1-1-1999

Effect of moisture on the state of stress and dimensional stability of photographic gelatin-latex coatings.

Duangdao, Aht-Ong
University of Massachusetts Amherst

EFFECT OF MOISTURE ON THE STATE OF STRESS AND DIMENSIONAL STABILITY OF PHOTOGRAPHIC GELATIN-LATEX COATINGS

A Dissertation Presented

by

DUANGDAO AHT-ONG

Submitted to the Graduate School of the
University of Massachusetts Amherst in partial fulfillment
of the requirements for the degree of

DOCTOR OF PHILOSOPHY

May 1999

Polymer Science and Engineering

EFFECT OF MOISTURE ON THE STATE OF STRESS AND DIMENSIONAL STABILITY OF PHOTOGRAPHIC GELATIN-LATEX COATINGS

A Dissertation Presented

by

DUANGDAO AHT-ONG

Approved as to style and content by:

Richard J. Farris, Chair

William J. MacKnight, Member

Thomas J. Lardner, Member

John M. Pochan, Consulting Member

Richard J. Farris, Department Head
Polymer Science and Engineering

DEDICATION

To my dearest twin sister, my very best friend, Duangduen Aht-Ong,

whose love and support has always been there since the day we were born.

ACKNOWLEDGMENTS

It is quite hard to know where to begin, since there have been so many people who have contributed to my education and my well-being throughout the years at UMASS in so many different ways. First and foremost, I would like to take this opportunity to acknowledge the Anandamahidol Foundation, an organization under the Royal Patronage of His Majesty the King of Thailand, for giving me the unique and honored opportunity to pursue my postgraduate degree abroad. Receiving this scholarship was the most prestigious award I ever received in my life.

Throughout the years at UMASS, my advisor, Professor Richard J. Farris, is foremost in my mind. I would like to express my sincere gratitude to him for his guidance, advice, and continuous support. I am truly grateful for his kind encouragement and patience throughout my time here as a graduate student. Having him as my Ph.D. advisor was one of the best decisions I ever made. I would also like to thank my other committee members, Professor William J. MacKnight and Professor Thomas J. Lardner, for their time and constructive comments and suggestions.

I would like to acknowledge Eastman Kodak Company for providing financial and material support for this research. Dr. John M. Pochan deserves a special mention for serving as a consulting member on my committee. I would like to thank him for all the discussions and very helpful suggestions. I would also like to thank him for giving me the opportunities to visit and work at Kodak for a month. It was a great experience for me to have a chance to carry out some of my experiments at the Kodak Laboratories. Many thanks also to Dr. Anthony Dai at Kodak for his help and thoughtful suggestions

over the years. His interest in my work and stimulating discussions has meant a lot to me. In addition, I want to thank Kathleen Bonsignore, Katherine Ann Shriner, and Sharon Girolmo at Kodak for their help at the very first stage of this research.

I would like to thank all the members in Farris research group, both past and present, for their friendship and generous help. In particular, I appreciate the assistance of previous group members : Kapil Sheth and Shalabh Tandon, who were my mentors both professionally and personally; Michael Chen for being a great office-mate and for his help. In addition, I want to thank Dr. Seung Koo Park who has been another wonderful office-mate for all his kind words and moral support during my last year. I also enjoyed very much the conversation I had with him. I would also like to thank Ru Feng for her help with the PVT apparatus. These friendships will always be part of the unforgettable memories of my graduate school days. Furthermore, I would like to thank Lou Raboin for assisting me with SEM. Also my thanks to Eileen Besse who has kept track of all the records and made all the paper work a lot easier for the graduate students.

I consider myself a very fortunate person to have gained many lasting friendships over the past few years. Many thanks to my dear friends, Vipavee, Kanokwan, and Saneh, for all the good times and memories and for making my stay in Amherst a pleasant and precious one. Especially, I would like to thank Vipavee for her help (since the first day I came to UMASS), kind and encouraging words, and technical discussions. Special thanks to Viboon for all his help and support both scientifically and nonscientifically. I owe him a great deal for his assistance. I would also like to thank my high school and college friends, Ning, Ong, Wit, Ake, P'Charn, Tak, Sang, Joe, Wut, for supporting, calling, emailing, lettering, and visiting me over the past few years. These

friendships do not fade with time or distance. Thanks to all of them for reminding me that a whole other world is out there.

Most of all, I would like to thank Tar, Julathep Kajornchaiyakul, for being so caring and supportive throughout the years since fate brought us together. His love and understanding has meant so much to me. I thank him for everything he has done for me and for making the last couple of years at UMASS so meaningful and the future so promising.

Finally, words cannot adequately express my feeling and gratefulness towards my family who have stood by me always. My mom and dad have always had consistent faith in me since I was a kid. It is really this faith that has kept me on the track and brought me here. I appreciate very much the sacrifice that they have made by letting me go to another country to pursue my education. I definitely would like to thank them for their unconditional love, support, and encouragement for all these years. Last but certainly not least, I want to thank my dearest sister, my very best friend, Duangduen Aht-Ong, for her endless love, kindness, support, and understanding both emotionally and technically since the day we were born. I want to thank her for always putting up with me, even when I may not have been the best sister. It is absolutely the love of her that drives me to have strength and confidence to overcome the obstacles I have met, and that is invaluable beyond my description. I know she is very proud of me but I am equally as proud of her. Without a doubt in my mind, this dissertation is totally dedicated to her, the most wonderful person I ever known and always will in this whole wide world. I love her more than words could ever explained.

ABSTRACT

EFFECT OF MOISTURE ON THE STATE OF STRESS AND DIMENSIONAL STABILITY OF PHOTOGRAPHIC GELATIN-LATEX COATINGS

MAY 1999

DUANGDAO AHT-ONG, B.Sc., CHULALONGKORN UNIVERSITY, THAILAND

M.S., UNIVERSITY OF MASSACHUSETTS AMHERST

Ph.D., UNIVERSITY OF MASSACHUSETTS AMHERST

Directed by : Professor Richard J. Farris

Gelatin has been used as a binder or dispersing agent for light-sensitive and non-light-sensitive photographic layers. The ability to keep the silver halide crystals finely dispersed and to protect the silver halide crystals and other additives from abrasion and other mechanical and chemical influences make gelatin desirable in photographic applications. However, gelatin is very sensitive to changes in humidity. Although this sensitivity to moisture is favorable when the film must be processed, it is also a drawback to the use of gelatin in an emulsion layer. The absorption of moisture can induce swelling stresses, causing dimensional instability commonly observed as bending or curling in the photographic films.

This dissertation focuses on the effects of moisture on the state of stress and dimensional stability of gelatin coatings. The hygroscopic effects on the thermal, mechanical, and transport properties were also investigated. Two types of polymer latices, poly(ethyl acrylate) and poly(ethyl methacrylate), were studied as additives to gelatin. The effects of latex concentration, latex particle size, drying condition at

vitrification, and gelatin concentration at set point were examined as a function of relative humidity. The goal is to develop an understanding of these properties and assist in controlling or selecting conditions which will minimize the dimensional instability of photographic films over a wide range of use conditions.

A vibrational holographic interferometry method and a thermomechanical analyzer were adopted to measure the stresses and dimensional changes as a function of relative humidity. The incorporation of a polymer latex can reduce the moisture sensitivity, and hence increases the dimensional stability of the emulsion layer exposed to the moisture. Composite theories for an isotropic composite filled with spherical particles were applied to determine the humidity expansion coefficient and elastic moduli of the gelatin-latex films. The experimental data were in excellent agreement with the theories. The decrease in swelling stress with an addition of the polymer latex was explained by the incremental linear elasticity theory. Based on this theory, the best material (i.e., minimum swelling stress, lowest $E\beta$ value) was found to be the gelatin film with 40 parts PEA and 15% gelatin concentration at set point, and was dried at the LMERH condition (130F / 5.5% RH).

CONTENTS

APPENDICES

LIST OF TABLES

LIST OF FIGURES

CHAPTER 1

INTRODUCTION AND BACKGROUND

Introduction

Gelatin is a fascinating material. It has been widely used in the food, pharmaceutical, and photographic industries for over a hundred years.[1] In photographic applications, gelatin has been used since its discovery in 1871 as a binder for a light-sensitive silver halide emulsion layer because it has many desirable characteristics for this purpose.[2] It has the ability to keep the silver halide crystals finely dispersed. Its main function as a binder is to protect the silver halide crystals, couplers, dyes, and other additives from abrasion and other mechanical and chemical influences.[3-5] Besides acting as a protective colloid or dispersing aid, it also serves as a sensitizer, ripening agent, and halogen acceptor.[6] In addition, gelatin is also used as a binder for non-light-sensitive photographic layers such as a protective layer, backing layer, subbing layer, etc. Details regarding the functions and properties of all these layers will be presented in chapter2.

However, due to its chemical composition, gelatin is very sensitive to moisture. It has a high propensity to absorb moisture, because of the hydrogen bonding of the water molecule to the amine or carboxyl groups in the peptide chain. The moisture content of photographic film is a function of the relative humidity of the atmosphere with which the film is in moisture equilibrium. Owing to this hydrophilicity of gelatin, the gelatin-silver

halide emulsion layer swells during processing which allows access of the imaging chemistry to the processing chemicals. This implies that the sensitivity of gelatin to moisture is favorable when the film must be processed or developed. However, it has been known that many of the physical and photographic properties of the gelatin film change dramatically, often deleteriously, with alteration in relative humidity or exposure to moisture.[7-11]

Relative humidity has a direct effect on the dimensional stability of photographic film. At low relative humidity, gelatin is a glassy polymer. It shrinks with water removal and when constrained by a relatively rigid support, this causes very high stresses, often resulting in curl. Problems such as static charges and brittleness cause difficulties in this humidity range.[12] In contrast, gelatin film at high relative humidity becomes soft and plastic. Photographic deterioration, friction, mottle, and ferrotyping effects are recognized as problems at high humidities.[12]

The maintenance of dimensional stability of photographic materials is especially important in many industrial applications, such as aerial mapping, drawing reproduction, graphic arts products, microfilm, x-ray products, and other applications with a premium on resolution.[4,5,12] The dimensional changes of photographic film depends not only on their composition and method of manufacture, but also on their thermal and moisture history. Although photographic materials may experience a wide range of temperature and humidity fluctuations during use; in general thermal expansion is less important than humidity expansion.[12] The absorption of moisture can induce swelling stresses, causing dimensional instability commonly observed as bending or curling in the photographic films. In an extreme case, the humidity fluctuation results in a cycling of

the stresses in the layers; as a result, this stress loading and unloading of the film can fatigue the material and eventually cause failure of the emulsion or delamination from the film support.

The use of photographic film in applications where dimensional stability is critical has increased in recent years. Considerable research has been conducted to understand and minimize dimensional instability.[13-20] Attempts have been made to find a substitute which would be suitable as a colloid carrier and dispersing agent for silver halide crystals and which would overcome the deficiencies of gelatin.[15-18] Such an emulsion must possess the sensitometric characteristics and permeability to the photographic processing solutions comparable to the emulsion composed of gelatin as the sole binder. Other attempts to solve the problem have been to seek an extender to mix with gelatin to modify the emulsion layer.[19,20] It is important that this substance should meet the following requirements. First, this material should be compatible with gelatin and the photographic emulsion. Further, it should not impair the optical properties of the photographic layers. Lastly, it should be completely inert to light-sensitive compounds, dyes, sensitizing agents, etc.[20] In manufacturing systems where curl is detrimental, films are coated with a gelatin coating on the opposite side of the emulsion coating. Since this gelatin backing layer responds similarly to the emulsion layer, it tends to counteract the curl of the film.[4]

In this research, the idea of partial replacement of gelatin was adopted. Polymer latices have been added to gelatin coatings because they are photographically inert and are compatible with gelatin. In addition, they have little affinity for water; thus, incorporation of latex should reduce swelling as a function of relative humidity and

increase the dimensional stability of the emulsion layer. It could also reduce brittleness and cracking, as well as increase the flexibility of the emulsion layer. Two types of polymer latices, poly(ethyl acrylate) and poly(ethyl methacrylate), were studied as additives to gelatin. The purpose of this research is to investigate the effects of latex particle size, latex concentration, drying conditions at vitrification, and concentration of gelatin at the set point on the state of stress, dimensional stability, and properties of gelatin coatings as a function of relative humidity. These properties include thermal properties, mechanical properties, and transport properties. The goal of the research is to develop an understanding of these properties and assist in controlling or selecting conditions which will minimize the dimensional instability of photographic films over a wide range of use conditions.

Background

As previously stated, there have been many studies [13-20] conducted to improve the properties of the gelatin emulsion by controlling the gelatin microstructure, e.g. by varying the degree of crystallinity and degree of hardening[6]. One of the approaches is to modify the chemical nature of the gelatin. Such modifications usually do not significantly alter the physical properties. The reactive side groups on the amino acid chain of the gelatin molecule can be reacted with specific reactants to provide the gelatin molecule with exceptional properties.[13]

Another way of modification is to improve the physical properties by the "grafting" of a polymeric material to the gelatin. For example, by polymerizing

acrylamides in a gelatin solution, the modified gelatins are claimed to be tougher, have less swell and lower solubility than unmodified gelatin.[14]

Synthetic polymers have been proposed for use as a binder instead of gelatin.[15-18] For example, emulsions based on polyvinyl alcohol, a water soluble hydrophilic polymer, are claimed to have improved physical properties over gelatin emulsions.[15] In addition, the gelatin emulsion can also be replaced by a synthetic copolymer. Such binders have been made from a styrene / butadiene copolymer, for instance, and have been claimed to be tough, low in curl, and have excellent dimensional stability. This is due to the hydrophobic nature of the synthetic elastomer used.[16] Other binder systems are made of cellulose ester [17] and the sodium salt of cellulose acetate hydrogen phthalate.[18] These systems show substantial improvements in diffusion transfer products and color film products, respectively.

Partial replacement of gelatin is another interesting approach. By replacing 15% of a gelatin binder with a low molecular weight polyacrylamide, for instance, the emulsion layer had no loss in photographic image density.[19] Another example is the emulsion in which 20% of the gelatin binder was replaced with a copolymer of butadiene and methyl methacrylate. This modified emulsion layer had improved dimensional stability, lower water absorption, and less brittleness.[20] Latices of rubbery polymers have been used because they are compatible with gelatin and are less hydrophilic than gelatin.

From this brief review of the modified binder systems, we can see a trend starting from the earliest days of photography. Originally, gelatin alone was used as the binder, whereas nowadays, although it is still dominates, we see part of it displaced in order to

achieve desirable physical properties. However, since the outstanding physical properties of gelatin derive from its tertiary structure and inter- and intrachain hydrogen bonding, efforts to completely replace gelatin with a synthetic polymers have failed to produce a fully satisfactory material.[5] Although some emulsions based on synthetic polymers are claimed to have improved physical properties over gelatin emulsions [15,16], other properties such as optical clarity or photographic properties have not been mentioned. Nevertheless, synthetic polymers play an important role for partial gelatin replacement. The above examples [19,20] show that both the physical and photographic properties can be improved by introducing hydrophobic polymers into the binder system. Therefore, as stated earlier, the idea of partial replacement of gelatin was adopted in this research. The binder systems comprised of poly(ethyl acrylate) and poly(ethyl methacrylate) partially mixed with gelatin were investigated.

Dissertation Overview

This dissertation focuses on the effects of moisture on the stress state and dimensional stability of photographic gelatin-latex films. The hygroscopic effects on the thermal, mechanical, and transport properties were also investigated. Two types of polymer latices, poly(ethyl acrylate), PEA, and poly(ethyl methacrylate), PEMA, were studied as additives to gelatin. The objective of this work is to examine the effects of latex concentration, latex particle size, drying conditions at vitrification, and concentration of gelatin at the set point on the state of stress, dimensional stability, and properties of gelatin coatings as a function of relative humidity. The goal of this research

is to develop an understanding of these properties and assist in controlling or selecting conditions which will minimize the dimensional instability of photographic films over a wide range of use conditions. Restated, the goal is to find the conditions which provide an emulsion layer with lower moisture absorption, improved dimensional stability (i.e., less swell and lower in curl), and better physical and mechanical properties (i.e., less brittleness, higher toughness, greater flexibility, etc.).

A brief introduction of the use of gelatin for photographic applications is presented in the current chapter 1. Problems and phenomena that occur in gelatin film with variations in relative humidity are addressed. Several approaches to solve the dimensional instability of photographic gelatin film are highlighted.

In chapter 2, a summary of systems investigated and parameters is introduced. A background for photographic film as well as the properties and functions of its components are described. The material properties, including the bulk modulus, of gelatin, poly(ethylene terephthalate), and the polymer latex are presented. The use of saturated salt solutions and the system designed to control relative humidity are also detailed.

Moisture absorption of gelatin and poly(ethylene terephthalate) is investigated in chapter 3. The conventional gravimetric measurement using a commercial Cahn 2000 recording electrobalance is employed to determine the moisture uptake of a material as a function of time at various relative humidities. Possible explanations for a moisture sorption hysteresis are reviewed. The influence of polymer latex, gelatin concentration at set point, and drying condition at vitrification on the moisture absorption of gelatin film are also examined.

Chapter 4 presents a comprehensive characterization of the thermal properties for pure gelatin and gelatin-latex films. The thermal stability is studied by thermogravimetric analysis (TGA). The effect of moisture on thermal transition temperatures is characterized by differential scanning calorimetry (DSC). A classical thermodynamic theory that predicts the effect of diluent on the glass transition temperature in polymer/diluent systems is applied to describe the plasticizing effect of moisture on the gelatin film. The effect of various parameters such as latex concentration, latex particle size, gelatin concentration at set point, and drying condition at vitrification on the thermal properties of gelatin film are also discussed.

The effect of moisture on the tensile properties of gelatin films is given in chapter 5 as a function of latex concentration, latex particle size, gelatin concentration at set point, and drying condition at vitrification. Composite theories for the elastic modulus of particulated-filled systems are highlighted. The experimental values of Young's modulus are compared with those predicted by the semi-empirical composite models. An optical microscope and a scanning electron microscopy (SEM) are used to investigate deformation morphology of the fractured gelatin film surfaces.

In chapter 6, the hygrothermal effect on the dimensional stability of gelatin and poly(ethylene terephthalate) films is presented. A thermomechanical analyzer (TMA) is employed to measure the dimensional changes of films as a function of time, temperature, and relative humidity. Humidity expansion coefficients (HEC) and thermal expansion coefficients (TEC) are discussed in term of latex concentration, latex particle size, gelatin concentration at set point, and drying condition at vitrification. Composite theories for the thermal expansion coefficient of an isotropic composite filled with spherical particles

are reviewed and applied to the moisture-induced expansion case. The experimental data comparing the model predictions are presented in both cases.

Chapter 7 involves the effect of moisture on the biaxial stress for pure gelatin and gelatin-latex films. A vibrational holographic interferometry method is adopted to determine the biaxial swelling stress as a function of relative humidity.[9] The change in stress with relative humidity is explained in view of moisture absorption, humidity expansion, and the modulus of the gelatin films.

The swelling strain associated with moisture diffusion behavior of pure gelatin and gelatin-latex films is detailed in chapter8. Using a thermomechanical Analyzer (TMA) equipped with a relative humidity generator, the swelling strains induced during absorption and desorption of moisture are monitored as a function of time at various relative humidities. A one dimensional hygrothermal elasticity theory is applied to correlate these swelling strains to the moisture diffusion through the thickness of the films. The mass diffusion coefficient is quantified. The effect of latex concentration, latex particle size, gelatin concentration at set point, and drying condition at vitrification on the mass diffuison coefficient are presented.

Finally, chapter 9 summarizes the research work of the entire dissertation. A few recommendations for future work in this area are also offered.

References

1. Rose, P.I. In *Encyclopedia of Polymer Science and Engineering*; Mark, H.F., Bikales, N.M., Overberger, C.G., Menges, G., and Kroschwitz, J.I., Eds.; John Wiley & Sons: New York, 1978; Vol. 7, pp. 488-573.

2. James, T.H., Ed.; *The Theory of the Photographic Process, 4th ed.*; Macmillan Publishing Co.: New York, 1977.

3. Fleischer, C.A., Bauer, C.L., Massa, D.J., and Taylor, J.F, "Film as a Composite material", *MRS Bulletin*, **21**(7), 14 (1996).

4. Stroebel, L., Compton, J., Current, I., and Zakia, R., Eds.; *Photographic Materials and process*; Focal Press: Boston, 1986.

5. Armour, E., Campbell, G.A., and Upson, D.A. In *Encyclopedia of Polymer Science and Engineering, 2nd ed.*; Mark, H.F., Bikales, N.M., Overberger, C.G., Menges, G., and Kroschwitz, J.I., Eds.; John Wiley & Sons: New York, 1985; Vol. 11, pp. 175-185.

6. Jolley, J.E., "The Microstructure of Photographic Gelatin Binders", *Photographic Science and Engineering*, **14**(3), 169 (1970).

7. Marshall, A.S. and Petrie, S.E.B., "Thermal Transitions in Gelatin and Aqueous Gelatin Solutions", *Journal of Photographic Science*, **28**, 128 (1980).

8. Ni, B.Y. and Faou, A.L., "Crystalline Structure and Moisture Effects on Deformation Mechanisms of Gelatin Films under Mode I Stress Field", *Mat. Res. Soc. Symp. Proc.*, **292**, 229 (1993).

9. Vrtis, J.K., "Stress and Mass Transport in Polymer Coating and Films", Ph.D. Dissertation, University of Massachusetts, Amherst, MA (1995).

10. Pinhas, M-F., Blanshard, J.M.V., Derbyshire, W., and Mitchell, J.R., "The Effect of Water on the Physicochemical and Mechanical Properties of Gelatin", *Journal of Thermal Analysis*, **47**, 1499 (1996).

11. Fakirov, S. et al., "Mechanical Properties and Transition Temperatures of Crosslinked Oriented Gelatin II Effect of Orientation and Water Content on Transition Temperatures", *Colloidal Polymer Science*, **275**, 307 (1997).

12. Adelstein, P.Z. In *SPSE Handbook of Photographic Science and Engineering*; Thomas, W., Ed.; John Wiley & Sons: New York, 1973; Section 8, pp. 473-500.

13. Ryan, W.H., "Process for Producing Silver Halide Emulsions Containing gelatin Derivatives", U.S. Patent No. 3,186,864 (June 1, 1965).

14. Coover, H.W.,Jr., "Modified Gelatins Obtained by Polymerizing and Alkenyl Carbonamide in an Aqueous Gelatin Solution", U.S. Patent No. 2,794,787 (June 4, 1957).

15. Oberth, A.E. and Shacklett, C.D., "Gelatin-Anion Soap Complex Dispersion in Polyvinyl Alcohol Photographic Emulsions", U.S. Patent No. 3,067,035 (December 4, 1962).

16. Dubosc, J-P.C.G. and Thiebaut, R.P.J.G., "Photographic Emulsion Having a Low Modulus of Elasticity and Process for Its Manufacture", U.S. Patent No. 3,359,108 (December 19, 1967).

17. Levenson, G.I.P., "Limiting Factors in Processing", *Journal of Photographic Science*, **17**, 2 (1969).

18. Rogers, H.G. and Lutes, H.W., "Photographic Process", U.S. Patent No. 3,239,336 (March 8, 1966).

19. Allentoff, N. and Minsk, L.M., "Photographic Silver Halide Emulsions Having High Wet Density Retention", U.S. Patent No. 3,271,158 (September 6, 1966).

20. Paesschen, A.J.V. and Vrancken, M.N., "Photographic material", U.S. Patent No. 3,397,988 (August 20, 1968).

CHAPTER 2

MATERIAL PROPERTIES

Introduction

The study of pure gelatin and gelatin-latex films is the primary focus of this thesis research. In addition, poly(ethylene terephthalate) has been investigated. This chapter offers a background for photographic film. The material properties of the gelatin, poly(ethylene terephthalate), and the polymer latices are highlighted. The bulk modulus of these materials was evaluated using a pressure-volume-temperature (PVT) apparatus. The results will be incorporated into composite theories for the coefficients of expansion in chapter 6. Details regarding the use of saturated salt solutions to generate relative humidity are also addressed.

Materials

The materials used in this investigation were alkaline processed bone gelatin coatings on a poly(ethylene terephthalate) substrate. All of these materials were provided by the Eastman Kodak Co., Rochester, NY. The samples were stored in a freezer in order to minimize any aging effect prior to experimentation. The systems investigated were pure gelatin as a control and gelatin with polymer latex additives. Two different kinds of polymer latices were studied. Table 2.1 lists the variables for each latex system,

including the particle size, concentration, and drying conditions. Details of the samples and the corresponding factors are summarized in Appendix A.

Table 2.1 : Description of the Coating Parameters Studied

Factors	System I	system II
Kodak ID	PWnMt	EmWnMt
Latex Type	Poly(ethyl acrylate)	Poly(ethyl methacrylate)
Latex Concentration (g of latex / 100 g of gelatin)	0, 20, 40	0, 20, 40
Latex Particle Size (μm)	0.051, 0.112	0.067, 0.150
Gelatin Concentration at Set Point (%)	10, 15	10, 15
Drying Condition at Vitrification	HMERH (80F / 29 %RH) LMERH (130F / 5.5 %RH)	HMERH (80F / 29 %RH) LMERH (130F / 5.5 %RH)

Photographic Film

Generally, photographic materials such as photographic films and papers, are composed of an emulsion layer consisting of silver halide in gelatin coated on a substrate, most commonly poly(ethylene terephthalate) or cellulose acetate. A schematic of a photographic film is illustrated in Figure 2.1. The physical properties of the photographic materials are determined by the composition of the support as well as the thin emulsion layer as outlined in the literature.[1-3]

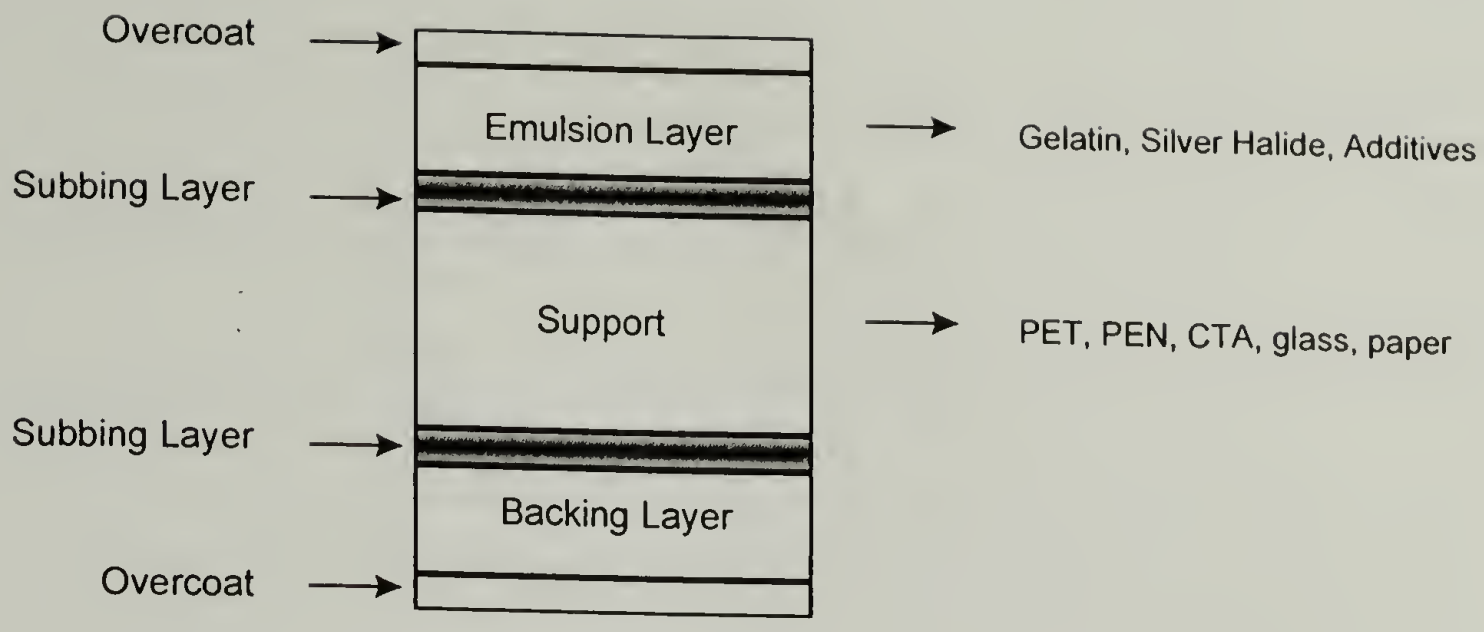

Figure 2.1 : Schematic of photographic material.

Support

The principal function of the substrate, typically 100 μm in thickness, is to provide mechanical strength and dimensional stability for the film, especially when it is transported through the camera and developing process.[4] In addition to dimensional stability and optical clarity, the polymer support must have good tear strength, provide antistatic protection, be abrasion-resistant, and be resistant to curling.[1-4]

Emulsion Layer

An emulsion layer is composed of a gelatin matrix or binder filled with silver halide crystals and other additives (e.g., hardeners, couplers, or dyes). The main function of the gelatin is to protect the silver halide and those additives in the emulsion layer from abrasion and other mechanical and chemical influences.[4-6] Compared to other

photochemical materials, silver halides are more sensitive to light and are used in the photographic manufacturing industry to produce the latent image that is later developed to produce a visible image.[5] The thickness for the emulsion layer is about 5-25 μm depending on use and can be adjusted by controlling viscosity and speed of coating.[5] The physical properties of photographic materials also depend upon the relative thickness of the emulsion and support layers.[1] As shown in Figure 2.1, the emulsion layer is usually overcoated with an abrasion-resistant layer to prevent scratching of negatives before, after, and during processing.[4]

Subbing Layer

Basically, the gelatin-based emulsion layer must adhere well to the support throughout its life time. Therefore, the adhesion of the layer must withstand all the handling, scratching, processing chemicals, etc., to which it is exposed during manufacturing and customer use. For example, the processing environment is quite harsh, including a development step in a high pH (12) aqueous bath at 38°C for 20 minutes.[4] The hydrophilic gelatin binder does not adhere well when applied directly to the hydrophobic support surface; hence, before coating the emulsion on the support, the support has to be prepared to make the emulsion layer adhere. One of the ways to achieve acceptable adhesion between the emulsion and the support is to coat a subbing layer or adhesion-promoter to the film support. This subbing layer has a thickness of 0.5-3 μm and is composed of polymers that are intermediate in hydrophilic-hydrophobic

balance compared with the emulsion layer and the support. Typically copolymers are used for the subbing layer, such that one monomer interacts with the gelatin emulsion layer, whereas the other monomer is compatible with the support. A frequently used subbing layer copolymer for the PET substrate is poly(acrylonitrile-*co*-vinylidene chloride-*co*-acrylic acid).[6] Furthermore, better adhesion is generally obtained if the support surface is treated before applying the subbing layer. For instance, solvent etching or a corona discharge treatment of the hydrophobic support surface may be used.[4,6]

Backing Layer

Unlike the emulsion layer, the back side of most photographic film does not contain any photosensitive elements. In fact a variety of different layers are used on the back side of the support to provide the physical properties needed for handling and use of the film. For example, a thin conductive layer is used for antistatic protection. The subbing layer is also used to adhere the backing layer to the support. In manufacturing systems where curl is detrimental and curl control is desired, films are also coated with a gelatin coating on the back side to balance the curl of the front side emulsion. Since this gelatin backing layer responds similarly to the emulsion layer, it tends to counteract the curl of the film. Similar to the emulsion layer, an abrasion-resistant overcoat is used on the outermost of the backing layer to prevent scratching and other damage to the film during use in the camera, during processing, and in postprocessing handling.[4,6]

Gelatin

Gelatin is a high molecular weight polypeptide, derived from collagen by alkaline or acid hydrolysis. Collagen is a right-handed triple helix polypeptide, consisting of three left-handed single helices. The structure of gelatin is a random coil polymer molecule made up of amino acids joined together by peptide bonds.[7] The chemical structure of gelatin is shown in Figure 2.2.

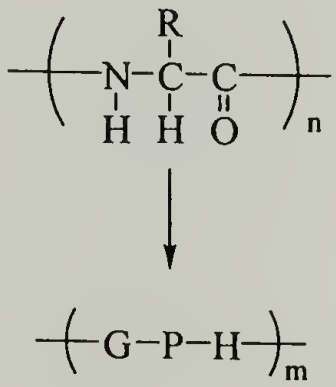

terpolymer sequence

Figure 2.2 : Chemical structure of gelatin.

Typically, there may be 500 - 1000 amino acid units in the chain. There are 18 different amino acids in gelatin.[7] Even though its precise sequence has not been elucidated, the general arrangement is clear that three amino acids; Glycine(G), Proline(P), and Hydroxy Proline(H), make up about 55% of the gelatin molecule, and occur as shown in the terpolymer sequence illustrated in Figure 2.2.

Therefore, it is obvious that because of its chemical composition, gelatin is very sensitive to moisture. It has a high tendency to absorb moisture, owing to the hydrogen

bonding of the water molecule to the amine or carboxyl groups in the peptide chain. This characteristic is of prime importance to the physical and photographic properties of the film. These properties are affected by changes in moisture content of the film as determined by the relative humidity with which the film is brought to equilibrium. Overall the properties of the gelatin matrix are highly dependent on the use environment. Under dry or standard room conditions, gelatin is a semicrystalline solid with glassy characteristics. However, in a wet environment or a swollen state, gelatin is a crosslinked polymeric matrix that can be considered a soft rubber.

Poly(ethylene terephthalate)

Poly(ethylene terephthalate), PET, is manufactured by Eastman Kodak Co. under the trade name ESTAR®. PET can absorb 0.5% moisture at 70F, 50% RH.[1] PET has a higher modulus than cellulose triacetate (CTA) and an-order-of magnitude less water absorption, which leads to higher dimensional stability.[1-4] PET's higher modulus is due principally to its method of manufacture, melt extrusion and casting followed by biaxial stretching and heat setting. This method creates a biaxially oriented film that is highly oriented in the plane of the film with about 40-50% crystallinity.[4]

Polymer Latex

Latex or emulsion polymers have been employed in modern photographic products. They improve physical properties in some cases and act as carriers for

hydrophobic additives in others.[6] Since latex polymers have little affinity for water [6,8], as partial gelatin replacements, in which latex is a dispersed phase and gelatin is the continuous phase, latex polymers increase the drying rate of coatings. In addition, other properties that can be affected include dimensional stability, flexibility, cracking, abrasion resistance, and swelling.[6] In this work, two types of polymer latices, Poly(ethyl acrylate), PEA, and Poly(ethyl methacrylate), PEMA were studied as additives to gelatin.

Poly(ethyl acrylate), PEA, obtained by radical polymerization in the 48 to -78°C range is amorphous. It is rubberlike, soft, and extensible. Poly(ethyl methacrylate), PEMA, is a hard polymer with much higher tensile strength and lower elongation than PEA. The chemical structures of PEA and PEMA are shown in Figure 2.3. The substitution of a methyl group at the α-H on the main chain of PEMA restricts the freedom of rotation and motion of the polymer back bone (steric hindrance) and thus produces harder, higher tensile strength, and a lower elongation polymer than their acrylate counterpart (PEA).[9,10] Table 2.2 summarizes the latices properties investigated.

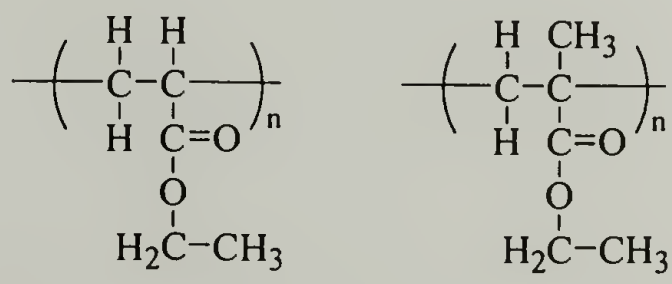

Figure 2.3 : Chemical structure of PEA and PEMA.

Table 2.2 : Latices Description [9,10]

Properties	PEA	PEMA
Glass Transition Temperature(°C)	-24	[a]atactic : 65 syndiotactic : 120 isotactic : 8
Density (g/cm^3) @ 25°C	[b]1.12	[b]1.12
Solubility Parameter (J/cm^3)	19.3	18.3
Refractive Index n_D^{25}	1.464	1.485
Tensile Modulus (MPa)	~ 1	~ 3000
Tensile Strength (MPa)	0.2	34
Elongation at Break (%)	1800	7

[a] PEMA provided by Eastman Kodak Co.
[b] values communicated per Kathleen Bonsignore, Eastman Kodak Co.[11]

Bulk Modulus

A pressure-volume-temperature (PVT) from Gnomix Research Inc. was employed to determine the bulk modulus of the materials used in this research. This instrument allows one to measure the specific volume change of a sample as a function of pressure (0.1-200 MPa) and temperature (30-400°C).[12] The sample weight of 0.5-2 g is confined in the sample cell filled with mercury. One end of the sample cell is sealed, whereas the other end of the cell is attached to a flexible stainless steel bellows which moves to suit the expansion or contraction of the sample assembly. The change in volume of the sample due to the applied pressure or temperature is measured by the deflection of the bellows which is attached to a linear variable differential transformer

(LVDT) displacement transducer. The starting conditions for all PVT experiments are D1 (displacement of the LVDT rod) = -2.000 mm, P = 10 MPa, and T = 30°C. According to the manual, the PVT apparatus has a sensitivity of < 0.0005 cm^3/g and an accuracy of $\pm$ 0.002 cm^3/g at temperatures less than 250°C and up to $\pm$ 0.004 cm^3/g at higher temperatures.[13]

In this research, the bulk compressibility, κ, was evaluated by carrying out an isothermal run at 30°C. At a constant temperature, the specific volume change was measured as pressure was varied from 10 MPa to 160 MPa. The slope of the dilatation vs. pressure curve is equal to the bulk compressibility of the sample as defined in equation (2.1). Finally, the bulk modulus, K, of the material is obtained by taking an inverse of the bulk compressibility.

$$\kappa = -\frac{1}{V_0}\left(\frac{\partial V}{\partial P}\right)_T \qquad (2.1)$$

Figure 2.4 shows a typical isothermal test for gelatin film. The changes in specific volume as a function of pressure at 30°C for gelatin and polymer latices, PEA and PEMA, are compared in Figure 2.5. The results from the isothermal runs of these materials are summarized in Table 2.3 which includes bulk compressibility and bulk modulus values. It is apparent from Figure 2.5 and also from the calculated values presented in Table 2.3, that gelatin has the greatest bulk modulus among the three materials tested. This is because of its glassy characteristic at the tested condition, especially when comparing to PEA which becomes soft and rubber-like at 30°C.

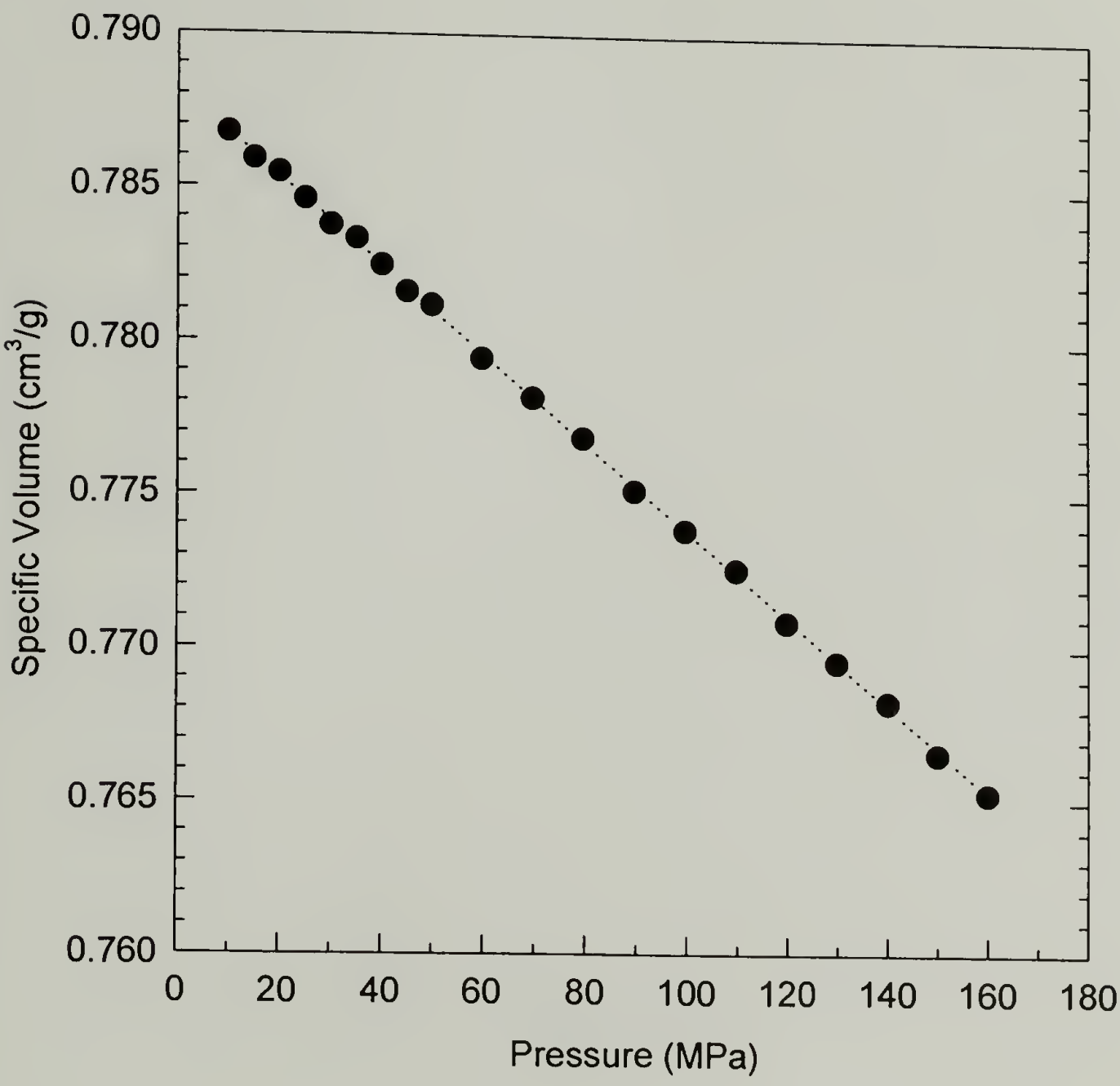

Figure 2.4 : Change in specific volume with applied pressure at 30°C for pure gelatin film in the PVT apparatus.

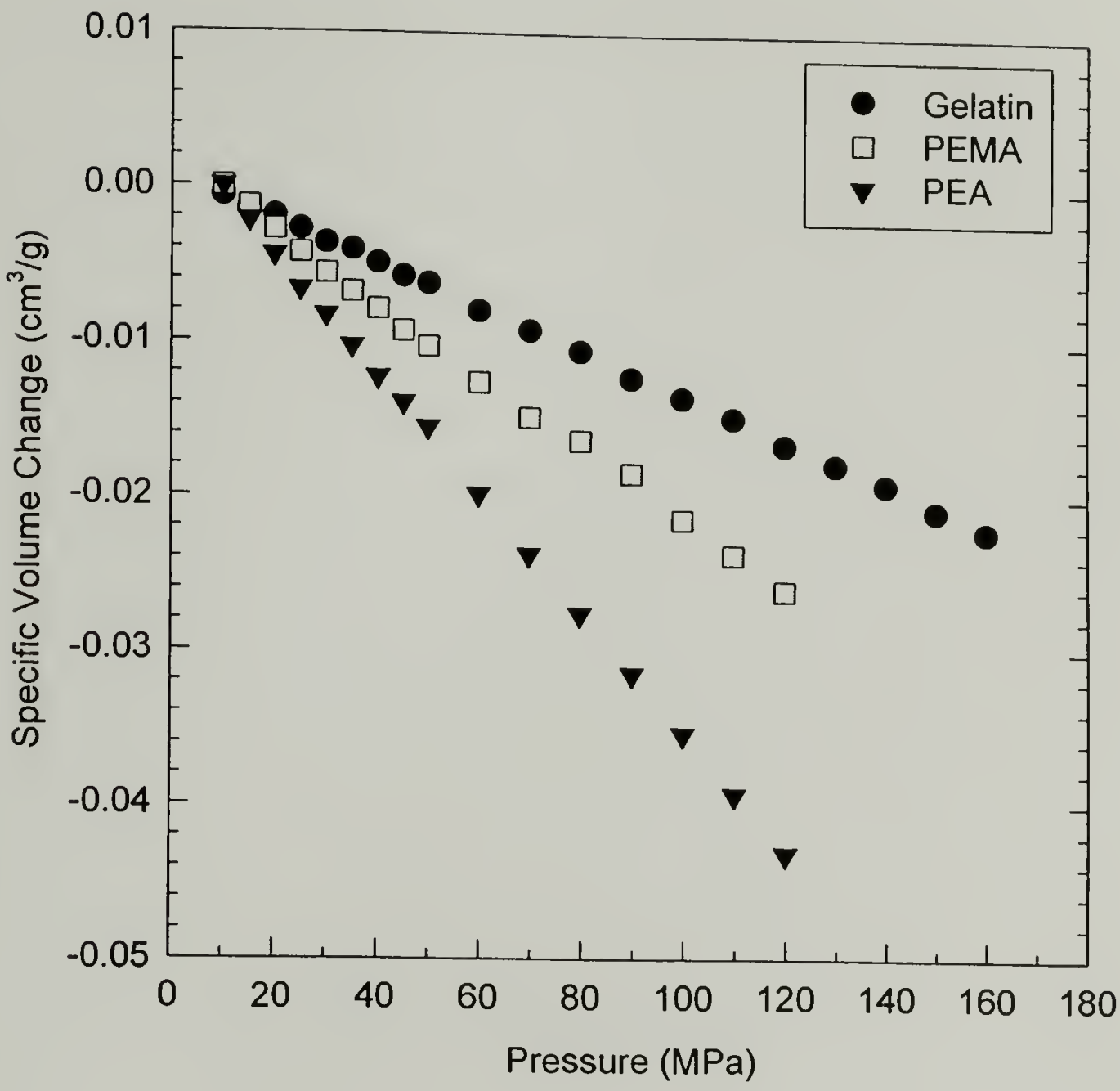

Figure 2.5 : Isothermal run at 30°C for gelatin, PEMA, and PEA to evaluate the bulk compressibility.

Additionally, in comparison to PEA, PEMA has a lower bulk compressibility and hence higher bulk modulus. This is due to the greater backbone rigidity in PEMA. These data will be used in the composite models for the prediction of the humidity expansion and thermal expansion coefficients in chapter 6.

Table 2.3 : Bulk Compressibility and Bulk Modulus from the PVT Apparatus

Material	Bulk Compressibility (GPa^{-1})	Bulk Modulus (GPa)
Gelatin	0.182	5.50
PEMA	0.258	3.88
PEA	0.435	2.30
Kodak PET	[a]0.140	7.14

[a] reported value at 25°C [14]

Relative Humidity Generation

Relative humidity is the ratio of the partial pressure of water vapor in air to the saturated pressure of water vapor at the same temperature. It can be generated by a number of different methods reported elsewhere.[15,16] However, it should be noted that some limitations must be considered. For example, by using water-sulfuric acid mixtures to generate relative humidity, care must be used as the humidity obtained depends on composition and temperature. Moreover, the vapor pressure of the solutions change with use as they become diluted or concentrated by interchange of moisture with

the conditioning material. These problems do not occur when saturated salt solutions are used to control humidity, and therefore, saturated salt solutions were used in this investigation. Table 2.4 presents the list of standard salt solutions that were used with their corresponding humidities. The saturated salt solution method is simple and inexpensive. Because the vapor pressure does not change as long as some of the solid phase is present, the mixture produces constant relative humidity which is independent of temperature. The valid temperature range is about ambient or room temperature which makes using saturated salt solutions very convenient.

Table 2.4 : Relative Humidity Generated by Standard Salt Solutions [17-19]

Saturated Salt Solutions	Relative Humidity (%)	Valid Temperature (°C)
Potassium Acetate	22 ± 1	15 - 30
Magnesium Chloride	32 ± 1	5 - 45
Sodium Iodide	38 ± 2	5 - 45
Calcium Nitrate	51 ± 2	10 - 30
Sodium Bromide	58 ± 2	0 - 35
Potassium Iodide	69 ± 2	5 - 30
Ammonium Sulfate	81 ± 1	10 - 40
Barium Chloride	90 ± 2	5 - 25

As depicted in Figure 2.6, a compressed gas, either nitrogen or helium, depending on the experiment being conducted, is bubbled through the gas washing bottle containing the saturated salt solution. The relative humidity is then transported to the sample. In order to attain 0% relative humidity, a compressed gas is passed through a drying agent or

Drierite® ($CaSo_4$). A gas dispersion tube is attached to the entrance tip of the gas washing bottle in order to generate a number of very small, fine bubbles, affording a great deal of surface area between the air and the solution. Small gas bubbles also have more residence time in the solution and a high surface to volume ratio. As a result, equilibrium conditions are rapidly established.

A Fisher® Digital Hygrometer/Thermometer was employed to monitor the humidity and temperature. Its relative humidity range is 5 to 95 %RH with an accuracy of $\pm$1.5 %RH. It provides humidity readings in less than 10 seconds.

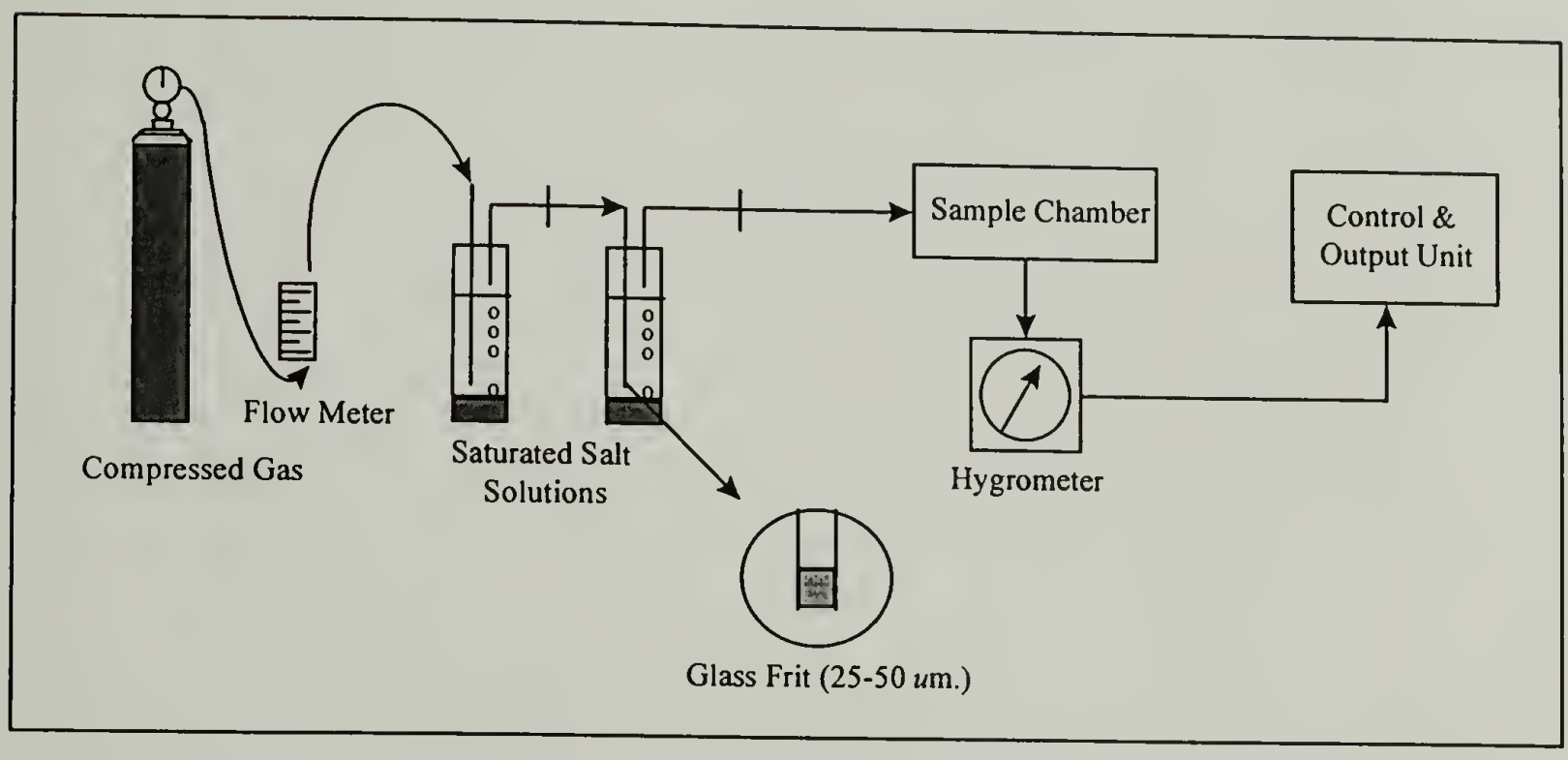

Figure 2.6 : Schematic of the relative humidity generation system.

References

1. Adelstein, P.Z. In *SPSE Handbook of Photographic Science and Engineering*; Thomas, W., Ed.; John Wiley & Sons: New York, 1973; Section 8, pp. 473-500.

2. "Physical and Chemical Behavior of Kodak Aerial Films", *Properties of Kodak Materials for Aerial Photographic Systems*; Eastman Kodak Co.: Rochester, NY, 1972; Vol. III.

3. "Physical Properties of Kodak Aerial Films", *Properties of Kodak Materials for Aerial Photographic Systems*; Eastman Kodak Co.: Rochester, NY, 1972; Vol. II.

4. Fleischer, C.A., Bauer, C.L., Massa, D.J., and Taylor, J.F, "Film as a Composite material", *MRS Bulletin*, **21**(7), 14 (1996).

5. Stroebel, L., Compton, J., Current, I., and Zakia, R., Eds.; *Photographic Materials and process*; Focal Press: Boston, 1986.

6. Armour, E., Campbell, G.A., and Upson, D.A. In *Encyclopedia of Polymer Science and Engineering, 2nd ed.*; Mark, H.F., Bikales, N.M., Overberger, C.G., Menges, G., and Kroschwitz, J.I., Eds.; John Wiley & Sons: New York, 1985; Vol. 11, pp. 175-185.

7. Jolley, J.E., "The Microstructure of Photographic Gelatin Binders", *Photographic Science and Engineering*, **14**(3), 169 (1970).

8. Harper, C.A., Ed.; *Handbook of Plastics, Elastomers, and Composites, 2nd ed.*; McGraw-Hill, Inc.: New York, 1992; Chapter 1, pp. 49-52.

9. Brendley, W.H., "Acrylic Polymers", *Paint and Varnish Production*, 19 (1973).

10. Kine, B.B. and Novak, R.W. In *Encyclopedia of Polymer Science and Engineering , 2nd ed.*, Mark, H.F., Bikales, N.M., Overberger, C.G., Menges, G., and Kroschwitz, J.I., Eds.; John Wiley & Sons: New York, 1985; Vol. 1, pp. 234-299.

11. Bonsignore, K., personal communication, 1996.

12. Zoller, P., Bolli, P., Pahud, V., and Ackermann, H., "Apparatus for Measuring Pressure-Volume-Temperature Relationships of Polymers to 350°C and 2200 kg/cm^2", *Review of Scientific Instruments*, **47**(8), 948 (1976).

13. Zoller, P., "PVT Manual (Version 2.01)", Gnomix Inc., Boulder, CO, 1987.

14. Chen, M.J., "Pressure-Volume-Temperature and Wave Propagation Studies of Polyimide Films", Ph.D. Dissertation, University of Massachusetts, Amherst, MA (1998).

15. Wexler, A. and Brombacher, W.G., "Methods of Measuring Humidity and Testing Hygrometers. A Review and Bibliography", U.S. Government Printing Office (1951).

16. "The Measurements of Humidity in Closed Spaces", Food Investigation Special Report No. 8 (1993).

17. Weast, R.C., Ed.; *Handbook of Chemistry and Physics, 55th ed.*; CRC Press: Ohio, 1974.

18. Greenspan, L, "Humidity Fixed Points of Binary Saturated Aqueous Solutions", *Journal of Research of the National Bureau of Standards: A. Physics and Chemistry*, **81A**(1), 89 (1977).

19. O'Brien, F.E.M. "Control of Humidity by saturated Salt Solutions", *Journal of Scientific Instrumentation*, **25**, 73 (1948).

CHAPTER 3

MOISTURE ABSORPTION

Introduction

Moisture absorption of both natural and synthetic polymers depends upon the chemical structure and morphology of the polymer, such as the polarity of the molecular structure, degree of crystallinity, degree of crosslinking, presence of residual monomers and/or other water attracting species.[1] Moisture can be distributed throughout the polymers at polar sites or within the free volume that is present. The degree of clustering of the water molecules, presumably within the free volume, is a function of molecular polarity.[1] Polymers with ketones and imides are more resistant to hydrolysis; they have fewer polar groups and this reduces their moisture sensitivity.[2] Polymers that are highly crystalline exhibit lower moisture absorption. The moisture absorption of a polymer is reduced by an increase in the cross-linking density.

The sorption of moisture by a material is of prime importance since many physical and mechanical properties of a moisture-sensitive material can be greatly modified by the presence of sorbed moisture. These properties are affected by changes in the moisture content of the material as determined by the relative humidity with which the material is brought to equilibrium. Property changes may be due to combinations of plasticization and mechanical damage from moisture induced swelling. For composite materials, mechanical damage may cause surface crazing/cracking and matrix

microcracking. Organic fibers, such as Kevlar and wood fibers, also absorb moisture, tend to exhibit softening and may even crack internally.

Moisture induced plasticization of polymers is a common occurrence. This plasticization process involves interruption of the van der Waals' bonds, e.g., ethers, secondary amines and hydroxyl groups, between polymer chains. The degree of plasticization is much stronger when water molecules can interact with the polymer chains in the form of hydrogen bonding, causing an increase in free volume. This allows more freedom of motion and reduces the glass transition temperature. Thus the reduction in Tg on moisture absorption is greater for polar polymers. In both nylon 66, studied by Starkweather [3], and high-performance epoxy resin, described by Moy and Karasz [4], the moisture is believed to hydrogen bond between polar sites in the polymers, acting as crosslinks at low temperatures but plasticizing at elevated temperatures because of greater thermal mobility of moisture compared to segments of the polymer chain.

The moisture-polymer interaction can be beneficial or detrimental to performance of commercial polymers. For photographic applications, the sensitivity to moisture of gelatin is advantages when films must be developed. However, it has been observed that many of the material properties change dramatically, often deleteriously, with variations in relative humidity or exposure to moisture. For example, the tensile strength, yield strength, and tensile modulus of gelatin decrease with increasing moisture content, while the elongation at break increases. Moreover, moisture absorption in gelatin can induce swelling stresses, causing dimensional instability commonly observed as bending or curling in photographic films.

Prior to discussing the influence of moisture uptake on the properties of photographic materials, in particular gelatin film, the measurement of moisture content in the material itself is essential. Colton and Wiegan [5] reviewed a number of analytical methods, chemical, physical, and electrical, for measuring the moisture content of photographic film. The shortcomings and advantages of each method are also discussed.

In this chapter, the conventional gravimetric measurement using a commercial Cahn 2000 recording electrobalance was employed. The objective of this chapter is to quantify the moisture uptake of gelatin film and the poly(ethylene terephthalate) substrate as a function of time at various relative humidities. The effect of polymer latex, gelatin concentration at set point, and drying condition at vitrification on the moisture absorption of gelatin film was also examined.

Experimental

There are several techniques available to measure moisture content and to determine moisture sorption isotherms of the material.[5-8] These methods can be divided into three main categories: 1) a gravimetric method which measures the weight change of samples in equilibrium with different water vapor pressures(RH), 2) manometric and hygrometric methods, which are suitable for rapid and convenient determination of water activity in process and quality control. For obtaining complete sorption isotherms, samples with different water content must be available. 3) special methods. More extensive details can be found in the literature.

In this study, the gravimetric method, which is the most common technique of measuring moisture content, was used. Direct measurement of weight changes was made using a commercially available Cahn 2000 electrobalance.[9] This apparatus allows one to measure weight changes as a function of time at various relative humidities. Figure 3.1 presents a schematic of a Cahn electrobalance set up with a relative humidity generator using saturated salt solutions.

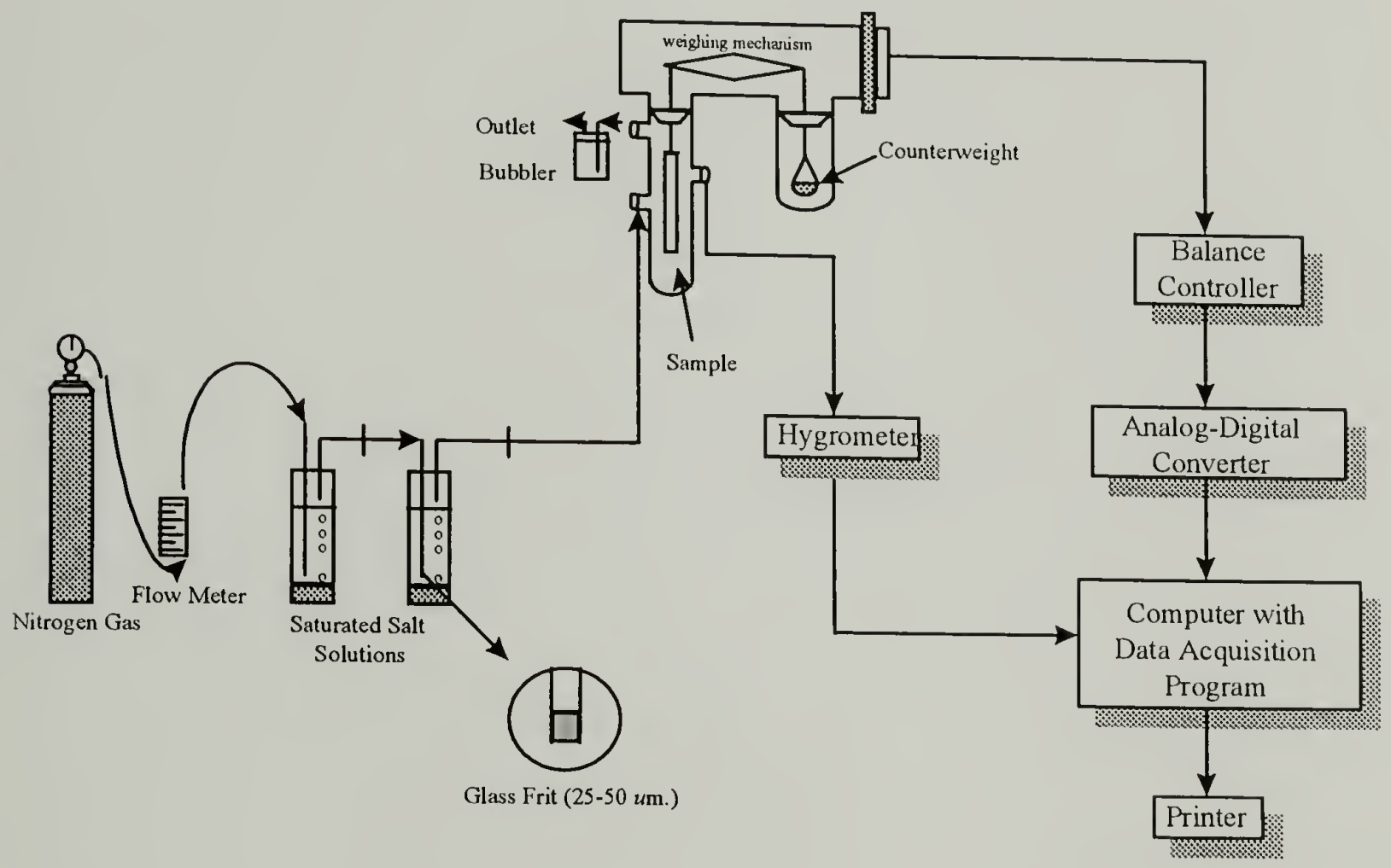

Figure 3.1 : Schematic of a Cahn 2000 electrobalance used to determine moisture content as a function of time at various relative humidities.

The system consists of three main parts which are: the relative humidity generator, the weight measuring unit (electrobalance), and the control and output unit. A uniaxial sample weight of 10 mg was used and the mass uptake as a function of time at

various relative humidities was recorded. Initially, the sample was dried at 0 %RH until no further weight change was observed. Then 20% RH was introduced into the system and the weight increase as a function of time was monitored. After equilibrium was reached, the sample was then subjected to a higher relative humidity and again the moisture uptake at each relative humidity was determined. Weight changes were measured as analog signals which were converted to digital signals by an A/D converter. A computer with a data acquisition program (Lab Tech Notebook) was used to capture the data.

Results and Discussion

Moisture Sorption

The moisture absorption isotherms at 20 %RH, 40 %RH, 60 %RH, and 80 %RH for pure gelatin film are shown in Figure 3.2. At 20 %RH, the gelatin absorbed 12.10 weight % moisture. It can be seen that the ability of gelatin to absorb moisture increases with increasing relative humidity. It is clear that gelatin films have a strong affinity for moisture. Gelatin can absorb 27.81 % moisture at 80%RH, which is very high when compared to other polymer and protein sorption systems such as a nylon-water system [10], a wool-water system [10,11], or a silk-water system [12]. Figure 3.3 presents the moisture absorption of PET film at various relative humidities. As seen in Figure 3.3, PET at 40 %RH absorbed only 0.43 % moisture. However, like the gelatin film, at higher

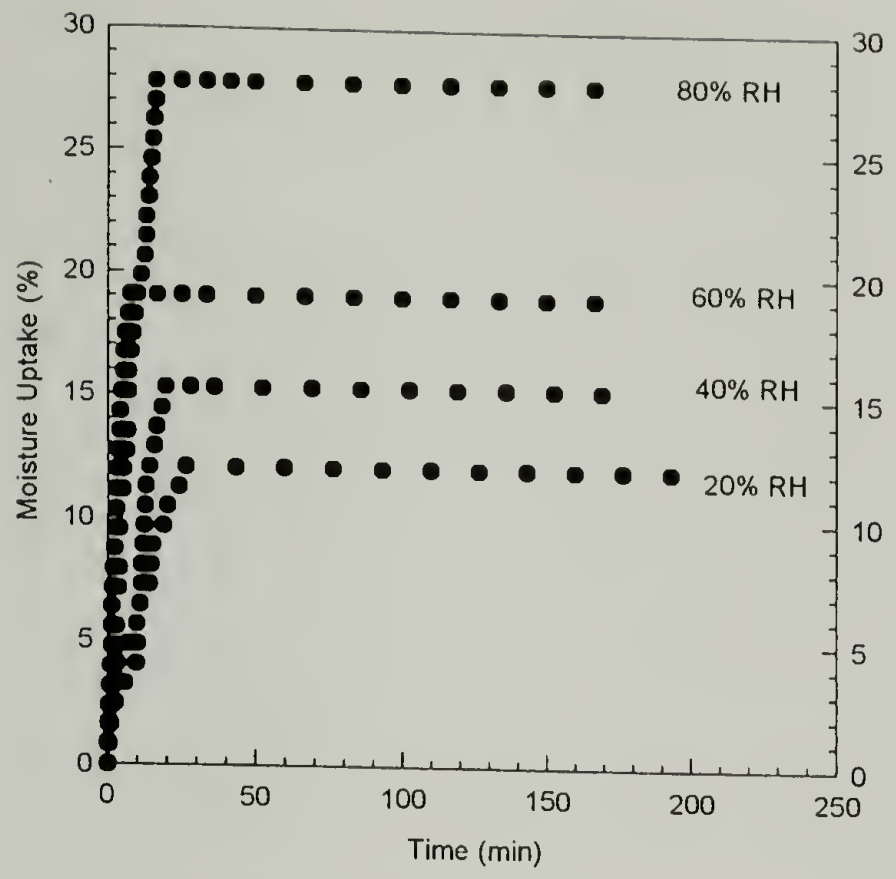

Figure 3.2 : Moisture absorption isotherms as a function of time at various relative humidities for gelatin film (BF 8362-1C).

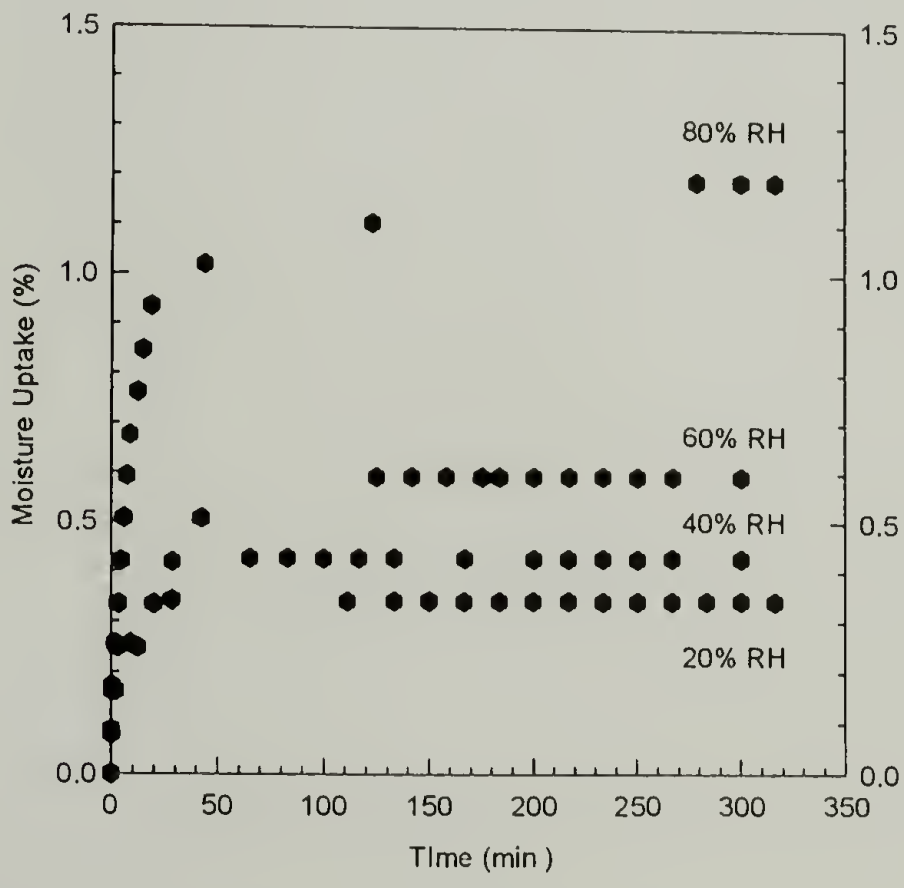

Figure 3.3 : Moisture absorption isotherms as a function of time at various relative humidities for PET film.

relative humidities, the amount of absorbed moisture also increases with increasing relative humidity.

Figure 3.4 provides a comparison of the percent moisture uptake of gelatin and PET at 40 %RH. It is obvious that at the same relative humidity, gelatin can absorb much more moisture than the PET substrate. This is due to the strong hydrophilic nature of gelatin film. The very low moisture absorption of the PET substrate, when compared to the very high moisture absorption of the gelatin film, is one of the reasons for the adverse effect which gelatin has on the dimensional stability of photographic film. The values of equilibrium moisture uptake for gelatin and PET films are tabulated in Table 3.1.

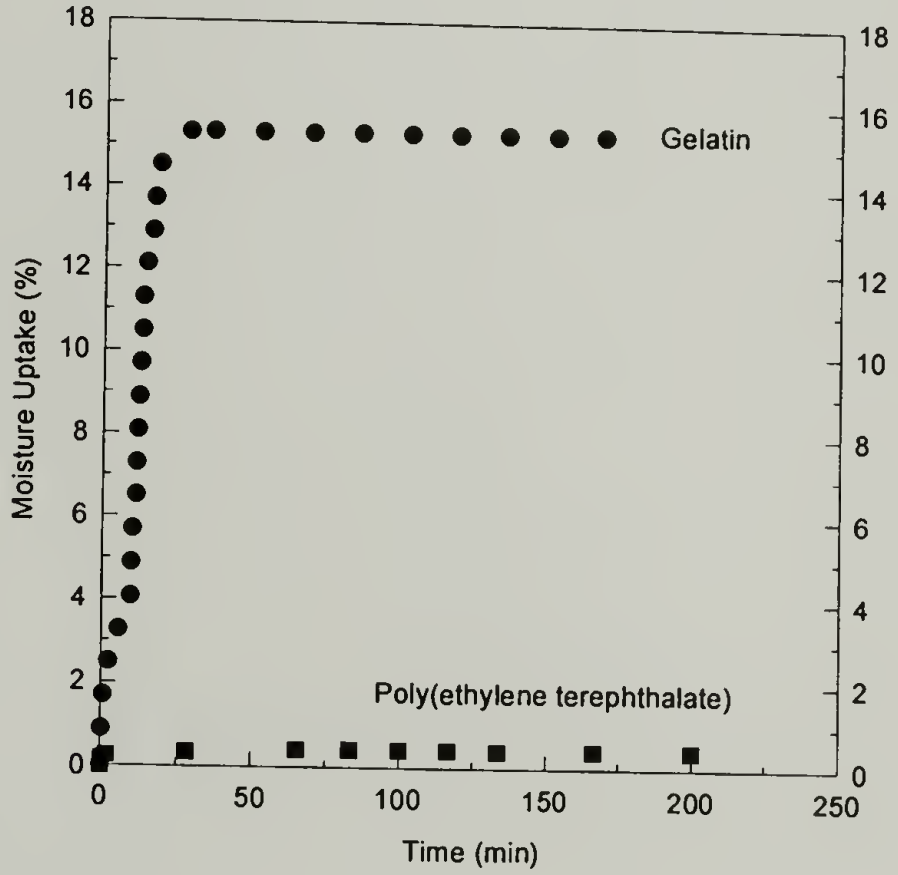

Figure 3.4 : Comparison of the moisture absorption isotherm for gelatin (BF 8362-1C) and PET films at 40% RH.

Table 3.1 : Comparison of the Equilibrium Moisture Uptake (%) for Gelatin Film (BF 8362-1C) and PET Substrate at Various Relative Humidities Measured by a Cahn 2000 Electrobalance

Relative Humidity (%)	Gelatin	Poly (ethylene terephthalate)
20	12.1	0.34
40	15.3	0.43
60	19.1	0.59
80	27.8	1.19

In both gelatin and PET films, the moisture sorption isotherms initially show a linear relationship between moisture uptake and time, followed by saturation. Gelatin reaches its equilibrium faster than the PET substrate. For example, at 40 %RH the mass uptake of gelatin reaches equilibrium within approximately 20 minutes, whereas it takes about one hour for PET substrate to reach equilibrium at the same relative humidity. This is due to the differences in their thickness and diffusion coefficients, which is another reason for the complex time dependency of dimensional instability in photographic film.

Figure 3.5 and 3.6 illustrate the absorption and desorption isotherms of gelatin and PET films conditioned at 20 %RH and 40 %RH, respectively. In a manner similar to the absorption isotherm, the initial linear relationship between moisture loss and time for the desorption behavior is observed in both gelatin and PET films and followed by equilibrium.

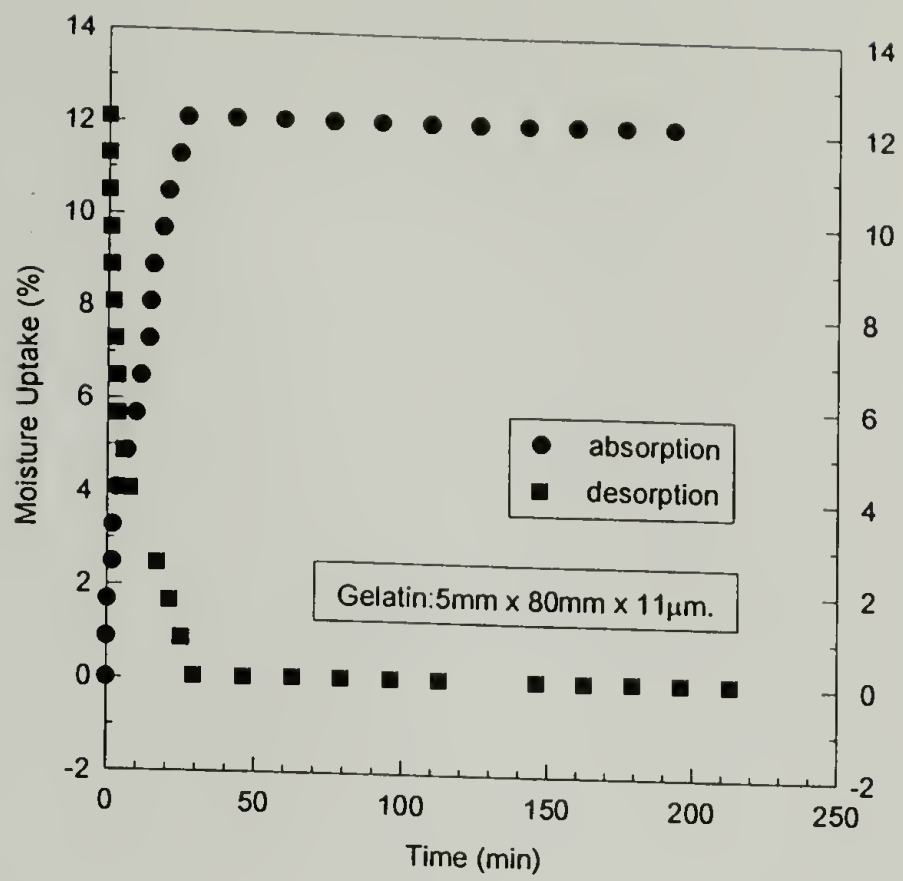

Figure 3.5 : Moisture absorption and desorption isotherms of gelatin film (BF 8362-1C) conditioned at 20% RH measured by a Cahn 2000 electrobalance.

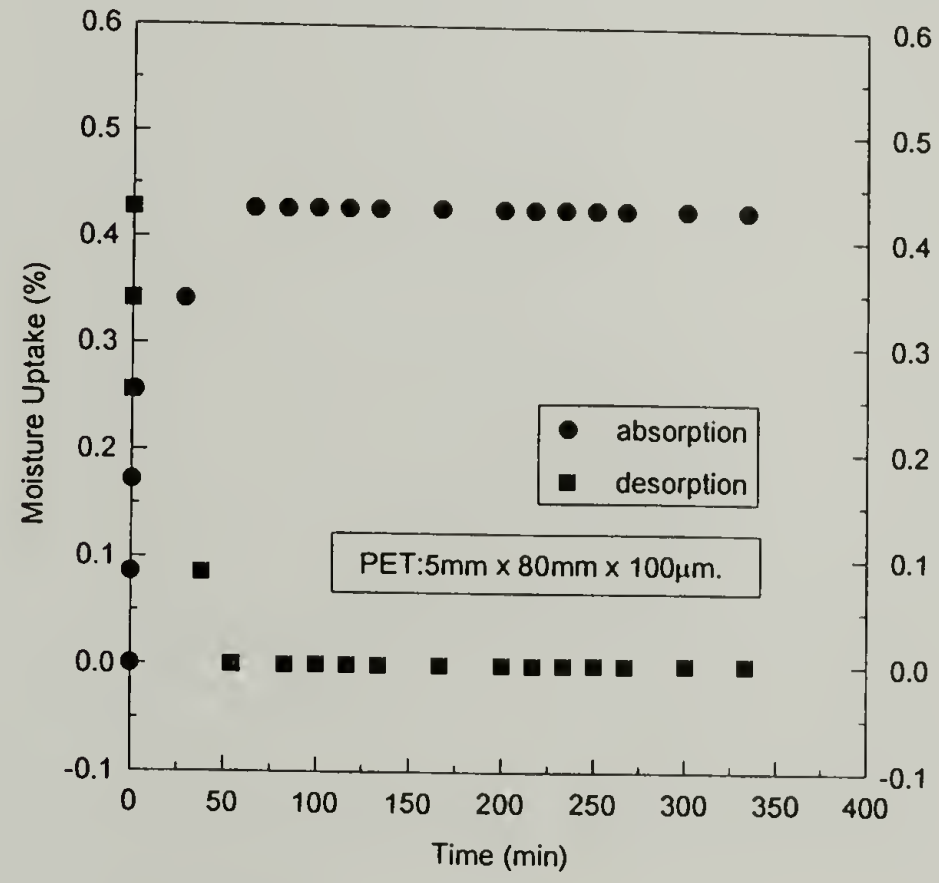

Figure 3.6 : Moisture absorption and desorption isotherms of PET film conditioned at 40% RH measured by a Cahn 2000 electrobalance.

Moisture Sorption Hysteresis

As displayed in Figure 3.7, absorption and desorption isotherms of moisture in gelatin follow different paths. The desorption isotherm gives a higher moisture uptake than the absorption isotherm at the same relative humidity. This phenomenon is the so ealled "moisture sorption hysteresis", which is generally observed in paper and other moisture-absorbing materials ineluding polymer and protein sorption systems such as a wool-water vapor system.[13-15]

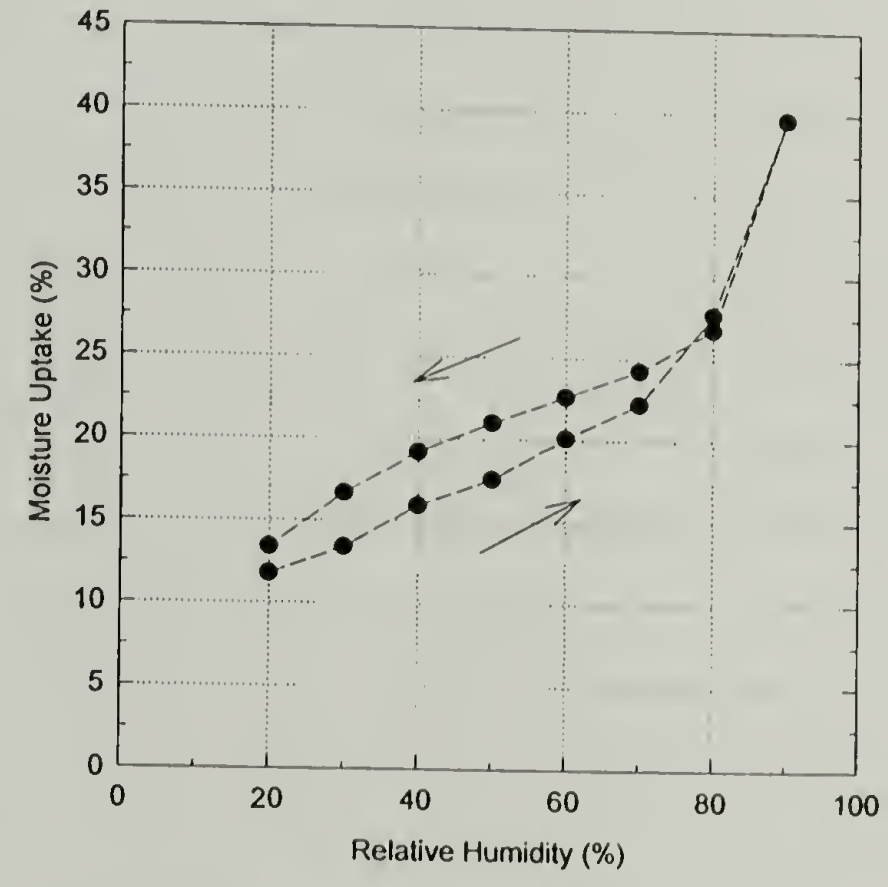

Figure 3.7 : Moisture sorption hysteresis of pure gelatin film (BF 8362-1C) measured by a Cahn 2000 eleetrobalanee.

Figure 3.8 illustrates the moisture sorption hysteresis of pure gelatin and gelatin-latex films. Both gelatin-PEA film and gelatin-PEMA film exhibit hysteresis when subjected to a sorption-desorption humidity eyele. However, their ability to absorb

moisture are different. It is very clear that at each relative humidity the amount of absorbed moisture in the emulsion layer decreases when polymer latex is added to the system, especially when adding the poly(ethyl acrylate). This is because both PEA and PEMA are less hydrophilic than gelatin. For example, at 90 %RH the moisture uptake of pure gelatin film is around 40%, where that of gelatin-PEMA and gelatin-PEA films are approximately 33 % and 30 %, respectively. This decrease in the moisture uptake is a desirable property, since it makes the composite emulsion layer less sensitive to moisture than the pure gelatin.

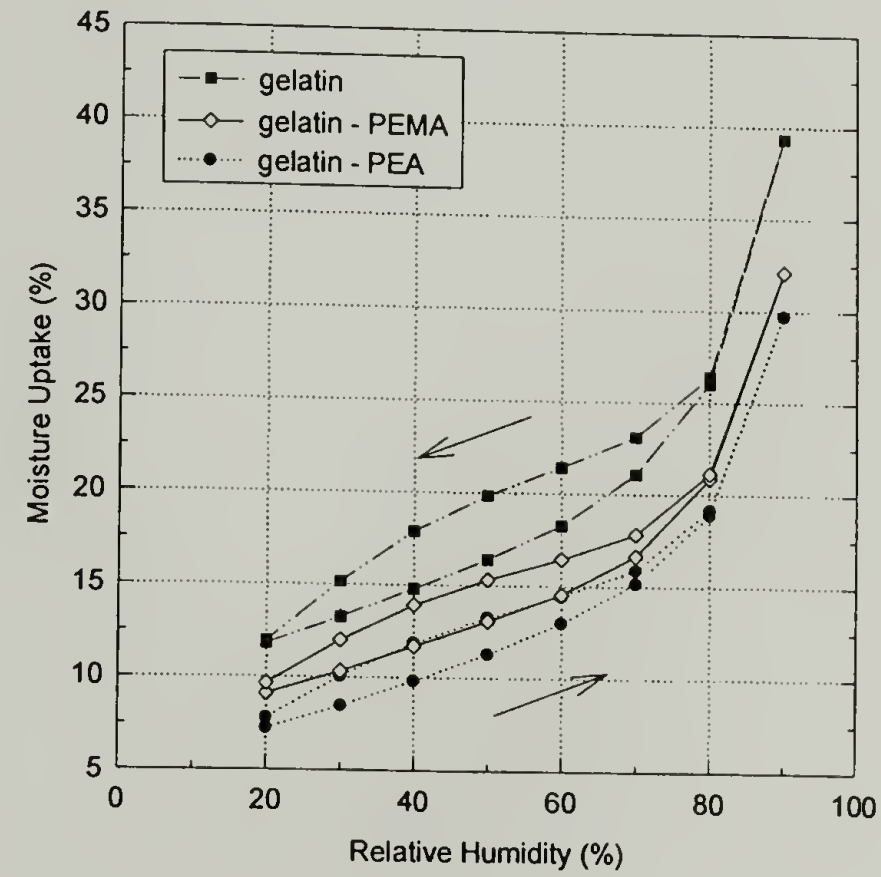

Figure 3.8 : Effect of polymer latex on the moisture sorption hysteresis : pure gelatin (BF 8483-133), gelatin-20 parts PEMA (BF 8483-123), and gelatin-20 parts PEA (BF 8483-173) films.

The effect of gelatin concentration at the set point is shown in Figure 3.9. The gelatin film with the lower gelatin concentration at the set point (10 %) absorbed more

moisture than the film with 15 % gelatin concentration at the set point. This can be explained by the molecular structure of the film. Usually, crystalline regions of polymers are not penetrated by absorbed moisture. The amorphous structure is the area that absorbs moisture. The film with a 10 % gelatin concentration at the set point has a higher amorphous structure than the film with 15 % gelatin concentration at the set point; therefore, it absorbs more moisture. This result correlates well with the effect of moisture on the thermal properties, especially the glass transition temperature and the heat of fusion, which are described in chapter 4.

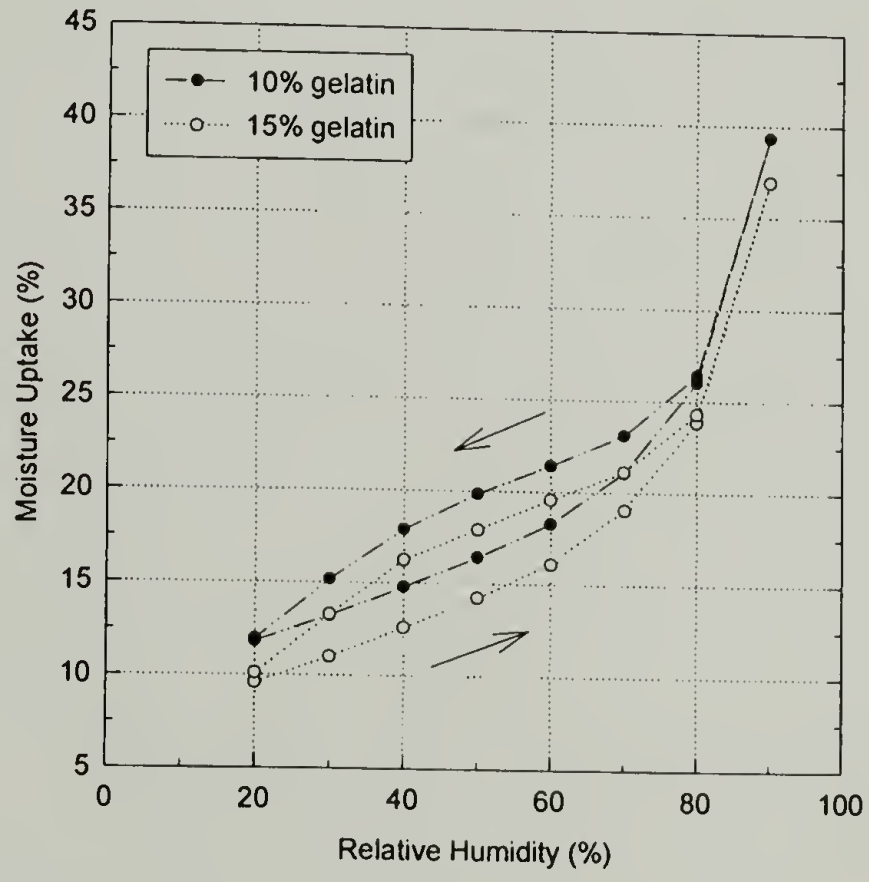

Figure 3.9 : Effect of gelatin concentration at set point on the moisture sorption hysteresis of pure gelatin films : (1) 10% gelatin (BF 8483-133) and (2) 15% gelatin (BF 8483-83).

The drying conditions also influence the moisture absorption of gelatin films. As shown in Table 3.2, the moisture uptake of gelatin film dried under the HMERH (80 F /

29 %RH) condition has slightly higher moisture uptake than the material dried under the LMERH (130 F / 5.5 %RH) condition.

Table 3.2 : Effect of Drying Condition on the Equilibrium Moisture Uptake (%) for Pure Gelatin at Various Relative Humidities : HMERH (BF 8483-83) and LMERH (BF 8483-73)

Relative Humidity (%)	HMERH	LMERH
20	9.57	8.94
30	11.0	10.2
40	12.6	11.5
50	14.2	12.7
60	16.1	14.5
70	19.1	17.6
80	23.9	22.7
90	36.9	35.8

These results can again be simply explained by the gelatin structure. It is known that the drying condition can greatly affect the molecular structure of gelatin materials. According to Jolley [16], the gelatin film dried at the low temperature (10°C) will have a crystalline structure, and the gelatin film dried at the higher temperature (50°C) will have an amorphous structure (the details regarding the drying conditions will be discussed shortly). As mentioned earlier, water can penetrate the amorphous regions but not the crystalline regions. It would therefore be expected that the moisture uptake of crystalline films, in our case the gelatin film dried under HMERH condition, should be less than that of the gelatin film dried under LMERH condition which has an amorphous structure.

However, Jolley did show that at 50 %RH the crystalline film absorbs essentially the same amount of moisture as an amorphous film. He suggested that this might be because water is a small molecule and has a very high affinity to form hydrogen bonds with the gelatin molecule and, as a result, it can penetrate both crystalline and amorphous regions. His statement can be confirmed by the x-ray diffraction studies of Bear in 1952.[17] Bear has shown that because of the absorption of moisture between the helices, the crystalline lattice of gelatin expands laterally upon absorption of moisture.

In our case, however, the crystalline film absorbs slightly more moisture than the amorphous film. Therefore, the effect of drying temperature alone cannot be used to explain the result completely. The extra amount of moisture absorbed by the crystalline film could also be explained as a relative humidity effect. The HMERH drying condition exposes the gelatin films to a higher humidity (29 %RH) than the film dried at the LMERH (5.5 %RH); therefore, the percent moisture uptake of the gelatin film dried at the HMERH condition must be higher than the gelatin film dried at the LMERH condition.

In summary, the ability of the gelatin films to absorb moisture when dried at different conditions depends on both temperature and relative humidity. Again, this result can be used to support the plasticizing effect of water on the glass transition temperature of gelatin coatings and will be discussed in chapter 4.

There are several proposed mechanisms to explain moisture sorption and moisture sorption hysteresis. Windle [18] proposed that adsorbed water exists in three forms : localized water, bound water, and liquid or free water. Localized water represents the water molecules that are hydrogen bonded to the hydrophilic polar groups of the gelatin. Bound water is the water attached by hydrogen bonds to the localized water. Finally, free

water is the water that fills the interstices in the polymer's amorphous regions. The amount of free water is dictated by the relative humidity. Windle did not discuss the moisture hysteresis phenomenon.

The earliest attempt to explain the hysteresis phenomenon is suggested by Zsigmondy in 1911.[19] His "Incomplete Wetting Theory" is based on the Kelvin equation ($RT\ln P/P_0 = -2\sigma V\cos\theta/r_m$ where R is the gas constant, P the vapor pressure of the liquid over the curved meniscus, P_0 the saturation vapor pressure at temperature T, σ the surface tension, V the molar volume of the liquid, θ the contact angle, and r_m the mean radius of curvature of the meniscus). Because of the presence of impurities (dissolved gases, etc.), the receding contact angle for desorption is smaller than that of the advancing contact angle for adsorption. This is the cause of the hysteresis. However, the Zsigmondy theory failed to explain the adsorption results at low relative humidities.

Later mechanisms proposed that porous structures exist in the polymer.[20-22] This is the so-called "Ink Bottle Neck Theory". This theory explains hysteresis on the basis of the differences in radii of the porous structure. A cavity consists of a large-diameter pore with a narrow neck as in the body and neck of an ink bottle. The absorption occurs into the large diameter cavity of the bottle, while the desorption happens at the neck or pore which is blocked by a meniscus. As a result, the moisture content is different along the absorption and desorption paths. In other words, moisture hysteresis occurs.

Others expanded upon these earlier proposed mechanisms by assuming multilayer absorption.[23,24] This "Open-Pore" theory was elaborated upon by Cohan in 1938.

Cohan's theory is based on the differences in vapor pressure between absorption and desorption as affected by the shape of meniscus, which he considered to be cylindrical and hemispherical on absorption and desorption, respectively.

Another attempt to explain moisture sorption hysteresis was proposed by York in 1981.[25] York's proposed mechanism can be described in three steps: First, the water molecules adsorb on the surface, forming a monomolecular layer known as monolayer-adsorbed moisture. Second, the absorption of moisture into the material by diffusional forces occurs and is referred to as absorbed moisture. Finally, multimolecular layers of water, termed condensed water, are formed when more moisture adheres to the surface. When the relative humidity is decreased, the water molecules at the surface are removed first, followed by the removal of the absorbed moisture. The hysteresis takes place because of the difference between the absorption rate and desorption rate.

Recently, a better understanding of moisture sorption hysteresis of gelatin was clarified by Wetzel et al. using circular dicroism(CD) measurements.[26] They discovered that the conformation of the gelatin chains resemble the conformation of the polyproline, Form II, the trans-peptide form of polyproline. Since gelatin has a glycyl residue at every third position along the chain, the trans-conformation of the single chains of gelatin is stabilized only in a triple helix structure. In general, "bound" water molecules stabilize the triple helix structure by interchain bridging, so called hydrogen bonding, between the water molecules and the CO-groups in gelatin. From experiments with decreasing relative humidity, the trans-conformation or the triple helix content decreases and, simultaneously, the cis-conformation is observed. It is known that the water molecules are less accessible to form hydrogen bonds with the CO-groups in the

cis-form than in the trans-form. Therefore, at low relative humidity, where the cis-conformation exists, the water content in gelatin decreases and the triple helix content decreases. Upon rehydration, or along the absorption path, the triple helix strands are regenerated and a cis- to trans- transition is observed. However, not all of the cis-form converts to the trans-form. The amount of cis-form in the absorption path is greater than in the desorption path, resulting in a hysteresis. In summary, "bound" water is the primary contributing factor to the hysteresis. The occurrence of a hysteresis can be attributed to the different amounts of cis- and trans- conformation in each sorption path. At the same relative humidity, the trans-form in the desorption path is greater than in the absorption path. Therefore, the desorption cycle shows a greater moisture content than the absorption cycle. In other words, hysteresis occurs.

Conclusions

The moisture sorption of gelatin and the PET substrate was measured using a Cahn 2000 electrobalance. As expected, the interaction of moisture with gelatin exhibits a hysteresis phenomenon. Some mechanisms explaining the moisture sorption hysteresis of gelatin were highlighted. At 80 %RH, gelatin absorbs as much as 27.81 % moisture, whereas PET can absorb only 1.19 %. This difference in the resulting swelling of the composite film causes large stresses and dimensional problems.

It is very clear that the amount of sorbed moisture in the emulsion layer decreases when polymer latices are added to the system, especially for the gelatin-PEA film. The addition of a polymer latex can reduce the sensitivity of the emulsion layer to moisture.

This is the desired effect, since it can reduce the mismatch of the moisture absorption between the emulsion coating and the PET substrate. The dimensional stability of the film is therefore improved.

The gelatin concentration at set point and the drying conditions at vitrification also have an influence on the moisture absorbing ability of the gelatin film. The gelatin film with the lowest gelatin concentration picks up more moisture. The moisture uptake of the films dried at the HMERH condition (80 F / 29 %RH) is slightly higher than the films dried at the LMERH condition (130 F / 5.5 %RH). These results correlate well with the effect of moisture on the Tg and heat of fusion of the films as will be presented in chapter 4.

References

1. Jones, F.R. In *Handbook of Polymer-Fibre Composites*; Jones, F.R., Ed.; Longman Scientific & Technical: Burnt Mill, Harlow, Essex, 1994; Chapter 6.3, pp. 371-375.

2. Wolff, E.G. In *Handbook of Polymer-Fibre Composites*; Jones, F.R., Ed.; Longman Scientific & Technical: Burnt Mill, Harlow, Essex, 1994; Chapter 6.1, pp. 362-366.

3. Starkweather, Jr., H.W. In *Water in Polymers*; Rowland, S.P., Ed.; American Chemical Society: Washington, D.C., 1980; Chapter 25, pp. 433-440.

4. Moy, P. and Karasz, F.E. In *Water in Polymers*; Rowland, S.P., Ed.; American Chemical Society: Washington, D.C., 1980; Chapter 30, pp. 505-513.

5. Colton, E.K. and Wiegand, E.J., "Moisture in Photographic Film and Its Measurement", *Photographic Science and Engineering*, **2**(3), 170 (1958).

6. Gal, S. In *Water Relations of Foods*; Duckworth, R.B., Ed.; Academic Press: London, 1975; pp. 139-153.

7. Gal, S. In *Water Activity: Influences on Food Quality*; Rockland, L.B. and Stewart, G.F., Eds.; Academic Press: New York, 1981; pp. 89-110.

8. Spiess, W.E.L. and Wolf, W. In *Water Activity: Theory and Applications to Food*; Rockland, L.B. and Beuchat, L.R., Eds.; Marcel Dekker, Inc.: New York, 1987; pp. 215-233.

9. Cahn Instruments, Inc., Cerritos, CA 90701.

10. D'Arcy, R.L. and Watt, I.C., "Analysis of Sorption Isotherms of Non-Homogeneous Sorbents", *Trans. Faraday Soc.*, **66**, 1236 (1970).

11. King, G. and Cassie, A.B.D., "Propagation of Temperature Changes Through Textiles in Humid Atmosphere : Part I. Rate of Absorption of Water Vapor by Wool Fibers", *Trans. Faraday Soc.*, 36, 445 (1940).

12. Agarwal, N., Hoagland, D.A., and Farris, R.J., "Effect of Moisture Absorption on the Thermal Properties of Bombyx mori Silk Fibroin Films", *Journal of Applied Polymer Science*, **63**, 401 (1997).

13. Kapsalis, J.G. In *Water Activity: Theory and Application to Food*; Rockland, L.B. and Beuchat, L.R., Eds.; Marcel Dekker, Inc.: New York, 1987; pp. 173-214.

14. D'Arcy, R.L. and Watt. In *Water Activity: Influences on Food Quality*; Rockland, L.B. and Stewart, G.F., Eds.; Academic Press: New York, 1981; pp. 111-142.

15. Kapsalis, J.G. In *Water Activity: Influences on Food Quality*; Rockland, L.B. and Stewart, G.F., Eds.; Academic Press: New York, 1981; pp. 143-177.

16. Jolley, J.E., "The Microstructure of Photographic Gelatin Binders", *Photographic Science and Engineering*, **14**(3), 169 (1970).

17. Bear, R.S., "The Structure of Collagen Fibrils", *Advance Protein Chemistry*, **7**, 69 (1952).

18. Windle, J.J., "Sorption of Water by Wool", *Journal of Polymer Science*, **21**, 103 (1956).

19. Zsigmondy, R., "Structure of Gelatious Silicic Acid. Theory of Dehydration", *Journal of Organic Chemistry*, **71**, 356 (1911).

20. Kraemer, E.O. *A Treatise on Physical Chemistry*; Van Nostrand: New York, 1931.

21. McBain, J.W., "An Explanation of Hysteresis in the Hydration and Dehydration of Gels", *Journal of American Chemical Society*, **57**, 699 (1935).

22. Rao, K.S., "Hysteresis in Sorption. I-IV", *Journal of Physical Chemistry*, **45**, 500 (1941).

23. Cohan, L.H., "Sorption Hysteresis and the Vapor Pressure of Concave Surfaces", *Journal of American Chemical Society*, **60**, 433 (1938).

24. Cohan, L.H., "Hysteresis and the Capillary Theory of Adsorption of Vapors", *Journal of American Chemical Society*, **66**, 98 (1944).

25. York, P., "Analysis of Moisture Sorption Hysteresis in Hard Gelatin Capsules and Maize Starch: Drug Powder Mixtures", *Journal of Pharmaceutical and Pharmacology*, **33**, 269 (1981).

26. Wetzel, R., Buder, E., Hermel, H., and Hüttner, "Conformations of Different Gelatins in Solutions and in Films: An Analysis of Circular Dicroism (CD) Measurements", *Colloid and Polymer Science*, **265**, 1036 (1987).

CHAPTER 4

EFFECT OF MOISTURE ABSORPTION ON THERMAL PROPERTIES

Introduction

As stated in the preceding chapter, moisture can cause a wide variety of mechanical and physical changes in polymers. The most important consequence of moisture absorption on a physical property is a reduction in the glass transition temperature, Tg, of the polymers as a result of moisture plasticization.[1] Moy and Karasz [2] showed that the lowering of Tg for an epoxy-diamine resin is proportional to the amount of water in the system. Fuzek [3] found that water absorbed by synthetic fibers and silk at room temperature and 65% RH substantially lowers Tg's. Pritchard [4] reported that, as moisture content increases from 0 to 6% by weight, the Tg of poly(vinyl alcohol) fiber decreases by approximately 64°C. This effect is not limited to synthetic polymers and resins; Scandola and Pezzin [5] noted the lowering of Tg of elastin by water. Elastin has a dry Tg of 200°C; upon hydration, it becomes a rubbery system with the Tg below room temperature.

Similarly, the Tg and Tm for gelatin is highly dependent upon its moisture content. Both Tg and Tm decrease with increasing relative humidity. The effect of moisture on these thermal transitions is essentially important in understanding the changes in the physical behavior and performance of gelatin in an environment with changing relative humidity. Although there has been a great deal of research performed

on the thermal properties of gelatin [6-17], relatively little is done on the influence of humidity on its thermal transitions [14-17]. In particular, no work has ever been reported on the gelatin-latex film. Therefore, in this chapter the study of both pure gelatin and gelatin-latex films was undertaken to obtain further understanding of the effect of moisture on these transition temperatures. The plasticization effect of moisture on Tg for pure gelatin and gelatin-latex films was detailed and compared to the predictions of a phenomenological theory derived from classical thermodynamics. The effects of latex concentration, latex particle size, gelatin concentration at set point, and drying conditions at vitrification on the thermal properties were investigated as a function of relative humidity. In addition, the thermal stability of the films was studied by thermogravimetric analysis (TGA).

Experimental

Thermogravimetric Analysis

Thermal degradation and weight loss as a function of temperature were studied using a TGA 2950 from TA Instruments in a nitrogen atmosphere at a flow rate of 100 ml/min. A heating rate of 10°C/min was used to heat the sample from room temperature to 400 °C. Specimens weighing 5 mg were used.

Differential Scanning Calorimetry

DSC thermograms were obtained using a Perkin-Elmer DSC 7 at a heating rate of 10 °C/ min in a nitrogen atmosphere. In order to study the effect of moisture on the calorimetric properties, three samples, BF 8483-133, BF 8483-173, and BF 8483-123, were selected as representatives of pure gelatin, gelatin-PEA, and gelatin-PEMA systems. Films were brought to equilibrium in different conditioning environments (15, 30, 50, 65, 70, 80 %RH) for a day prior to performing the DSC experiments. However, in order to study other variables, such as latex concentration, drying condition, etc., all the samples were prepared in a conditioning environment of 70 °F and 50 %RH only.

In each case, sample sizes with an average weight of 10 mg encapsulated in a hermetically sealed aluminum pan were prepared for each condition. Each sample was analyzed twice. The same temperature history was applied to all samples: first heating from 0 °C to 110 °C at 10 °C/min, followed by quenching the sample using liquid nitrogen to 0 °C, and finally heating to 110 °C at a 10 °C/min rate. The melting temperature was taken as the maximum of the endothermic peak from the first heating, while the glass transition temperature was taken as the midpoint of the heat capacity jump from the second heating, i.e., the glass transition temperature was estimated using a half-width method.

Crystallinity Determination

The degree of crystallinity of the gelatin was calculated using the following formula:

$$\chi_c = \frac{\Delta H_{sc}}{\Delta H_c} \times 100 \qquad (4.1)$$

where, ΔH_{sc} = heat of fusion for the semi - crystalline polymer (cal / g)
ΔH_c = heat of fusion for completely crystalline polymer (cal / g)

The degree of crystallinity was estimated using two different values for the heat of fusion for the fully crystalline polymer. The first calculation was based on the ΔH_c of collagen, which is 24 cal/g.[13] This is valid because gelatin is a random coil polymer derived from collagen. The second method was calculated by using the heat of fusion of completely crystalline gelatin. In general, the heat of fusion of crystalline polymers can be obtained from the depression of their melting point by a diluent. Jolley measured the depression of the melting point of cold dried gelatin caused by water and found that the heat of fusion of completely crystalline gelatin is 17 cal/g.[10] In this work, both ΔH_c of collagen and fully crystalline gelatin were adopted to determine two measures of the degree of crystallinity of gelatin.

Results and Discussion

Thermogravimetric Analysis

Figure 4.1 represents a typical TGA experiment for gelatin film. Gelatin shows an initial weight loss at 100 °C as a result of water loss. The amount of water loss is dependent upon the initial moisture content of the sample. As can be seen from Figure 4.1, the water loss for the gelatin film dried at the HMERH condition is greater when compared with the gelatin film dried at the LMERH condition. This is because the film dried at the HMERH condition has a greater initial moisture content and also has a greater moisture uptake, as described earlier. With a further rise in temperature from 100 °C to 400 °C, both gelatin films exhibit no substantial changes in weight and are stable to 270 °C. Thermal degradation of the gelatin begins near 275 °C, with the weight decreasing rapidly to 400 °C. The temperature at the onset of the degradation and the percentage weight loss at different temperatures are summarized in Table 4.1.

Differential Scanning Calorimetry and Degree of Crystallinity

Effect of Moisture on Transition Temperatures. The DSC thermograms for pure gelatin film equilibrated at 15 %RH are illustrated in Figure 4.2. This is a typical DSC scan for the gelatin film. The first heating profile exhibits two endothermic peaks. A

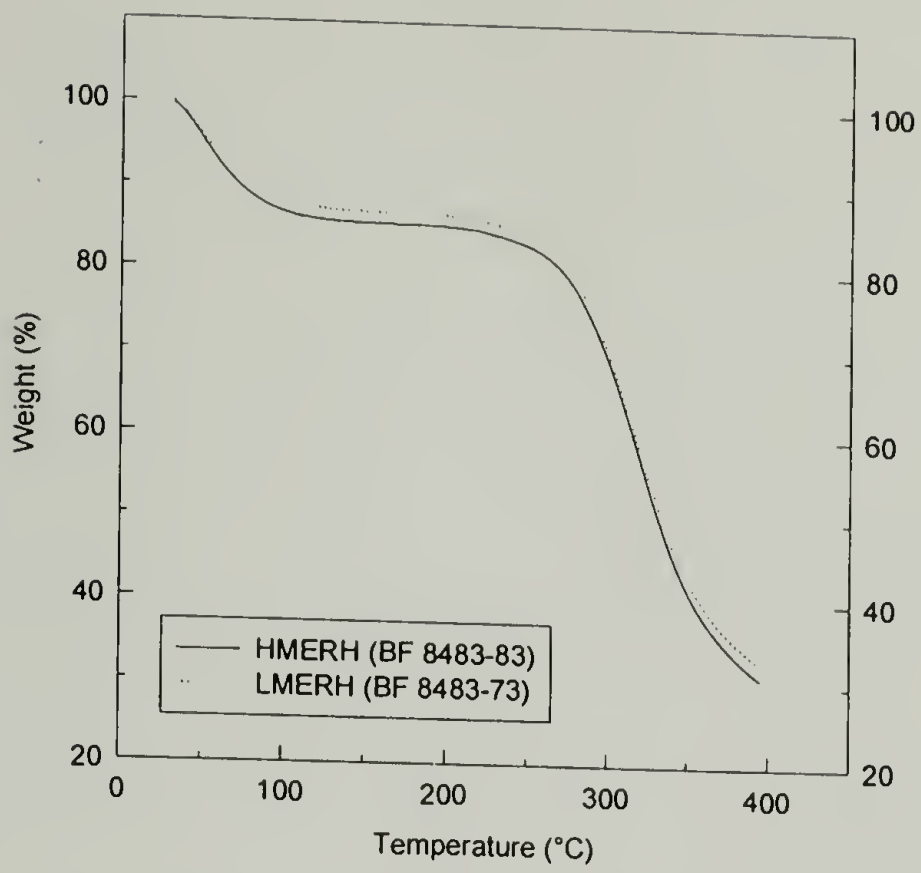

Figure 4.1 : Weight loss as a function of temperature for pure gelatin film measured by a thermogravimetric analyzer.

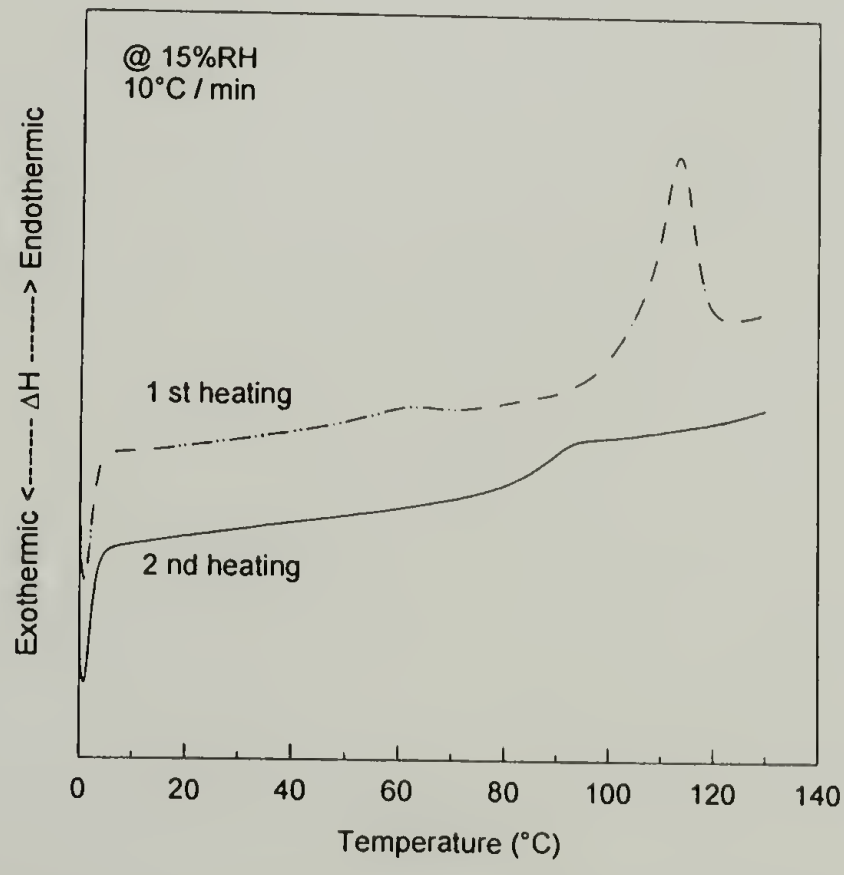

Figure 4.2 : DSC thermograms for pure gelatin film (BF 8483-133) equilibrated at 15 %RH.

Table 4.1 : Onset of Degradation Temperature and Percent Weight Loss at Three Different Temperatures for Pure Gelatin and Gelatin-Latex Films

ID	Latex Type	Latex Size (μm)	Latex Conc (parts)	Gel Conc (%)	Drying Condition	Td (°C) (onset)	Percent Weight Loss		
							100 °C	150 °C	300 °C
8483-13	-	-	-	10	HMERH	273.6	11.9	12.9	29.3
8483-23	-	-	-	10	LMERH	275.2	11.6	13.0	28.7
8483-173	PEA	0.051	20	10	HMERH	274.7	10.4	11.1	24.9
8483-183	PEA	0.051	20	10	LMERH	273.5	9.7	10.4	23.9
8483-43	PEA	0.112	20	10	HMERH	275.1	11.3	12.3	25.6
8483-33	PEA	0.112	20	10	LMERH	274.3	11.9	13.0	28.0
8483-123	PEMA	0.067	20	10	HMERH	276.1	11.6	12.7	25.2
8483-113	PEMA	0.067	20	10	LMERH	275.2	9.9	10.8	25.1
8483-163	PEMA	0.15	20	10	HMERH	275.6	11.0	11.8	25.0
8483-153	PEMA	0.15	20	10	LMERH	275.7	10.9	11.9	27.3
8483-83	-	-	-	15	HMERH	275.0	13.3	14.4	30.7
8483-73	-	-	-	15	LMERH	273.7	11.9	13.1	29.6
8505-482	PEA	0.051	20	15	HMERH	273.3	10.1	10.9	25.6
8505-472	PEA	0.051	20	15	LMERH	273.1	10.0	10.9	25.8
8505-362	PEA	0.112	20	15	HMERH	274.1	12.9	14.0	30.3
8505-352	PEA	0.112	20	15	LMERH	274.0	11.7	12.7	29.4
8483-93	PEMA	0.067	20	15	HMERH	275.3	10.9	11.8	25.5
8483-103	PEMA	0.067	20	15	LMERH	274.4	10.7	11.6	29.4
8483-213	PEMA	0.15	20	15	HMERH	276.0	11.4	12.2	25.9
8483-223	PEMA	0.15	20	15	LMERH	273.8	8.4	9.1	23.4
8505-372	PEA	0.112	40	10	HMERH	277.4	10.9	11.7	23.0
8505-382	PEA	0.112	40	10	LMERH	275.9	9.9	10.6	23.5
8483-63	PEA	0.051	40	15	LMERH	274.5	8.0	8.5	22.2
8505-402	PEMA	0.067	40	10	HMERH	276.9	9.8	10.5	23.6
8505-392	PEMA	0.067	40	10	LMERH	276.6	8.4	9.0	22.5
8505-412	PEMA	0.15	40	10	HMERH	274.8	9.2	9.8	22.9
8505-422	PEMA	0.15	40	10	LMERH	275.2	9.1	9.8	22.7
8505-292	PEA	0.051	40	15	HMERH	274.6	8.9	9.6	21.5
8505-302	PEA	0.051	40	15	LMERH	273.2	8.5	9.1	22.7
8505-442	PEA	0.112	40	15	HMERH	274.4	10.8	11.5	23.9
8505-432	PEA	0.112	40	15	LMERH	273.5	8.2	8.8	22.7
8505-282	PEMA	0.067	40	15	HMERH	275.9	10.3	11.2	23.8
8505-272	PEMA	0.067	40	15	LMERH	275.6	8.9	9.6	22.7
8505-242	PEMA	0.15	40	15	HMERH	276.2	8.3	9.1	21.4
8505-232	PEMA	0.15	40	15	LMERH	274.8	8.1	8.8	21.5

small, broad endothermic peak near 60 °C corresponds to the aging enthalpy relaxation.[18] At higher temperatures, a relatively sharp melting endothermic peak (Tm) or a helix-to-coil transition is observed. It is well known that the area enclosed under this melting endothermic peak, (called the heat of fusion), can be used to calculate the degree of crystallinity. Therefore, by knowing the heat of fusion of fully crystalline gelatin, the degree of crystallinity can be determined. Since the crystalline gelatin structure does not reform during the cooling cycle, the structureless amorphous film only exhibits a well-defined glass transition on the second heating.

The effect of relative humidity on the thermal transition temperatures of pure gelatin and gelatin-latex films are shown in Figure 4.3 and 4.4. It is very clear that both types of transitions, Tm and Tg, are very sensitive to moisture; both shift to lower temperatures with increasing moisture content.

The effect of relative humidity and moisture uptake on the transition temperatures for pure gelatin is shown in Figure 4.5. Obviously, as relative humidity increases, the gelatin film absorbs more and more moisture, resulting in a decrease of the transition temperatures. This lowering of Tg indicates the plasticizing effect of moisture on gelatin film. However, it has to be noted that Tg is more sensitive to moisture than Tm. Tg varies between 27 °C and 87 °C while Tm varies between 71 °C and 113 °C for the range of relative humidity (15 %RH - 80 %RH). This again clearly demonstrates that the depression in Tg is actually a result of the plasticizing effect of water.

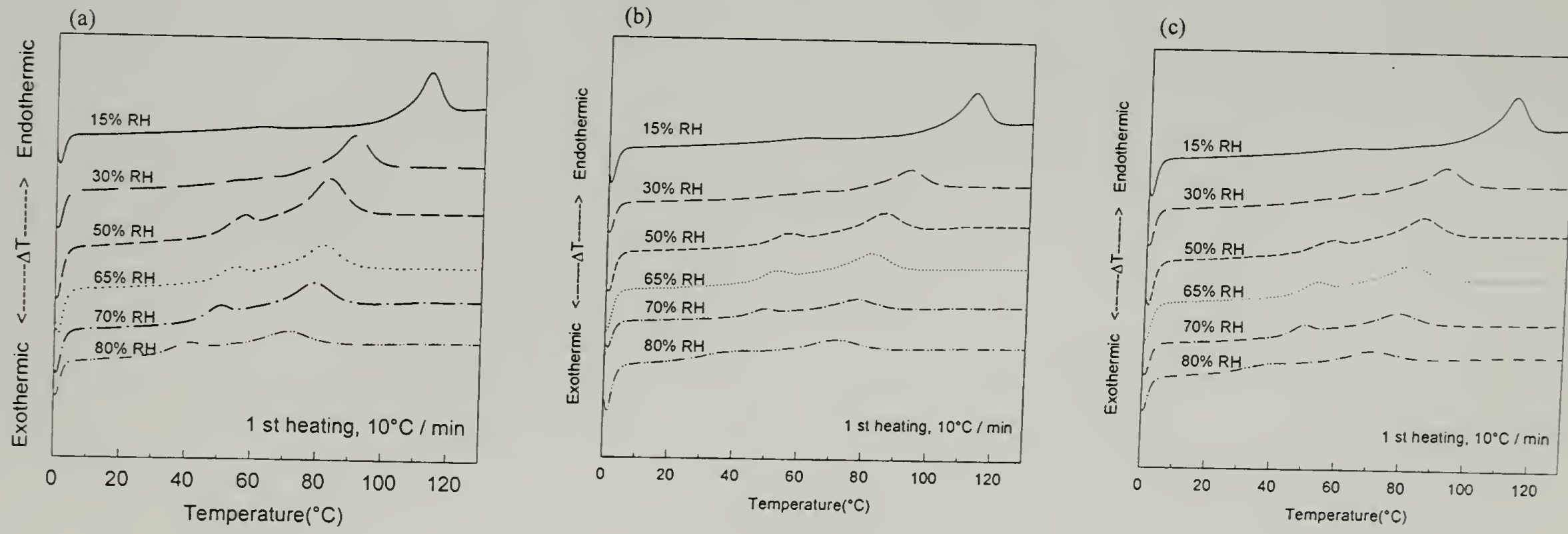

Figure 4.3 : Effect of relative humidity on the melting temperatures of gelatin films : (a) pure gelatin(BF 8483-133), (b) gelatin-20 parts PEA(BF 8483-173), and (c) gelatin-20 parts PEMA(BF 8483-123).

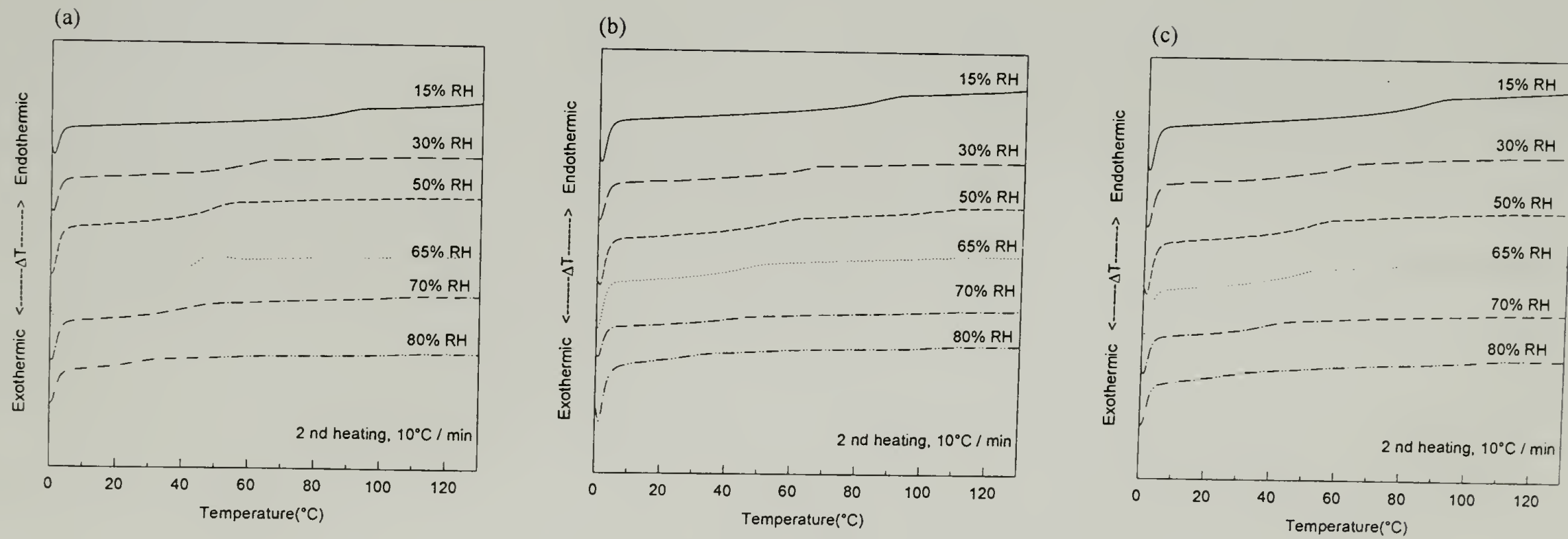

Figure 4.4 : Effect of relative humidity on the glass transition temperatures of gelatin films : (a) pure gelatin(BF 8483-133), (b) gelatin-20 parts PEA(BF 8483-173), and (c) gelatin-20 parts PEMA(BF 8483-123).

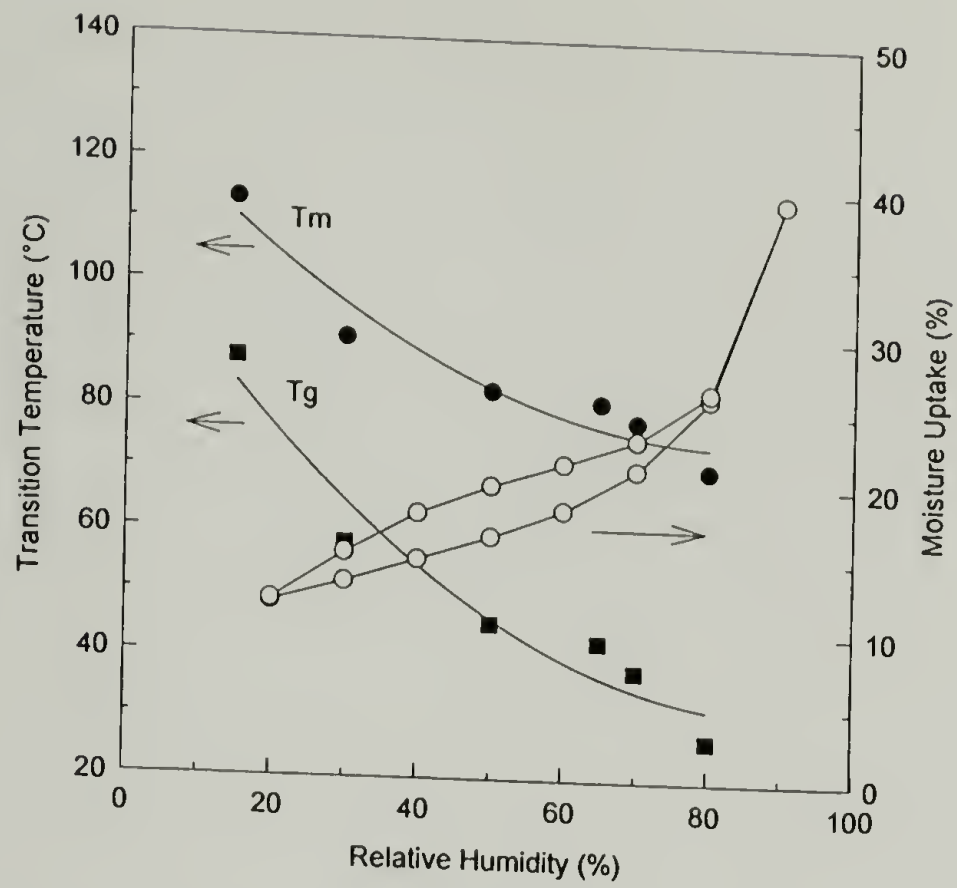

Figure 4.5 : Thermal transition temperatures and moisture sorption hysteresis of pure gelatin film(BF 8483-133) as a function of relative humidity.

The decrease in both transition temperatures as a function of moisture is also true for the gelatin-latex systems as displayed in Figure 4.6. Table 4.2 summarizes the glass transition temperature, melting temperature, heat of fusion ,and degree of crystallinity of pure gelatin and gelatin-latex films at various relative humidities.

Although both Tm and Tg respond to the moisture in a similar fashion, the decrease in Tm with the increase in moisture content can not be described as a plasticizing effect. Many researchers have studied the decrease in transition temperatures, especially the Tg as a function of moisture, for a variety of water-compatible natural polymers. Fakirov et al. [17] proposed that the decrease in Tm with the increase in moisture can be explained by the influence of crystallization temperature on Tm.

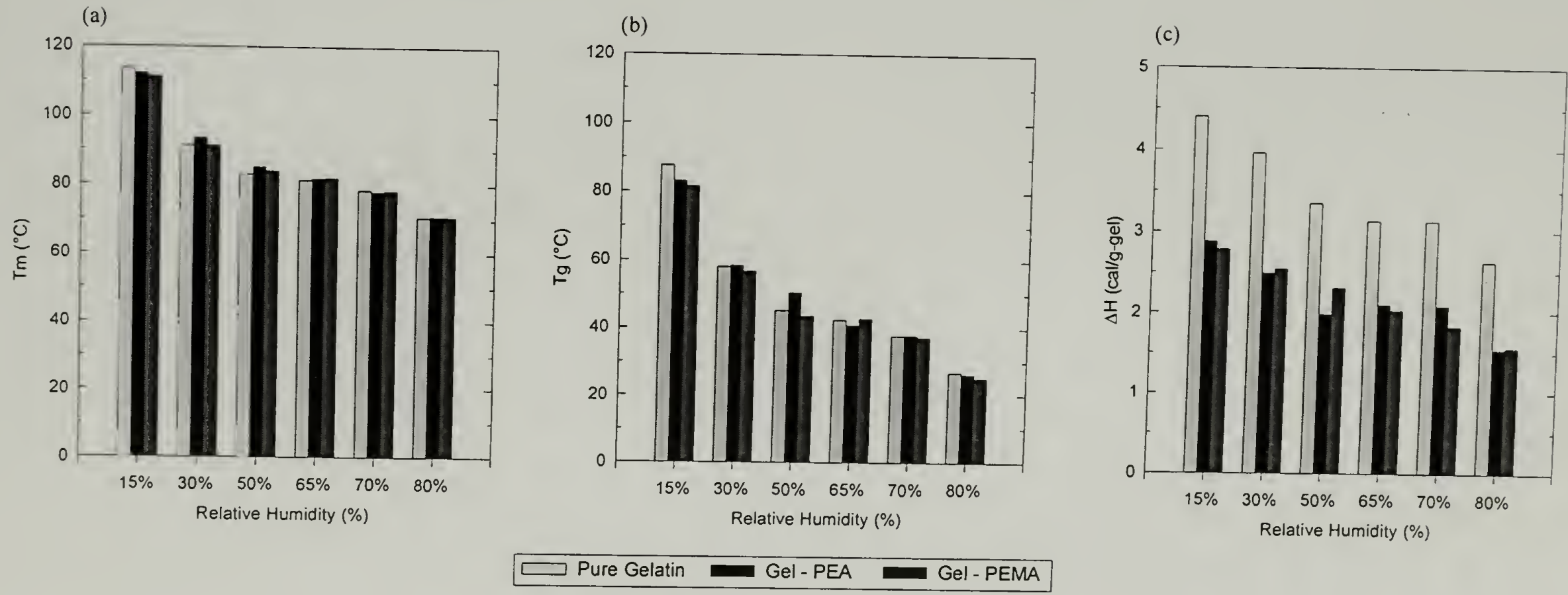

Figure 4.6 : Effect of relative humidity on the thermal properties of pure gelatin(BF 8483-133), gelatin-20 parts PEA (BF 8483-173), and gelatin-20 parts PEMA(BF 8483-123) films.

Table 4.2 : Thermal Properties and Degree of Crystallinity for Pure Gelatin and Gelatin-Latex Films at Various Relative Humidities

ID	sample	%RH	Tm(°C)	Tg(°C)	ΔH		Degree of Crystallinity (%)			
							(1) ΔHc = 24 cal/g		(2) ΔHc = 17 cal/g	
					cal/g(total)	cal/g(gel)	/total	/gel	/total	/gel
8483-133	control 10% gel HMERH	15 30 50 65 70 80	113.5 91.2 83.0 81.4 78.4 70.7	87.7 57.9 45.2 42.5 37.9 26.9	4.4 4.0 3.4 3.1 3.1 2.6	4.4 4.0 3.4 3.1 3.1 2.6	18.3 16.5 14.0 13.1 13.1 11.0	18.3 16.5 14.0 13.1 13.1 11.0	25.9 23.3 19.7 18.4 18.4 15.5	25.9 23.3 19.7 18.4 18.4 15.5
8483-173	PEA 20 parts 0.051 μm 10%gel HMERH	15 30 50 65 70 80	112.1 93.4 85.2 81.8 78.0 70.9	83.1 58.5 50.4 41.0 38.0 26.3	3.5 3.0 2.4 2.5 2.5 1.9	2.9 2.5 2.0 2.1 2.1 1.6	14.5 12.5 9.9 10.5 10.5 7.8	12.0 10.4 8.3 8.8 8.7 6.5	20.4 17.6 14.0 14.9 14.8 11.0	16.9 14.7 11.7 12.4 12.3 9.1
8483-123	PEMA 20 parts 0.067 μm 10%gel HMERH	15 30 50 65 70 80	111.1 91.1 84.0 81.9 78.3 70.8	81.5 56.7 43.7 42.9 37.4 25.2	3.4 3.1 2.8 2.4 2.2 1.9	2.8 2.5 2.3 2.0 1.8 1.6	14.0 12.7 11.6 10.2 9.2 7.9	11.6 10.6 9.6 8.5 7.6 6.5	19.7 18.0 16.4 14.4 13.0 11.1	16.4 14.9 13.6 11.9 10.8 9.2

It is generally accepted that the lower the crystallization temperature Tc, the larger the undercooling temperature ($\Delta T = Tm - Tc$), resulting in less perfect crystals. Since Tg is greatly lowered by moisture, permitting crystallization to occur at a temperature far below Tm, rather small and imperfect crystals should be expected. This results in a lowering of Tm with an increase in moisture content. Figure 4.6 (C) illustrates the decrease in the heat of fusion for both pure gelatin and gelatin-latex films with increasing relative humidity. An interesting result is that the heat of fusion of the gelatin-latex films is much less than that of the pure gelatin film. The latex particles could interfere with the cyrstallization of the gelatin and will be discussed in the next section.

A classical thermodynamic theory that predicts the effect of diluents on the glass transition temperature in polymer/diluent systems was applied to describe the plasticizing effect of moisture on the gelatin film. There are several theories that predict the compositional dependence of the glass transition temperature of binary and ternary mixtures.[19-21] In most cases, these expressions arise from the underlying principles that assume additivity of both entropy and volume. An analysis of the experiments using the widely accepted theory developed by Couchman and Karasz has produced the best results.[22,23] In this model, they relate the glass transition temperature of a homogeneous blend of several compositions to their weight fractions and thermodynamic characteristics of the pure components as expressed in equation (4.2).

$$\ln Tg = \frac{\Sigma W_i \Delta Cp_i \ln Tg_i}{\Sigma W_i \Delta Cp_i} \qquad (4.2)$$

where T_g is the glass transition of the system, w_i is the weight fraction of component i, Tg_i is the glass transition of the pure compound i, and ΔCp_i is the incremental change in specific heat at Tg_i of the pure compound i. For a binary system, if the ratio Tg_1 / Tg_2 is close to unity, which means the two glass transition temperatures do not differ greatly, then the above equation can be approximated as :

$$Tg = \frac{\Sigma W_i \Delta Cp_i Tg_i}{\Sigma W_i \Delta Cp_i} \qquad (4.3)$$

The experiments were analyzed using both equations. The glass transition temperature and incremental change in specific heat for each component are taken from the literature (gelatin : Tg = 493 K [14] and ΔCp = 0.50 J/gK [16]; water : Tg = 136 K [24] and ΔCp = 1.94 J/gK [25]).

A comparison of the experimental Tg behavior of gelatin with that predicted from the Couchman and Karasz equations is presented in Figure 4.7. The data shows fair agreement to the theoretical predictions of equation (4.2). As expected, equation (4.3) does not predict the experimental data well due to the large differences between the Tg of gelatin and water. However, as the weight fraction of moisture increases, the decrease in the predicted values is greater than those obtained from experimental data. This depression of Tg as a function of the moisture content of gelatin is consistent with the result observed by Pinhas et al.[16] In their work, the experimental Tg followed the theoretical values up to 25 % water and after that the Tg remains almost constant.

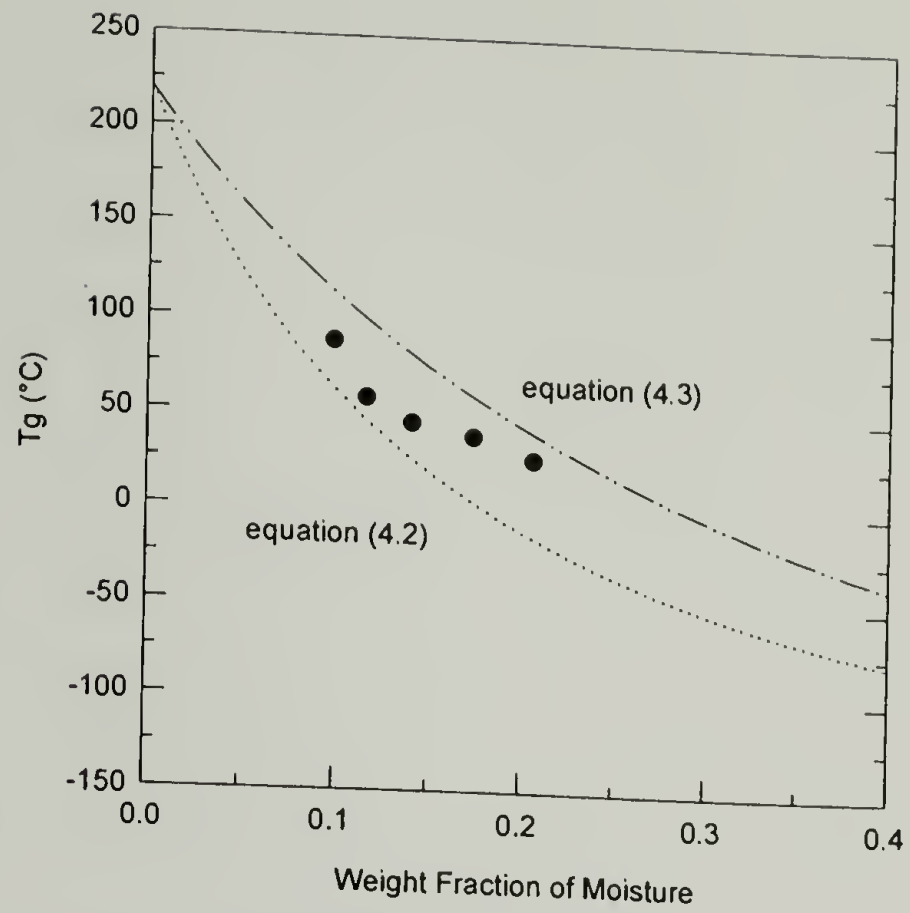

Figure 4.7 : Effect of moisture absorption on the glass transition temperature of gelatin film compared with theoretical prediction.

Latex Concentration vs. Thermal Properties. The effect of latex concentration on the melting temperature, glass transition temperature, and heat of fusion of both pure gelatin and gelatin-latex systems are presented in Figures 4.8 (a) through (c), respectively. As shown in Figure 4.8 (a) and (b), at 50% relative humidity, there is no difference in the Tm or Tg between the pure gelatin and the gelatin-latex films. The Tg of each system remains close to the Tg of pure gelatin, regardless of the latex concentration used, suggesting that phase separation occurs. Neither gelatin-PEA nor gelatin-PEMA systems can be classified as miscible. The DSC spectra, as displayed in Figure 4.9, show only one Tg, which might make the systems look homogeneous, but no temperature shift is observed with changing composition. In fact, the only thermal transitions shown by the blends are those typical of the pure gelatin, which shift to lower

temperature as a function of moisture as displayed in Figure 4.3 and 4.4. It is therefore concluded that the binary blends investigated are heterogeneous systems. The reason no transitions associated with the latices could be detected by DSC is likely because of the inability of the instrument to detect the relatively small heats associated with the small amount of the latex present.

In both latex systems, the heat of fusion of gelatin decreases as the latex concentration increases as shown in Figure 4.9 (c). There is no difference between the two latex systems. As can be seen, the heat of fusion of pure gelatin is approximately 4 cal/g , while that of the 20 parts and 40 parts gelatin-latex systems reduces to 2.5 and 1.5 cal/g-gel, respectively. The added latex appears to act as an impurity, interfering with the crystallite formation of gelatin by interacting with the gelatin in such a way as to block an interchain hydrogen bonding, i.e., at the peptide bonds of gelatin molecules. A small amount of interference will lead to a weaker gel while a larger amount may completely prevent crystallite formation. This result is somewhat similar to those reported by Veis.[26] In his work, he studied the effect of copper salts and other compounds such as urea, calcium chloride, and potassium thiocyanate on gel formation and found that they greatly suppressed gelation. It can be concluded that substances that compete for the hydrogen bonding sites on the gelatin molecule will interfere with the crystallite formation resulting in the suppression of gelation, or more precisely, decrease the degree of crystallinity.

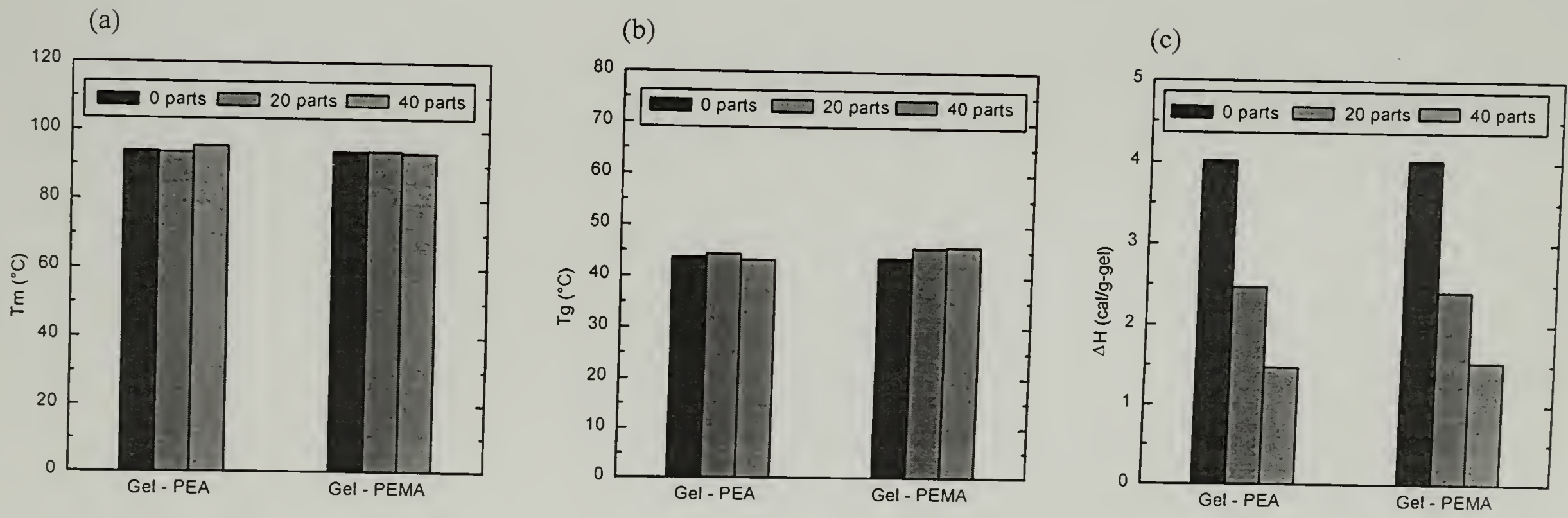

Figure 4.8 : Effect of latex concentration on the thermal properties of gelatin films conditioned at 50% RH.

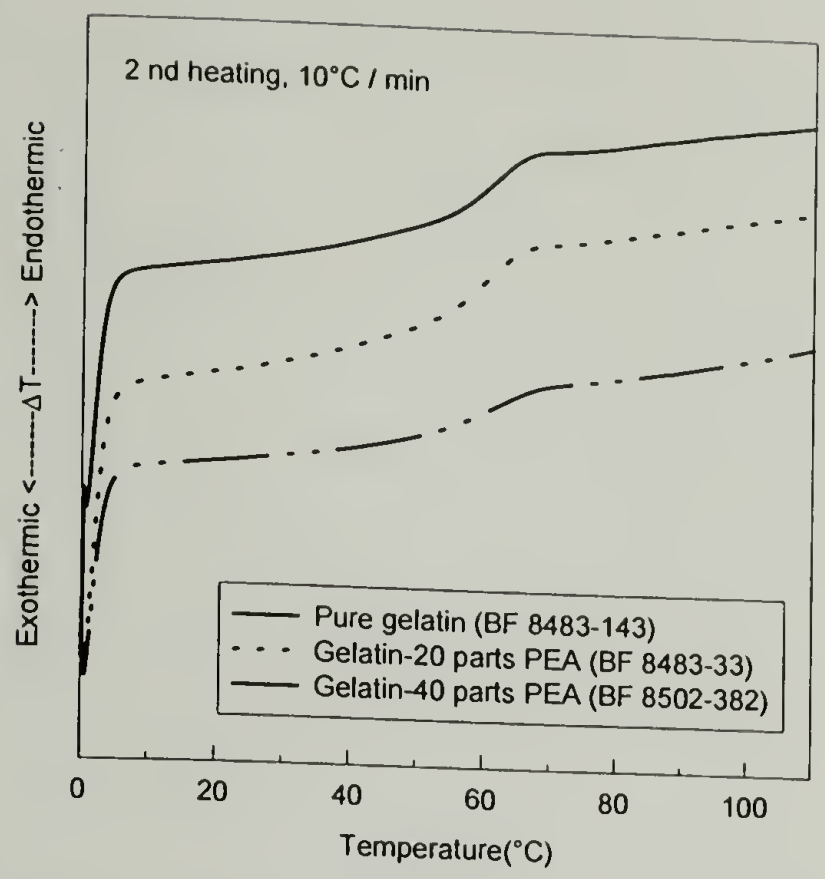

Figure 4.9 : Effect of latex concentration on the glass transition temperature for gelatin films conditioned at 50% RH.

Latex Particle Size vs. Thermal Properties. Figures 4.10 (a) through (c) present the effect of latex particle size on the melting temperature, glass transition temperature, and heat of fusion of the gelatin-latex films, respectively. As can be seen, both latex systems show that the latex particle size has no effect on the thermal properties; Tm, Tg, and ΔH remain constant regardless of the particle size of polymer latex.

Gelatin Concentration at Set Point vs. Thermal Properties. Gelatin concentration at set point has no effect on the melting temperature of both pure gelatin and gelatin-latex film as shown in Figure 4.11 (a). However, it has an effect on both glass transition temperature and heat of fusion of the films as presented in Figure 4.11 (b) and (c),

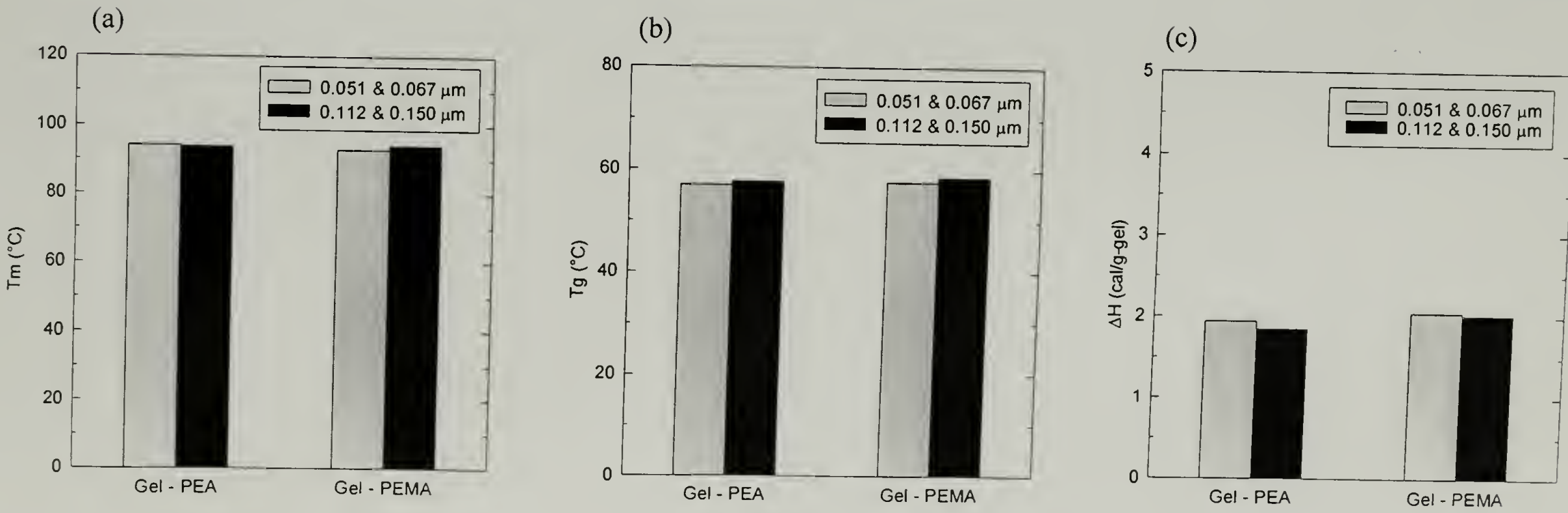

Figure 4.10 : Effect of latex particle size on the thermal properties of gelatin-20 parts latex films conditioned at 50% RH.

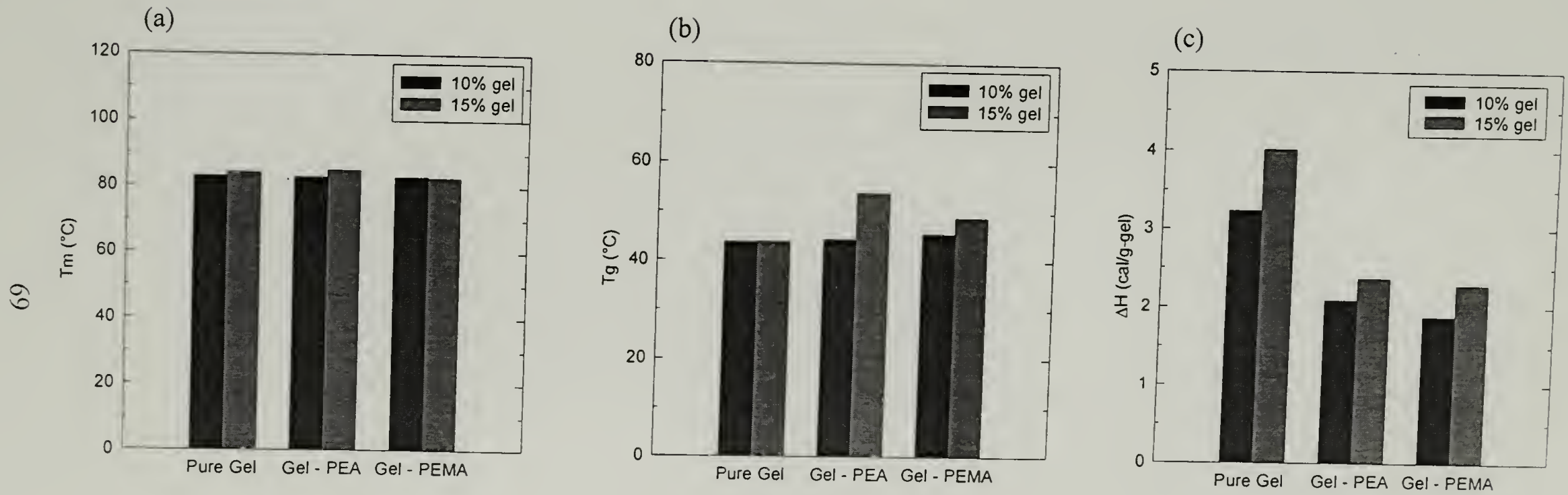

Figure 4.11 : Effect of gelatin concentration at set point on the thermal properties of pure gelatin and gelatin-20 parts latex films conditioned at 50% RH.

respectively. In both latex systems, the films containing 10 % gelatin show lower glass transition temperatures. This result correlates well with the moisture absorption behavior as shown in Figure 3.9 (chapter 3). The films with 10 % gelatin concentration can absorb more moisture than the films with 15 % gelatin concentration; therefore, their glass transition temperatures are lower than that of the films with 15 % gelatin concentration due to the plasticizing effect of water as described earlier. Similarly, the heat of fusion of the films with 15 % gelatin are higher than that of the films with 10 % gelatin concentration. This observation can be explained in term of their gel structure. The films with 15 % gelatin concentration have more gel structure and a higher degree of crystallinity; as a result, they require more energy to melt or change their structures.

Drying Condition at Vitrification vs. Thermal Properties. It has long been known that the molecular structure, physical properties, and photographic properties of dried gelatin coatings are complex and dependent upon the drying conditions. There are many problems that can occur as a result of the drying process. For example, high internal stress in the coating causes curl and cracking. Other defects such as mottle or blush can result from air contact during the drying process. In general, the dry gelatin film must be transparent, colorless, flexible, abrasion resistant, a latent-image stabilizer, and be capable of being swollen by water in order to permit aqueous processing.[27]

Generally, the drying temperature greatly affects the dried film properties and hence, product performance. In aqueous solutions the gelatin molecules exist as single chains surrounded by water molecules, which is referred to as a random coil configuration. Upon drying, gelation may be initiated by rapid chilling, followed by

gradual drying in controlled stages to about 10 % moisture content. The resulting film will have a microstructure and properties dependent upon the drying temperature and relative humidity. Jolley has divided the dried film into two extreme cases : "hot-dried" film and "cold-dried" film.[10] Hot-dried film is obtained when the film is dried at 50 °C (122 F), while cold-dried film is obtained at 10 °C (50 F). From his x-ray diffraction work, it can be concluded that the hot-dried films consist of an amorphous structure of randomly arranged single gelatin molecules. In contrast, the cold-dried films show evidence of a high degree of order and thus a crystalline structure of single gelatin chains tied together by triple-stranded crystallites.

Photographic emulsions are very complex systems that include not only gelatin but silver halides and other additives as well. Therefore, it is important to consider how the added materials can affect the structure of the composite film, especially in terms of the drying conditions. Figure 4.12 (a) through (c) shows the effect of drying conditions on the calorimetric properties of both pure gelatin and gelatin-latex films. Even though the drying temperatures studied were not the same as those "hot" and "cold" drying conditions described by Jolley, they were conditions recommended by Kodak for these studies. These conditions are known to alter the properties of these materials and they are practical conditions that can be used in the production of photographic materials.

As displayed in Figure 4.12 (a), the melting temperatures of the films dried at the HMERH condition (80 F / 29 %RH) are lower than that of the films dried at the LMERH condition (130 F / 5.5 %RH). This result can be explained by differences in crystallization. Crystallization is a process which takes place between Tg and Tm in two distinct steps, nucleation and growth. Upon cooling a polymer melt, crystallization

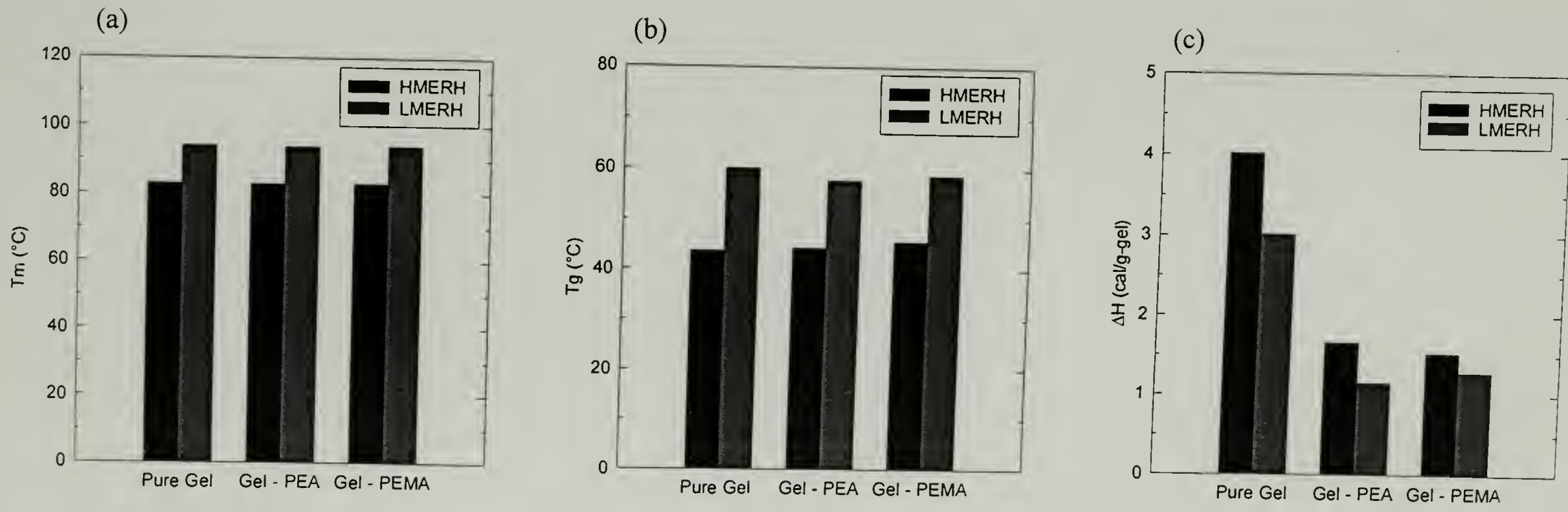

Figure 4.12 : Effect of drying condition on the thermal properties of pure gelatin and gelatin-40 parts latex films conditioned at 50% RH.

slowly begins at the melting point. The random coil molecules become aligned and form small ordered regions randomly throughout the melt. In the case of gelatin, nucleation occurs via the formation of triple-stranded crystallites and is believed to involve regions containing the pyrrolidine-rich amino acid triplets Gly-Pro-Pro or Gly-Pro-Hyp.[27] This nucleation process increases as the temperature is lowered because there is a greater tendency to have the chain segments in their lower energy crystalline configuration. In contrast, the second step, which is the growth of crystal nuclei, requires motion of the chain segments at the growing nuclei surface, thus this step is favored by higher temperatures. The number, size, perfection, and morphology of nuclei formed depends upon the crystallization temperature. At undercooling only a few degrees below the melting temperature, a small number of large and perfect crystals are formed because of the preponderance of growth over nucleation. Conversely, when the undercooling is increased, a large number of small and less perfect crystals are obtained. The lower the crystallization temperature, the more crystalline the material becomes, but the crystals are smaller and less perfect. Since melting is the reverse of crystallization, the melting of cold dried gelatin film is due to the melting of the ordered triple-stranded crystallites to the disordered single-stranded or the random coil arrangement of the gelatin molecules.[10] The melting temperature of gelatin films formed at the LMERH condition (130F / 5.5 %RH) are higher than those formed at lower temperatures, the HMERH condition (80F / 29 %RH), owing to the greater stability of the more perfect crystallites. At the HMERH condition, gelatin films were dried at higher relative humidity than the films dried at the LMERH condition. As a result, the films have higher moisture content

and lower Tg as mentioned earlier. Again, the lower Tg causes the crystallization process to take place at a temperature far below Tm, resulting in small and imperfect crystallites.

Again, the plasticizing effect can be used to explain the glass transition temperature of the gelatin films dried at different conditions. Although the moisture uptake of the gelatin film dried at the HMERH condition (80 F / 29 %RH), as presented in Table 3.2 (chapter 3), is slightly higher than the film dried at the LMERH condition (130 F / 5.5 %RH), the glass transition temperatures of the films dried the at HMERH condition, as shown in Figure 4.12 (b), are much lower than those of the films dried at the LMERH condition. This is strong evidence to confirm the significant effect of moisture on the properties of the gelatin films, especially the glass transition temperature. Only a slight difference in the moisture content can cause a significant difference in the glass transition temperature.

Figure 4.12 (c) illustrates the heat of fusion of the gelatin films dried at two different conditions. Clearly, the films dried at the HMERH condition (80 F / 29 %RH) show a higher heat of fusion than the films dried at the LMERH condition (130 F / 5.5 %RH). The films dried at the HMERH condition have a greater amount of crystalline structure compared to the films dried at the LMERH condition. This result is consistent with the one reported by Jolley, although our drying temperatures are not exactly the same as he defined in his work. The films dried at the HMERH and the LMERH conditions can be considered, according to Jolley's definition, as cold-dried and hot-dried films, respectively.

In summary, at a constant relative humidity, the calorimetric properties of both gelatin-latex systems are the same in terms of the effect of latex particle size,

concentration of gelatin at set point, and drying condition at vitrification. Both latex systems show the same magnitude for all the calorimetric properties.

Conclusions

The thermal properties of pure gelatin and gelatin-latex films of various moisture content have been measured directly through the use of differential thermal techniques and hermetically sealed pans. The decrease in the melting temperature and the glass transition temperature with an increase in moisture content can be explained by the effect of crystallization temperature and the plasticizing effect of water, respectively. The classical thermodynamic theory of the Tg (i.e. the Couchman-Karasz equation) was adopted to describe the plasticizing effect of water on the films. The experimental results show fair agreement to the theoretical prediction.

An absence of any Tg shift with latex concentration in both latex systems demonstrates that the blend components are immisible. Latex particle size has no effect on the calorimetric properties. However, both the gelatin concentration at set point and the drying condition at vitrification have a significant influence on the thermal properties of the gelatin films. The greater amorphous structure in the film containing 10 % gelatin concentration enables the film to absorb more moisture and thus, show a lower Tg and heat of fusion. The glass transition temperature of the film dried at the LMERH condition (130 F / 5.5 %RH) is higher than that of the film dried at the HMERH condition (80 F / 29 %RH). This is due to the plasticizing effect of the moisture. The

film dried at the HMERH condition has a lower Tm and higher ΔH compared to the film dried at the LMERH condition and can be explained by crystallization theory. The lower the gelation temperature, the more crystalline it is, but the smaller and less perfect are its crystallites.

In summary, moisture plays an important role in determining the properties of gelatin film. The addition of a polymer latex can reduce the sensitivity of the emulsion layer to moisture. Other factors, such as the gelatin concentration or drying conditions, also affect the thermal properties of the gelatin film. It can be seen that the effect of the PEA and PEMA latices on the thermal properties of the gelatin-latex films is not different. Both latices have the same effect on the thermal properties; however, the effect of these two latices on the mechanical properties of the gelatin film is significantly different and will be presented in chapter 5.

References

1. Jones, F.R. In *Handbook of Polymer-Fibre Composites*; Jones, F.R., Ed.; Longman Scientific & Technical: Burnt Mill, Harlow, Essex, 1994; Chapter 6.3, pp. 371-375.

2. Moy, P. and Karasz, F.E. In *Water in Polymers*; Rowland, S.P., Ed.; American Chemical Society: Washington, D.C., 1980; Chapter 30, pp. 505-513.

3. Fuzek, J.F. In *Water in Polymers*; Rowland, S.P., Ed.; American Chemical Society: Washington, D.C., 1980; Chapter 31, pp. 515-530.

4. Pritchard, J.G. *Poly(vinyl alcohol)-Basic Properties and Uses*; Gordon and Breach Science Publishers: New York, 1970; pp. 60.

5. Scandola, M. and Pezzin, G. In *Water in Polymers*; Rowland, S.P., Ed.; American Chemical Society: Washington, D.C., 1980; Chapter 13, pp. 225-234.

6. Koleske, J.V. and Faucher, J.A., "Transitions in Gelatin and Vitrified Gelatin-Water Systems", *The Journal of Physical Chemistry*, **69**(11), 4040 (1965).

7. Yannas, I.V and Tobolsky, A.V., "Transitions in Gelatin-Nonaqueous-Diluent Systems", *Journal of Macromolecular Chemistry*, **1**(4), 723 (1966).

8. Yannas, I.V and Tobolsky, A.V., "High-Temperature Transformations of Gelatin", *European Polymer Journal*, **4**, 257 (1968).

9. Petrie, S.E.B. and Becker, R. In *Analytical Calorimetry*; Porter, R.S. and Johnson, J.F., Eds.; Plenum Press: New York, 1970; Vol. 2, pp.225-238.

10. Jolley, J.E., "The Microstructure of Photographic Gelatin Binders", *Photographic Science and Engineering*, **14**(3), 169 (1970).

11. Macsuga, D.D., "Thermal Transitions in Gelatin: Optical Rotation and Enthalpy Changes", *Biopolymers*, **11**, 2521 (1972).

12. Godard, P., Biebuyck, J.J., Daumerie, M., Naveau, H., and Mercier, J.P., "Crystallization and Melting of Aqueous Gelatin", *Journal of Polymer Science: Polymer Physics Edition*, **16**, 1817 (1978).

13. Vrtis, J.K., "Stress and Mass Transport in Polymer Coating and Films", Ph.D. Dissertation, University of Massachusetts, Amherst, MA (1995).

14. Marshall, A.S. and Petrie, S.E.B., "Thermal Transitions in Gelatin and Aqueous Gelatin Solutions", *Journal of Photographic Science*, **28**, 128 (1980).

15. Marshall, A.S. and Petrie, S.E.B., "Thermal Transitions and Physical Aging in Gelatin", *Proceedings of the Eleventh North American Thermal Analysis Society Conference*, **2**, 183 (1981).

16. Pinhas, M-F., Blanshard, J.M.V., Derbyshire, W., and Mitchell, J.R., "The Effect of Water on the Physicochemical and Mechanical Properties of Gelatin", *Journal of Thermal Analysis*, **47**, 1499 (1996).

17. Fakirov, S. et al., "Mechanical Properties and Transition Temperatures of Crosslinked Oriented Gelatin II Effect of Orientation and Water Content on Transition Temperatures", *Colloidal Polymer Science*, **275**, 307 (1997).

18. Ni, B.Y. and Faou, A.L., "Crystalline Structure and Moisture Effects on Deformation Mechanisms of Gelatin Films under Mode I Stress Field", *Mat. Res. Soc. Symp. Proc.*, **292**, 229 (1993).

19. Gordon, J.M., Rouse, G.B., and Risen, W.M., Jr., "The Compositional Dependence of Glass Transition Properties", *The Journal of Chemical Physics*, **66**(11), 4971 (1977).

20. Gordon, M. and Taylor, J.S., "Ideal Copolymers and the Second-Order Transitions of Synthetic Rubbers. I. Non Crystalline Copolymers", *Journal of Applied Chemistry*, **2**, 493 (1952).

21. Kelley, F.N. and Bueche, F., "Viscosity and Glass Temperature Relations for Polymer-Diluent Systems", *Journal of Polymer Science*, **50**, 549 (1961).

22. Couchman, P.R. and Karasz, F.E., "A Classical Thermodynamic Discussion of the Effect of Composition on Glass Transition Temperature", *Macromolecules*, **11**, 117 (1978).

23. Couchman, P.R., "Compositional Variation of Glass Transition Temperature. 2. Application of the Thermodynamic Theory to Compatible Polymer Blends", *Macromolecules*, **11**, 1156 (1978).

24. Johari, J.P., Hallbrucker, A., and Mayer, E., "The Glass-Liquid Transition of Hyper Quenched Water", *Nature*, **330**, 552 (1987).

25. Sugisaki, M., Suga, H., and Seki, S., "Calorimetric Study of the Glass State. IV. Heat Capacities of Glassy Water and Cubic Ice", *Bull. Chem. Soc. Jpn.*, **41**, 2591 (1968).

26. Veis, A. *The Macromolecular Chemistry of Gelatin*; Academic Press: New York, 1964; pp. 367-387.

27. Rose, P.I. In *Encyclopedia of Polymer Science and Engineering*; Mark, H.F., Bikales, N.M., Overberger, C.G., Menges, G., and Kroschwitz, J.I., Eds.; John Wiley & Sons: New York, 1978; Vol. 7, pp. 488-573.

CHAPTER 5

EFFECT OF MOISTURE ABSORPTION ON TENSILE PROPERTIES

Introduction

Owing to its high glass transition temperature, gelatin film behaves as a glassy material at room temperature resulting in high stiffness and low toughness. The idea of rubber toughening of glassy polymers was adopted in this research in an attempt to improve the physical, mechanical, and photographic properties of gelatin. As detailed in chapter 2, two types of polymer latices, poly(ethyl acrylate) and poly(ethyl methacrylate) were studied as additives to gelatin.

Similar to commercial engineering polymers, such as high impact polystyrene (HIPS) or acrylonitrile-butadiene-styrene (ABS), by adding latex polymers into the gelatin, the toughness of the system should be increased by a variety of mechanisms such as shear yielding or crazing. The optimum combination of stiffness and toughness is the most desirable requirement in all of materials.

The most common method of investigating mechanical properties is to carry out stress-strain, or more precisely load-extension, measurements using a tensile tester. Determination of the stress-strain behavior of a material is useful as it provides information concerning important mechanical properties such as Young's modulus, yield strength, and elongation. These are significant parameters which are vital in design considerations when the material is used in a practical situation.

Moisture serves as a plasticizer, so it can affect both physical and mechanical properties of gelatin film.[1-8] Thus, this chapter will focus on the effect of moisture on the tensile properties of pure gelatin and gelatin-latex films. Although it is well known that the tensile properties of gelatin film are greatly influenced by relative humidity, little is known about the gelatin-latex film. Therefore, the objective of this work is to further supplement the general understanding of the effect of moisture on the tensile properties of gelatin film, especially for the gelatin-latex film. The effects of latex concentration, latex particle size, drying conditions at vitrification, and gelatin concentration at the set point on the tensile properties of gelatin coatings were investigated as a function of relative humidity. Further, the experimental values of Young's moduli were compared with the predictions of models based on composite theory. Lastly, an optical microscope and a scanning electron microscope (SEM) were employed to investigate the deformation morphology of the fractured gelatin film surfaces.

Experimental

Tensile Testing

The tensile properties of gelatin and gelatin-latex films were determined as a function of relative humidity using a Sintech tensile tester (MTS System Corporation) with a strain rate of 50%/min and a cross head speed of 20 mm/min. A 1-5 pound range load cell was used to measure the force. The gelatin coatings were cut by a JDC precision sample cutter (Twing-Albert Instrument Company) and then carefully peeled

from the PET substrate at a take off angle of about 5°. All the samples were prepared in a conditioning room environment of 70 °F and 50 %RH. The tests, however, were performed in different conditioning rooms (15, 30, 50, 70, 80 %RH) at the Physical Performance Laboratory, Eastman Kodak Co., Rochester, NY. For each sample, five uniaxial specimens with dimensions of 15 mm wide, 150 mm long, and 10 μm thick were tested. The gauge length was 100 mm. Experimental values of Young's Modulus were compared with the predicted semi-empirical composite models.

Fracture Surfaces and Deformation Mechanisms

The fracture topography and deformation mechanism were studied by an optical microscope (Olympus BH-2) and a scanning electron microscope (JEOL JSM-35CF). For the SEM studies, the fracture surfaces were coated with a thin layer of gold using a Polaron Instruments sputter coater.

Results and Discussion

Tensile Properties

Effect of Moisture on Stress-Strain Relationship. The effect of moisture on the tensile properties of pure gelatin and gelatin-latex films are shown in Figure 5.1(a) through (c). It is very clear that the tensile properties are highly dependent on relative humidity. As the relative humidity increases, the gelatin film absorbs more and more

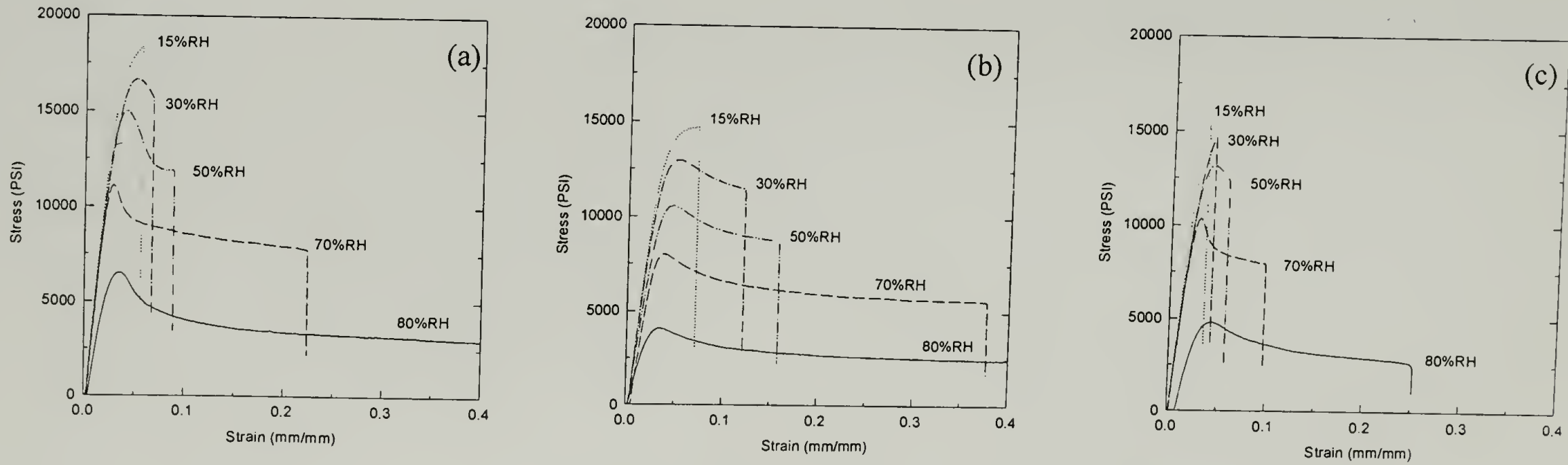

Figure 5.1 : Effect of relative humidity on the tensile properties of (a) pure gelatin (BF 8483-143), (b) gelatin-20 parts PEA (BF 8505-472), and (c) gelatin-20 parts PEMA (BF 8483-103) films.

moisture, resulting in a decrease of the tensile strength and tensile modulus. In contrast, the elongation at break increases with increasing relative humidity. These results indicate the plasticization effect of moisture on the gelatin film.

For both gelatin and gelatin-latex films at low relative humidity (15% RH), the films are brittle and show no plastic deformation. They fractured without showing much deviation from a linear stress-strain curve, immediately after or even before yielding. Their elongations at break are less than 20%. This is because at low relative humidity gelatin behaves as a glassy material owing to its high glass transition temperature.

At high relative humidity (80% RH), gelatin can absorb much more moisture than at low relative humidity. Water acts as plasticizer lowering the glass transition temperature by increasing free volume of the polymer. As a result, at room temperature and high humidity, gelatin films become soft and ductile. Their elongation at break is much greater than 20%. In some cases, for example, pure gelatin or gelatin-PEA films, their elongation at break is as high as 100%. The stress-strain curves of these films show that films have reached their yield points and further elongate until break. In other words, plastic deformation occurs. This is a general characteristic for most ductile polymers. Their stress-strain curves show a load drop immediately after reaching the maximum load, due to a combination of strain softening and localized necking.

The brittle to ductile transition of gelatin film is dependent upon the relative humidity. This transition of the pure gelatin and gelatin-PEA films occurs at 30% RH, whereas that of the gelatin-PEMA films is at 50% RH, due to the higher in Tg of the PEMA inclusions. Although a yield point is observed, most of the gelatin films form unstable necks which continues to thin-down until fracture occurs. However, at 70% and

80% RH, a few samples have the ability to form stable necks and undergo cold-drawing. The gelatin films show some stress-whitening when they are stretched to large extensions at 70% and 80% RH. The onset of stress-whitening followed yielding and neck formation. This observation of whitening upon stretching can be due to crazing of the glassy matrix (gelatin), cavitation or dewetting of the particles (PEA and PEMA). The details regarding the deformation mechanisms and fracture behavior of the gelatin films at 80% RH are confirmed by the optical micrographs and scanning electron micrographs (SEM) of the fracture surfaces.

Figure 5.2(a) through (d) present the effect of latex on the tensile properties of gelatin films at various relative humidities. It is apparent that, at each relative humidity, the tensile strength and Young's modulus of the gelatin-latex films are lower than those of the pure gelatin films, especially the films containing PEA as an additive. The PEA latex lowers the tensile strength and Young's modulus of the gelatin films more than the PEMA latex. However, the elongation to break of the gelatin-PEA films is much greater than that of the gelatin-PEMA films, in fact even greater than the elongation to break of the pure gelatin films. Clearly, the addition of the PEA latex increases the elongation to break and toughness of the gelatin emulsion layer, whereas the PEMA latex reduces both the elongation to break and toughness of the gelatin film. At 30% RH, for example, the gelatin-PEMA film is still brittle. Its stress-strain curve shows no yield point. Its elongation at break is less than 5%. These results can be explained in term of the glass transition temperature. Because the Tg of PEMA (65°C) is higher than that of PEA (-20°C), the films containing PEMA are stiffer and have lower elongation at break. Also, dewetting of the hard PEMA particles could trigger failure. In contrast to the gelatin-

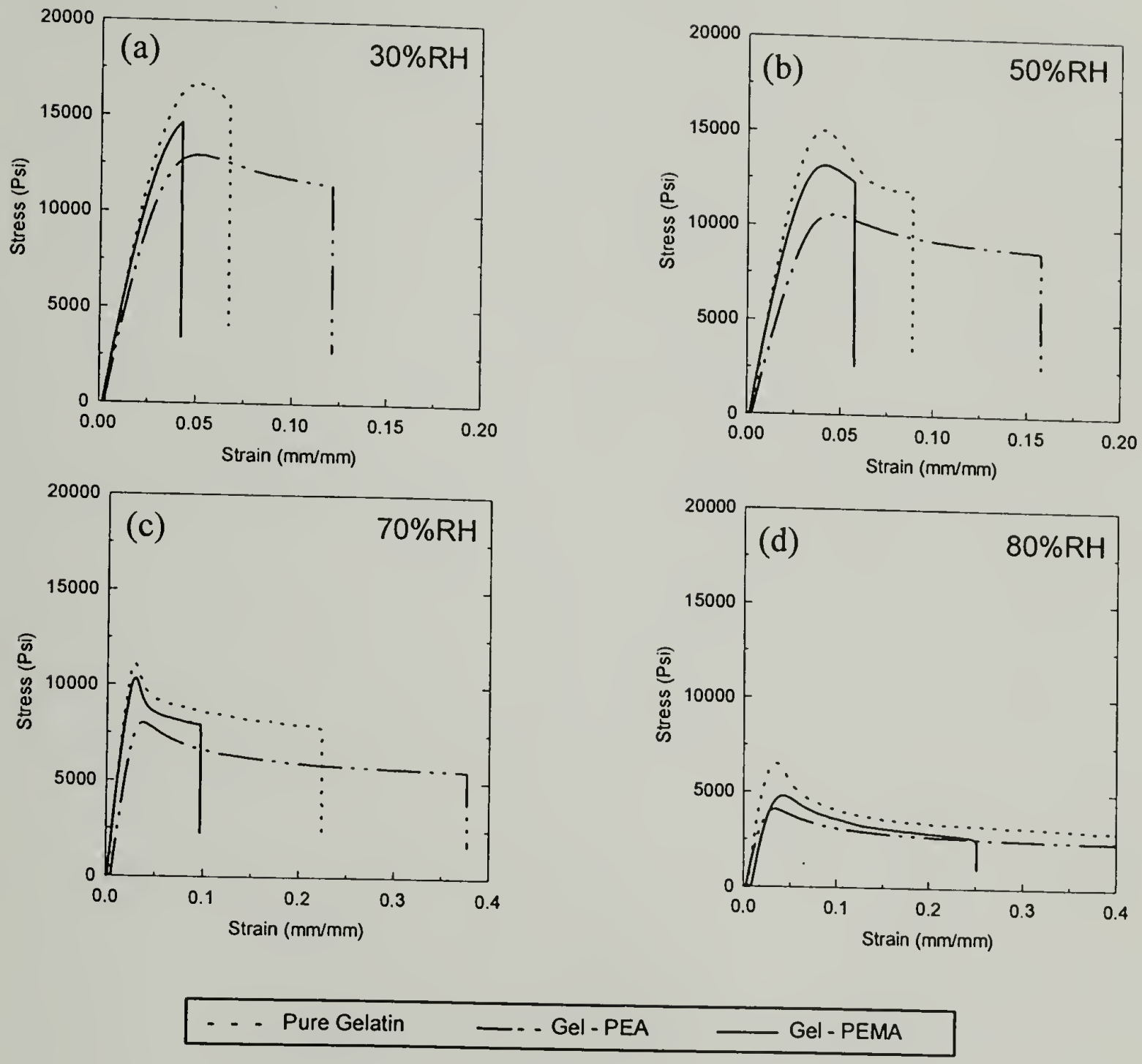

Figure 5.2: Effect of 20 parts latex on the tensile properties of gelatin films at (a) 30% RH, (b) 50% RH, (c) 70% RH, and (d) 80% RH.

PEA films, the low Tg latex helps decrease the tensile strength and modulus and increase the elongation at break and toughness of the gelatin coatings.

The increase in the toughness due to the presence of the PEA latex particles in the gelatin film can be explained by the concept of the rubber toughening of glassy polymers. The PEA latex particles typically have a Young's modulus about 3 orders of magnitude lower than that of glassy matrix, which is gelatin in this case. This leads to a stress concentration at the equators of the latex particles during mechanical deformation. The presence of the stress concentration can lead to crazing or shear yielding around latex particles and hence throughout the entire material. It is known that both crazing and shear yielding involve the absorption of energy [9]; thus, the gelatin matrix absorbs a large amount of energy during deformation and is toughened. In other words, the incorporation of a PEA particle into a gelatin film can lead to significant degrees of toughening by inducing high levels of crazing and/or shear yielding.

Latex Concentration vs. Tensile Modulus. The effect of latex concentration on the tensile modulus of the gelatin films is shown in Figure 5.3. All the films in this plot were dried at the LMERH condition (130F / 5.5% RH), and the concentration of gelatin at the set point is 15%. For the gelatin-latex films, the particle size of PEA and PEMA is 0.051 μm and 0.067 μm, respectively.

In both latex systems, the tensile modulus decreases with increasing latex concentration. The pure gelatin films have the highest tensile modulus, while the gelatin films with 40 parts PEA have the lowest tensile modulus. Experimental values of the Young's moduli compared with composites theories will be presented in the next section.

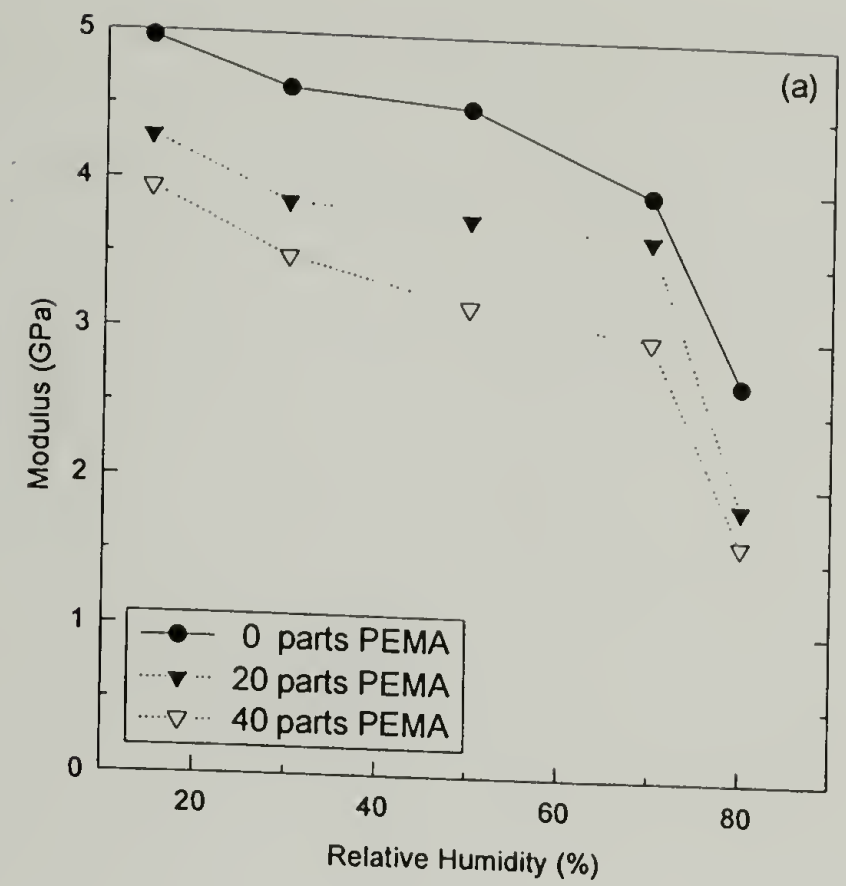

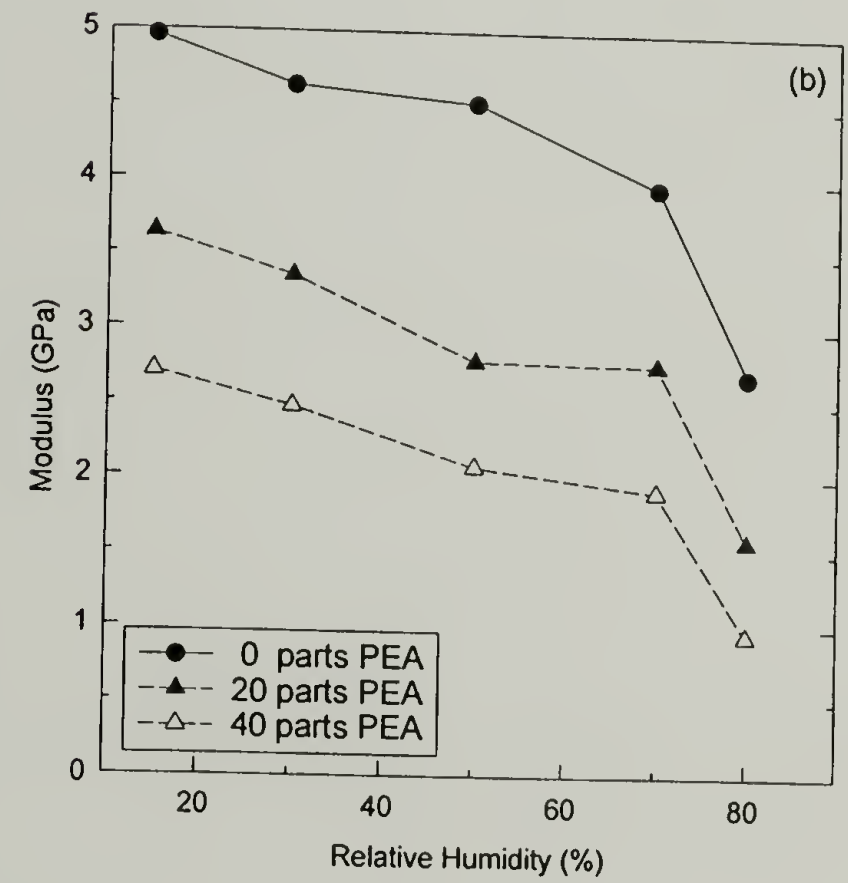

Figure 5.3 : Effect of latex concentration on the tensile modulus for (a) gelatin-PEMA and (b) gelatin-PEA films.

Latex Particle Size vs. Tensile Modulus. As shown in Figure 5.4, latex particle size does not affect the tensile modulus of the gelatin-latex films in the investigated diameter range. Again, the gelatin films with 20 parts latex and 15% gelatin concentration at the set point were dried at the HMERH condition (130F / 5.5% RH). In both gelatin-latex systems, the tensile moduli of the films with larger latex particle size (0.112 and 0.15μm) are approximately equal to those of the ones with smaller latex particle size (0.051 and 0.067 μm). This should be expected. The various composite theories have no modulus dependency on the particle size of the additive, only the volume fraction of each component is used to predict the modulus of the composite material.

Gelatin Concentration at Set Point vs. Tensile Modulus. Figures 5.5 presents the effect of gelatin concentration at the set point on the tensile modulus of the pure gelatin and gelatin-latex films. Here, the films were dried at the LMERH condition. The latex concentration of the gelatin-latex films is 40 parts, and the latex particle sizes of PEA and PEMA is 0.112 μm and 0.15 μm, respectively. As shown in each system, no difference is observed in the tensile modulus of the films for all relative humidities investigated. The tensile modulus of both the gelatin and gelatin-latex films is unaffected by the concentration of gelatin at the set point.

Drying Condition at Vitrification vs. Tensile Modulus. The effect of drying condition at vitrification on the tensile modulus of the pure gelatin and gelatin-latex films is shown in Figure 5.6. In this case, the gelatin concentration at the set point of the films

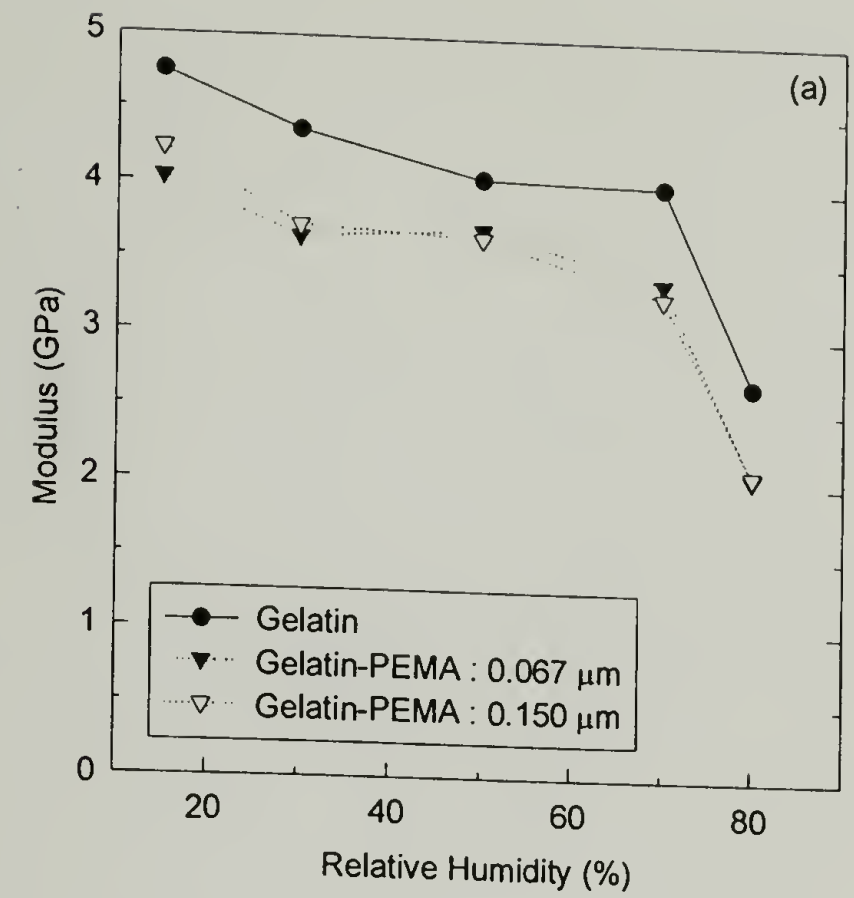

Figure 5.4 : Effect of latex particle size on the tensile modulus for (a) gelatin-PEMA and (b) gelatin-PEA films.

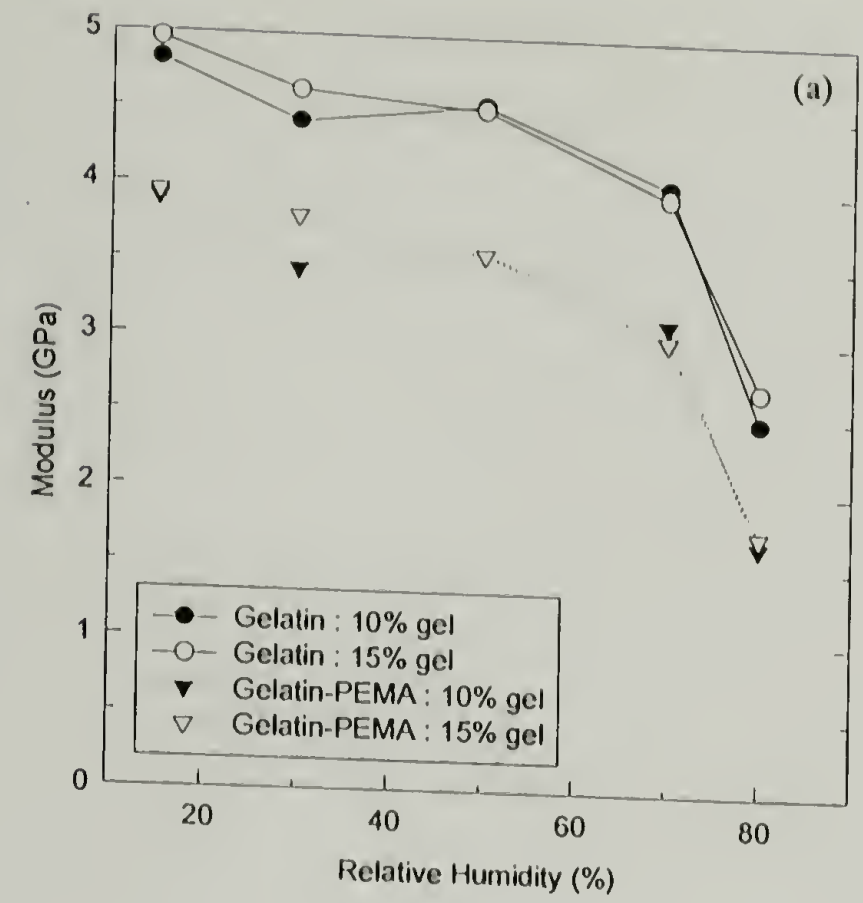

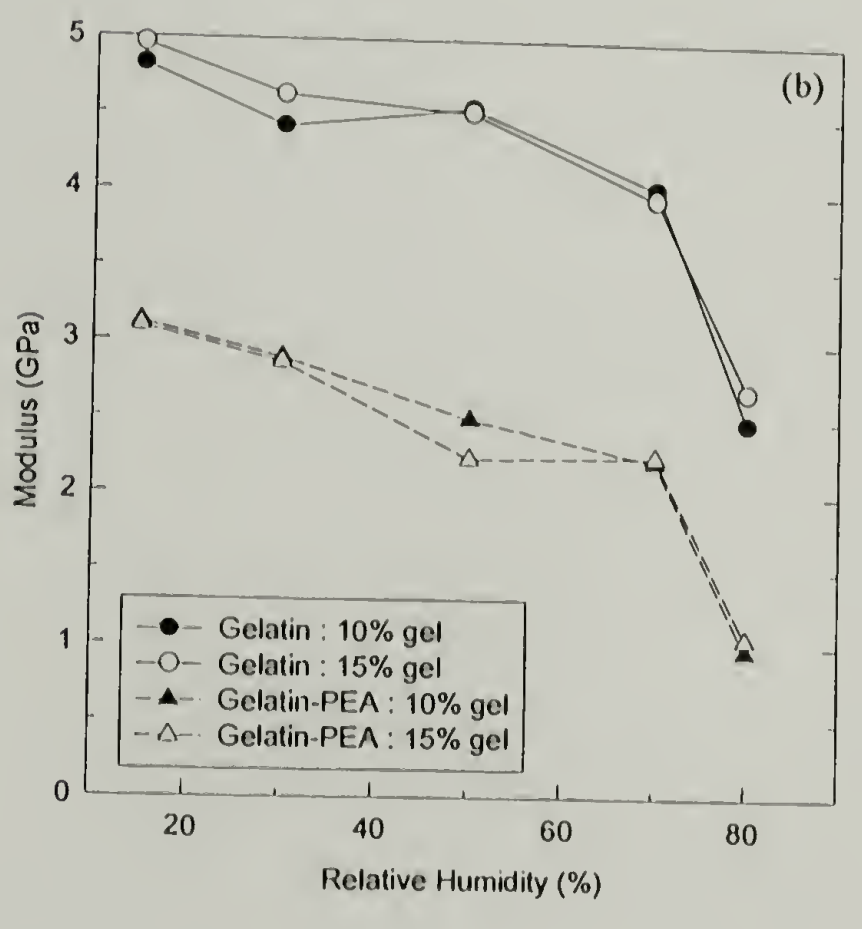

Figure 5.5: Effect of gelatin concentration at set point on the tensile modulus for pure gelatin and gelatin-latex films: (a) gelatin-PEMA and (b) gelatin-PEA films.

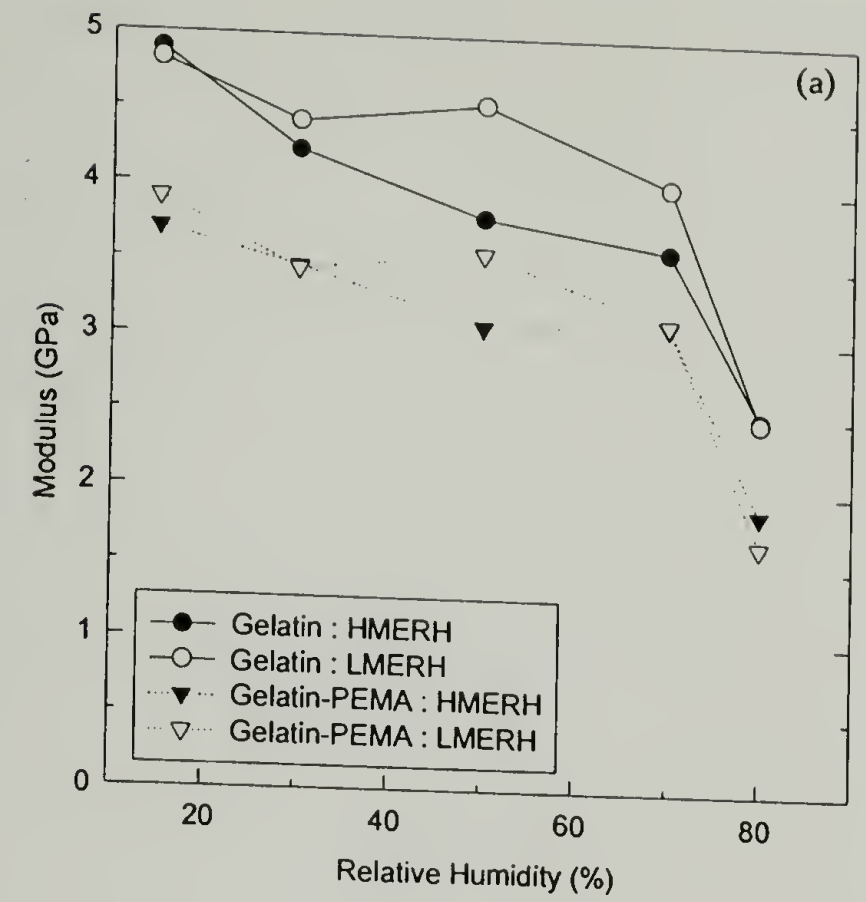

Figure 5.6 : Effect of drying condition at vitrification on the tensile modulus for pure gelatin and gelatin-latex films : (a) gelatin-PEMA and (b) gelatin-PEA films.

is 10%. The latex concentration of both latices is 40 parts. The particle size of PEA and PEMA is 0.112 μm and 0.15 μm, respectively. Similar to the effect of latex particle size and gelatin concentration at the set point, no significant effect on the tensile modulus is observed when the latex is present. There does appear to be an effects at 50% RH for the pure gelatin.

Composite Theories for Particulate Reinforcement

Several theories have been developed to predict the stress-strain behavior of composite materials. Most of the models are based on the relations between any two independent elastic constants among a Young's modulus (E), a shear modulus (G), and a bulk modulus (K) to predict the elastic response of reinforced materials.

One model for describing the mechanical properties of particulate-filled polymers was successfully provided by Dewey [10] in 1974 as shown in equation (5.1) and (5.2). In spite of the accuracy in calculating the shear modulus for an elastic medium, its limitation is that the model valid only at a small volume fraction ($\phi_f < 0.1$) of spherical inclusions.

$$\frac{G}{G_m} = 1 - \frac{15(1-\nu_m)\left(1-\frac{G_f}{G_m}\right)\phi_f}{7-5\nu_m+2(4-5\nu_m)\left(\frac{G_f}{G_m}\right)} \qquad (5.1)$$

$$K = K_m + \frac{(K_f - K_m)\phi_f}{1 + \left[(K_f - K_m) \Big/ \left(K_m + \frac{4}{3}G_m\right)\right]} \tag{5.2}$$

where ϕ is the volume fraction, ν is the Poisson's ratio, and the subscript m and f refer to matrix and filler, respectively.

Other models attempt to be applicable for the entire range of filler concentration (from 0% to 100% by volume). One of the widely used theories was proposed by Van der Poel [11] in 1958. In general, the comparisons of model predictions to experimental data give good agreement; however, it predicts a shear modulus that is far too high when the matrix is a rigid material. This is because the model inherently assumes that the matrix is soft and so is simply not applicable to the rigid matrix case.

Another extensively used theory is the so-called three-phase model developed by Kerner [12]. This model assumes that a spherical filler particle is surrounded first by a matrix layer and then by a certain equivalent medium showing the properties of the composite. The general form of this model is defined as equation (5.3):

$$\frac{E}{E_m} = \frac{G_f\phi_f \Big/ \left[(7-5\nu_m)G_m + (8-10\nu_m)G_f\right] + \phi_m \Big/ \left[15(1-\nu_m)\right]}{G_m\phi_f \Big/ \left[(7-5\nu_m)G_m + (8-10\nu_m)G_f\right] + \phi_m \Big/ \left[15(1-\nu_m)\right]} \tag{5.3}$$

The Kerner equation can be greatly simplified in some cases. For fillers that are much more rigid than the polymer matrix ($G_f >> G_m$), equation (5.3) becomes:

$$\frac{G}{G_m} = 1 + \frac{15(1-\nu_m)}{8-10\nu_m}\frac{\phi_f}{\phi_m} \tag{5.4}$$

For foams and rubber-modified rigid polymers ($G_f << G_m$), such as HIPS, the Kerner equation reduces to:

$$\frac{1}{G} = \frac{1}{G_m}\left[1 + \frac{15(1-\nu_m)}{7-5\nu_m}\frac{\phi_f}{\phi_m}\right] \tag{5.5}$$

Halpin and Tsai [13-15] have shown that the Kerner equation and many other equations for moduli can be put in a more general form. Lewis and Nielsen [16] then presented how those equations can be further generalized to:

$$\frac{M}{M_m} = \frac{1 + AB\phi_f}{1 - B\Psi\phi_f} \tag{5.6}$$

where M is any modulus - Young's, shear, or bulk

$A = K_E - 1$, where K_E is the Einstein Coefficient

$$B = \frac{(M_f/M_m) - 1}{(M_f/M_m) + A}$$

$$\Psi = 1 + \left(\frac{1-\phi^*}{\phi^{*2}}\right)\phi_f$$

The constant A takes into account such factors as geometry of the filler phase and Poisson's ratio of the matrix. For example, K_E equals to 2.5 for a spherical filler particle. The factor Ψ depends upon the maximum packing fraction, ϕ^*, of the filler.

It is apparent that most of the models have a common feature that is a particular idealized geometry and packing arrangement has to be assumed. In reality, the material can not be identified with any specific arrangement throughout the entire structure.

In order to improve these models, Farber and Farris [17] developed a model as described in equation (5.7) and (5.8) based on the mathematical similarity between the elastic deformation of solids (Christensen [18]) and the motion of suspended particles in viscous media (Navier-Stokes equations). The model is a differential approach to composite modulus theory for spherical inclusions. It assumes perfect adhesion and should represent a lower bound to the rigidity. This model has no adjustable parameters, unlike other models, and is valid over a wide range of filler concentrations.

$$\frac{dG}{d\phi_f} = \frac{-15G(1-\nu)\left(1-\frac{G_f}{G}\right)}{\left(7-5\nu+2(4-5\nu)\frac{G_f}{G}\right)(1-\phi_f)} \tag{5.7}$$

$$\frac{dK}{d\phi_f} = \frac{(K_f-K)}{\left(1+\frac{K_f-K}{K+\frac{4}{3}G}\right)(1-\phi_f)} \tag{5.8}$$

where $\nu = \frac{3K-2G}{2(3K+G)}$

The above equations can be numerically integrated using the following initial and boundary conditions:

$$\phi_f = 0 \quad , \quad G = G_m \quad , \quad K = K_m \tag{5.9}$$

$$\phi_f = 1 \quad , \quad G = G_f \quad , \quad K = K_f \tag{5.10}$$

For the limiting case of a low modulus incompressible filler ($\nu_f = 0.5$ and $G_f \approx 0$), equation (5.7) gives an analytical solution as:

$$\frac{G}{G_m} = \left(1 - \phi_f\right)^{5/3} \tag{5.11}$$

In this research, a new approach to analytically simplify Farber and Farris model (equation (5.7) and (5.8)) for rubber toughening glassy polymers system will be presented by assuming as follows:

(1) $\frac{dK}{d\phi_f} = 0$ (K is constant)

(2) $\frac{G_f}{G} \approx 0$ $\left(G_f << G_m\right)$

Therefore, equation (5.7) can be reduced to

$$\frac{dG}{d\phi_f} = \frac{-15G(1-\nu)}{(7-5\nu)\left(1-\phi_f\right)} \tag{5.12}$$

By substituting $\nu = \frac{3K - 2G}{2(3K + G)}$, equation (5.12) can then be expressed as

$$\frac{dG}{d\phi_f} = \frac{-5G(3K + 4G)}{(9K + 8G)\left(1-\phi_f\right)} \tag{5.13}$$

This differential expression can now be analytically integrated. The result can be written as

$$\left(1-\phi_f\right)^5=\left(\frac{G}{G_m}\right)^3\left(\frac{3K+4G_m}{3K+4G}\right) \tag{5.14}$$

By substituting $G=\frac{3K(1-2\nu)}{2(1+\nu)}$, equation (5.14) can be described as

$$\left(1-\phi_f\right)^5=\left(\frac{G}{G_m}\right)^3\left(\frac{1-\nu_m}{1-\nu}\right)\left(\frac{1+\nu}{1+\nu_m}\right) \tag{5.15}$$

Finally, equation (5.15) can be rearranged to

$$\frac{G}{G_m}=\left[\left(1-\phi_f\right)^5\left(\frac{1-\nu}{1-\nu_m}\right)\left(\frac{1+\nu_m}{1+\nu}\right)\right]^{1/3} \tag{5.16}$$

Or by substituting $\frac{G}{G_m}=\left(\frac{1+\nu_m}{1+\nu}\right)\left(\frac{E}{E_m}\right)$ into equation (5.15), then

$$\frac{E}{E_m}=\left[\left(1-\phi_f\right)^5\left(\frac{1-\nu}{1-\nu_m}\right)\left(\frac{1+\nu}{1+\nu_m}\right)^2\right]^{1/3} \tag{5.17}$$

The prediction of the proposed model (Equation (5.17)) compared with Farber-Farris model (Equation (5.11)) and Kerner Equation (Equation(5.5)) for the gelatin-latex system is presented in Figure 5.7. Also, Figure 5.7 shows the relative Young's moduli in comparison with those predicted from models for gelatin-PEA films at various relative humidities. The experimental data are in close agreement to the theoretical predictions, especially at 50 and 70% RH.

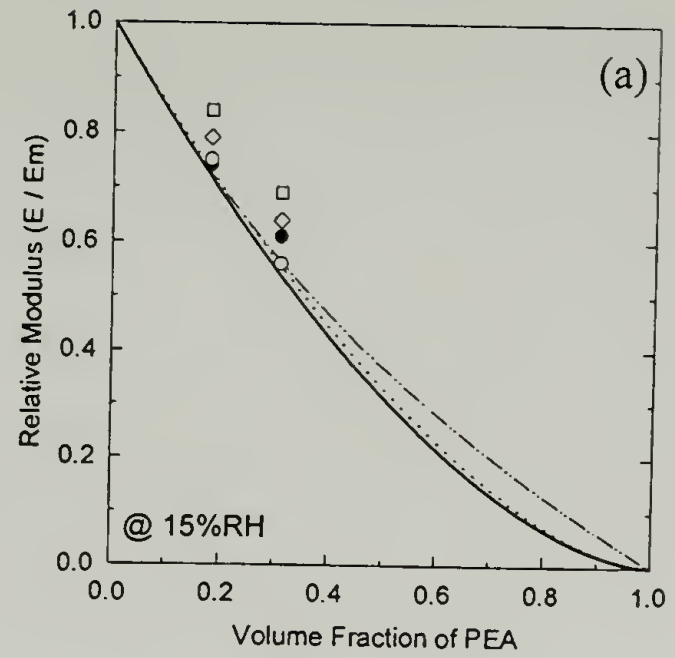

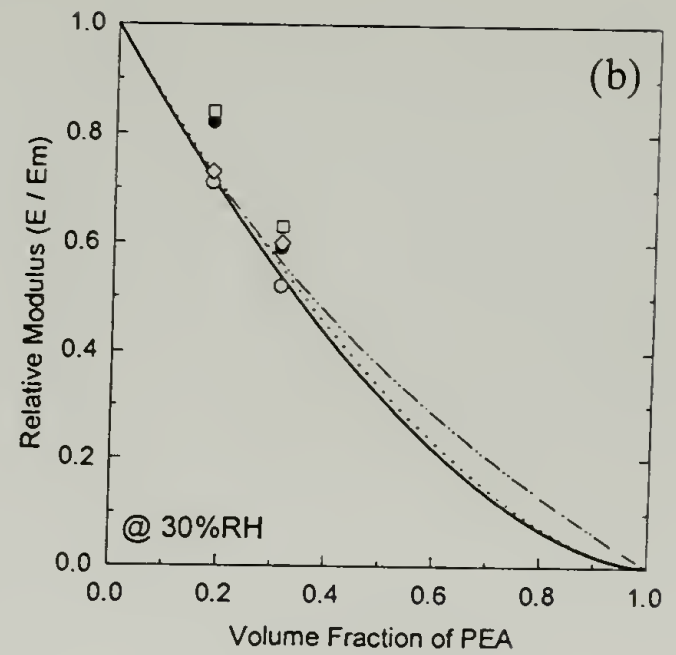

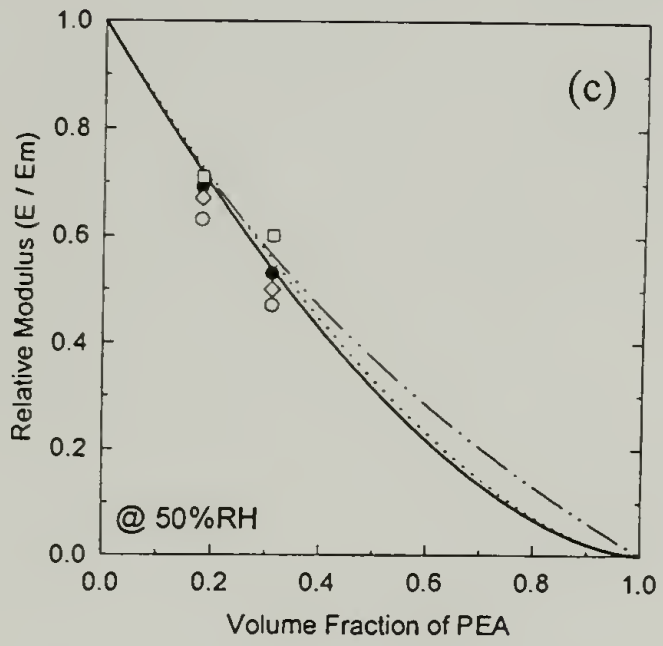

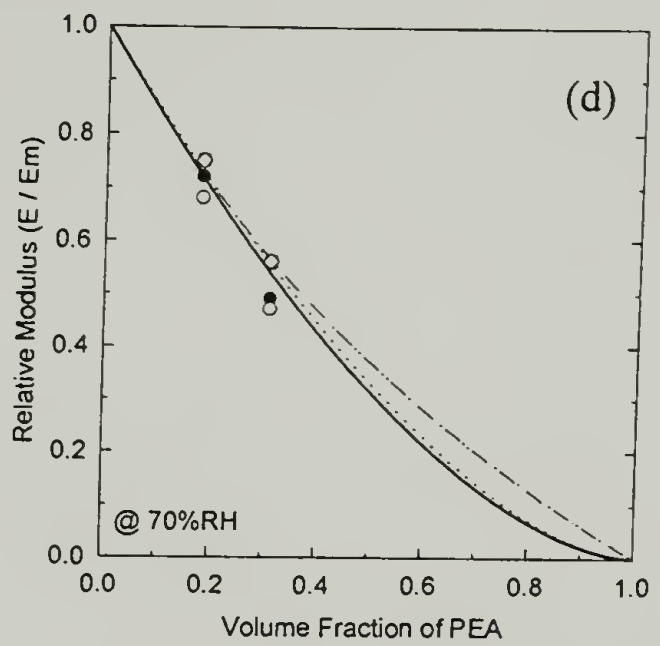

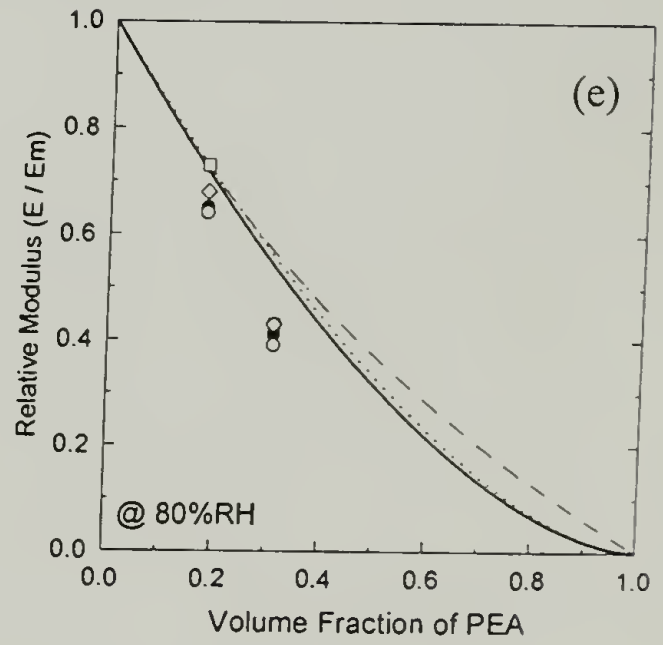

Figure 5.7 : Relative modulus of gelatin-PEA films vs. volume fraction of PEA predicted with different models : (—) model performance (equation (5.17)); (·····) Farber-Farris; (—··) Kerner at various RHs. Experimental data for (1) 0.051μm-15% gel-HMERH (●); (2) 0.051μm-15% gel-LMERH (O); (3) 0.112μm-15% gel-HMERH (□); (4) 0.112μm-15% gel-LMERH (◊).

Fracture Surfaces and Deformation Mechanisms

In order to understand the effect of moisture on the deformation mechanisms of the gelatin film, fracture surfaces of the gelatin and gelatin-latex films were examined by an optical microscope and a scanning electron microscope (SEM). In fact, the interesting results were obtained from the gelatin films stretched at 80%RH where the films behave as a ductile material. Optical micrographs, along with SEM micrographs, of gelatin and gelatin-latex films are shown in Figure 5.8 through 5.11.

Figure 5.8(a) and (b) show the optical micrographs of unstretched and stretched pure gelatin films (BF 8483-13) at 80%RH, respectively. The micrographs reveal that micro-voids, or perhaps bubbles of entrapped air, exist in the unstretched gelatin films. After being stretched, these structures become oval and are elongated parallel to the tensile stress direction. (Note that the direction of the applied tensile stress is vertical in each case.) Similar results are also observed in the gelatin-PEA film (BF 8483-173) as shown in Figure 5.8(c) and (d). A comparative study was performed by taking SEM micrographs of the unstretched and stretched pure gelatin film (BF 8483-13), as presented respectively in Figure 5.8(e) and (f). The direction of the applied tensile stress is indicated by the arrow. Figure 5.8(f) indicates that the tiny oval shape seen in optical micrographs is likely to be the bubbles of entrapped air.

Besides these micro-voids, small cracks also form on the gelatin surface. As shown in Figure 5.9(a), the crack orientation of the pure gelatin film (BF 8483-23) is preferentially aligned in a direction approximately 90° to the principle tensile stress. In

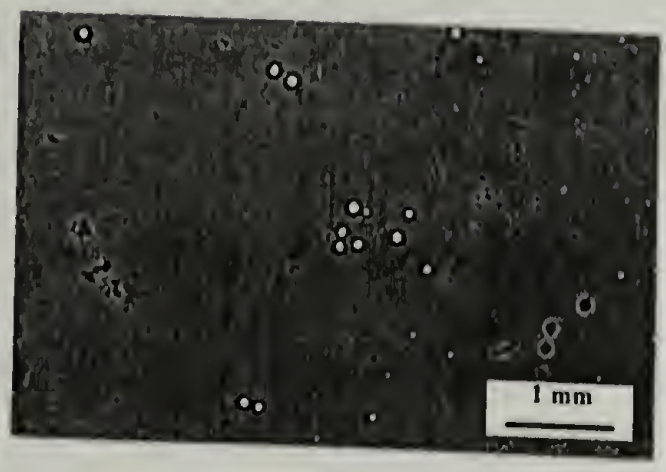

(a) As received pure gelatin film
(BF 8483-13)

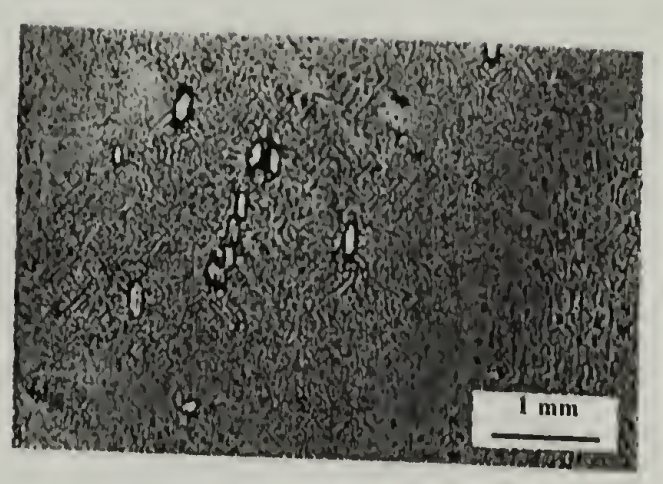

(b) Stretched pure gelatin @ 80%RH
(BF 8483-13)

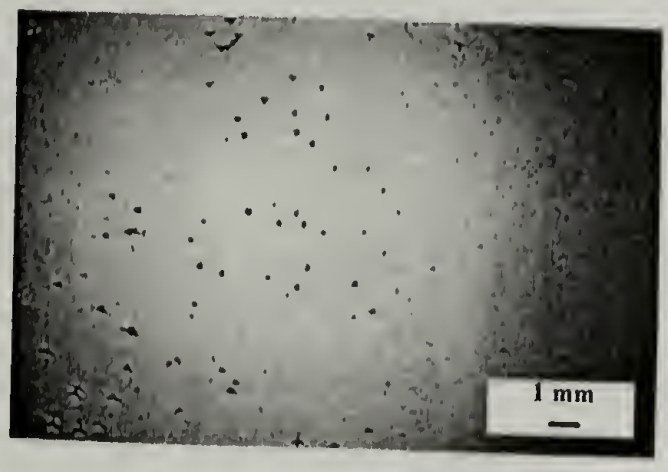

(c) As received gelatin-PEA film
(BF 8483-173)

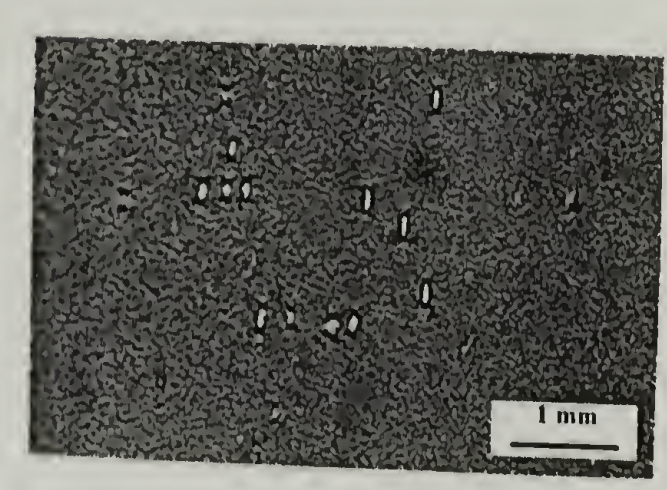

(d) Stretched gelatin-PEA @80%RH
(BF 8483-173)

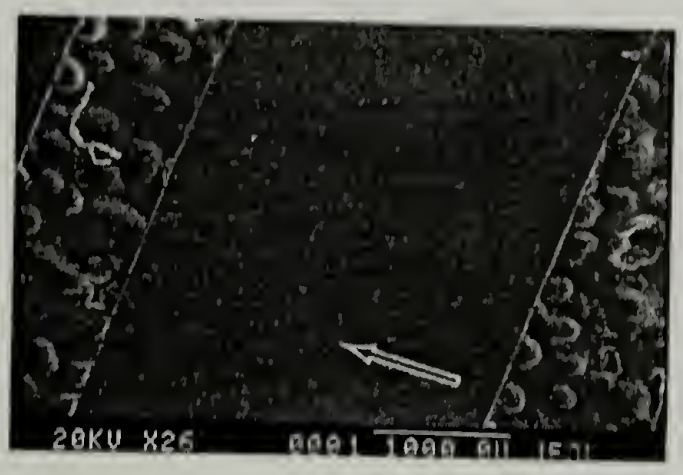

(e) As received pure gelatin film
(BF 8483-13)

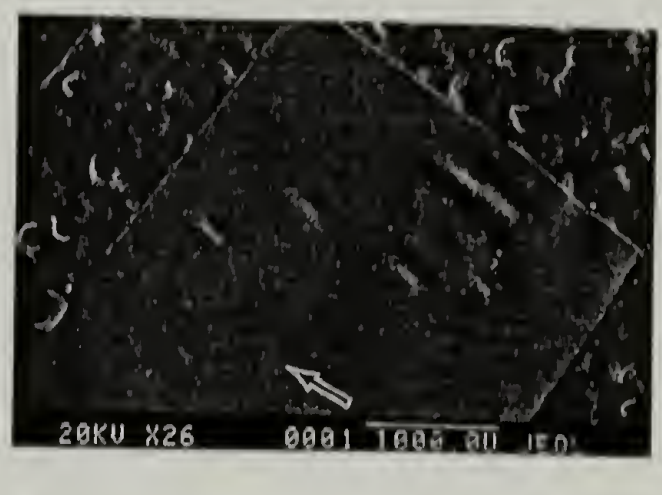

(f) Stretched pure gelatin @ 80%RH
(BF 8483-13)

Figure 5.8 : Optical (a-d) and SEM (e and f) micrographs of as received and fracture surfaces for pure gelatin and gelatin-PEA films.

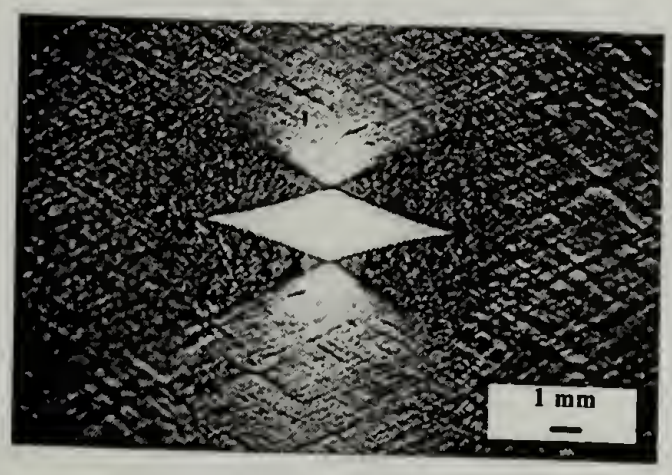

(a) Pure gelatin (BF 8483-23)

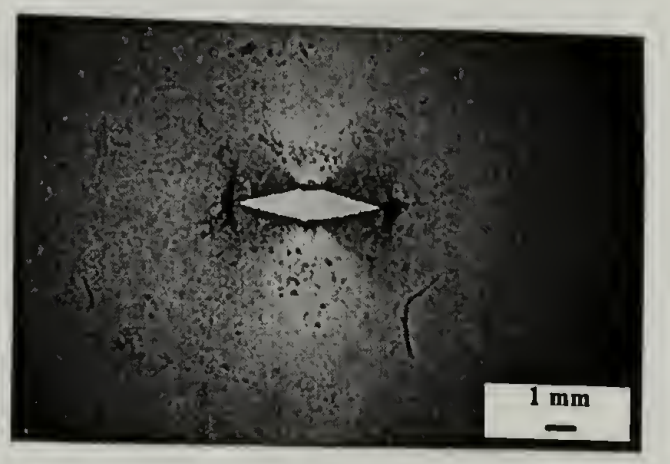

(b) Gelatin-PEA film (BF 8505-442)

(c) Gelatin-PEMA (BF 8483-113)

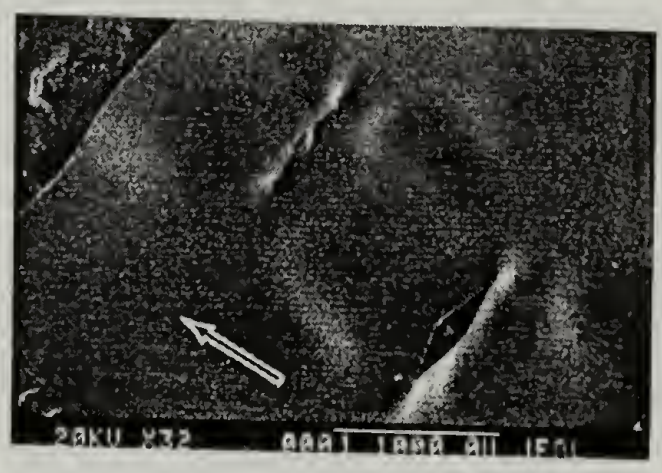

(d) Gelatin-PEMA (BF 8483-113)

Figure 5.9 : Optical (a-c) and SEM (d) micrographs of cracks surfaces for gelatin and gelatin-latex films after being stretched to 80% RH.

other words, the cracks are generated as typical tensile microcracks in the direction normal to the maximum principle stress.[9,19,20]

Similar cracking failure mechanisms are also observed in both gelatin-PEA (BF 8505-442) and gelatin-PEMA (BF 8483-113) films, as illustrated in Figure 5.9(b) and (c), respectively. In addition, it is interesting to note that unlike any other materials, these cracks are obviously in a 'diamond' shape with the very sharp edges. Since these 3 micrographs were taken at the same magnification, and it is apparent that the size of the cracks in both gelatin-latex films are smaller than that of the pure gelatin film. This might suggest that latex particles help in decreasing the size of the cracks in the gelatin films. Evidence of the cracks is given in Figure 5.9(d), where the SEM micrograph of the fracture surface of the gelatin-PEMA (BF 8483-113) film is shown.

The cracks or voids are initiated at some imperfection in the film or on the surface.[16] Such fracture due to the presence of flaws, could be associated scratches, impurities, chain ends, or interfaces between crystallites and amorphous regions.[19,21] These flaws have the effect of causing a stress concentration. As clearly seen in Figure 5.9(b), a large stress concentration should exist at the crack tip, which means that the local stress in this area is much higher than that applied to the whole body; as a result, fracture starts at the crack tip and the crack then continues to propagate.[19] Besides these flaws, in the case of gelatin-latex films, the fracture of the films may start at the interface between gelatin matrix and latex particles due to weak adhesion between the two phases.

Figure 5.10(a) and (b) show a deformed specimen of pure gelatin film (BF 8483-83) which has undergone crazing. The crazes are oriented perpendicular to the maximum

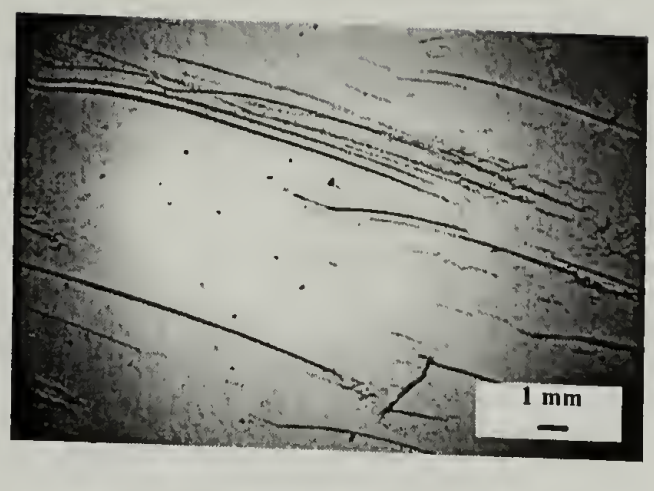

(a)

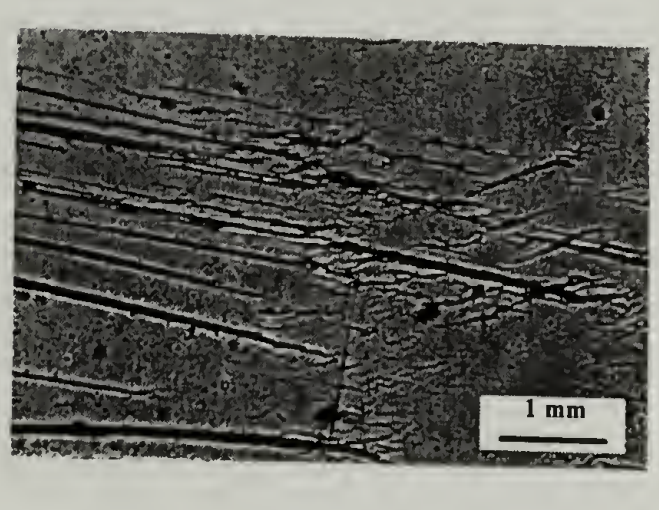

(b)

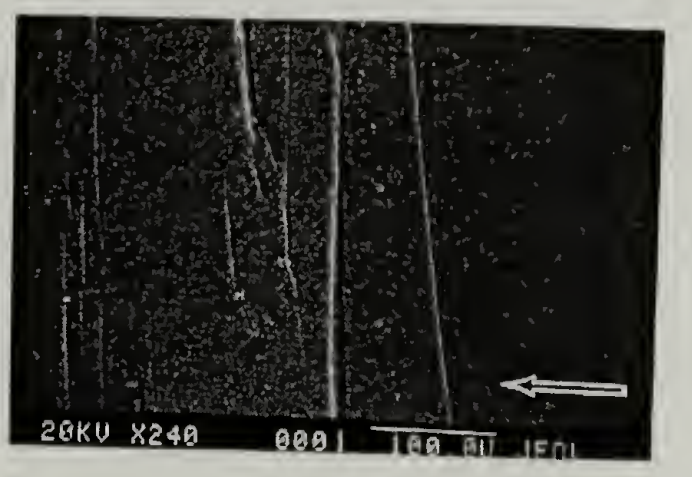

(c)

Figure 5.10 : Optical (a and b) and SEM (c) micrographs of crazes in pure gelatin film (BF 8483-83) after being stretched to 80% RH.

applied tensile stress.[9,19,20] Normally, crazes are initiated at flaws, such as scratches or other imperfection, either within or at the surface of the specimen. Although they appear to be similar to cracks due to their lower refractive index than their surroundings, they actually contain fibrils of polymer within their bulk whereas cracks do not. It is the presence of the relatively strong craze fibrils that makes the crazes load bearing and consequently differently from the cracks.[9,19,20] And also because of their void-fibril structure; they are less dense than the uncrazed material and so reflect and scatter light. As a result, they can be seen by naked eye.[19] The SEM micrograph of the fracture surface of the pure gelatin film (BF8483-83) is presented in Figure 5.10(c).

Another deformation mechanism that can be observed in the fracture surface of gelatin film, especially at 80% RH, is shear yielding. Figure 5.11(a) through (d) present the optical micrographs of the fracture surfaces at 80% RH of four pure gelatin films with different gelatin concentration and drying condition of: (a) 10% gel at the HMERH (BF 8483-13); (b) 10% gel at the LMERH (BF 8483-23); (c) 15% gel at the HMERH (BF 8483-83) ; and (d) 15% gel at the LMERH (BF 8483-73). Intense shear bands were observed on the gelatin surfaces. It can be seen that these shear bands develop along the direction of maximum shear stress which is 45° to the maximum applied tensile stress.[9,19,20] Not only does this mechanism act as an energy absorbing process but the shear bands also present a barrier to the propagation of crazes (Figure 5.10(b)) and thus crack growth (Figure 5.9(a) and (c)), therefore delaying failure of the material.[9] As can be seen in Figure 5.10(b), crazing and shear yielding could occur simultaneously. When crazes meet pre-existing shear bands, they may be arrested or their path may be diverted and , in particular, the direction of propagation may rotate away from lying perpendicular

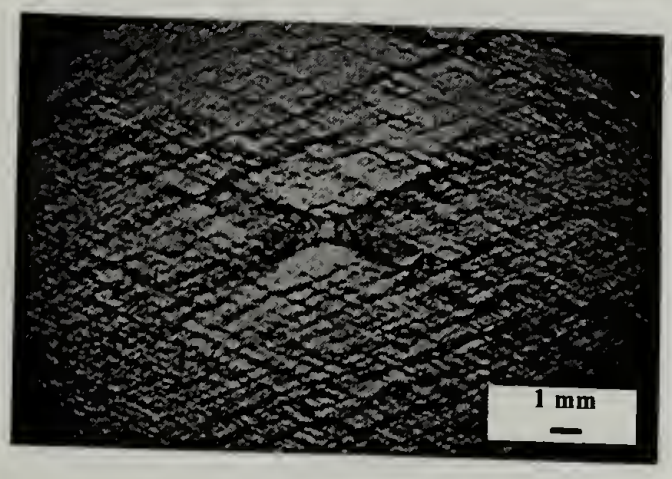

(a) BF 8483-13

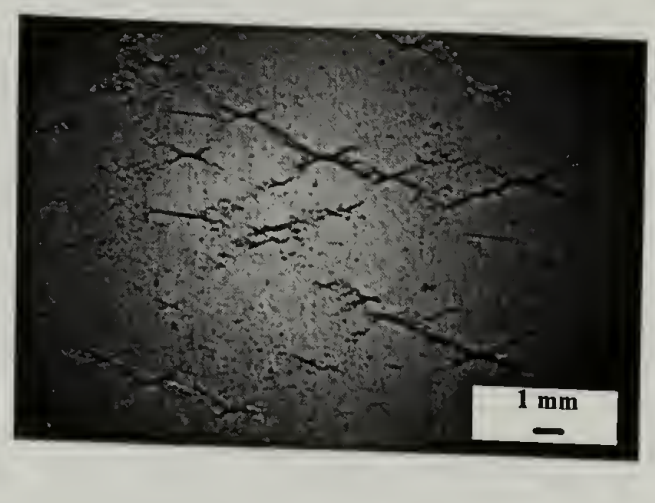

(b) BF 8483-83

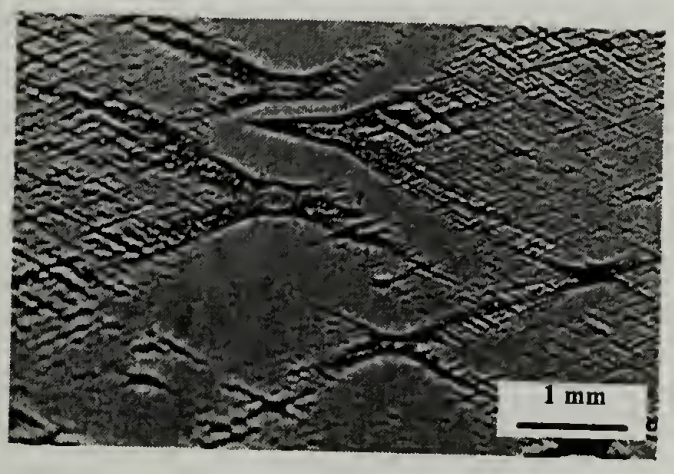

(c) BF 8483-23

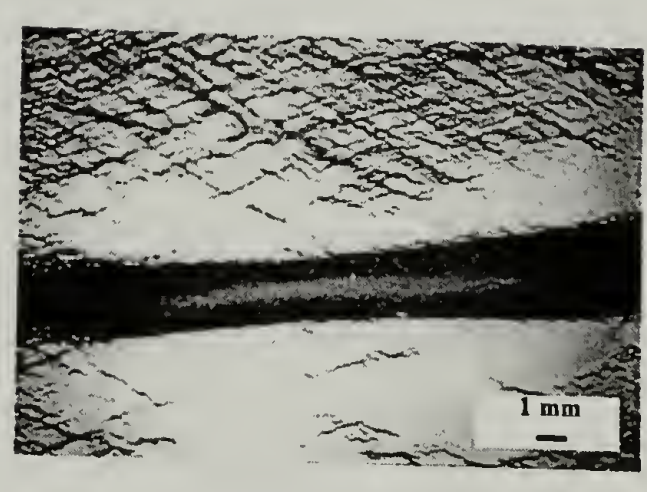

(d) BF 8483-73

Figure 5.11 : Optical micrographs of shear bands in pure gelatin films after being stretched to 80% RH : (a) 10% gel-HMERH, (b) 15% gel-LMERH, (c) 10% gel-LMERH, and (d) 15% gel-LMERH.

to the applied tensile stress owing to the molecular orientation in the shear band.[20] This observation leads to the conclusion that shear bands are effective craze stoppers.[9]

Conclusions

Similar to other moisture sensitive materials, such as nylon or silk, the tensile properties of gelatin are greatly affected by relative humidity. While the tensile strength and Young's modulus of gelatin decrease with increasing moisture content, the elongation to break increases. Observation of the fractured gelatin film surfaces after they had been stretched at 80% RH shows the presence of either micro-voids or bubbles of entrapped air, small cracks, crazes, and shear banding.

At fixed relative humidity, the incorporation of polymer latex, PEA and PEMA, into a gelatin has a profound effect upon the tensile properties as shown from the stress-strain curves. For instance, at 15% RH gelatin is relatively brittle but following the addition of soft latex particles, especially the PEA latex, the material is able to undergo yield and deform plastically. In other words, gelatin films have higher tensile strength and Young's modulus, but a lower strain to break, than gelatin-PEA films. However, this is not the case for gelatin-PEMA films. Although the PEMA latex also lowers the tensile strength and Young's modulus, it reduces the toughness and elongation to break of the gelatin films.

In both gelatin-latex systems, the tensile strength and Young's modulus decrease with increasing filler content. The pure gelatin films have the highest tensile strength and Young's modulus, while the gelatin films with 40 parts PEA have the lowest tensile

strength and Young's modulus. No effect of latex particle size is observed on the tensile properties of the gelatin-latex films in the investigated diameter range. Similarly, neither drying condition at vitrification nor gelatin concentration at the set point affect the tensile modulus of both pure gelatin and gelatin-latex films.

References

1. Eliassaf, J. and Eirich, F.R., "Creep Studies on Gelatin at 100% relative Humidity", *Journal of Applied Polymer Science*, **4**(11), 200 (1960).

2. "Physical Properties of Kodak Aerial Films", *Properties of Kodak Materials for Aerial Photographic Systems*; Eastman Kodak Co.: Rochester, NY, 1972; Vol. II.

3. Calhoun, J.M., "Properties and Dimensional Stability of Safety Aerographic Film", *Photogrammetric Engineering*, **13**, 163 (1974).

4. Marshall, A.S. and Petrie, S.E.B., "Thermal Transitions in Gelatin and Aqueous Gelatin Solutions", *Journal of Photographic Science*, **28**, 128 (1980).

5. Marshall, A.S. and Petrie, S.E.B., "Thermal Transitions and Physical Aging in Gelatin", *Proceedings of the Eleventh North American Thermal Analysis Society Conference*, **2**, 183 (1981).

6. Ni, B.Y. and Faou, A.L., "Crystalline Structure and Moisture Effects on Deformation Mechanisms of Gelatin Films under Mode I Stress Field", *Mat. Res. Soc. Symp. Proc.*, **292**, 229 (1993).

7. Pinhas, M-F., Blanshard, J.M.V., Derbyshire, W., and Mitchell, J.R., "The Effect of Water on the Physicochemical and Mechanical Properties of Gelatin", *Journal of Thermal Analysis*, **47**, 1499 (1996).

8. Fakirov, S. et al., "Mechanical Properties and Transition Temperatures of Crosslinked Oriented Gelatin II Effect of Orientation and Water Content on Transition Temperatures", *Colloidal Polymer Science*, **275**, 307 (1997).

9. Walker, I. and Collyer, A.A. In *Rubber Toughened Engineering Plastics*; Collyer, A.A., Ed.; Chapman & Hall: New York, 1994; Chapter 2, pp.29-56.

10. Dewey, J.M., "The Elastic Constants of Materials Loaded with Non-Rigid Fillers", *Journal of Applied Physics*, **18**, 578 (1947).

11. Van Der Poel., C., "On the Rheology of Concentrated Dispersions", *Rheologica Acta*, **1**, 198 (1958).

12. Kerner, E.H., "The Elastic and Thermo-Elastic Properties of Composite Media", *Proceedings of the. Physical Society, London*, **69B**, 808 (1956).

13. Tsai, S.W., U.S. Government Report AD 834851, 1968.

14. Ashton, J.E., Halpin, J.C., and Petit, P.H. *Primer on Composite Analysis*; Technomic: Lancaster, Pennsylvania, 1969.

15. Halpin, J.C., "Stiffness and Expansion Estimates for Oriented Short Fiber Composites", *Journal of Composite Material*, **3**, 732 (1969).

16. Lewis, T.B. and Nielsen, L.E., "Dynamic Mechanical Properties of Particulate-Filled Composites", *Journal of Applied Polymer Science*, **14**, 1449 (1970).

17. Farber, J.N. and Farris, R.J., "Model for Prediction of Elastic Response of Reinforced Materials over Wide Ranges of Concentration", *Journal of Applied Polymer Science*, **34**, 2093 (1987).

18. Christensen, R.M. *Mechanic of Composite Material*; Wiley-Interscience: New York, 1979; Chapter 2, pp.31-72.

19. Young, R.J. and Lovell, P.A. *Introduction to Polymers, 2nd ed.*; Chapman & Hall: New York, 1991; Chapter 5, pp.310-428.

20. Donald, A.M. In *Rubber Toughened Engineering Plastics*; Collyer, A.A., Ed.; Chapman & Hall: New York, 1994; Chapter 1, pp.1-28.

21. Williams, H.L., *Polymer Engineering*; Elsevier: New York, 1975; pp.110-113.

CHAPTER 6

HYGROTHERMAL EFFECT ON DIMENSIONAL STABILITY

Introduction

Dimensional stability is one of the most significant physical requirements of photographic films. It is of prime importance in a number of applications such as lithographic products, radiographic products, topographic maps, aerial mapping, reproduction of mechanical drawings, motion picture industry, and graphic arts, etc.[1-3] In recent years, various synthetic polymers such as polystyrene, polyester, and poly(vinyl chloride) have been used to replace former types of photographic supports which are cellulose nitrate, cellulose triacetate, or cellulose acetate butyrate.[2] This is due to their superior moisture resistance and improved dimensional stability. Among these newer types of supports, poly(ethylene terephthalate), PET, is the top choice for most applications. This is because of the small magnitude of the swelling and its uniformity.

In general, dimensional changes are due to one of these factors : temperature, humidity, processing, or aging.[1,4] However, it has to be noted that all these causes may play their roles concurrently. As a result, they may promote or partially cancel one another. For example, when the temperature increases, the relative humidity usually decreases, or vice versa. Usually, the decrease in film size owing to the temperature change is less than the decrease due to the humidity change. Practically, thermal expansion is much less important than humidity expansion, because photographic film is

not frequently used over a wide temperature range.[1,4] In other words, thermal effects are normally overshadowed by humidity effects.

At low relative humidity, the emulsion is in tension and the support is in compression, resulting in a concave of emulsion layer so called "positive" curl.[5,6] This is because when the relative humidity is lowered, the emulsion has both a higher contraction and a higher stiffness due to the increasing in the modulus at low humidities than the support.[5] As a result, the emulsion pulls the support into a curl. On the other hand, at high relative humidity, a "negative" curl occurs when the emulsion is in compression.[5,6] This phenomenon can be explained that when the humidity is raised, the emulsion expands more than support, causing the emulsion to push the support into a convex configuration.[5] At very high humidities, the emulsion becomes soft and the curl is reduced.

The reasons for processing dimensional changes differ for different kinds of support. For cellulose ester and polycarbonate base films, a shrinkage occurs due to loss of residual coating solvents from the support during photographic processing.[1,4] This is not the case for PET and PS base films. Processing dimensional changes are due to mechanical interactions of the gelatin layers and the support.[1,2,4] More details will be discussed shortly.

In addition to the different types of dimensional changes already mentioned, permanent shrinkage caused by aging is another concern, although it is of little practical importance unless the atmospheric conditions are extreme. Once again the reasons behind the aging shrinkage, including the amount of shrinkage, vary in each particular film. For instance, the relatively high shrinkage of the cellulose ester base film is caused

by the loss of residual solvents from the support.[1,4] As the film ages, these solvents gradually diffuse from the support, resulting in a permanent shrinkage. In contrast, the relatively low shrinkage of polyester base film (PET) is caused by relaxation shrinkage and plastic flow of the support due to internal and external stresses, respectively.[4] The external stresses on the polyester base are due to the compressive force of the emulsion layer. High or low relative humidity should be avoided since it may accelerate permanent film shrinkage. Therefore, film should be stored at approximately 70-80 F and 40-50% RH in order to minimize aging shrinkage.[1] The amount of shrinkage will increase with (1) increase in the thickness of emulsion layer and (2) decrease in storage relative humidity because these two factors increase the compressive force on the support. In addition, the magnitude of shrinkage will also increase with an increase in storage temperature. This is due to the fact that at elevated temperature the modulus of the support decreases.[2]

Another major factor contributing to film curl is "plastic-flow". Typically, when film is wound into a roll, it is flat across its width but assumes a lengthwise curvature. Consequently, under that condition film is subjected to stresses and undergoes plastic flow in the length direction of the film. This phenomenon of lengthwise plastic flow is know as "core set".[5] Core set increases with an increase in storage temperature and time. Moreover, it will also increase with a reduction in roll diameter since film becomes more highly stressed when wound into a small radius. Part of this phenomena is plastic and part is viscoelastic.

In conclusion, the various types of dimensional changes can be classified as follows [7]:

(1) Temporary or reversible dimensional changes due to

(1.1) humidity expansion or contraction

(1.2) thermal expansion or contraction

(2) Permanent shrinkage (in processing or aging) due to

(2.1) loss of residual solvent

(2.2) plastic flow of the base caused by contraction of the emulsion

(2.3) release of the mechanical strain

(2.4) mechanical effects of the emulsion layer due to humidity and moisture history

As discussed earlier, the magnitude of the change depends on the chemical composition and thickness of the support and emulsion.[3,8] Moreover, the storage conditions and treatment received during the manufacturing process also influence the dimensional changes in photographic film.

Although the dimensional changes can be caused by several factors, the dimensional instability discussed throughout this research is mainly focused on those caused by humidity. Nonetheless, a comparative study on the effect of temperature was also performed. Due to the difference in the ability to absorb moisture between hydrophilic gelatin layer and hydrophobic substrate[1,2,5], the photographic film will curl when exposed to moisture. In other words, the dimensional instability of photographic film is caused primarily by the mismatch of in-plane humidity expansion coefficients between the emulsion layer and the support. This results in a bending

moment resulting in curl. Figure 6.1 illustrates this bending phenomenon of gelatin coated on a PET substrate.

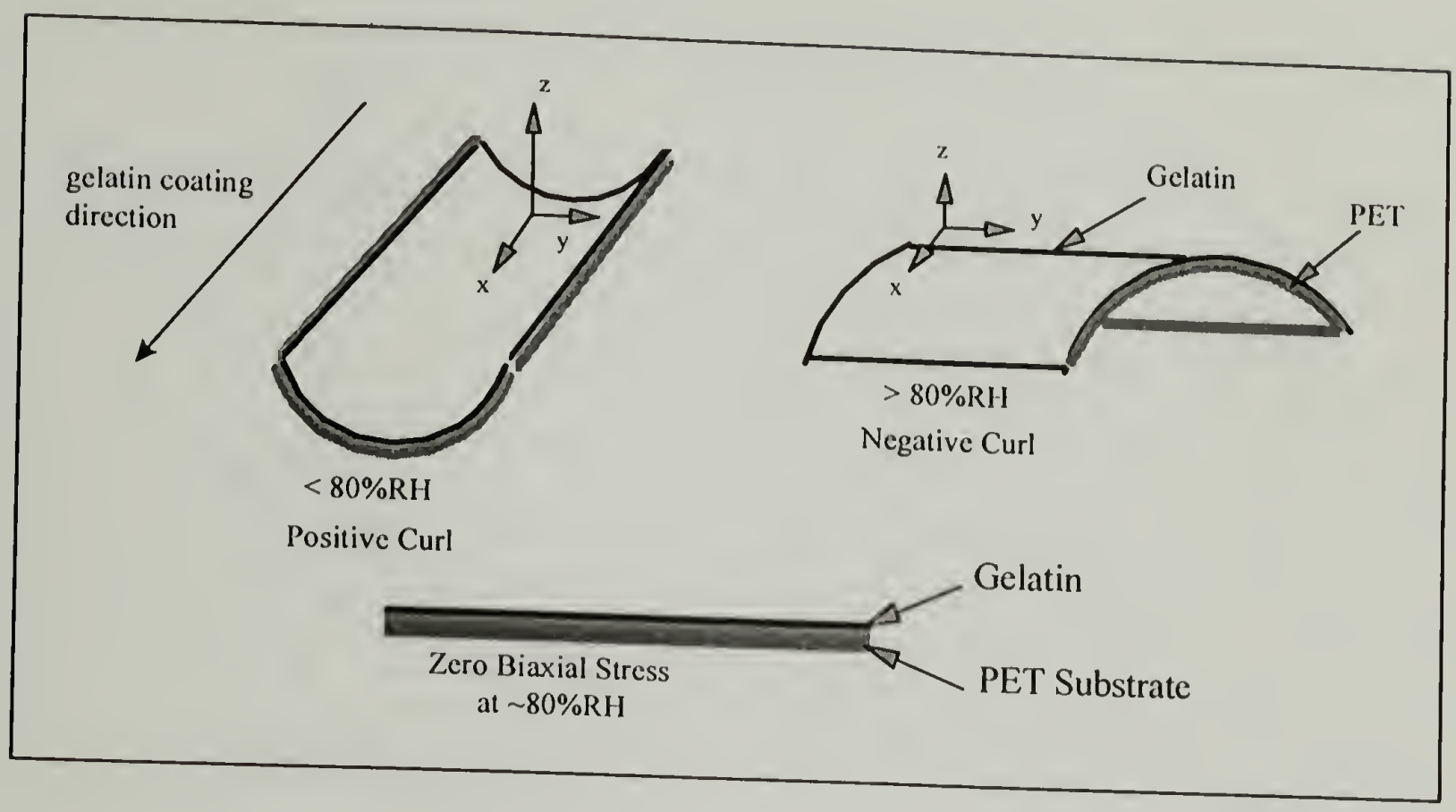

Figure 6.1 : Schematic of dimensional instability in a bilayer system of gelatin coated on a PET substrate.

As shown, each bending mode depicts the bilayer as a cylindrical shape. It is the stress in the system that causes bending to occur. For the gelatin/PET bilayer investigated in this work, the zero state of stress, i.e., stress at which the photographic film lies flat, occurred at around 75-80% RH and room temperature. It should be noted that this specific humidity can be very different for other bilayer systems. For instance, it was observed that the gelatin/cellulose acetate bilayer lies flat at 54% RH.[6] Besides the choice of substrate, the zero state of stress in photographic film is also dependent upon

drying conditions, gelatin coating thickness, etc.[6] Chapter 7 will present the details regarding the relationship of stress as a function of relative humidity including the zero state of stress for the gelatin/PET bilayer system.

In this research, the effect of humidity and temperature on the dimensional changes of the pure gelatin and gelatin-latex films were measured using a thermomechanical analyzer (TMA). The humidity expansion coefficients were determined by plotting the humidity swelling strain at equilibrium as a function of relative humidity. The first derivative of this curve or the slope is the humidity expansion coefficient. The humidity expansion coefficient can be defined as:

$$\beta = \left.\frac{\partial \varepsilon}{\partial \mathrm{RH}}\right|_{\text{stress, temp}} \tag{6.1}$$

The results of the in-plane humidity swelling experiment will be incorporated into an incremental linear elasticity theory in chapter 7.

Theoretical Models for Predicting the Coefficients of Expansion

Thermal Expansion

A number of different equations, relating to the properties and concentration of the individual components, have been proposed for calculating the coefficient of thermal expansion (CTE) (or thermal expansion coefficient (TEC)) of particulate-filled polymers.

[9-21] The different equations often predict quite different values for the coefficient of expansion of a given composite. Some experimental data agree with one equation, while other data agree with a different equation.[9]

As a first approximation, use is often made of the rule of mixtures:

$$\alpha_c = \alpha_f \phi_f + \alpha_m \phi_m \tag{6.2}$$

where α_c, α_f, and α_m are the coefficients of thermal expansion of the composite, particulate filler, and matrix, respectively.

However, in most cases the coefficient of expansion of the mixture is not a linear function of the concentration of the filler and the coefficients of expansion of the two components. The first model for calculating the coefficient of expansion based on the modulus of elasticity of each component was proposed by Turner [10] in 1946. Assuming that stresses are nowhere sufficient to disrupt the material (the sum of the internal forces can be equal to zero), that each component is constrained to change dimensions with temperature changes at the same rate as the aggregate, and that there is negligible shear deformation, Turner has calculated the effective coefficient of thermal expansion, α_c, as:

$$\alpha_c = \frac{\alpha_f \phi_f K_f + \alpha_m \phi_m K_m}{\alpha_f K_f + \alpha_m K_m} \tag{6.3}$$

where K_m and K_f are the bulk modulus of matrix and filler. In addition, this model also assumes that the filler particles are isotropic and that the coefficient of expansion does not depend upon the size and shape of the filler particles.

For nearly spherical particles dispersed in a matrix, Kerner [11] derived the following equation for the coefficient of linear thermal expansion of a composite:

$$\alpha_c = \alpha_f \phi_f + \alpha_m \phi_m - (\alpha_m - \alpha_f)\phi_m \phi_f \frac{\left(\frac{1}{K_m} - \frac{1}{K_f}\right)}{\left(\frac{\phi_m}{K_f} + \frac{\phi_f}{K_m} + \frac{3}{4}G_m\right)} \qquad (6.4)$$

where G_m is the shear modulus of matrix and is defined as: $G_m = \frac{3K_m(1-2\nu_m)}{2(1+\nu_m)}$

This equation does not deviate strongly from the rule of mixture since spheres do not impose mechanical restrictions on the matrix to the extent that fibers do.[12] The interaction term in this equation becomes zero when the bulk modulus of the filler is the same as that of the matrix, and it goes through a maximum at $\phi_f = \phi_m = 0.5$. On substituting G_m into equation (6.4), the effective linear thermal expansion coefficient for the particulate-filled polymer composite can then be expressed as:

$$\alpha_c = \alpha_m - (\alpha_m - \alpha_f)\phi_f \left[1 + \frac{(1-\phi_f)(K_f - K_m)}{K_m(1-\phi_f) + K_f\phi_f + \frac{9}{8}K_f K_m^2 \frac{(1-2\nu_m)}{(1+\nu_m)}}\right] \qquad (6.5)$$

Another extensively used model was proposed by Levin [13] in 1967. Levin has shown that a simple relationship can be established between the effective thermal expansion coefficients, α_c, and the effective elastic moduli of two phase materials. For an isotropic composite with two isotropic phases the basic relationship can be written in the form:

$$\alpha_c = \bar{\alpha} + \frac{\alpha_f - \alpha_m}{\frac{1}{K_f} - \frac{1}{K_m}}\left[\frac{1}{K_c} - \overline{\left(\frac{1}{K}\right)}\right] \tag{6.6}$$

where $\bar{\alpha} = \alpha_f \phi_f + \alpha_m \phi_m$ and $\overline{\left(\frac{1}{K}\right)} = \frac{\phi_f}{K_f} + \frac{\phi_m}{K_m}$

K_c is the effective bulk modulus of the composite. Its value can be determined experimentally or theoretically. The simplest case for an isotropic material is that of a dilute suspension of spherical particles ($\phi_f < 0.1$) when we can make use of the relation derived by Hashin [14] or by Christensen [15] as shown in equation (6.7) and (6.8), respectively.

$$K_c = K_m + \frac{\phi_f}{\frac{1}{K_f - K_m} + \frac{3}{3K_m + 4G_m}} \tag{6.7}$$

$$K_c = K_m + \frac{(K_f - K_m)\phi_f}{1 + \left[(K_f - K_m)\Big/\left(K_m + \frac{4}{3}G_m\right)\right]} \tag{6.8}$$

For higher particle concentration or volume fraction, the effective bulk modulus can be calculated from equation (6.9) given by Kerner [11]:

$$K_c = \frac{\frac{K_m \phi_m}{3K_m + 4G_m} + \frac{K_f \phi_f}{3K_f + 4G_m}}{\frac{\phi_m}{3K_m + 4G_m} + \frac{\phi_f}{3K_f + 4G_m}} \tag{6.9}$$

An expression corresponding to equation (6.9) for the effective bulk modulus was also obtained later by Hashin and Shtrikman [16] and by Christensen [15] as presented in equation (6.10) and (6.11), respectively. And from a close comparison it can be shown algebraically that there is an exact mathematical equivalence among three sets of equations derived by Kerner (equation (6.9)), Hashin and Shtrikman (equation (6.10)), and by Christensen (equation (6.11)).[17]

$$K_c = K_m + \frac{\phi_f}{\frac{1}{K_f - K_m} + \frac{3(1-\phi_f)}{3K_m + 4G_m}} \tag{6.10}$$

$$K_c = K_m + \frac{(K_f - K_m)\phi_f}{1 + \left[(1-\phi_f)(K_f - K_m) \Big/ \left(K_m + \frac{4}{3}G_m\right)\right]} \tag{6.11}$$

It is apparent from equation (6.10) and (6.11) that when ϕ_f is small, the term $(1-\phi_f)$ can be neglected and these relations then become identical with equations (6.7) and (6.8), respectively. By substituting the effective bulk modulus equations in Levin's

equation (equation (6.6)), the effective linear thermal expansion coefficient for the composite sphere assemblage can be written as:

$$\alpha_c = \alpha_m - (\alpha_m - \alpha_f)\phi_f \left[1 + \frac{(1-\phi_f)(K_f - K_m)}{K_m(1-\phi_f) + K_f\phi_f + \frac{K_f(1+\nu_m)}{2(1-2\nu_m)}} \right] \tag{6.12}$$

It should be noted that relationship represented by equation (6.6) has also been obtained independently by several authors including Schapery [18], Rosen [19], Cribb [20], and Steel [21].

If the geometry of the composite is not clearly defined, it can be argued that it is better to use rigorous bounds rather than an uncertain approximation. Bounds on the effective thermal expansion coefficient of an isotropic composite can be obtained by using the bounds derived by Hashin and Shtrikman [16], which may be written in the form:

For the upper bound:

$$K_c = K_f + \frac{\phi_m}{\frac{1}{K_m - K_f} + \frac{3\phi_f}{3K_f + 4G_f}} \tag{6.13}$$

For the lower bound:

$$K_c = K_m + \frac{\phi_f}{\frac{1}{K_f - K_m} + \frac{3\phi_m}{3K_m + 4G_m}} \tag{6.14}$$

Substitution of these upper and lower bounds into equation (6.6) yields the following bounds for the effective thermal expansion coefficients of an isotropic composite of arbitrary geometry:

$$\alpha_c^{(-)} = \alpha_f - \frac{(\alpha_f - \alpha_m)K_m(3K_f + 4G_f)\phi_m}{K_f(3K_m + 4G_f) + 4(K_m - K_f)G_f\phi_m} \tag{6.15}$$

$$\alpha_c^{(+)} = \alpha_m - \frac{(\alpha_m - \alpha_f)K_f(3K_m + 4G_m)\phi_f}{K_m(3K_f + 4G_m) + 4(K_f - K_m)G_m\phi_f} \tag{6.16}$$

It should be noted that the lower bound on bulk modulus (equation (6.14)) yields the upper bound on the thermal expansion coefficient (equation (6.16)), and vice versa. [18]

Humidity Expansion

Generally, the analytical treatment of moisture-induced expansion in polymer matrix composites is similar to the temperature effects.[22,23] In other words, the humidity expansion coefficient (HEC) is analytically analogous to the coefficient of thermal expansion (CTE).[24] This approach serves as a first approximation to the calculation of HEC. In some literature it has also been called the coefficient of moisture expansion (CME) [23,25], the hygral expansion coefficient [26], or the coefficient of hygroelasticity [27]. Thus, based on the above equations for the thermal expansion

behavior, the effective linear humidity expansion coefficient for the particulate-filled polymer composite can be predicted from the following set of equations:

Rule of Mixtures

$$\beta_c = \beta_f \phi_f + \beta_m \phi_m \tag{6.17}$$

where β_c, β_f, and β_m are the coefficients of humidity expansion of the composite, particulate filler, and matrix, respectively.

Turner's Equation

$$\beta_c = \frac{\beta_f \phi_f K_f + \beta_m \phi_m K_m}{\beta_f K_f + \beta_m K_m} \tag{6.18}$$

Kerner's Equation

$$\beta_c = \beta_m - (\beta_m - \beta_f)\phi_f \left[1 + \frac{(1-\phi_f)(K_f - K_m)}{K_m(1-\phi_f) + K_f \phi_f + \frac{9}{8} K_f K_m^2 \frac{(1-2\nu_m)}{(1+\nu_m)}} \right] \tag{6.19}$$

Levin's Equation

$$\beta_c = \beta_m - (\beta_m - \beta_f)\phi_f \left[1 + \frac{(1-\phi_f)(K_f - K_m)}{K_m(1-\phi_f) + K_f\phi_f + \frac{K_f(1+\nu_m)}{2(1-2\nu_m)}} \right] \tag{6.20}$$

Hashin and Shtrikman's Equations

$$\beta_c^{(-)} = \beta_f - \frac{(\beta_f - \beta_m)K_m(3K_f + 4G_f)\phi_m}{K_f(3K_m + 4G_f) + 4(K_m - K_f)G_f\phi_m} \tag{6.21}$$

$$\beta_c^{(+)} = \beta_m - \frac{(\beta_m - \beta_f)K_f(3K_m + 4G_m)\phi_f}{K_m(3K_f + 4G_m) + 4(K_f - K_m)G_m\phi_f} \tag{6.22}$$

Experimental

Humidity Expansion

The in-plane humidity expansion coefficient (HEC) was determined using a Dupont TMA 2940 equipped with a relative humidity generator to measure uniaxial humidity swelling strains in the planar direction of the films. Relative humidity was generated and controlled using saturated binary aqueous salt solutions which was described in chapter 2. A schematic of the apparatus is shown in Figure 6.2. The system

consists of three main parts which are: the relative humidity generator, the TMA, and the control and output unit. This set-up allows one to measure length changes as a function of time at various relative humidities under isothermal condition at room temperature. A small force of 0.001N was applied to the uniaxial sample with dimensions of 5 mm wide, 25 mm long, and 10 μm thick.

Initially, the sample was dried at 0% RH until no further length change was observed. Then 30% RH was introduced into the system and the length increase as a function of time was monitored. After equilibrium was reached, the sample was then subjected to a higher relative humidity, and again the length change at each relative humidity was determined. The swelling strain was then calculated as the length change due to humidity exposure divided by the initial length of the sample. A plot of humidity swelling strain at equilibrium vs. relative humidity was generated. The slope of the curve is considered the humidity expansion coefficient.

Thermal Expansion

The in-plane coefficient of thermal expansion (CTE) was measured using a TMA 2940 from TA Instruments under a nitrogen purge with a typical flowrate of approximately 80 ml/min and at a heating rate of 5°C/min. Similar to the humidity expansion experiment, a thin ribbon sample of 5 mm wide, 25 mm long, and 10 μm thick was subjected to a small constant force of 0.001N prior to start heating.

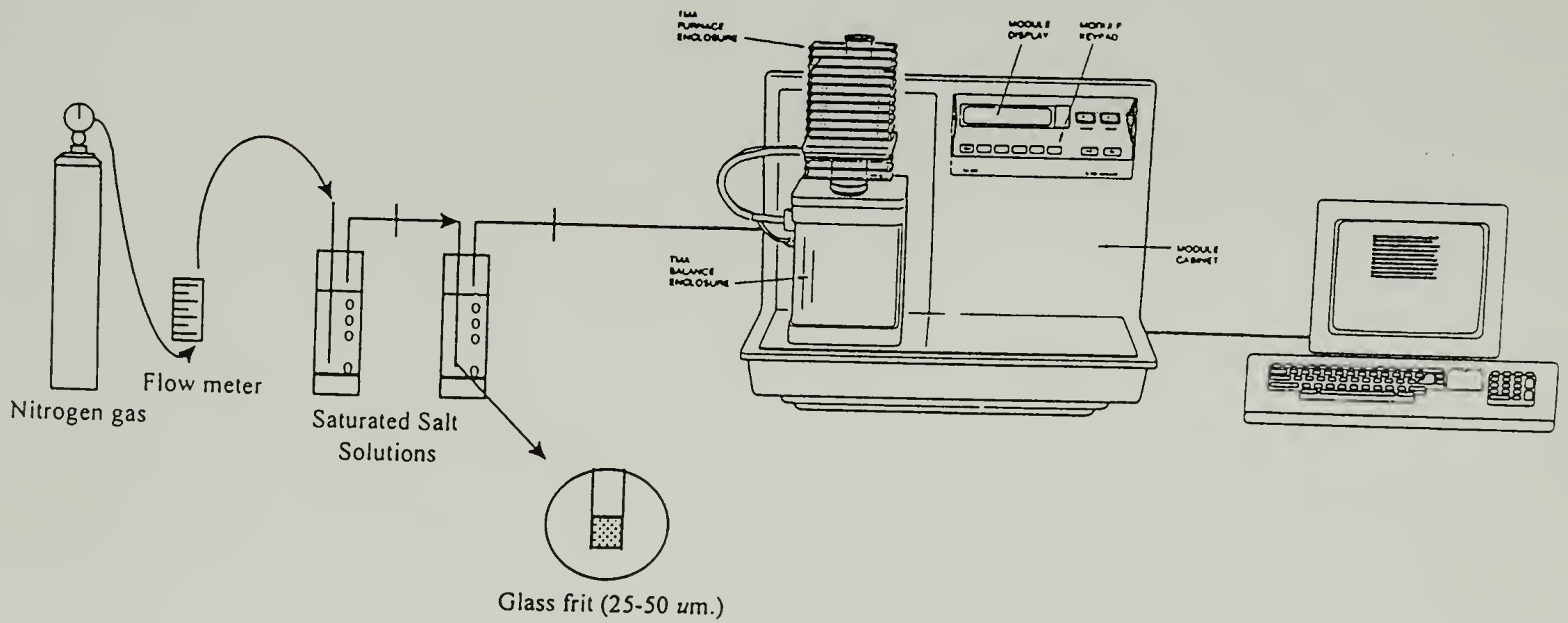

Figure 6.2 : Schematic of Thermomechanical Analyzer equipped with a relative humidity generator employed to measure the in-plane uniaxial humidity swelling strain.

Results and Discussion

Humidity Expansion Coefficients

The in-plane humidity expansion coefficients were determined for gelatin and PET by monitoring the swelling strain as a function of time at various relative humidities. Figure 6.3(a) and (b) represent respectively the characteristic absorption and desorption curves for pure gelatin film (BF8483-133). As Figure 6.3(a) and (b) indicate, the swelling strain increases with increasing relative humidity, and vice versa. Gelatin-latex and PET films also show similar characteristics.

Figure 6.4(a) and (b) present typical swelling strain vs. relative humidity curves during moisture absorption for gelatin (BF8483-133) and PET, respectively. These curves were generated from the equilibrium swelling strain vs. time. Because of the independence of the humidity expansion coefficient and tensile modulus on direction in the plane, it was determined that the gelatin is an in-plane isotropic material. However, this is not the case for PET film. As indicated in Figure 6.4(b), due to the tenter frame processing, PET is an anisotropic material; thus, its humidity swelling strains are different in the machine (MD) and transverse (TD) directions. The samples were prepared along the processing axes of the PET which are oriented parallel (MD) and perpendicular (TD) to the gelatin coating direction.

Table 6.1 summarizes the in-plane humidity expansion coefficients for gelatin (BF 8483-133), PET, and gelatin coated on PET. The humidity expansion coefficients for unsupported gelatin (i.e., gelatin removed from the substrate) and PET differ by an

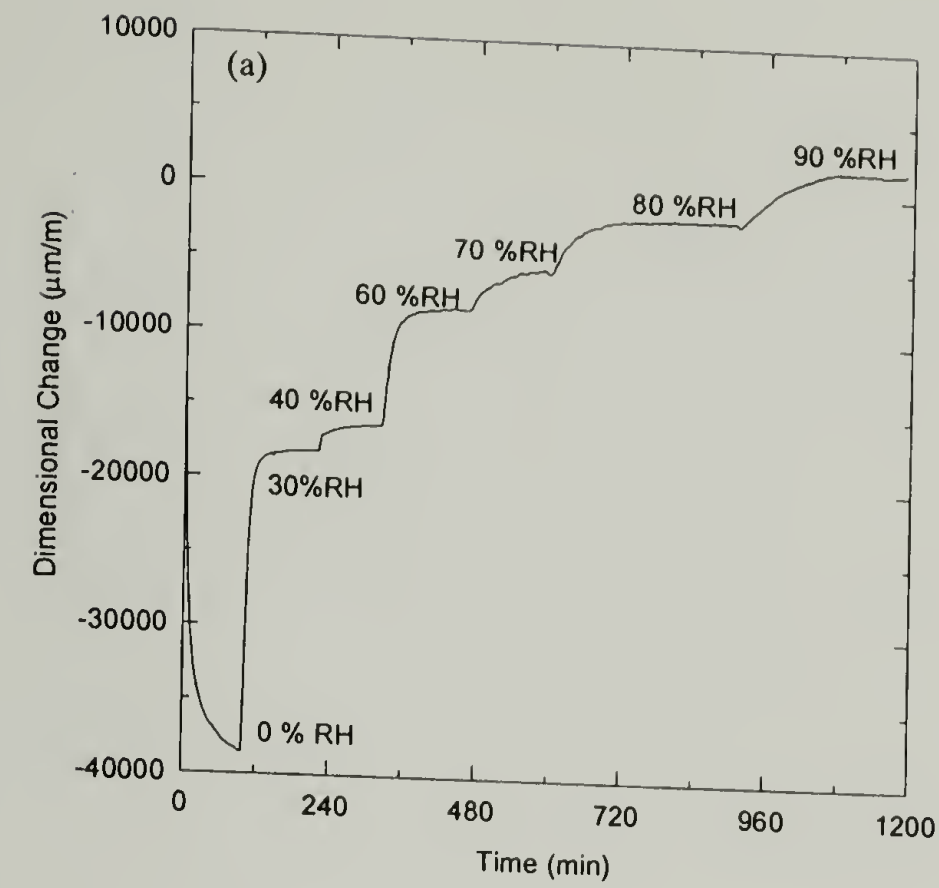

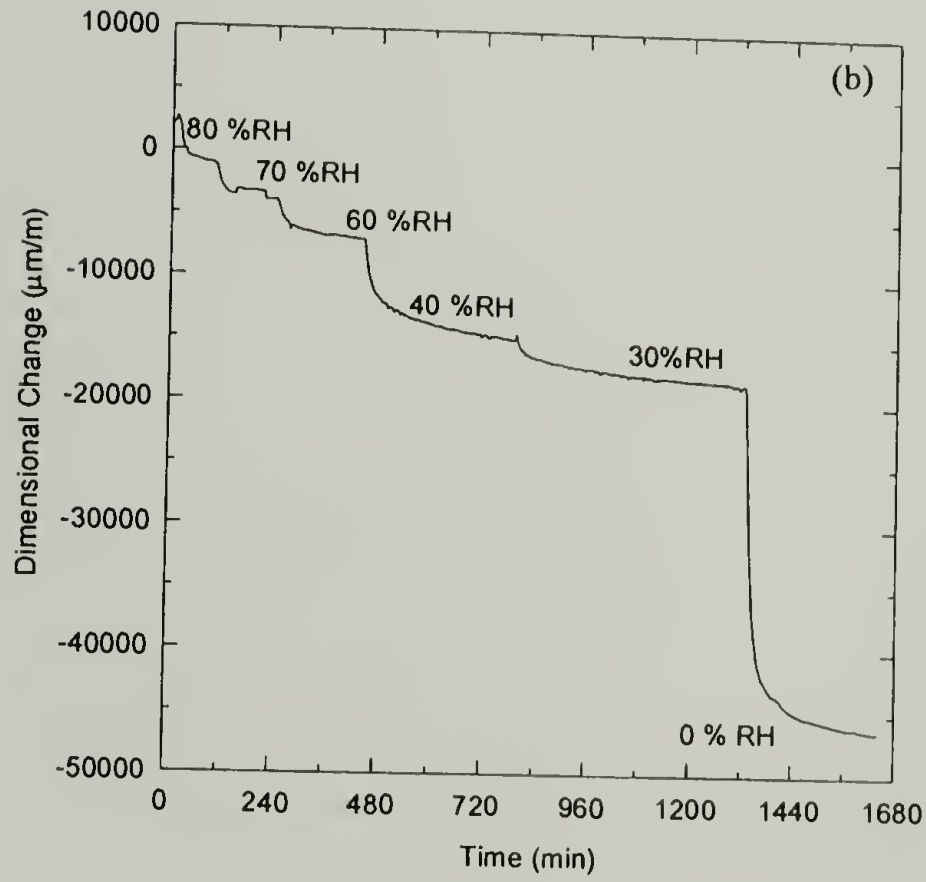

Figure 6.3 : Characteristic dimensional changes as a function of time at various relative humidities for pure gelatin film (BF 8483-133) through an (a) absorption and (b) desorption cycle.

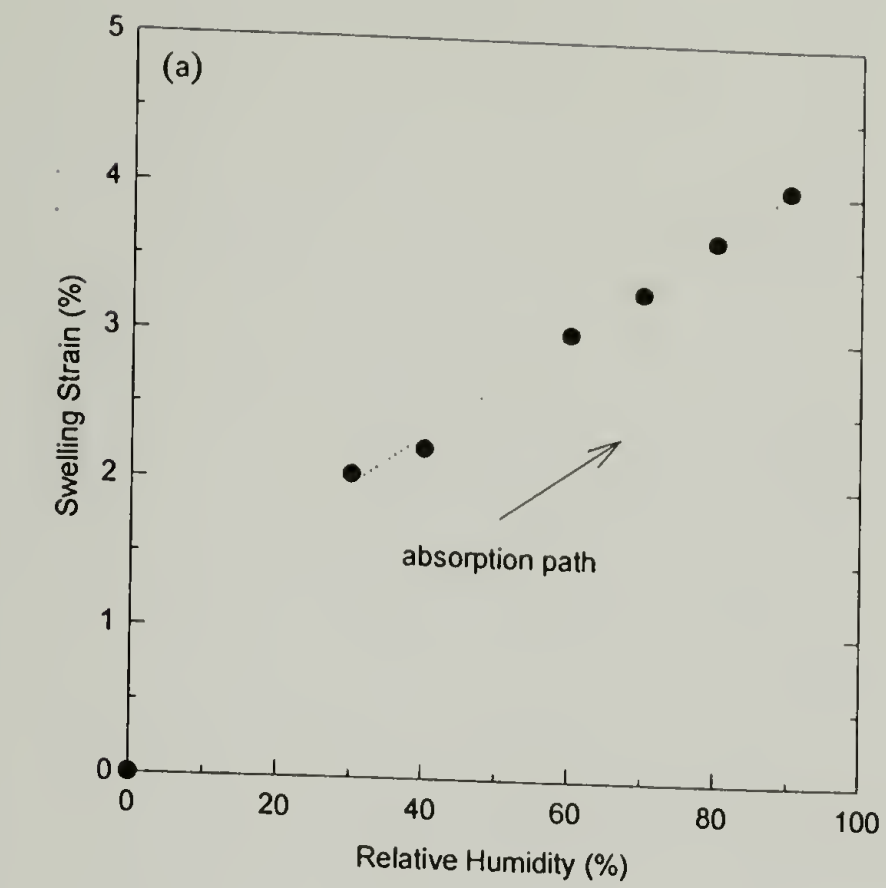

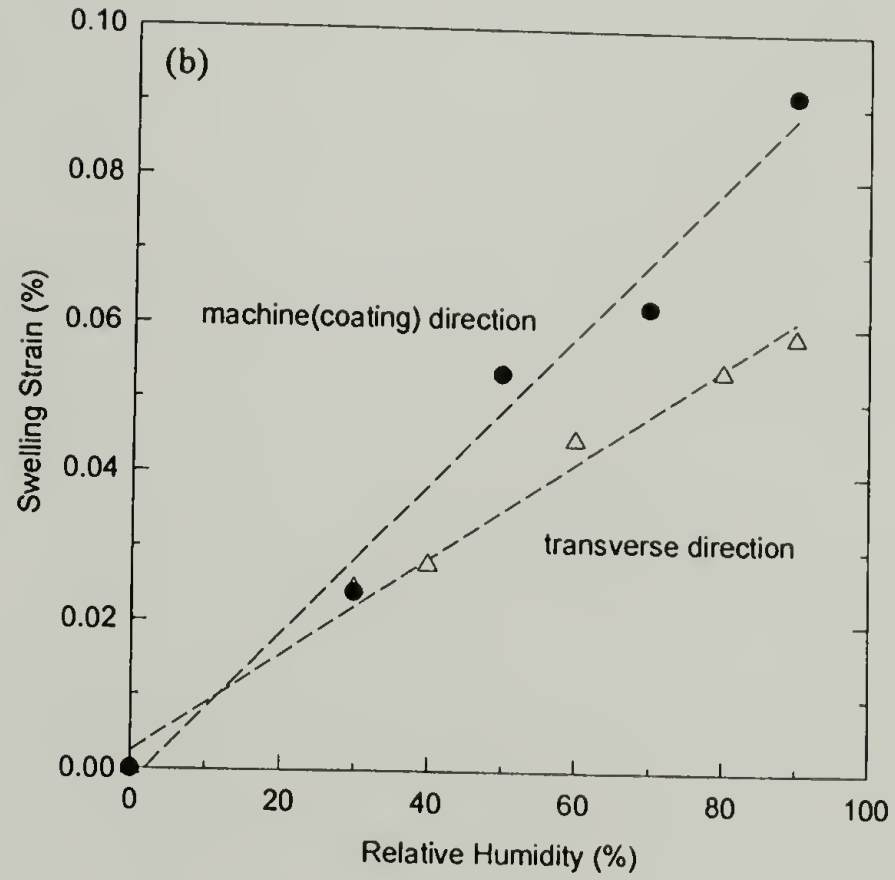

Figure 6.4 : Typical swelling strain vs. relative humidity curves during moisture absorption for (a) gelatin film (BF 8483-133) and (b) PET film, respectively.

Table 6.1 : Summary of the Humidity Expansion Coefficients for Gelatin Film (BF 8483-133) and PET Substrate

Material	Sorption Path	Humidity Range(%)	HEC (β) (μm/m%RH)
Pure Gelatin (BF 8483-133)	absorption desorption	30-90 30-90	343 340
PET (MD) PET (TD)	absorption absorption	30-90 30-90	10.5 5.97
Gelatin & PET (MD)	absorption	30-70	18.4

order of magnitude along the gelatin coating direction. This is due to the lower water absorption and greater stiffness of the PET substrate.[1] It is this mismatch that causes the bending moment in a bilayer system of gelatin and PET. In addition, the HEC of the unsupported gelatin is greater than that of the gelatin coated on PET. This would imply that the PET substrate assists in decreasing the dimensional instability of the gelatin caused by the humidity exposure. This is expected and has been observed by others.[2] Obviously, the anisotropy of the PET is confirmed by the dependence of the humidity expansion coefficient on the direction. The HEC for an uniaxial PET film parallel to the gelatin coating direction (MD) is greater than that perpendicular to the gelatin coating

direction. For the unsupported gelatin, the absorption HEC is greater than the desorption HEC. The difference between the absorption and desorption swelling characteristics for gelatin has been published although the dependence of the HEC on the sorption path was not noted.[2,4,6] The photographic industry customarily determines the humidity expansion coefficient from the absorption path of the cycle.[2]

Latex Concentration vs. Humidity Expansion Coefficients. Table 6.2 shows the effect of latex concentration on the humidity expansion coefficients of the gelatin films. In both latex systems, the HEC is reduced with increase in the latex concentration; the film with higher latex concentration offers greater resistance to the humidity expansion. Consequently, pure gelatin film yields the highest HEC, while gelatin films with 40 parts latex show the lowest HEC.

Table 6.2 : Effect of Latex Concentration on the Humidity Expansion Coefficient

ID	Description	Latex Conc (parts)	Humidity Range (%)	HEC (μm/m%RH)	
				Absorption	Desorption
BF 8483-133	gelatin-PEA	0	30-90	343 ± 5	341 ± 4
BF 8483-43		20	30-80	320 ± 3	295 ± 5
BF 8505-372		40	30-80	297 ± 4	250 ± 5
BF 8483-133	gelatin-PEMA	0	30-90	343 ± 5	341 ± 4
BF 8483-163		20	30-80	305 ± 6	275 ± 6
BF 8505-412		40	30-80	274 ± 4	252 ± 3

Figure 6.5 and 6.6 present the experimental results of the humidity expansion coefficients in comparison with those predicted from equations (6.17) through (6.20) for the gelatin-PEA and gelatin-PEMA films, respectively. The theoretical curves have been calculated using values presented in Table 6.3 for the properties of the PEA and PEMA fillers and gelatin matrix.

Table 6.3 : Material Properties Used in the Calculation of the Humidity Expansion Coefficient

Properties	Gelatin	PEA	PEMA
β (μm/m %RH)	343	[a]50	[a]50
K (GPa)	5.50	2.30	3.88
ν	[b]0.37	-	-

[a] value regenerated from the literature [28]
[b] reported value [6]

It is very clear from Figure 6.5 and 6.6 that the experimental data for the humidity expansion coefficients in two systems are in excellent agreement with the model prediction based on modulus-modified rules of mixtures or Turner's equation (equation (6.18)). The decrease in the HEC owing to the presence of the latex particles in the gelatin film can be explained by the moisture sorption behavior. Both latices are less hydrophilic than gelatin; thus, the amount of absorbed moisture in the emulsion layer decreases when latex is introduced into the system. As a result, the HEC of gelatin-latex film is less than that of the pure gelatin film.

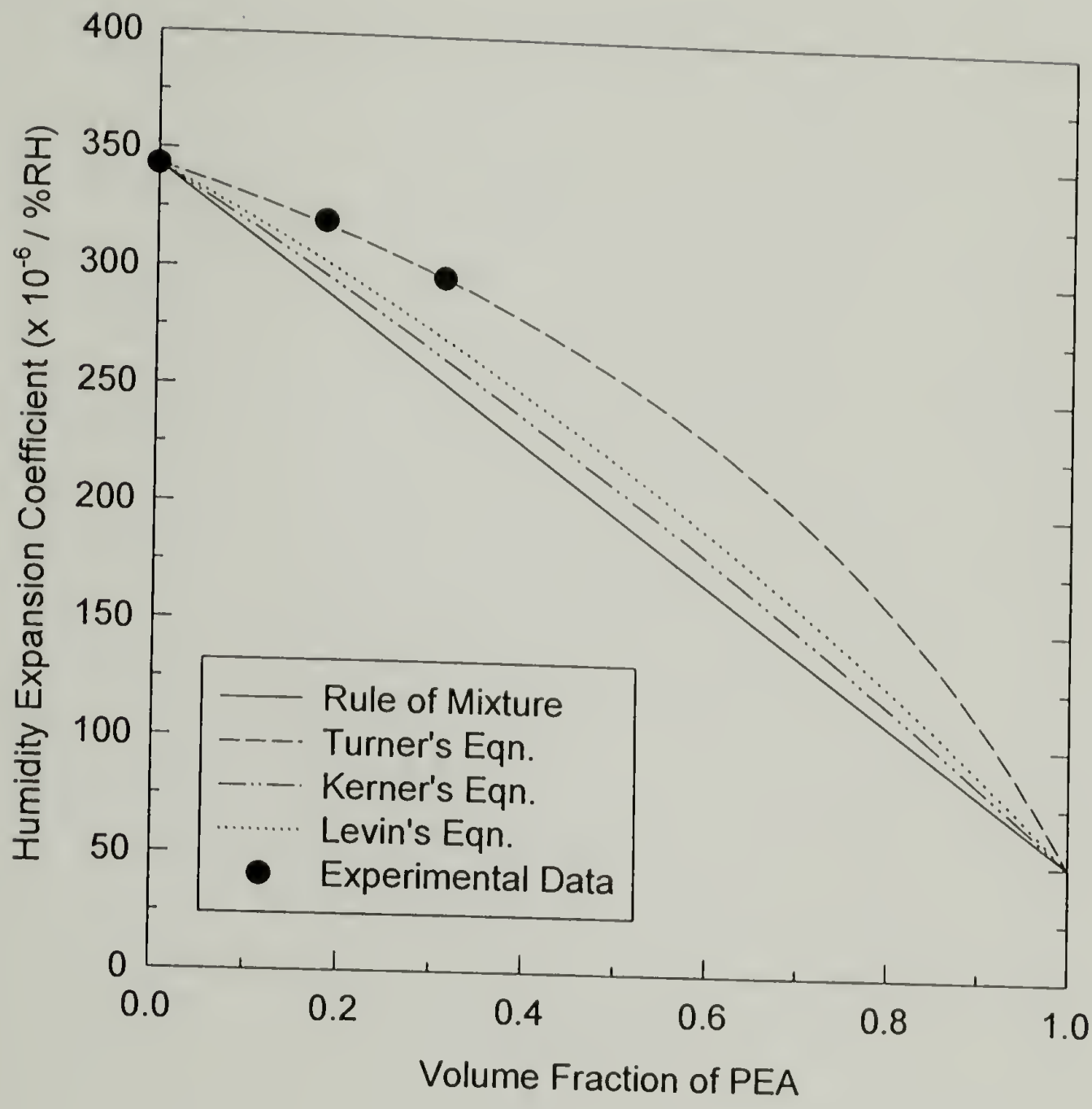

Figure 6.5 : Comparison of the experimental data with the theoretieal predietions for the humidity expansion eoefficient of a gelatin-PEA system : Rule of mixture (equation (6.17)), Turner's equation (equation (6.18)), Kerner's equation (equation (6.19)), and Levin's equation (equation (6.20)).

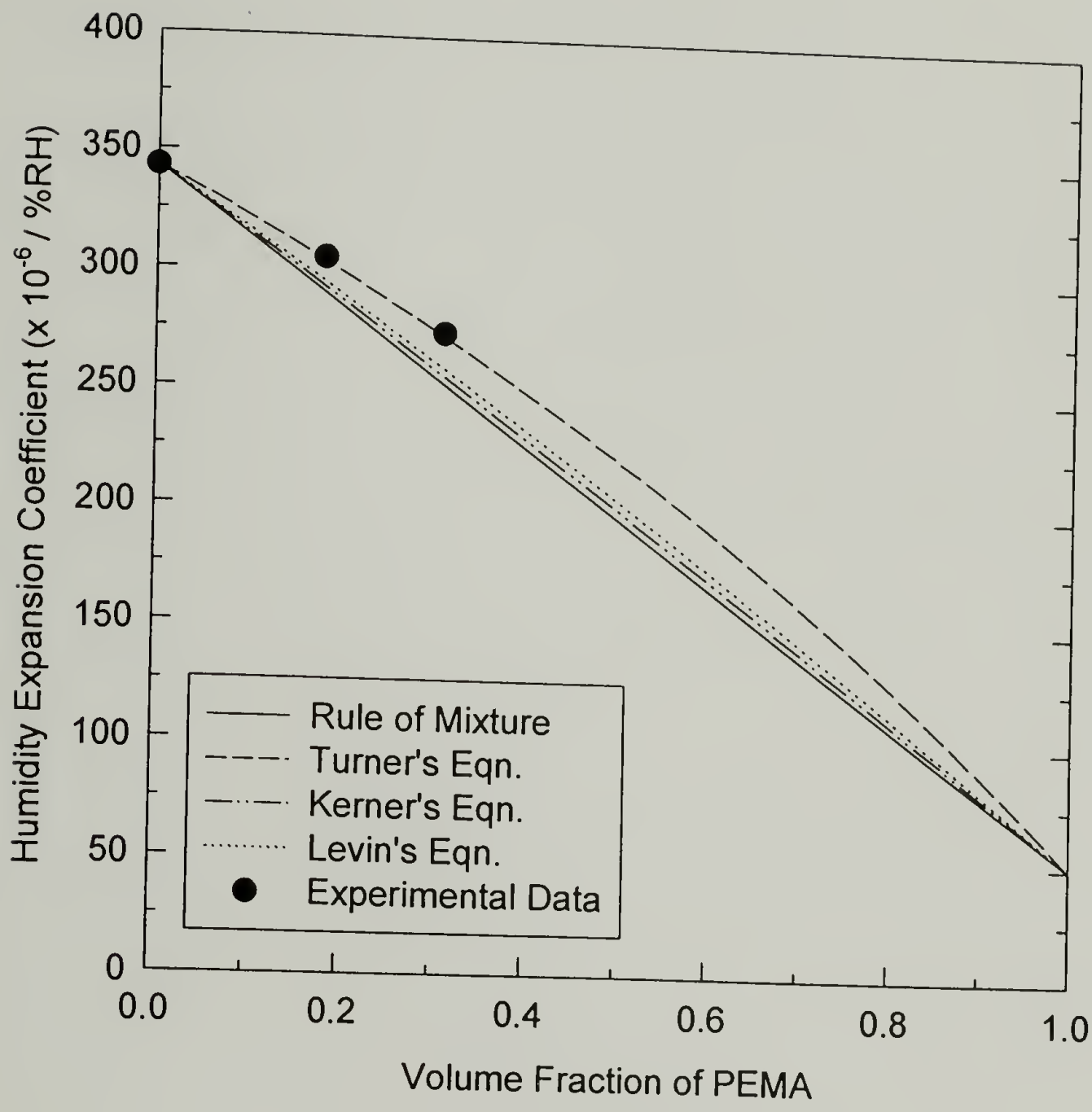

Figure 6.6 : Comparison of the experimental data with the theoretical predictions for the humidity expansion coefficient of a gelatin-PEMA system : Rule of mixture (equation (6.17)), Turner's equation (equation (6.18)), Kerner's equation (equation (6.19)), and Levin's equation (equation (6.20)).

Latex Particle Size vs. Humidity Expansion Coefficients. As presented in Table 6.4, the humidity expansion coefficients of both PEA and PEMA systems are unaffected by the latex particle size.

Gelatin Concentration at Set Point vs. Humidity Expansion Coefficients. The effect of gelatin concentration at set point on the humidity expansion coefficients of the pure gelatin and gelatin-latex films is given in Table 6.5. The HEC of gelatin decreases with increasing the gelatin concentration at set point. This result correlates well with their moisture absorption behavior presented in chapter 3 (Figure 3.9). Since the films with 10% gelatin can absorb more moisture than the films with 15% gelatin; as a result, their HECs are greater than those of the films with 15% gelatin concentration.

Drying Concentration at Vitrification vs. Humidity Expansion Coefficients. The drying condition also influences the humidity expansion coefficients of both pure gelatin and gelatin-latex films. As shown in Table 6.6, the HEC of the films dried at the HMERH condition (80F / 29% RH) is greater than that of the films dried at the LMERH condition (130F / 5.5% RH). Again, this observation can be explained in term of their difference in the ability to absorb moisture. Analogous to the effect of gelatin concentration on the HEC of the gelatin, the moisture uptake of the films dried under the HMERH condition has higher moisture uptake than the material dried under the LMERH condition (Table 3.2); therefore, the films dried at HMERH yield lower resistance to the humidity expansion.

Table 6.4 : Effect of Latex Particle Size on the Humidity Expansion Coefficient

ID	Description	Latex Size (μm)	Humidity Range (%)	HEC (μm/m%RH)	
				Absorption	Desorption
BF 8483-173	gelatin-PEA	0.051	30-90	319 ± 4	245 ± 8
BF 8483-43		0.112	30-80	320 ± 3	295 ± 5
BF 8483-123	gelatin-PEMA	0.067	30-90	291 ± 7	231 ± 9
BF 8483-163		0.15	30-80	305 ± 6	275 ± 6

Table 6.5 : Effect of Gelatin Concentration at Set Point on the Humidity Expansion Coefficient

ID	Description	Gelatin Conc (%)	Humidity Range (%)	HEC (μm/m%RH)	
				Absorption	Desorption
BF 8483-133	pure gelatin	10	30-90	343 ± 5	341 ± 4
BF 8483-83		15	30-90	255 ± 6	238 ± 6
BF 8483-173	gelatin-PEA	10	30-90	319 ± 4	245 ± 8
BF 8505-482		15	30-80	290 ± 6	240 ± 5
BF 8483-123	gelatin-PEMA	10	30-80	291 ± 7	231 ± 9
BF 8483-93		15	30-80	217 ± 7	170 ± 8

Table 6.6 : Effect of Drying Condition at Vitrification on the Humidity Expansion Coefficient

ID	Description	Drying Condition	Humidity Range (%)	HEC (μm/m%RH)	
				Absorption	Desorption
BF 8483-133	pure gelatin	HMERH	30-90	343 ± 5	341 ± 4
BF 8483-143		LMERH	30-90	293 ± 9	244 ± 5
BF 8483-173	gelatin-PEA	HMERH	30-90	319 ± 4	245 ± 8
BF 8483-183		LMERH	30-90	270 ± 8	259 ± 7
BF 8483-123	gelatin-PEMA	HMERH	30-80	291 ± 7	231 ± 9
BF 8483-113		LMERH	30-90	246 ± 5	164 ± 7

Similar to the data presented in Table 6.1, as indicated in Table 6.2 and Table 6.4 through 6.6, the absorption HEC in every case is greater than the desorption HEC. In addition, it is also interesting to note that the HECs of gelatin-PEA films are greater than those of gelatin-PEMA films, even though their moisture absorption are less than that of the gelatin-PEMA films (Figure 3.8). These results imply that the moisture absorption behavior alone is not sufficient to explain the HEC results.

Recall from equation (6.18) through (6.21) that the HEC of the composite material is expressed in term of both the HEC and the bulk modulus of each component. Thus, in the case of gelatin-latex films it is reasonable to state that not only the moisture absorption behavior but also the stiffness of the latex has to be considered.

As shown in chapter 2, PEMA has a greater bulk modulus than PEA, this leads to the greater stiffness in the gelatin-PEMA film. Supportive evidence is also presented in chapter 5 that the gelatin-PEMA films have higher tensile modulus than the gelatin-PEA films. As a result, the gelatin-PEMA films have higher resistance to the humidity expansion (i.e. lower HEC) than the gelatin-PEA films. In other words, the greater moisture absorption of the gelatin-PEMA films is dominated by its greater stiffness.

In summary, in order to obtain the film with low HEC, which is the desirable property, the latex should have low moisture absorption and high bulk stiffness so that it can resist the dimension change due to the humidity exposure. However, in the case of pure gelatin vs. gelatin-latex films, it has been shown that the greater stiffness of the pure gelatin is dominated by its greater moisture absorption; consequently, the pure gelatin films have higher in HEC values. In contrast to the case of gelatin-PEA vs. gelatin-PEMA, the HEC has been shown to depend upon the stiffness of the film. Another factor is adhesion. If the stresses are high enough, the particles debond creating voids which greatly complicates the swelling.

Dimensional Hysteresis

Figure 6.7 presents the typical dimensional hysteresis observed between the absorption and desorption swelling strains for the unsupported gelatin. This particular sample was of gelatin-PEA film (BF 8483-173). As seen in Figure 6.7, the desorption path was greater than the absorption path. This behavior is similar to the moisture

sorption hysteresis of gelatin (Figure 3.7) and suggests that the dimensions of the film at any given relative humidity are dependent upon the direction from which that humidity is approached. Similar results can also be found in the literature.[2,6]

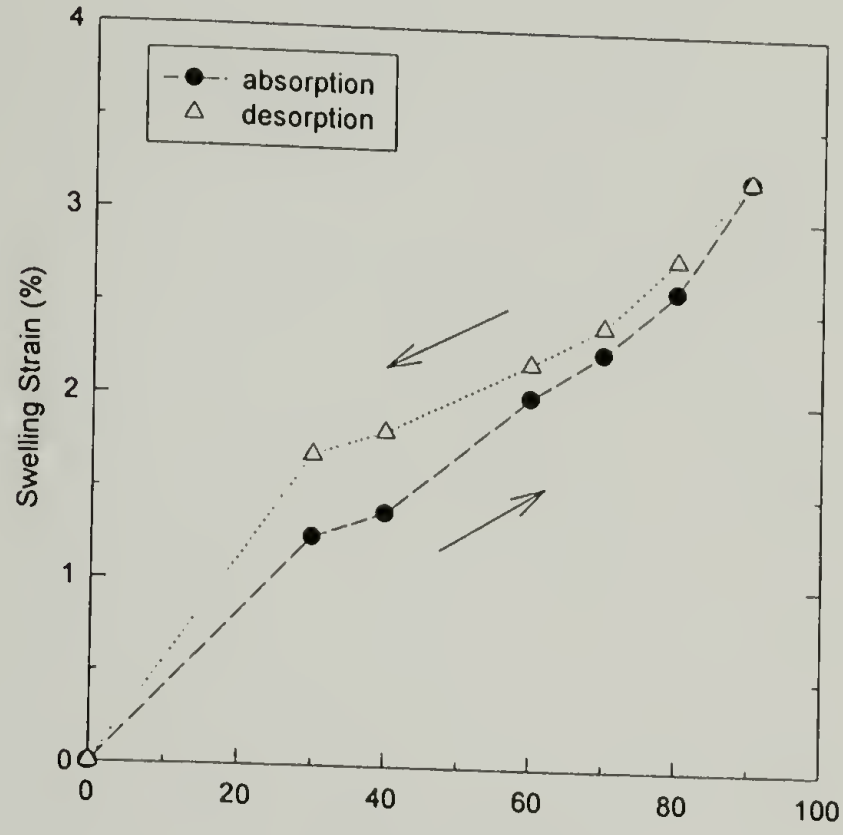

Figure 6.7 : Dimensional hysteresis for the unsupported gelatin-PEA film (BF 8483-173).

However, not all of the gelatin samples behave in this way. Figure 6.8(a) and (b) show a "reversed dimensional hysteresis" for gelatin-PEA (BF 8505-372) and gelatin-PEMA (BF 8483-412), respectively. That is, the absorption swelling strain falls above the desorption swelling strain. The absorption curve exhibits a drop between 80% and 90% RH. This behavior is opposite to the moisture sorption hysteresis (Figure 3.7) and also opposite to the normal dimensional hysteresis (Figure 6.7) for unsupported gelatin film.

The result here is not uncommon and has been reported by others as well.[2,4] The reason for this behavior has been explained as being due to the moisture -induced relaxation shrinkage at the high conditioning relative humidity of the gelatin.[2]

Figure 6.9(a) and (b) represent the TMA profiles corresponding to the reversed dimensional hysteresis for unsupported gelatin-PEA (BF 8505-372) and gelatin-PEMA (BF 8483-412), respectively. It is clear from these curves that the gelatin-latex films show relaxation as a function of time at 90% RH. In fact, the films first lengthen as the moisture is absorbed and then shrink over a period of time until it reaches equilibrium. This is because when the gelatin layer coated on substrate is dried, most of the lateral shrinkage is confined by the substrate. In other words, the gelatin molecules remain extended. However, when the gelatin layer is peeled off the substrate and rehumidified, especially at a high relative humidity where the Tg is near room temperature [29], the gelatin molecules are free to contract because the internal viscosity of gelatin is lowered enough for the extended molecules to move. As a result, the gelatin layer shrinks to its preferred position. In fact, this relaxation shrinkage is analogous to that observed by Leaderman [30] when a cellulose filament is stretched while wet and dried under tension. When rewetted, the filament shrinks. He describes this phenomenon as "swelling recovery".

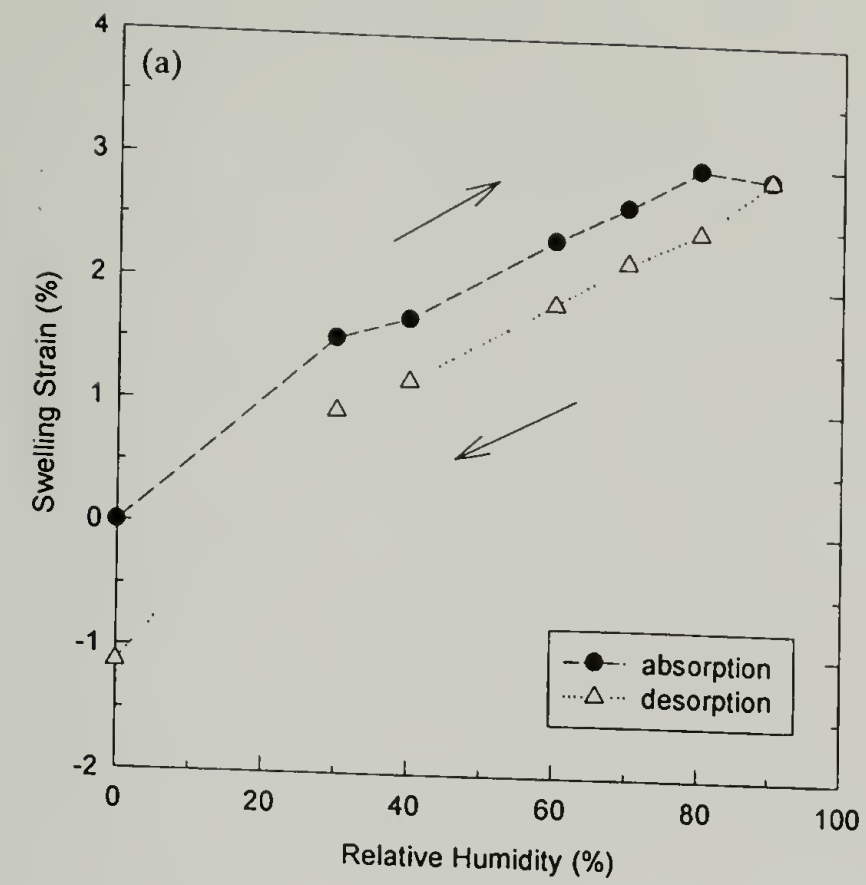

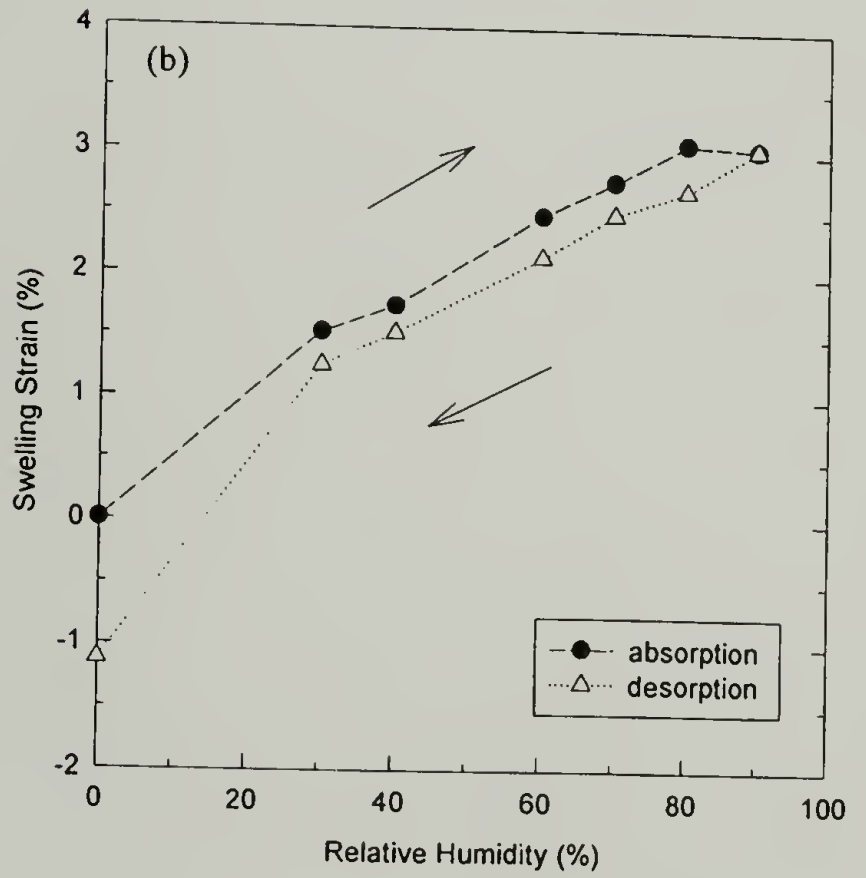

Figure 6.8 : Reversed dimensional hysteresis for (a) gelatin-PEA (BF 8505-372) and (b) gelatin-PEMA (BF 8483-412) films, respectively.

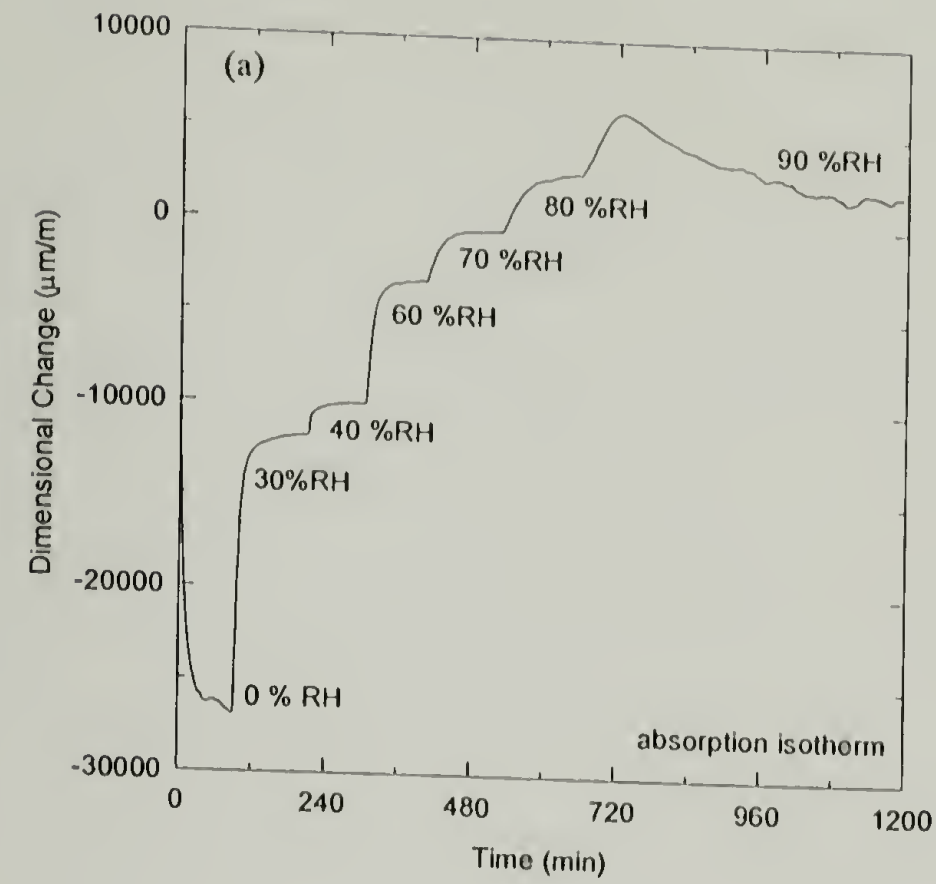

Figure 6.9 : Dimensional changes as a function of time for (a) gelatin-PEA (BF 8505-372) and (b) gelatin-PEMA (BF 8483-412) films through an absorption path corresponding to the reversed dimensional hysteresis presented in Figure 6.8.

Thermal Expansion Coefficients

Figure 6.10(a) and (b) represent the thermal expansion behavior of PET and gelatin, respectively. As seen in Figure 6.10(a), the PET substrate, like most of the materials, expands when the temperature increases and contracts when it decreases. On the other hand, as shown in Figure 6.10(b), gelatin starts contracting rapidly upon heating to 120°C owing to moisture desorption. The second heating and cooling profiles are completely reversible. Gelatin expands upon heating and shrinks upon cooling. The coefficient of thermal expansion (CTE) for gelatin and PET were determined from their second heating profiles. The CTE for pure gelatin is 33 μm/m °C, whereas that for PET is 16.6 μm/m °C. Although as stated earlier that the effect of humidity is greater than the effect of temperature, the mismatch between the gelatin coating and PET substrate's CTE also contributes to the dimensional instability in the bilayer systems studied.

The effect of latex concentration on the thermal expansion coefficient of the gelatin films is shown in Table 6.7. In contrast to the HEC, the coefficient of thermal expansion (CTE) of gelatin-latex film increases as the latex concentration increases. This is because both gelatin and the latex want to expand when heated, especially since the CTE of latex is approximately 75 μm/m °C (from 0 to 38°C) [28] which is greater than that of the gelatin. The greater CTE of the latex promotes the increase in thermal expansion of the emulsion layer. The soft and rubber-like characteristics of latex, particularly for the PEA, has a very high thermal expansion coefficient and causes the very large effect. It should be noted that the particles experience little distortion but

considerable hydrostatic stresses. Hence relaxation in molecular motion is not an issue. Qualitatively, this result is in good agreement with composite theory regarding the thermal expansion of the composite material.

Table 6.8 through Table 6.10 summarize the effect of latex particle size, gelatin concentration at set point, and drying condition at vitrification, respectively, on the thermal expansion behavior. Unlike the humidity expansion coefficients discussed earlier, these parameters have no effect on the thermal expansion coefficients. In addition, no difference between the two latex systems is observed. Both gelatin-PEA and gelatin-PEMA films show the same magnitude for all the CTEs, which are approximately 60 μm/m °C and 90 μm/m °C for the films with 20 parts and 40 parts latex, respectively. It is not surprising because both PEA and PEMA behave similarly as a rubbery material for the calculated temperature range (30-140°C).

Figure 6.11. and 6.12 show the experimental data in comparison with the model predictions for the thermal expansion coefficients of the gelatin-PEA and gelatin-PEMA films, respectively. The calculated curves shown are based on the values presented in Table 6.11 for the properties of the gelatin matrix and PEA and PEMA fillers. The thermal expansion coefficient of rubber is used to calculated the CTE of the gelatin-latex films. This is due to the fact that both latices behave similarly as a rubber-like material at the calculated temperature range (30-140°C).

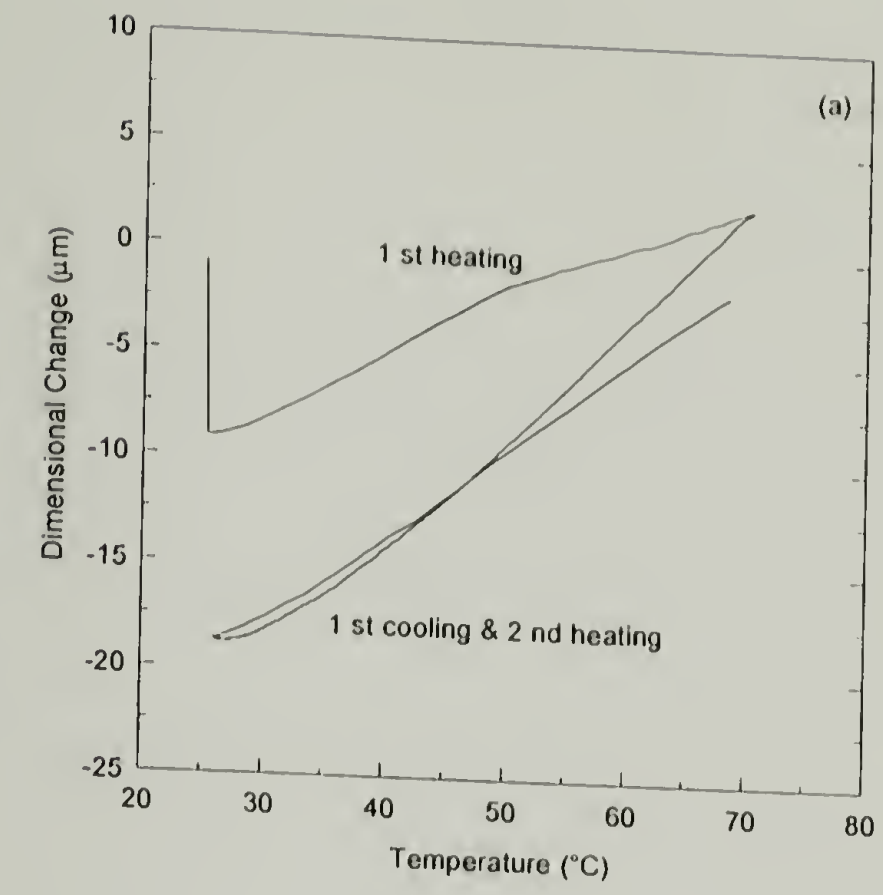

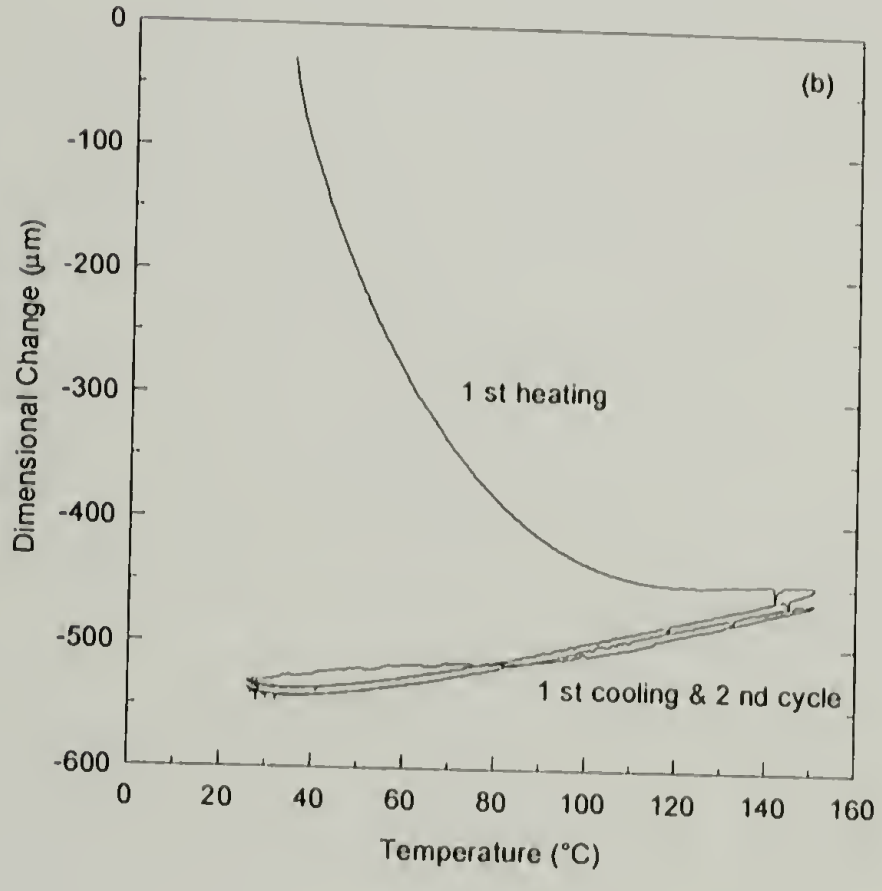

Figure 6.10 : The effect of thermal history on dimensional changes for (a) PET film and (b) gelatin film (BF 8483-143), respectively.

Table 6.7 : Effect of Latex Concentration on the Thermal Expansion Coefficient

ID	Description	Latex Conc (parts)	α (30-140°C) (μm/m°C)
BF 8483-133	gelatin-PEA	0	33
BF 8483-43		20	61.1
BF 8505-372		40	87.2
BF 8483-133	gelatin-PEMA	0	33
BF 8483-163		20	62.4
BF 8505-412		40	89.5

Table 6.8 : Effect of Latex Particle Size on the Thermal Expansion Coefficient

ID	Description	Latex Size (μm)	α (30-140°C) (μm/m°C)
BF 8483-173	gelatin-PEA	0.051	62.4
BF 8483-43		0.112	61.1
BF 8483-123	gelatin-PEMA	0.067	63.1
BF 8483-163		0.15	62.4

Table 6.9 : Effect of Gelatin Concentration at Set Point on the Thermal Expansion Coefficient

ID	Description	Gelatin Conc (%)	α (30-140°C) (μm/m°C)
BF 8483-133	pure gelatin	10	33
BF 8483-83		15	32.6
BF 8483-173	gelatin-PEA	10	62.4
BF 8505-482		15	64.7
BF 8483-123	gelatin-PEMA	10	63.1
BF 8483-93		15	67.3

Table 6.10 : Effect of Drying Condition at Vitrification on the Thermal Expansion Coefficient

ID	Description	Drying Condition	α (30-140°C) (μm/m°C)
BF 8483-133	pure gelatin	HMERH	33
BF 8483-143		LMERH	34.5
BF 8483-173	gelatin-PEA	HMERH	62.4
BF 8483-183		LMERH	65
BF 8483-123	gelatin-PEMA	HMERH	63.1
BF 8483-113		LMERH	63.1

Table 6.11 : Material Properties Used in the Calculation of the Thermal Expansion Coefficient

Properties	Gelatin	PEA	PEMA
α (μm/m °C) K (GPa) ν	33 5.50 [b]0.37	[a]200 2.30 -	[a]200 3.88 -

[a] reported value for rubber [31]
[b] reported value [6]

As can be seen, the experimental data for the thermal expansion coefficients of the gelatin-PEA film are in good agreement with the rule of mixtures (equation (6.2)). As for the gelatin-PEMA system, however, three of the theoretical curves, except the Turner's equation (equation (6.3)), are so close that it is difficult to say which of the equations is best. Nevertheless, the rule of mixture is probably more accurate than any other equation since the experimental points fall much closer to this curve, especially at the higher concentration of latex particle. In both figures, several samples containing 20 parts latex are plotted to show that there is no influence from the latex particle size, gelatin concentration at set point, or drying condition at vitrification on the thermal expansion coefficient of the gelatin-latex film.

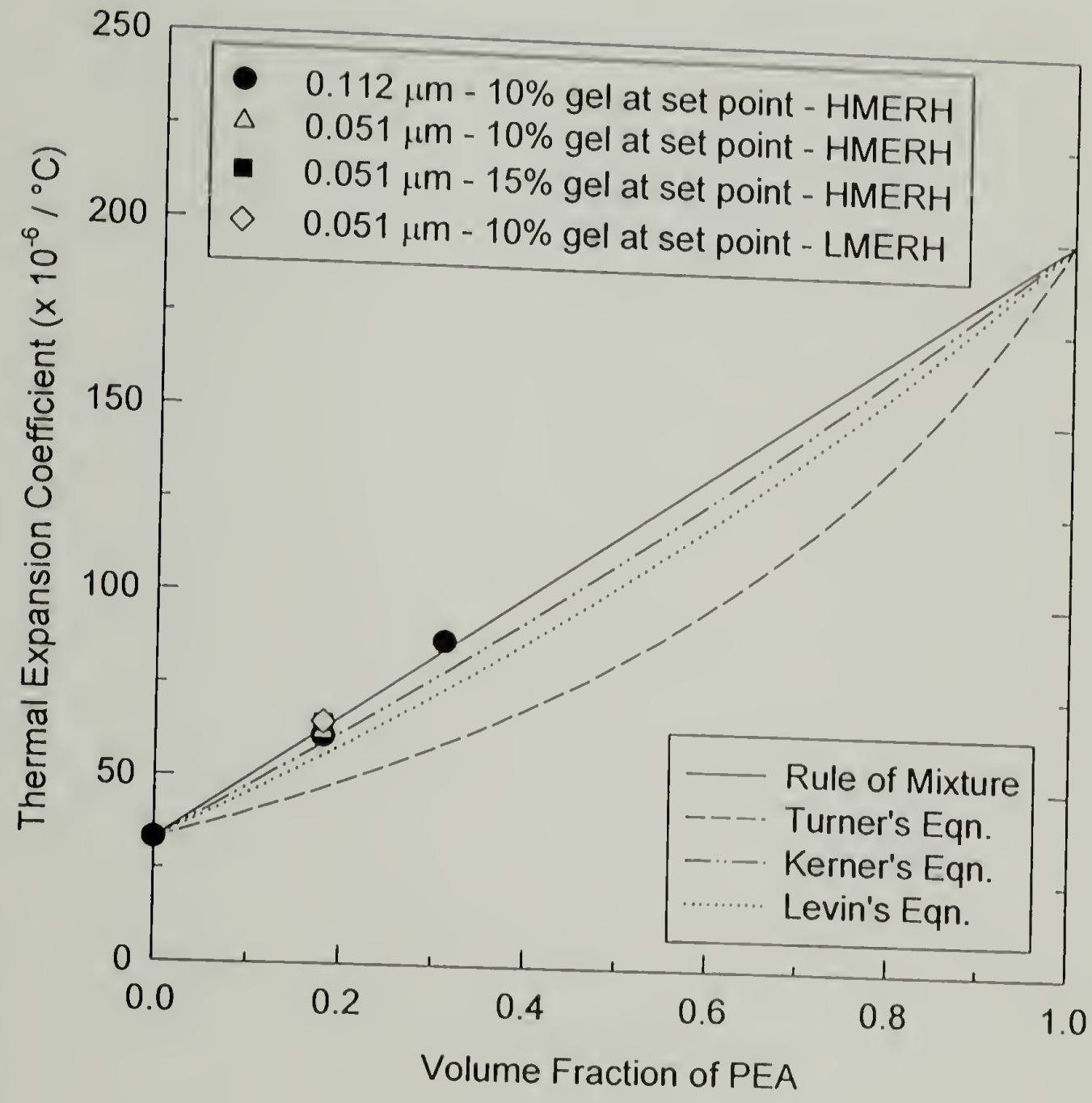

Figure 6.11 : Comparison of the experimental data with the theoretical predictions for the thermal expansion coefficient of a gelatin-PEA system : Rule of mixture (equation (6.2)), Turner's equation (equation (6.3)), Kerner's equation (equation (6.5)), and Levin's equation (equation (6.12)).

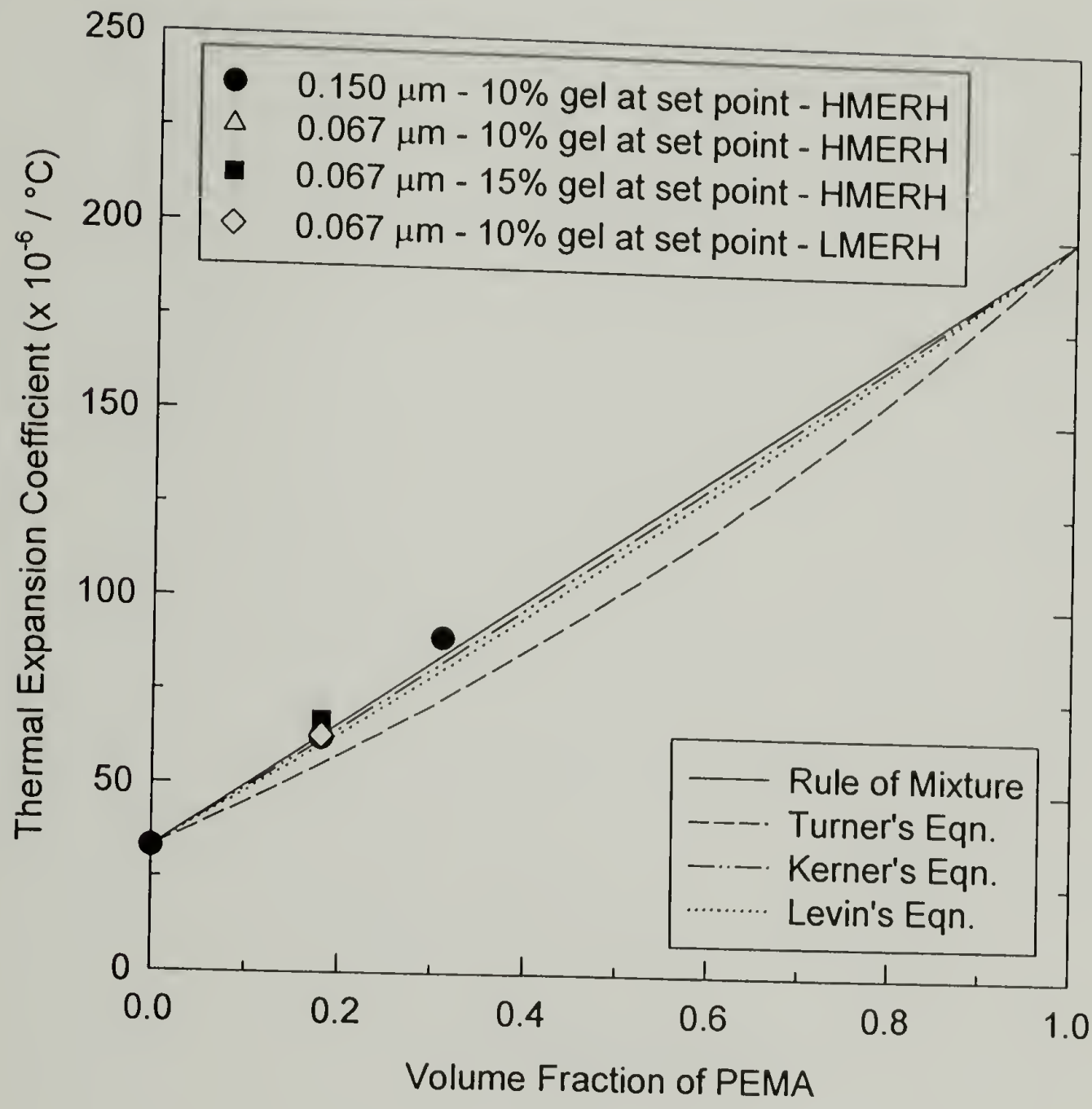

Figure 6.12 : Comparison of the experimental data with the theoretical predictions for the thermal expansion coefficient of a gelatin-PEMA system : Rule of mixture (equation (6.2)), Turner's equation (equation (6.3)), Kerner's equation (equation (6.5)), and Levin's equation (equation (6.12)).

Interesting results occurred when gelatin and PET were heated to temperatures above their glass transition temperatures. As shown in Figure 6.13(a), PET first enlarges as temperature increases and then shrinks when it goes through the Tg. This thermal-induced relaxation shrinkage is analogous to when a rubber is stretched while hot and cooled to low temperatures under tension. When the rubber is reheated after removal of the external stress, it contracts. Also, this phenomenon is somewhat similar to moisture-induced relaxation shrinkage of gelatin at high relative humidity as discussed earlier. In both cases, the polymer molecules are stretched and then "frozen" in a position either by drying or cooling. When they are "unfrozen" at a later time by heat or moisture, the molecules are free to contract to their preferred position. For gelatin, relaxation shrinkage can be induced not only by the moisture but also by the heat, as presented in Figure 6.13(b). Again, gelatin shows an initial contraction as a result of moisture loss. With a further rise in temperature to 200°C, its dimension stays nearly unchanged. However, another contraction is observed at the Tg when gelatin acquires rubber-like elasticity.

Figure 6.14 provides a comparison of the contraction at the Tg of gelatin and gelatin-latex films. Evidently, all the films show a substantial decrease in the dimension at the Tg. It is also clear that the magnitude of this "super contraction" remains unaffected when the latex is introduced into the gelatin film. These results coincide with the investigations by Bourdygina.[32] In his work, low molecular weight compounds, such as glycerol or urea, were shown to decrease the magnitude of super contraction and the Tg of gelatin up to a temperature of 120°C; whereas a polymeric compound like polyethylene glycol did not affect the thermophysical properties of the gelatin film.

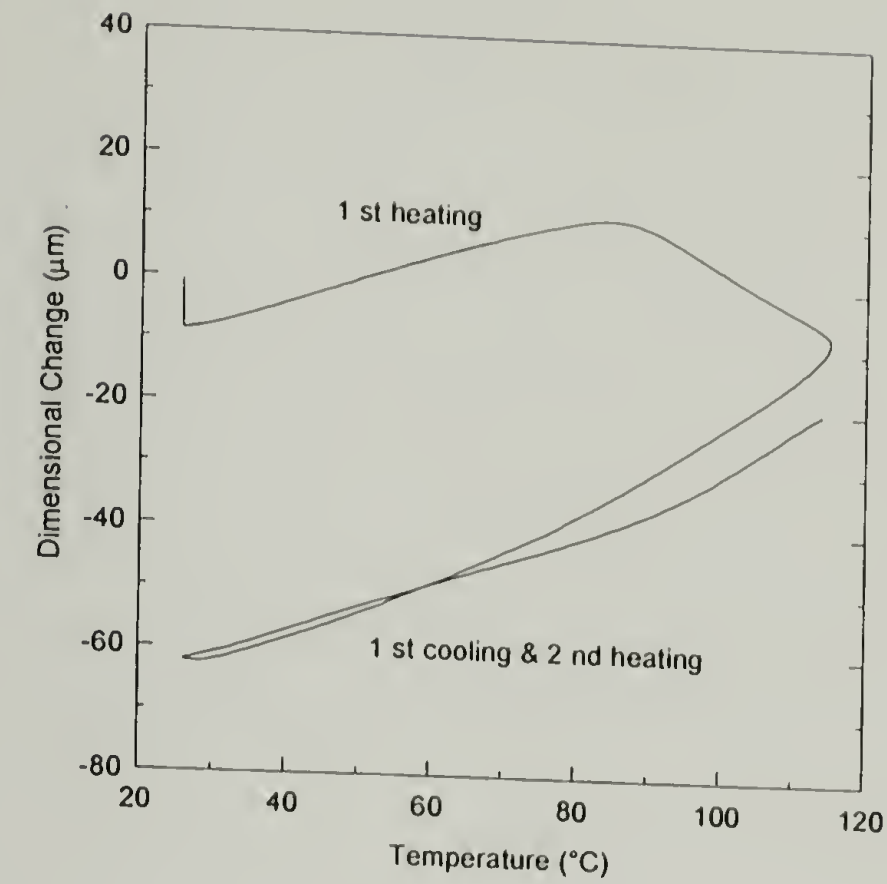

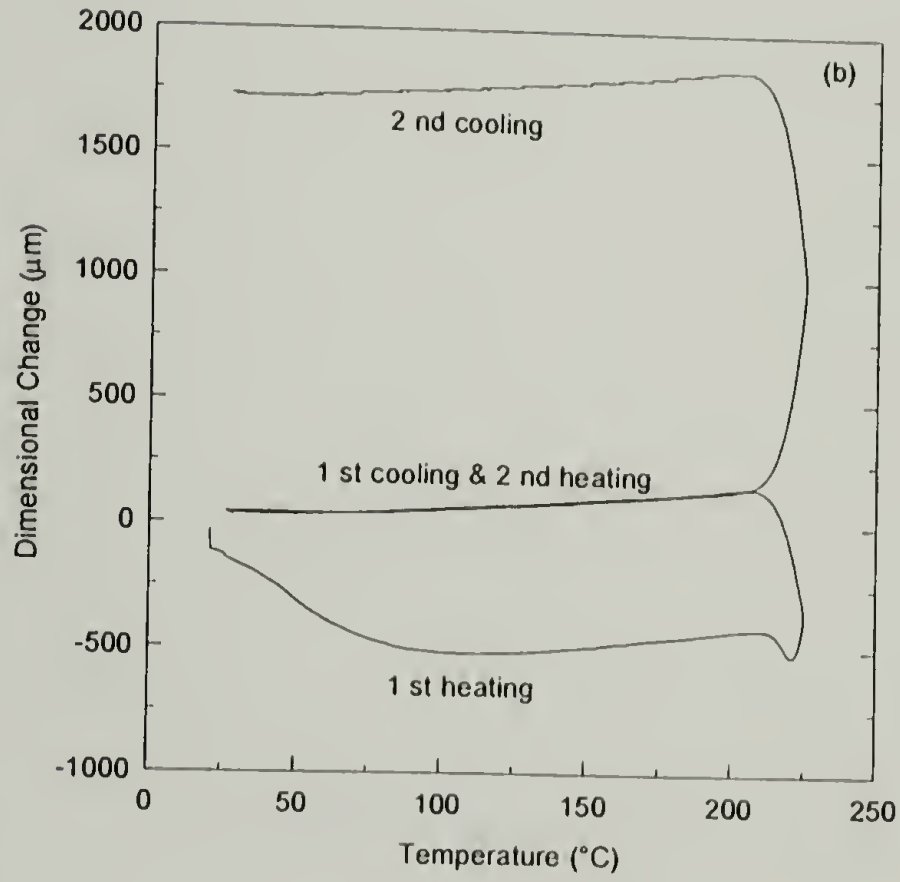

Figure 6.13 : Thermal expansion behavior for (a) PET film and (b) gelatin film (BF 8362-2C) when heated above their glass transition temperatures.

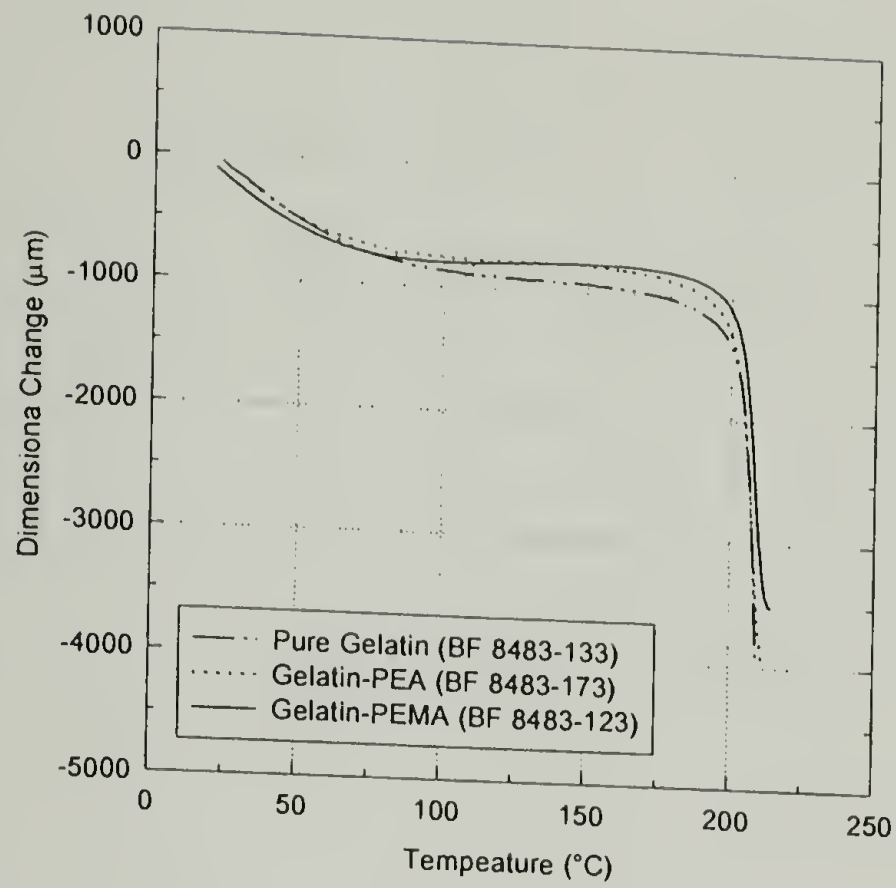

Figure 6.14 : Thermal effect on the dimensional contraction at the glass transition temperature for gelatin and gelatin-latex films.

Conclusions

The effect of moisture and temperature on the dimensional stability of gelatin and PET films were studied. The effect of latex concentration, latex particle size, drying condition at vitrification, and gelatin concentration at set point of the gelatin film were also investigated. Table 6.12 summarizes the in-plane humidity expansion and thermal expansion coefficients of gelatin and the PET substrate. Obviously, it is not only the mismatch of the HEC but also the CTE between the gelatin and PET substrate that contributes to the dimensional instability in a bilayer system.

It is also clear that the effect of humidity on the dimensional change of gelatin is much more pronounced than the effect of temperature. For example, based on a unit length of one meter for pure gelatin film, one percent change in relative humidity leads to a linear expansion of 340 μm, as oppose to only 33 μm caused by a change in temperature of one degree Celsius.

In addition, results indicate that the gelatin is in-plane isotropic whereas the PET is an in-plane anisotropic material. This anisotropy of the PET is a primary contributor to the inversion of the cylindrical shapes observed at various relative humidities.[6] It is also evident that an incorporation of latex particles into the gelatin helps improve the dimensional stability of the films exposed to the moisture, which is a desirable property. A comparison of the HEC and CTE from the other effects, such as latex particle size, drying condition at vitrification, and gelatin concentration at set point, is presented in Table 6.13. While the HEC decreases and the CTE increases with an increase in the latex concentration, the latex particle size has no effect on both HEC and CTE. It was also found that the gelatin concentration at set point and the drying condition at vitrification do not affect the CTE; nevertheless, these two parameters show significant effects on the HEC of the gelatin films. The film with higher gelatin concentration (15%) exhibits greater stability to the moisture than the film with 10% gelatin concentration. Also, the film dried at LMERH condition (130F / 5.5% RH) yields lower HEC which means that it has higher resistance to the humidity expansion than the film dried at HMERH condition (80F / 29% RH).

Table 6.12 : Comparison of the Effect of Moisture and Temperature on the Dimensional Stability of Gelatin and PET Films

Material	Humidity Expansion			Thermal Expansion	
	Sorption Path	Humidity Range(%)	HEC (β) (μm/m%RH)	Temp. Range(°C)	TEC (α) (μm/m°C)
Pure Gelatin BF 8483-133	absorption desorption	30-90 30-90	343 341	30-140	33
Gelatin-PEA BF 8483-173	absorption desorption	30-90 30-90	319 245	30-140	62.4
Gelatin-PEMA BF 8483-123	absorption desorption	30-90 30-90	291 231	30-140	63.1
PET (MD) PET (TD)	absorption absorption	30-90 30-90	10.5 5.97	30-60	16.6
Gelatin & PET (MD)	absorption	30-70	18.4	25-50	20.5

Table 6.13 : Summary of the Effect of Latex Type, Latex Concentration, Latex Particle Size, Gelatin Concentration at Set Point, and Drying Condition at Vitrification on the Humidity Expansion Coefficient (HEC) and Coefficient of Thermal Expansion (CTE) for the Gelatin Films

	HEC (μm/m%RH)	CTE (μm/m°C)
Latex Type	Gel-PEA > Gel-PEMA	Gel-PEA = Gel-PEMA
Latex Concentration (parts)	0 > 20 > 40	0 < 20 < 40
Latex Particle Size (μm)	no effect	no effect
Gelatin Concentration (%)	10 > 15	no effect
Drying Condition	HMERH > LMERH	no effect

Comparisons between the gelatin-PEA and gelatin-PEMA films show the HEC values have been shown to depend upon the bulk stiffness of the film. Chapter 5 shows that the stiffness of the film, in turn, depends upon the relative humidity, and therefore the moisture content. As a result, the HEC is a combination of moisture content and stiffness. The film with low moisture absorption and high stiffness should have a greater resistance to the dimensional change due to the humidity exposure. In addition, based on the scope of this investigation as shown in Table 6.13, in order to obtain a gelatin film with greatest dimensional stability to moisture exposure, the film has to be dried at the LMERH condition, contain 40 parts PEMA and 15% gelatin concentration at set point.

Lastly, besides a typical dimensional hysteresis, a "reversed dimensional hysteresis" of the gelatin film, caused by moisture-induced relaxation shrinkage at high relative humidity, was also observed. In addition, thermal-induced relaxation shrinkage was found in both gelatin and PET substrate heated to temperatures above their Tg. These observations agree very well with those reported in the literature.

References

1. Adelstein, P.Z. In *SPSE Handbook of Photographic Science and Engineering*; Thomas, W., Ed.; John Wiley & Sons: New York, 1973; Section 8, pp. 473-500.

2. Calhoun, J.M. and Leister, D.A., "Effect of Gelatin Layers on the Dimensional Stability of Photographic Film", *Photographic Science and Engineering*, **3**(1), 8 (1959).

3. Umberger, J.Q., "The Fundamental Nature of Curl and Shrinkage in Photographic Films", *Photographic Science and Engineering*, **1**(2), 69 (1957).

4. "Physical and Chemical Behavior of Kodak Aerial Films", *Properties of Kodak Materials for Aerial Photographic Systems*; Eastman Kodak Co.: Rochester, NY, 1972; Vol. III.

5. "Physical Properties of Kodak Aerial Films", *Properties of Kodak Materials for Aerial Photographic Systems*; Eastman Kodak Co.: Rochester, NY, 1972; Vol. II.

6. Vrtis, J.K., "Stress and Mass Transport in Polymer Coating and Films", Ph.D. Dissertation, University of Massachusetts, Amherst, MA (1995).

7. Adelstein, P.Z. and Calhoun, J.M., "Interpretation of Dimensional Changes in Cellulose Ester Base Motion-Picture Films", *Journal of the SMPTE*, **69**, 157 (1960).

8. Centa, J.M., "Effect of Base and Emulsion Thickness on Dimensional Stability of Graphic Arts Films", *Proceeding of the Annual Technical Meeting: Technical Associates of Graphic Arts*, **8**, 75 (1956).

9. Nielsen, L.E., "Mechanical Properties of Particulate-Filled Systems", *Journal of Composites Materials*, **1**, 100 (1967).

10. Turner, P.S., "Thermal-Expansion Stresses in Reinforced Plastics", *Journal of Research of the National Bureau of Standards*, **37**(4), 239 (1946).

11. Kerner, E.H., "The Elastic and Thermo-Elastic Properties of Composite Media", *Proceedings of the Physical Society*, **69**B, 808 (1956).

12. Nielsen, L.E. and Landel, R.F. *Mechanical Properties of Polymers and Composites, 2nd ed.*; Marcel Dekker, Inc.: New York, 1994; Chapter 7, pp. 377-459.

13. Levin, V.M., "On the Coefficients of Thermal Expansion of Heterogeneous Materials (in Russian)", *Mekhanika Tverdogo Tela*, **1**, 88 (1967).

14. Hashin, Z. *Proceedings of the IUTAM Symposium on Nonhomogeneity in Elasticity and Plasticity, Warsaw Poland*; Pergamon Press: New York, 1959; p. 463.

15. Christensen, R.M. *Mechanics of Composite Materials*; John-Wiley & Sons: New York, 1979; Chapter 2, pp. 31-72.

16. Hashin, Z. and Shtrikman, S., "A Variational Approach to Theory of the Elastic Behavior of Multiphase Materials", *Journal of the Mechanics and Physics of Solids*, **11**, 127 (1963).

17. Cuevas, J.E., "Effective Moduli Calculations of Isotropic Composites", *Journal of Composite Materials*, **2**(1), 113 (1968).

18. Schapery, R.A., "Thermal Expansion Coefficients of Composite Materials Based on Energy Principles", *Journal of Composite Materials*, **2**(3), 380 (1968).

19. Rosen, B.W., "Thermal Expansion Coefficients of Composite Materials", Ph.D. Dissertation, University of Pennsylvania, PA (1968).

20. Cribb, J.L., "Shrinkage and Thermal Expansion of a Two Phase Material", *Nature, London*, **220**, 576 (1968).

21. Steel, T.R., "Determination of the Constitutive Coefficients for a Mixture of Two Solids", *International Journal of Solids and Structures*, **4**, 1149 (1968).

22. Christensen, R.M. *Mechanics of Composite Materials*; John-Wiley & Sons: New York, 1979; pp. 208, 337.

23. Wolff, E.G. In *International Encyclopedia of Composites, Vol.4*; Lee, S.M., Ed.; VCH Publishers: New York, 1991; pp. 279-323.

24. Wolff, E.G. In *Handbook of Polymer-Fibre Composites*; Jones, F.R., Ed.; Longman Scientific & Technical: Burnt Mill, Harlow, Essex, 1994; Chapter 6.1, pp. 362-366.

25. Crossman, F.W., Warren, W.J., and Pinoli, P.C., "Time and Temperature Dependent Dimensional Stbility of Graphite-Epoxy Composites", *Proceedings of the 21st National SAMPE Symposium*, **21**, 424 (1976).

26. Crossman, F.W. and Wang, A.S.D., "Stress Field Induced by Transient Moisture Sorption in Finite-width Composite Laminates", *Journal of Composite Materials*, **12**, 2 (1978).

27. Treloar, L.R.G. *The Physics of Rubber Elasticity, 2nd ed.*; Clarendon Press: Oxford, 1958; p. 135.

28. Harper, C.A., Ed.; *Handbook of Plastics, Elastomers, and Composites, 2nd ed.*; McGraw-Hill, Inc.: New York, 1992; Chapter 1, pp. 49-52.

29. Marshall, A.S. and Petrie, S.E.B., "Thermal Transitions in Gelatin and Aqueous Gelatin Solutions", *Journal of Photographic Science*, **28**, 128 (1980).

30. Leaderman, H., "Elastic and Creep Properties of Filamentous Materials and Other High Polymers"; Textile Foundation, Inc.: Washington, D.C., 1943; pp. 98, 128.

31. Sheldon, R.P. *Composite Polymeric Materials*; Applied Science Publishers: London, 1982; Chapter 4, p. 98.

32. Bourdygina, G.I. and Kozlov, P.V., "Modification of the Physico-Mechanical Properties of Gelatin in the Coiled Conformation", *European Polymer Journal*, **28**(2), 135 (1992).

CHAPTER 7

EFFECT OF MOISTURE ON SWELLING STRESS

Introduction

The common failures of polymer coatings such as curling, buckling, cracking, and delamination are directly related to the state of stress in the coating resulting from a combination of material properties, processing conditions, and environmental exposure. [1] In general, the principal causes contributing to the development of stresses in the coatings are : 1) physical aging or degradation in which the molecular rearrangement or relaxation over time changes the material properties [2], 2) solvent removal during the curing process resulting in volume shrinkage [3], 3) the mismatch in thermal or humidity expansion coefficient between coating and substrate [1,4,5]. These factors can alone or in combination with one another result in high residual stress to cause coating failure. For example, the stresses in polyimide films are due to solvent removal and the mismatch in the thermal expansion coefficients of the coating and the substrate.[6,7]

For a photographic system, the stresses develop in the film due to physical aging and also due to the mismatch in the humidity expansion coefficients between the coating and the substrate.[8-10] Solvent removal may also play a role in a particular substrate such as cellulose ester or polycarbonate.[10,11] Hence, it is important to be able to measure stress in films especially under conditions which closely resemble those conditions the film will see when in service.

Various techniques are available to measure stresses in polymer coatings and films. However, we can divide these methods into three main categories 1) the most common technique such as beam bending which measure strain or radius of curvature of the system and then correlate to the stress by linear elastic assumptions [12,13], 2) techniques such as membrane deflection which measure the displacement due to the applied force [14], and 3) techniques such as vibrational holographic interferometry which measure the response of the material due to vibration [6-8,15].

Each of these techniques has advantages and disadvantages. For instance, the versatile technique of beam bending requires linear elastic assumptions and elastic constants of the material and substrate to be able to calculate the stress. Therefore, if a material is not linear elastic, this method only provides an approximate stress value. Besides that, it is a one dimensional uniaxial method so in order to analyze a two dimensional biaxial system, the Poisson's ratio of the coating is required. The membrane deflection technique is a simple and straight-forward method for measuring stresses in polymer coatings. One of its advantages is that no knowledge of material properties is required. However, only isotropic stresses can be measured by this method. Details regarding this technique are discussed elsewhere.

In this research, a direct method, vibrational holographic interferometry was used to determine the biaxial swelling stresses in gelatin film as a function of relative humidity. The effect of latex concentration, latex particle size, gelatin concentration at set point, and drying condition at vitrification on the swelling stress of gelatin and gelatin-latex films were also investigated.

Vibrational Holographic Interferometry

Vibrational holographic interferometry was used to directly measure the state of stress in the gelatin films. This technique is only briefly discussed here. Further details regarding the mathematical derivation and air damping effect can be found elsewhere.[6] Generally, this technique is based on the classical theory of membrane vibrations. The governing equation is:

$$\sigma \nabla^2 u = \rho \frac{\partial^2 u}{\partial t^2} \tag{7.1}$$

where

σ = biaxial stress in the membrane (N / m^2)

u = out - of - plane displacement (m)

ρ = density of the membrane (kg / m^3)

t = time (s)

∇^2 = laplacian operator, $\frac{\partial^2}{\partial r^2} + \frac{1}{r}\frac{\partial}{\partial r} + \frac{1}{r^2}\frac{\partial^2}{\partial \theta^2} + \frac{\partial^2}{\partial z^2}$

By applying the appropriated boundary condition that the out-of-plane displacement is zero at the edges, $u(r = R) = 0$, where R is the outer radius of the membrane, then the solution of equation (7.1) for a circular membrane is:

$$\sigma_{2D} = 4\pi^2 \rho R^2 \left(\frac{f_{ni}}{Z_{ni}} \right)^2 \tag{7.2}$$

where

σ_{2D} = biaxial stress (N / m^2)
ρ = density of the membrane (kg / m^3)
R = radius of the sample (m)
f_{ni} = resonant frequency for the $(n,i)^{th}$ mode (Hz)
Z_{ni} = i^{th} zero of the n^{th} order Bessel function

It is apparent from equation (7.2) that the only material property needed is the density of the film. This is an advantage because no linear elastic assumptions are necessary and the elastic constants of the material are not required.[15] Therefore, the stresses in the film can be calculated from equation (7.2) by finding the unique mode patterns [$(n,i)^{th}$ modes] and their respective resonant frequencies (f_{ni}).

The order of Bessel function is determined from the observed vibration pattern at a specific frequency. As can be seen from Figure 7.1, vibration of the zero order shows no lines of axial symmetry and produces a circular vibration pattern while vibration of the

Figure 7.1 : Typical vibration patterns and mode numbers for the vibration of a circular membrane. The indices n and i represent the order of the Bessel function and the number of the zero of that Bessel function and are determined by counting the number of radial and tangential nodal lines, respectively.[6]

first order will have one line of symmetry, etc.[7] In other words, the number of lines of symmetry in the vibration pattern determine the order of the Bessel function.

The zero of integer order Bessel functions have been tabulated in the literature.[16] A table of the first twenty zeros of the Bessel functions in their order of appearance is provided in Table 7.1.

Table 7.1 : Mode Numbers, Mode Shape Indices (n,i), and the First Twenty Zeros of the Integer Order Bessel Function ($Z_{n,i}$)

Mode Number	n,i	Z n,i
1	0,1	2.405
2	1,1	3.831
3	2,1	5.136
4	0,2	5.520
5	3,1	6.380
6	1,2	7.016
7	4,1	7.586
8	2,2	8.417
9	0,3	8.654
10	5,1	8.708
11	3,2	9.760
12	6,1	9.953
13	1,3	10.173
14	4,2	11.064
15	7,1	11.115
16	2,3	11.620
17	0,4	11.792
18	8,1	12.270
19	5,2	12.339
20	3,3	13.017

Besides its ability to measure the state of stress in coating, the vibrational holographic interferometry can also be employed to determine the principal directions and principal stresses in an anisotropic material. In addition, it can couple with other techniques to fully characterize all of the orthotropic elasticity coefficients and the transport coefficients (thermal and mass diffusion coefficients).[6-8,15,17]

Vibrational holographic interferometry can be operated at temperatures up to 400°C and at various relative humidities.[8,17] A schematic of the holographic interferometry set-up with the relative humidity generator is shown in Figure 7.2. Normally, the measurements are made under vacuum to avoid air damping effects. In our experiment, helium was used as a transport gas by bubbling it through saturated salt solutions. Vrtis concluded that, because of its low molecular weight, the use of helium gas does not change the apparent stress values; hence, no correction is required.[8]

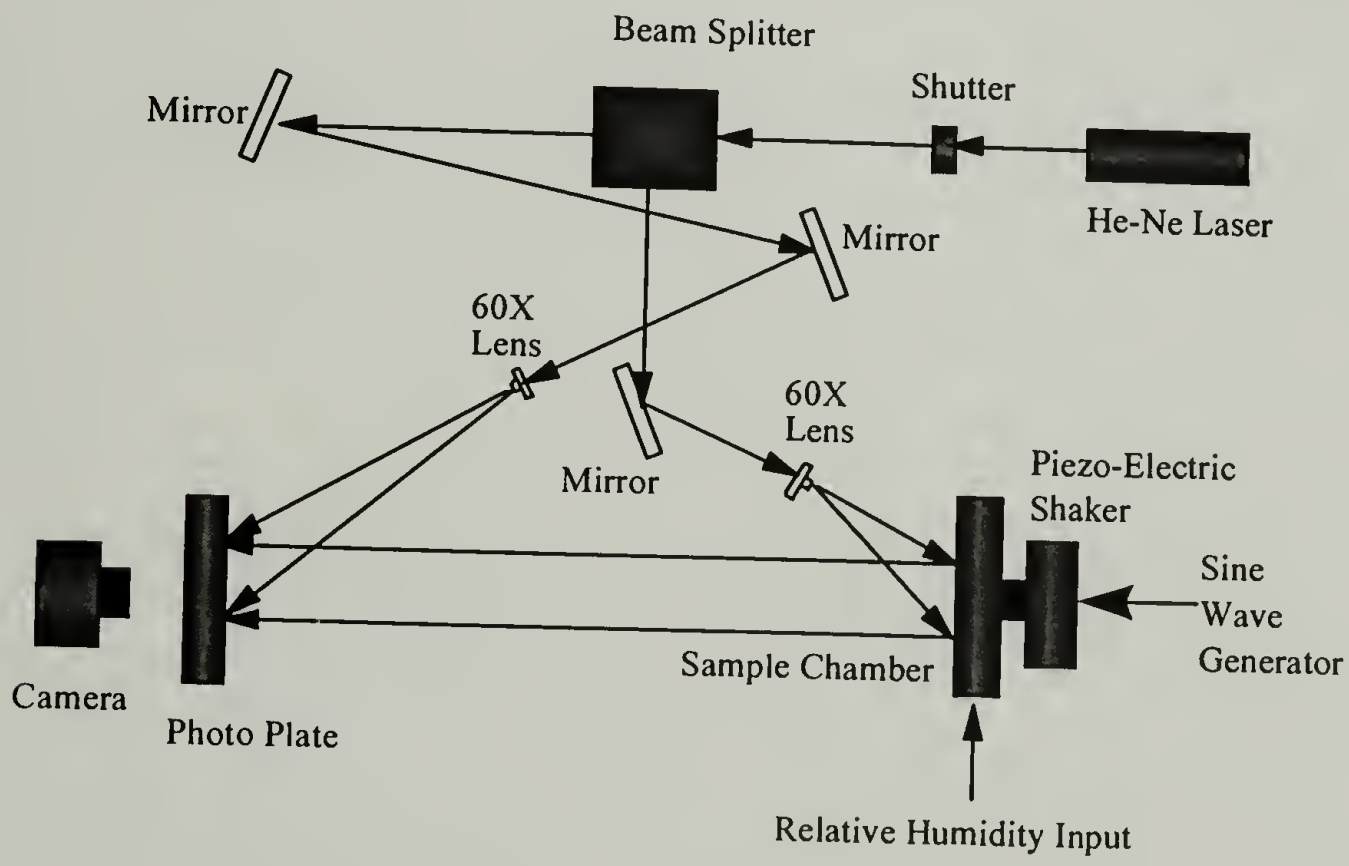

Figure 7.2 : Schematic of vibrational holographic interferometry set-up with relative humidity generator.[8]

Experimental

Sample Preparation

The sample preparation is crucial. In order not to alter the state of stress in the film, various special sample preparation methods have been developed depending upon each coating / substrate system. Typically, for a rigid substrate there are no shear or normal stresses between the coating and the substrate beyond a few film thicknesses from the edges of the film. The state of stress in the film away from the edges will not depend on the presence of the substrate. We can, therefore, remove a part of the substrate in the middle of the film without significantly affecting the stress state.

A sample of gelatin film was made by mounting a steel washer on top of the gelatin coating using Super Glue® and applying some pressure to ensure uniform adherence. The substrate was removed by peeling, after the glue is dried, at about a 5° degree take off angle to avoid introducing additional stresses.[8] However, it should be noted that, prior to this step, the sample should be preconditioned at a specific relative humidity which makes the sample free from stress resulting in a flat bilayer system. This particular relative humidity differs in each system. For gelatin coated on a poly(ethylene terephthalate) substrate, for instance, the sample is flat at around 75-80% RH.

Holographic Interferometry and Relative Humidity

As mentioned earlier, using holographic interferometry, the membrane sample is normally tested in a vacuum environment in order to eliminate pressure effects, so called air damping effects or mass loading effects, that result in deflated stress values. If air damping effects occur, the deflated stress values would require a data correction similar to that proposed by Lax [18].

However, the vacuum environment can not be used in this work since various relative humidities are needed to be transported into the chamber in order to study the effect of moisture. For that reason, a suitable transport medium is required. According to Vrtis, helium should be used as a transport gas because of its low molecular weight.[8]

In order to verify this statement, a gelatin membrane was used to investigate the possible air damping effects of relative humidity on the actual stress values by testing under 50% RH transported via helium gas. Relative humidity was generated and controlled using saturated binary aqueous salt solutions as described in chapter 2. For a comparison study, the gelatin membrane was also subjected to other three environments: vacuum, air (opened chamber), and air (closed chamber). The resonant frequencies were monitored in each case. At least 15 modes of vibration were recorded for each test run. The effect of the environment on the actual stress values was analyzed by comparing the stress vs. vibration mode for each environment.

Swelling Stress Dependence on Relative Humidity

For a moisture sensitive material, relative humidity can induce stress by swelling the material resulting in dimensional instability commonly observed as bending or curling.[1,2,4,19,20] This moisture induced swelling stress in a coating/substrate bilayer can impose a bending moment which may cause difficulty in processing.[13,21]

An investigation of the effect of moisture on the swelling stress of gelatin film was performed using the Real-Time Holographic Interferometry. The gelatin membrane was placed in the holographic interferometry chamber, which was connected to a piezoelectric shaker driven by a frequency generator and a power amplifier (Figure 7.2). The sorption cycle began after the gelatin was equilibrated for about two hours at 80% RH and room temperature. An image of the static membrane sample was recorded on a thermoplastic plate using a Newport Research Corporation HC301 holographic camera. After that, using the frequency generator, the frequency of vibration of the chamber and membrane was increased steadily until a resonant frequency of the membrane was reached. This is evidenced by the appearance of a vibration pattern superimposed on the static pattern. The resonant frequency along with the density and the radius of the membrane were then used to calculate the biaxial stress in the film. Desorption began at two hours intervals allowing for the gelatin membrane to equilibrate at each relative humidity. The sorption cycle was run as follows: 80% RH to70% RH to 60% RH to 50% RH to 30% RH to 50% RH to 60%RH to 70% RH to 80% RH. At each humidity, the equilibrium swelling stress in the membrane was determined.

Results and Discussion

Holographic Interferometry and Relative Humidity

Plots of biaxial stresses vs. mode numbers for gelatin membrane conditioned at four different environments are presented in Figure 7.3. Obviously, when the experiment was performed under vacuum, each resonant frequency yields a redundant stress value with a standard deviation of about 1%. For this specific sample (BF 8505-332), we were able to observe vibration patterns as high as the twentieth mode of vibration. Similarly for the tests conducted at 50% RH in helium, it is clear that the no air damping is observed. The stress values fall within the experimental error; as a result, no corrections of the apparent stress values are required if helium is used as the transport gas. The lower stress value for the test carried out at 50% RH is due to the plasticizing effect of moisture. In contrast, the experiments done in air (both closed and opened chamber) show that air damping effects cause resonant vibrations to occur at lower frequencies than normal, especially for the lower modes of vibration. Nevertheless, the effect of air loading on the lowering of the resonant frequency of a membrane is seen to decrease for higher modes of vibration. It is important to note that the air damping or the mass loading of the medium on the membrane does not actually lower the stress in the film, but offers resistance to vibration thereby lowering the frequency at which the membrane resonates resulting in erroneous stress calculations.[6]

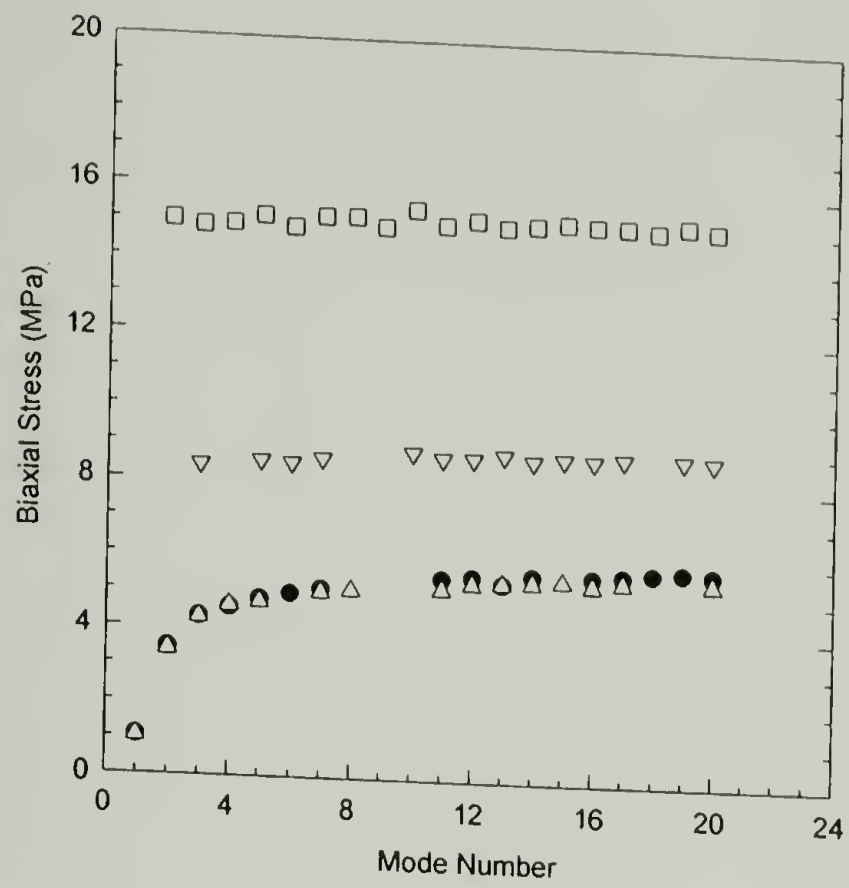

Figure 7.3 : Stress as a function of mode number for a gelatin (BF 8505-332) membrane measured at four different environments : (1) vacuum (□), (2) helium 50% RH (▽), (3) air-opened chamber (●), and (4) air-closed chamber (Δ).

Swelling Stress Dependence on Relative Humidity

Figure 7.4 illustrates the equilibrium biaxial swelling stress vs. mode of vibration of the gelatin membrane subjected to various relative humidities. It is clear that the stress values at each relative humidity are consistent within the experimental error, no air damping effects occurred as would be the case if air was used as the transport medium. These data confirm that vibrational holographic interferometry is an excellent technique to obtain the accurate stress values. The average of these equilibrium stress values are plotted as a function of relative humidity as shown in Figure 7.5. As expected , because of the plasticizing effect of moisture an increase in relative humidity decreases the

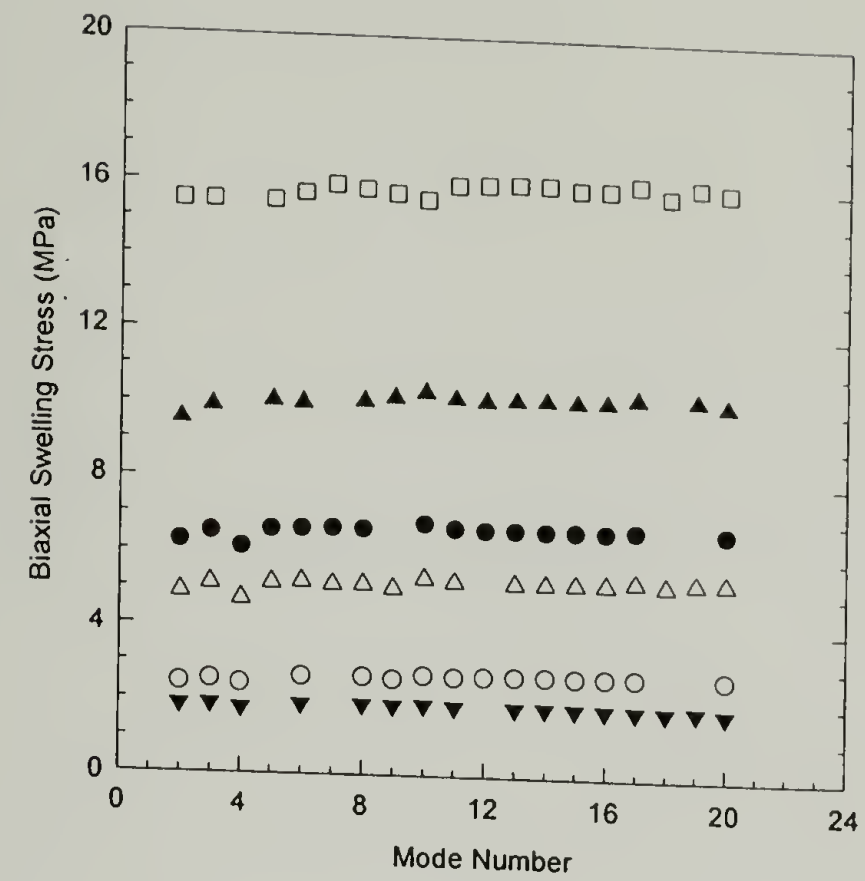

Figure 7.4 : Equilibrium biaxial swelling stress vs. mode number for a gelatin-PEMA (BF 8483-213) membrane under various relative humidities : (1) desorption : 60% RH (o), 50% RH (Δ), 30% RH (□) and (2) absorption : 50% RH (▲), 60% RH (●), 70% RH (▼).

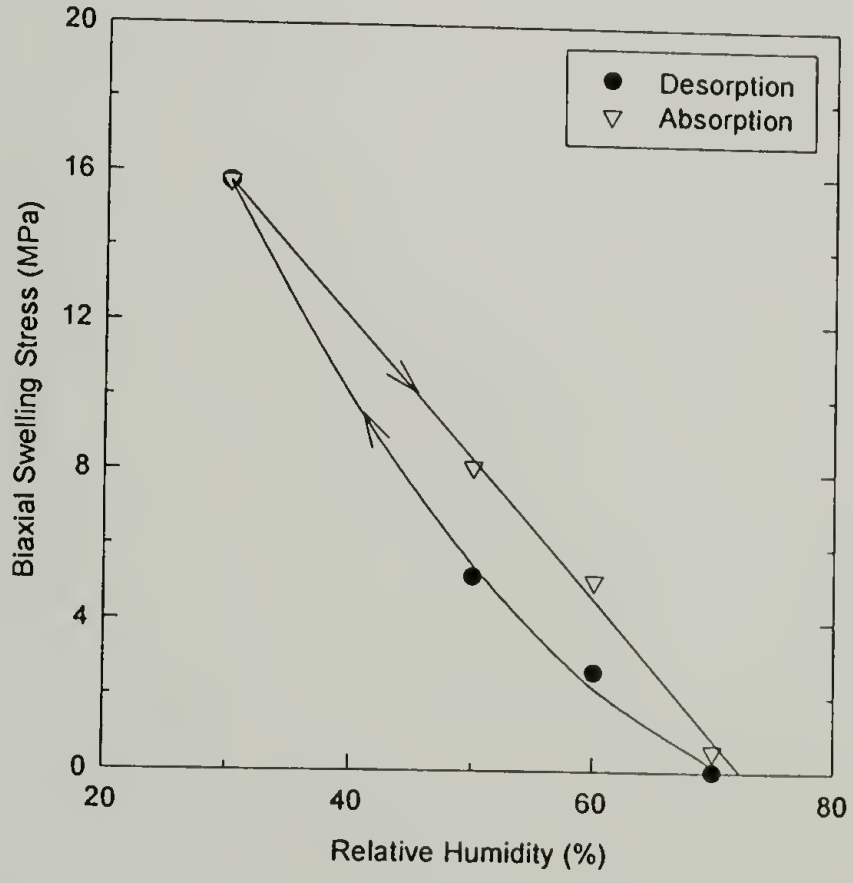

Figure 7.5 : Biaxial swelling stress as a function of relative humidity for a gelatin-PEMA (BF 8483-213) membrane. Each data point was averaged from the equilibrium biaxial swelling stress values at a specific relative humidity as presented in Figure 7.4.

magnitude of swelling stress of gelatin. The stress reaches zero at around 75% RH. Below 75% RH, it is in tension, while above 75% RH the gelatin membrane is in compression which is observed as buckling of the membrane.

As seen in Figure 7.5, a stress hysteresis is evident with an absorption path generating greater swelling stress. The desorption path in gelatin differs from the absorption path as indicated by the non-linearity of the desorption curve. The hysteresis of biaxial swelling stress of gelatin has also been observed by others[8,9]. However, their results showed that the desorption path was greater than the absorption path. The discrepancy in the direction of the hysteresis could be explained in term of the difference in the experimental procedures. In their work, gelatin film was brought to a very low relative humidity, 0% RH [8] or 10% RH [9]. A plot between the stress vs. time revealed that a stress relaxation occurred in the gelatin film at 20% RH or lower.[9] Hence, they concluded that this stress relaxation with time is a contributor to a reversed hysteresis of gelatin under tension at low relative humidity. In contrast to our experiment, the gelatin membrane was brought to only 30% RH and no stress relaxation was observed.

For a better understanding of the discussion to follow, recall from incremental linear elasticity theory that for an isotropic, linear elastic, homogeneous material the stress is proportional to the product of the modulus and the expansion coefficient as shown in equation (7.3):

$$E\left[\delta\varepsilon_{ij} - \delta_{ij}\left(\alpha\delta T - \beta\delta RH\right)\right] = (1+\nu)\delta\sigma_{ij} - \nu\delta_{ij}\delta\sigma_{kk} \qquad (7.3)$$

where

E = tensile modulus
ε_{ij} = strain
σ_{ij} = stress
ν = Poisson's ratio
δ_{ij} = Kronecker delta

α = thermal expansion coefficient
T = temperature
β = humidity expansion coefficient
RH = relative humidity
δ = differential operator

Although linear in stress and strain, this incremental or differential equation allows both mechanical properties and material coefficients to depend upon the temperature and relative humidity. However, in a coating, the material is constrained in two dimensions. Therefore, under isothermal condition, $\delta T = 0$, and by definition of a two dimensionally constrained, linear elastic, isotropic, homogeneous material, $\delta\varepsilon_{11} = \delta\varepsilon_{22} = 0$, $\delta\sigma_{33} = 0$, and $\delta\sigma_{11} = \delta\sigma_{22} = \delta\sigma$. This reduces equation (7.3) to:

$$\frac{d\sigma}{dRH} = -\frac{E\beta}{(1-\nu)} \tag{7.4}$$

Thus, the change in stress with relative humidity is proportional to the product of the modulus and humidity expansion coefficient (HEC). It is often assumed that the material constants are independent of humidity changes.[1,8] As a result, as the relative humidity increases, the stress in the gelatin coating decreases (Figure 7.5). Keeping these concepts in mind, one should be able to explain the effects of the following parameters on the biaxial swelling stress of the gelatin film.

Swelling Stress Dependence on Polymer Latex

The biaxial swelling stresses for pure gelatin and gelatin-latex films at various relative humidities are presented in Figure 7.6. All these gelatin samples contained 15% gelatin concentration at set point, and were dried at the HMERH condition (80F / 29% RH). The latex concentration of the gelatin-latex film in this specific case is 20 parts, and the latex particle size of PEA and PEMA is 0.112 μm and 0.15 μm, respectively.

Latex polymers have low affinity to moisture but since the majority part of the coating layer is still gelatin, it is obvious that the biaxial swelling stresses for the gelatin-latex films are also dependent upon the relative humidity. The swelling stress decreases with increasing relative humidity. However, the hydrophobic nature of polymer latex helps reduce the magnitude of swelling stress in the gelatin coating. It is apparent that, at each relative humidity, the biaxial swelling stresses of the gelatin-latex films are lower than those of the pure gelatin films, especially for the films containing PEA as an additive.

Besides, the decrease in the swelling stress due to the presence of the latex particles in the gelatin film can be explained by comparing the humidity expansion coefficient and the tensile modulus of the pure gelatin film with those of the gelatin-latex film. Recall from chapter 3 that the amount of absorbed moisture in the emulsion layer decreases when latex is introduced into the system. This causes a reduction in the in-plane HEC of the gelatin-latex film compared to the pure gelatin film as explained in chapter 6. In addition, it was demonstrated in chapter 5 that the tensile modulus of the

gelatin-latex film is lower than that of the pure gelatin film. Accordingly, the biaxial swelling stress of the pure gelatin film, which is proportional to the product of the HEC and tensile modulus (equation(7.3)), is greater than those of the gelatin-latex films.

Similar explanations can be applied to the case of gelatin-PEA and gelatin-PEMA films. As described in chapter 6, although the gelatin-PEMA is more hydrophilic than the gelatin-PEA, the gelatin-PEMA film has a greater resistance to the moisture expansion (i.e. lower HEC). Therefore in comparison with the gelatin-PEA, the larger tensile modulus of the gelatin-PEMA film is solely responsible for the greater biaxial swelling stress of the gelatin-PEMA film.

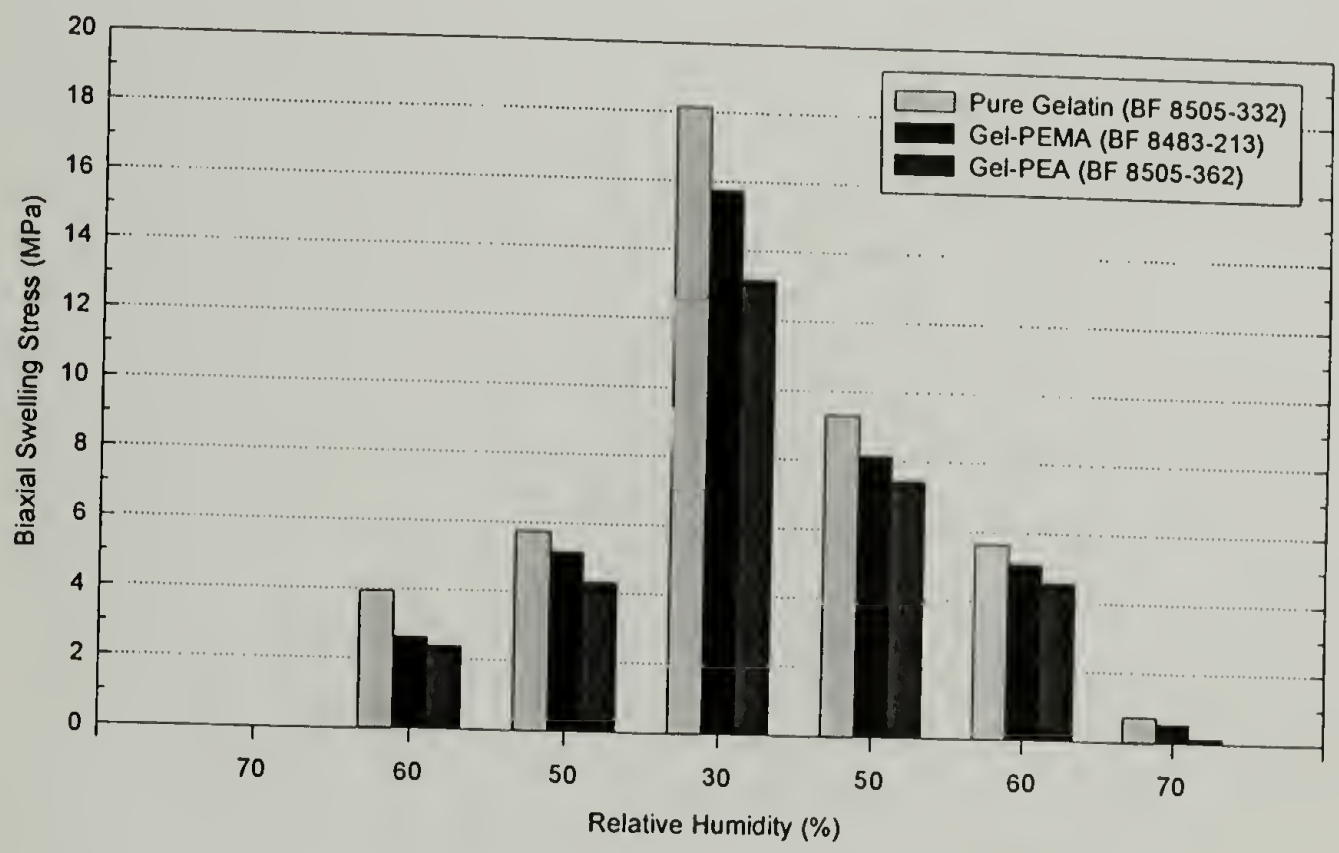

Figure 7.6 : Effect of polymer latex on the biaxial swelling stress of gelatin membrane at various relative humidities.

Latex Concentration vs. Swelling Stress

The effect of PEMA and PEA concentration on the biaxial swelling stress of the gelatin film is given in Figure 7.7. Similar to the samples shown in Figure 7.6, all these films were dried at the HMERH condition (80F / 29% RH). The gelatin concentration at set point is 15%. The latex particle size of PEA and PEMA is also 0.112 μm and 0.15 μm, respectively. For both latex systems, the biaxial swelling stress decreases as the latex concentration increases. Again, as already described in chapter 5 and 6, the tensile modulus and the in-plane HEC are reduced with an increase in the latex concentration. The film with higher latex concentration has a lower tensile modulus and greater resistance to the humidity expansion (lower HEC). As a result, the pure gelatin film yields the greatest swelling stress, whereas the gelatin film with 40 parts latex shows the lowest swelling stress.

Latex Particle Size vs. Swelling stress

Figure 7.8 represents the effect of latex particle size on the biaxial swelling stress for both gelatin-PEMA and gelatin-PEA films. These two particular figures are plotted from the gelatin films with 40 parts latex and 15% gelatin concentration at set point. Again, these two films were dried at the HMERH condition (80F / 29% RH). As can be seen, the latex particle size does not have an appreciable effect on the swelling stress in both PEMA and PEA systems. It was shown in chapter 5 and 6 respectively that the latex

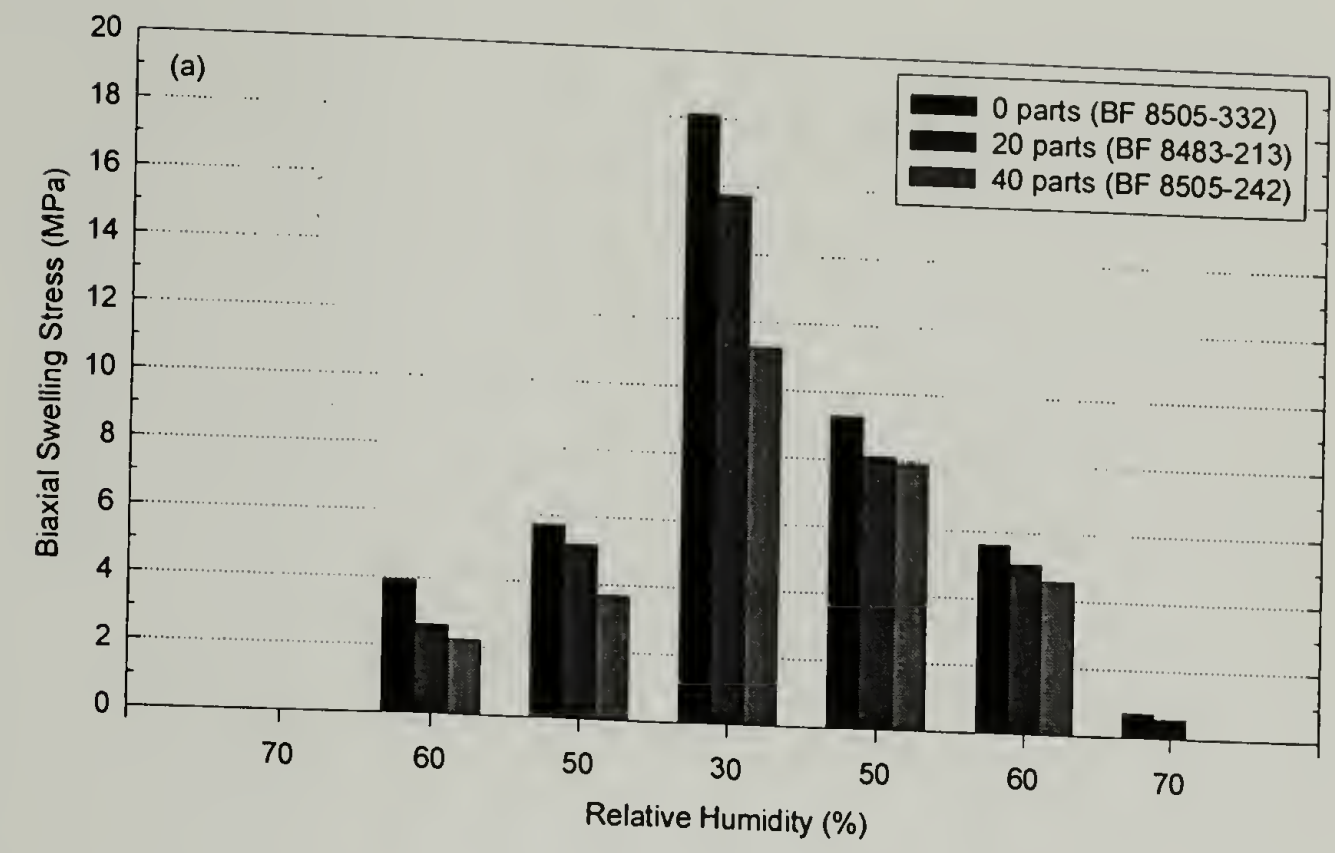

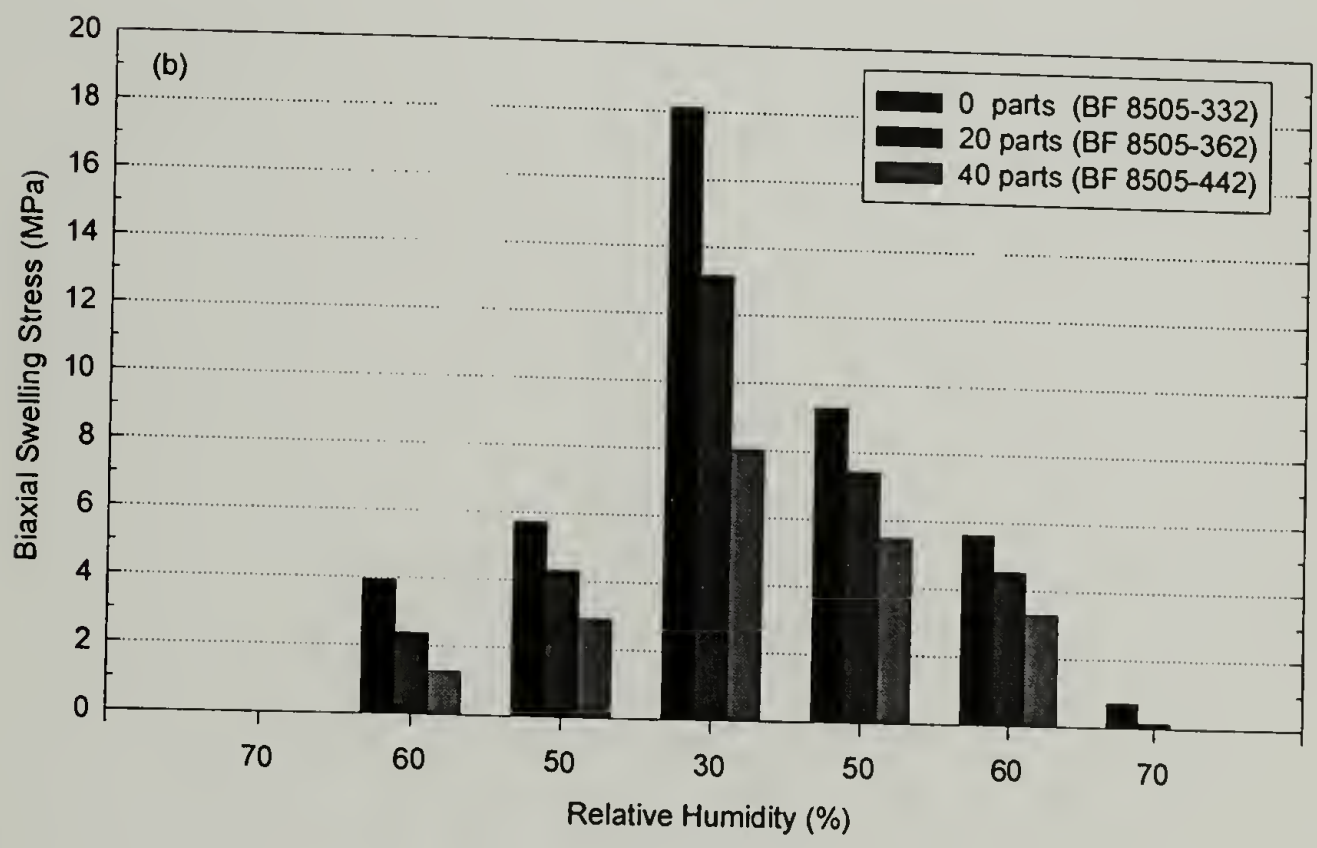

Figure 7.7 : Effect of latex concentration on the biaxial swelling stress of gelatin membrane at various relative humidities : (a) gelatin-PEMA and (b) gelatin-PEA.

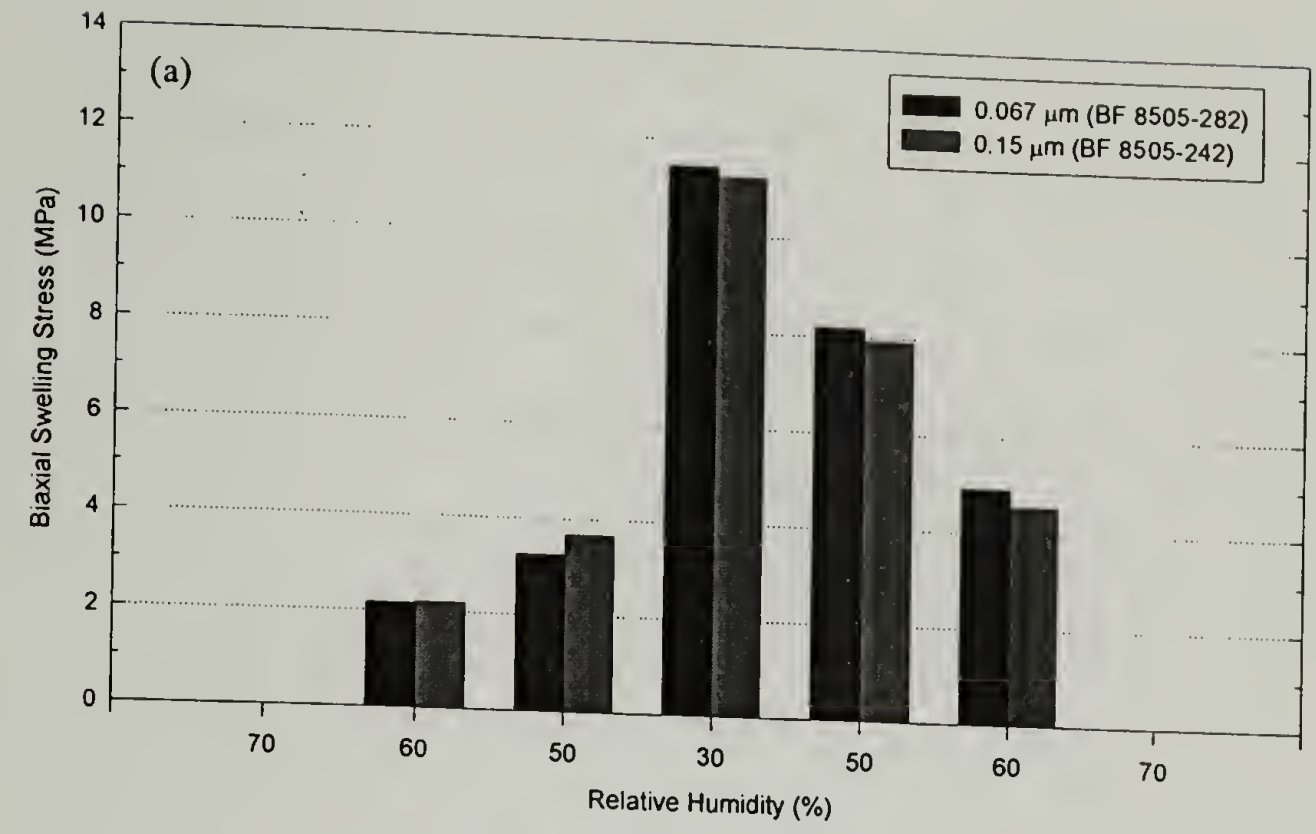

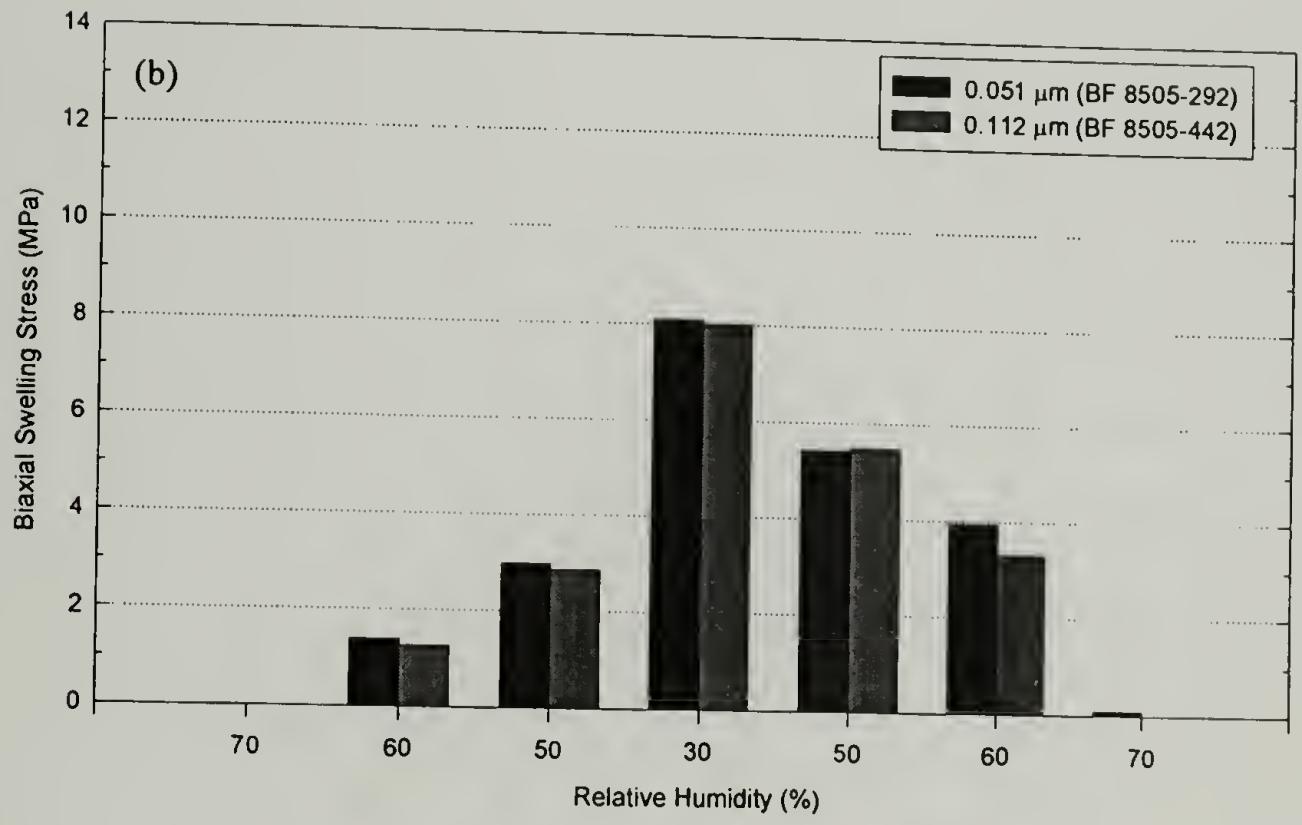

Figure 7.8 : Effect of latex particle size on the biaxial swelling stress of gelatin membrane at various relative humidities : (a) gelatin-PEMA and (b) gelatin-PEA.

particle size does not have any noticeable effect on the tensile modulus or the HEC. Consequently, the swelling stress is unaffected by the latex particle size.

Gelatin Concentration at Set Point vs. Swelling Stress

The effect of gelatin concentration at set point on the biaxial swelling stress was also investigated. Figure 7.9(a) through (c) illustrate the effect of gelatin concentration on the biaxial swelling stress of the pure gelatin, gelatin-PEMA, and gelatin-PEA, respectively. All the films were dried at the LMERH condition (130F / 5.5% RH). For the gelatin-latex films, the latex concentration is 20 parts and the latex particle size for the PEA and PEMA is 0.112 μm and 0.15 μm, respectively. Although it was demonstrated in chapter 5 that the tensile modulus of both pure gelatin and gelatin-latex films are independent of the gelatin concentration at set point, Figure 7.9 shows that the films with lower gelatin concentration (10%) have greater swelling stresses. This is a consequence of the HEC of the films with 10% gelatin concentration being greater than that of the films with 15% gelatin as discussed in chapter 6.

Drying Condition at Vitrification vs. Swelling Stress

Figure 7.10(a) through (c) show how the drying condition at vitrification affect the biaxial swelling stress of the pure gelatin, gelatin-PEMA, and gelatin-PEA, respectively. The gelatin concentration for all the films in this case is 15%. In both

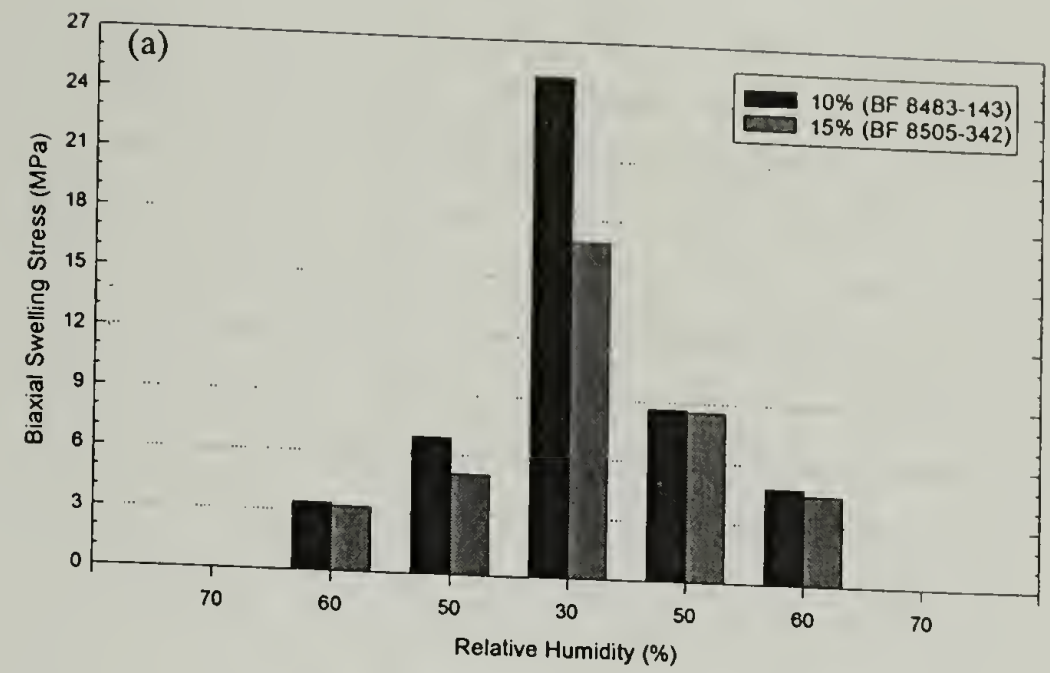

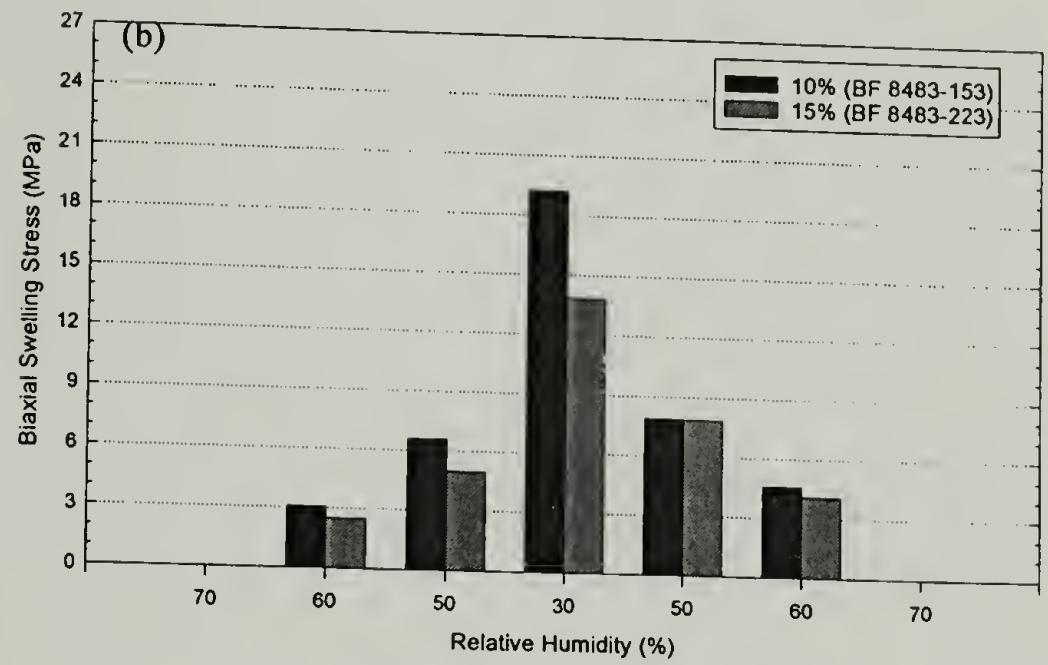

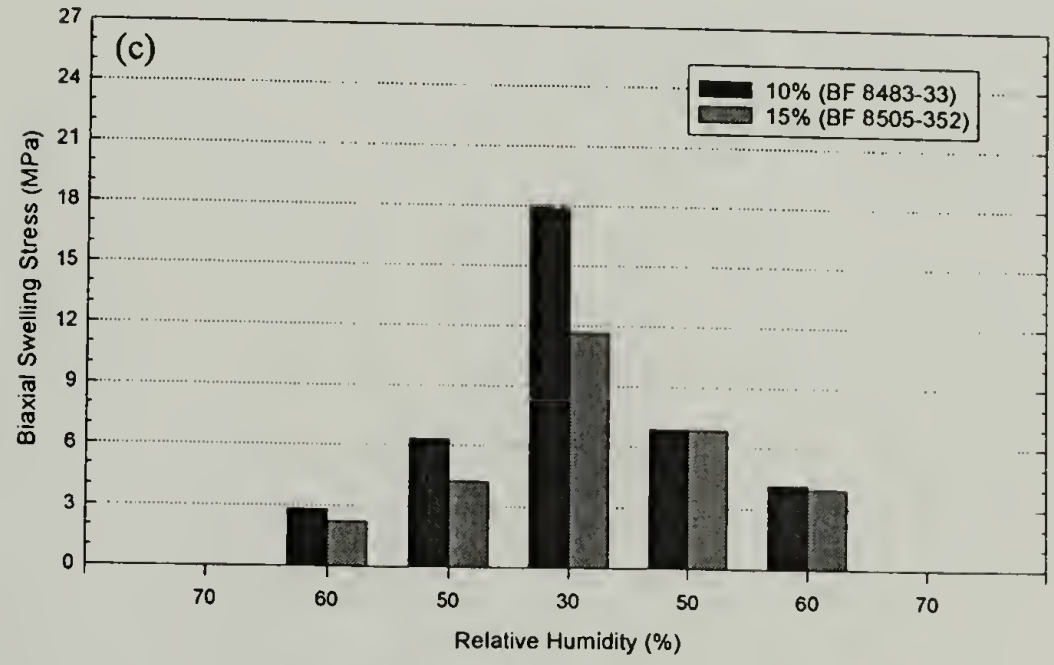

Figure 7.9 : Effect of gelatin concentration at set point on the biaxial swelling stress of gelatin membrane at various relative humidities : (a) pure gelatin, (b) gelatin-PEMA, and (c) gelatin-PEA.

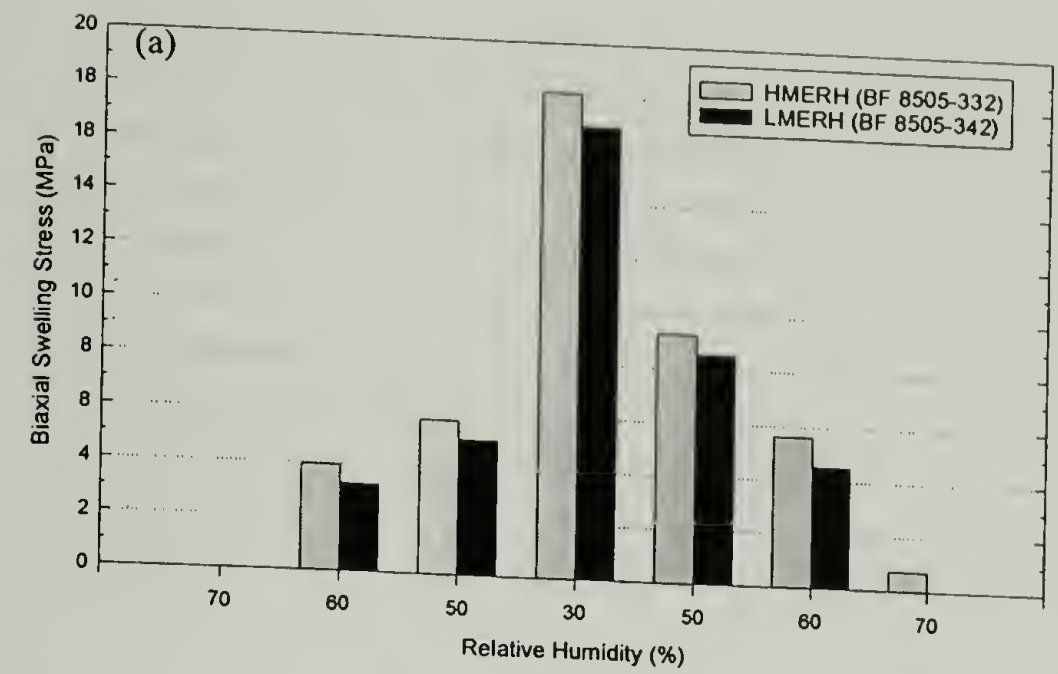

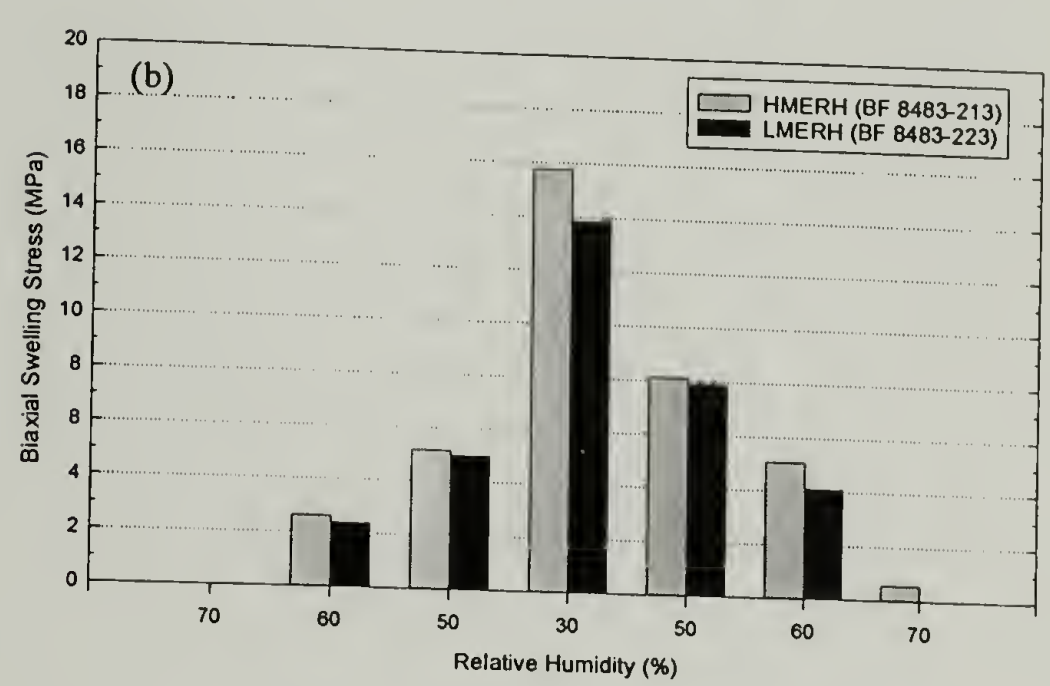

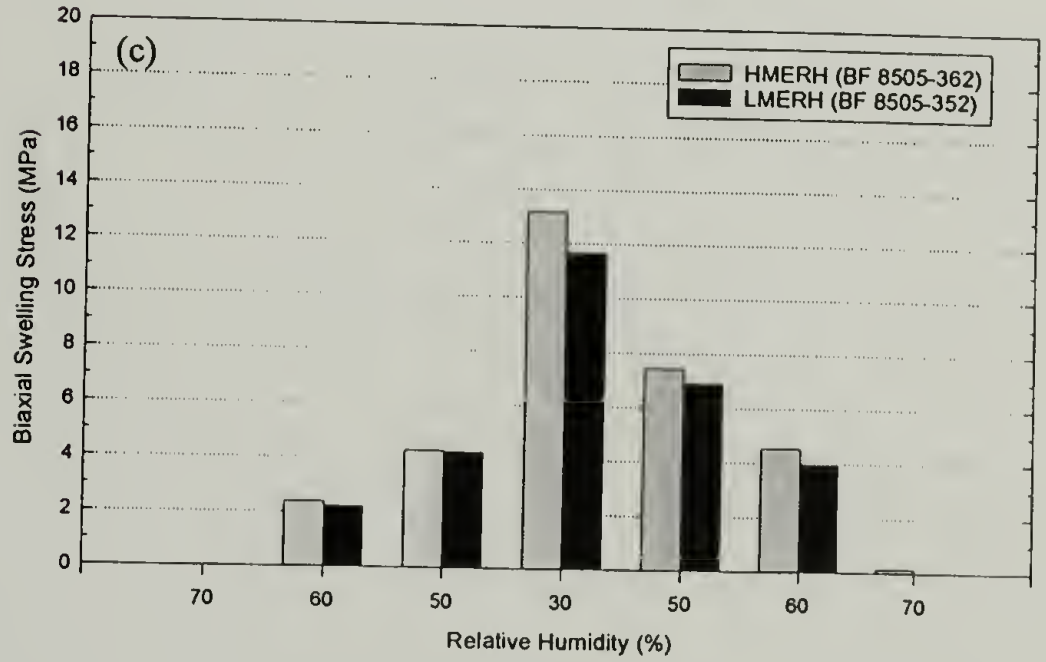

Figure 7.10 : Effect of drying condition at vitrification on the biaxial swelling stress of gelatin membrane at various relative humidities : (a) pure gelatin, (b) gelatin-PEMA, and (c) gelatin-PEA.

gelatin-latex films, the latex concentration is 20 parts. The particle size of PEA and PEMA in these films is 0.112 μm and 0.15 μm, respectively. As seen in Figure 7.10(a), pure gelatin films show a difference in the swelling stresses for the two drying conditions. The films dried at the HMERH condition (80F / 29% RH) have greater swelling stresses than the films dried at the LMERH condition (130F / 5.5% RH). Analogous to the effect of gelatin concentration, even though the drying condition has no effect on the tensile modulus, it does affect the humidity expansion behavior of the pure gelatin film. As shown in chapter 6 that the HEC of the pure gelatin films dried at the HMERH condition is greater than that of the films dried at the LMERH condition. This is the reason why films dried at the HMERH condition have greater swelling stresses than the films dried at the LMERH condition. Gelatin-PEMA and gelatin-PEA films also exhibited similar behavior as shown in Figure 7.10(b) and Figure 7.10(c), respectively.

Conclusions

It is a well known fact that moisture influences the durability of photographic materials. When a gelatin coating and its substrate are exposed to variations in relative humidity, dimensional changes are almost always induced. If these changes are prevented by the adhesion of the gelatin coating to its substrate and if the expansion coefficients of the coating and the substrate are different, which is usually the case, a swelling stress will develop in the coating. Swelling stress can cause dimensional instability commonly observed as curling or bending of the bilayer system. However, in

extreme cases, swelling stress can, alone or in combination with the stress already developed during film formation, overcome the cohesive and/or adhesive forces leading to cracking or delamination of the gelatin coating from the substrate. Therefore, understanding the effect of moisture on the biaxial swelling stress in gelatin coating is essential to controlling dimensional stability in post-coating processes as well as the development of the end-product design.

Holographic interferometry was employed successfully to quantify the biaxial stress in pure gelatin and gelatin-latex films as a function of relative humidity. The influence of latex concentration, latex particle size, gelatin concentration at set point, and drying condition at vitrification on the biaxial swelling stress were also investigated. The effect of air damping on the vibration behavior was evaluated in experiments performed on the pure gelatin film (BF 8505-332). Results indicate that in order to avoid this air damping phenomenon when introducing relative humidity to the membrane sample inside a holographic interferometry chamber, helium gas should be used as a transport gas due to its low molecular weight and no correction to the apparent stress values was required.

The plot of equilibrium biaxial swelling stress as a function of relative humidity of gelatin reveals that the swelling stress decreases as the relative humidity increases and vice versa. The gelatin film has a fairly non-linear equilibrium desorption path which differs from the absorption path. Thus, hysteresis of biaxial swelling stress is observed between the absorption and desorption paths, with absorption generating higher swelling stress. The highest swelling stress value is reached at the lowest relative humidity.

The pure gelatin film possesses higher biaxial swelling stress than the gelatin-latex film through the entire range of investigated relative humidity. According to

incremental linear elasticity theory, the change in stress with relative humidity is proportional to the product of the modulus and humidity expansion coefficient (HEC). Hence the lower biaxial swelling stress of the gelatin-latex film results from its lower tensile modulus and the in-plane HEC when compared to the pure gelatin film. Likewise, it was found that for both latex systems the biaxial swelling stress decreases as the latex concentration increases, in particular for the gelatin film having a PEA as an additive. Specifically, the pure gelatin film yields the highest swelling stress, while the gelatin film with 40 parts PEA has the lowest swelling stress. All of these results can be explained in terms of both the humidity expansion behavior and the tensile modulus of the films.

For both gelatin-PEA and gelatin-PEMA films, changing the particle size from smaller (0.051 and 0.067 μm) to larger (0.112 and 0.15 μm) does not cause any noticeable change in the biaxial swelling stress. This result is in good agreement with the fact that the tensile modulus and the in-plane HEC are unaffected by the latex particle size as well.

The effect of gelatin concentration at set point and the drying condition at vitrification on the biaxial swelling stress were also investigated using holographic interferometry. The biaxial swelling stress for both pure gelatin and gelatin-latex films was found to decrease with increasing the gelatin concentration. The films with 15% gelatin concentration have lower swelling stress. It was also discovered that the films dried at the LMERH condition (130F / 5.5% RH) have less swelling stresses than the films dried at the HMERH condition (80F / 29% RH). Since the tensile modulus of these films are independent of the gelatin concentration and drying condition; therefore, the

logical factor responsible for the lower swelling stress, either for the films dried at the LMERH condition or for the film with 15% gelatin concentration, is the humidity expansion behavior.

In summary, the level of the swelling stress can be considerable and is dependent on the coating composition, the nature of the substrate, and any variation in temperature and /or in relative humidity to which the coating is exposed. Based on the scope of this investigation, in order to obtain a gelatin film with minimum biaxial swelling stress, the film should be dried at the LMERH condition (130F / 5.5% RH) and should contain 40 parts PEA and 15% gelatin concentration at set point.

References

1. Perera, D.Y. and Vanden Eynde, D., "Moisture and Temperature Induced Stresses (Hygrothermal Stresses) in Organic Coatings", *Journal of Coatings Technology*, **59**(748), 55 (1987).

2. Oosterbroek, M., Lammers, R.J., Van Der Van, L.G.J., and Perera, D.Y., "Crack Formation and Stress Development in an Organic coatings", *Journal of Coatings Technology*, **63**(797), 55 (1991).

3. Shimbo, M., Ochi, M., and Arai, K., "Effect of Solvent and Solvent Concentration on the Internal Stress of Epoxide Resin Coatings", *Journal of Coatings Technology*, **57**(728), 93 (1985).

4. Jou, J., Huang, R., Huang, P., and Shen, W., "Structure Effect on Water Diffusion and Hygroscopic Stress in Polyimide Films", *Journal of Applied Polymer Science*, **43**, 857 (1991).

5. Morinaka, A. and Asano, Y., "Residual Stress and Thermal Expansion Coefficients of Plasma Polymerized Films", *Journal of Applied Polymer Science*, **27**, 2139 (1982).

6. Maden, M.A., "The Determination of Stresses and Material Properties of Polyimide Coatings and Films Using Real Time Holographic Interferometry", Ph.D. Dissertation, University of Massachusetts, Amherst, MA (1992).

7. Maden, M.A. and Farris, R.J., "Stress Analysis of Thin Polyimide Films Using Holographic Interferometry", *Experimental Mechanics*, **31**(2), 178 (1991).

8. Vrtis, J.K., "Stress and Mass Transport in Polymer Coatings and Films", Ph.D. Dissertation, University of Massachusetts, Amherst, MA (1995).

9. Calhoun, J.M. and Leister, D.A., "Effect of Gelatin Layers on the Dimensional Stability of Photographic Film", *Photographic Science and Engineering*, **3**(1), 8 (1959).

10. "Physical and Chemical Behavior of Kodak Aerial Films", *Properties of Kodak Materials for Aerial Photographic Systems*; Eastman Kodak Co.: Rochester, NY, 1972; Vol. III.

11. Adelstein, P.Z. In *SPSE Handbook of Photographic Science and Engineering*; Thomas, W., Ed.; John Wiley & Sons: New York, 1973; Section 8, pp. 473-500.

12. Tong, H.M. and Saenger, K.L., "Bending Beam Characterization of Thin Polymer Films" In *New Characterization Techniques for Thin Polymer Films*; Tong, H.M. and Nguyen, L.T., Eds.; John Wiley and Sons, Inc.: New York, 1990.

13. Berry, B.S. and Pritcher, W.C., "Bending-Cantilever Method for the Study of Moisture Swelling in Polymers", *IBM Journal of Research and Development*, **28**(6), 662 (1984).

14. Jennings, R.M., Taylor, J.F., and Farris, R.J., "Determination of Residual Stress in Coatings by a Membrane Deflection Techniques", *Journal of Adhesion*, **49**, 57 (1995).

15. Vrtis, J.K. and Farris, R.J., "Experimental Stress Analysis and Some Thin Film Applications", *Materials Research Society Symposium Proceedings*, **338**, 527 (1994).

16. Arfken, G. *Mathematical Methods for Physicists, 3rd Ed.*; Academic Press: New York, 1985; pp. 572.

17. Sheth, K.C., "Stress, Mechanical and Thermal Characterization of Anisotropic Polyimide Thin Films and Coatings", Ph.D. Dissertation, University of Massachusetts, Amherst, MA (1996).

18. Maden, M.A., Tong, K., and Farris, R.J., "Measurement of Stresses in Thin Films Using Holographic Interferometry : Dependence on Atmospheric Conditions", *Material Research Society Symposium*, **188**, 29 (1990).

19. Vrtis, J.K. and Farris, R.J., "Hysteresis of Biaxial Swelling Stresses in Humidity Sensitive Polymer Coatings", *Proceedings of the American Chemical Society: Division of Polymeric Materials: Science and Engineering*, **69**, 440 (1993).

20. Sackinger, S.T., "The Determination of Swelling Stress in Polyimide Films", Ph.D. Dissertation, University of Massachusetts, Amherst, MA (1990).

21. Fu, T.Z., Durning, C.J., and Tong, H.M., "Simple Model for Swelling-Induced Stresses in a Supported polymer Thin Film", *Journal of Applied Polymer Science*, **43**, 709 (1991).

22. Plepys, A., "A Study of the Evolution of residual Stresses in Three Dimensionally Constrained Epoxy Resins", Ph.D. Dissertation, University of Massachusetts, Amherst, MA (1992).

CHAPTER 8

SWELLING STRAIN ASSOCIATED WITH MOISTURE DIFFUSION

Introduction

Diffusion is the movement of one material, such as a gas or a liquid , in the body of another material. The study of penetrant transport in glassy polymers has received considerable attention for decades because of its growing significance in polymer processing and related applications such as in the electronics industry, microlithography, controlled-release applications, etc. In polymer utilization, when a sample is exposed to a solvent, structure failure may occur due to mechanical softening, embrittlement, or crazing. As a result, application of polymer materials as structure components and as coating or packaging materials requires an understanding of how environmental conditions limit material performance. In the photographic industry, it is of importance to investigate how moisture influences and penetrates coating materials under various environmental conditions, especially relative humidity.

Generally, the diffusion behavior in a polymer depends upon both the characteristics of the polymer (i.e., glass transition temperature, molecular structure, water affinity, etc.) and the characteristics of the penetrant (i.e., molecular size and shape, solubility, etc.).[1] For a plane sheet, the direction of diffusion is usually normal to the plane of polymer film. When a penetrant diffuses into a polymer sample, the macromolecular chains rearrange toward new conformations where the rate of relaxation

depends on the penetrant concentration. The relative rates of penetrant diffusion and macromolecular chains relaxation to new conformations determine the nature of the transport process and lead to a wide variety of penetrant transport phenomena including Fickian, Case II, Super Case II, and anomalous transport. However, the general case of diffusion in materials is usually governed by Fick's laws as mathematically described in equation (8.1):

$$\frac{\partial c}{\partial t} = D_{eff} \frac{\partial^2 c}{\partial x^2} \qquad (8.1)$$

where
- c = concentration of the penetrant
- t = time
- x = distance in the direction of the diffusion
- D_{eff} = diffusion coefficient

By applying the following initial and boundary conditions to equation (8.1):

I.C. $c(x,0) = 0$
B.C. $c(0,t) = c(h,t) = c_{eq}$

where
- c_{eq} = equilibrium concentration
- h = film thickness

Yields the solution expressed in equation (8.2) [2,3]:

$$\frac{M_t}{M_\infty} = 1 - \frac{8}{\pi^2} \sum_{n=0}^{\infty} \frac{1}{(2n+1)^2} \exp\left\{ \frac{-D(2n+1)^2 \pi^2 t}{h^2} \right\} \qquad (2)$$

where M_t and M_∞ are mass uptake at time t and at equilibrium, respectively

The diffusion coefficient can be determined from the plot between M_t / M_∞ vs. $\sqrt{t}$ which is known as the "sorption" curve.[4] In some cases, D_{eff} can be calculated from the "reduced" sorption curve which is the plot between M_t / M_∞ vs. $\sqrt{t} / h$ as well.

According to the "sorption" curve (unless otherwise specified), the classical Fickian diffusion behavior can be characterized by the following measures [4]:

(1) Both absorption and desorption curves are essentially linear in the square root of time for $M_t/M_\infty < 0.60$. This means that the mass uptake is proportional to the square root of time.

(2) Beyond the linear region both absorption and desorption curves are concave to the abscissa axis and should be identical when superimposed.

(3) At fixed initial and final concentration, a superimposed single curve is obtained if each absorption (or desorption) curve for films of different thicknesses is replotted in the form of a reduced curve. Clearly, the curve of M_t / M_∞ vs. $\sqrt{t} / h$ should be independent of the thickness h.

Note that for criterion (3), films of at least two different thicknesses need to be measured which may not be practical. Therefore, in these experiments the diffusion behavior is considered as Fickian if criteria (1) and (2) are valid.

However, not every polymer follows Fickian diffusion. Some factors have to be taken into account such as glass transition temperature(Tg) of the material. According to Alfrey et al.'s work [5], at a temperature far above Tg, the diffusion behavior is Fickian. In this region, the polymers are soft and rubbery; hence, the motion of polymer chains

rcsponds rapidly to the presence of the penetrant. In other words, the relaxation rate is much greater than the diffusion rate. In contrast, the "non-Fickian" behavior is observed at temperatures below Tg in which the polymers are hard or glassy. In this case, the motion of the polymer chains is not fast enough to completely homogenize the penetrant; in other words, the rate of diffusion is very fast compared with that of relaxation. In addition, in the vicinity of Tg (10-15°C above Tg) in which the diffusion and relaxation processes are comparable, the diffusion becomes anomalous or "non-Fickian".[6,7] Examples for "non-Fickian" behavior can be found in the sorption of water by cellulose, keratin, and vinyl acetate.[8-10]

Alfrey, Gurnee, and Lloyed [5] have proposed a simple case for anomalous diffusion so called "Case II diffusion" which can be described as follows:

(1) In contrast to Fickian diffusion, at a temperature well below Tg, a linear relationship exists between the initial mass uptake and time.

(2) Case II diffusion is associated with swelling behavior in which a sharp boundary separates an outer swollen, rubbery shell of uniform concentration from an inner glassy core of zero penetrant concentration.

(3) The swelling front moves through the material at a constant velocity.

(4) The diffusion rate is very fast compared with the relaxation rate. On the other hand, the diffusion process of Fickian behavior is much less than the relaxation process.

Typical absorption and desorption curves for various categories of diffusion behaviors are graphically presented in Figure 8.1.[11] Besides judging from the

definitions and graphs, a common means of defining the type of transport in a planar geometry involves fitting transport data to the heuristic expression: [4]

$$\frac{M_t}{M_\infty} = kt^n \tag{8.3}$$

where k is a constant incorporating characteristics of macromolecule and penetrant systems and n is the diffusional exponent, which is indicative of the transport mechanism. A value of n of 0.50 implies Fickian diffusion, a value of 1.00 implies Case II transport, and for values of n of $0.50 < n < 1.00$ anomalous transport is observed. Values of n greater than 1.00 defines Super Case II transport. It is usually stipulated that this equation is only valid for short times and $M_t/M_\infty < 0.60$.

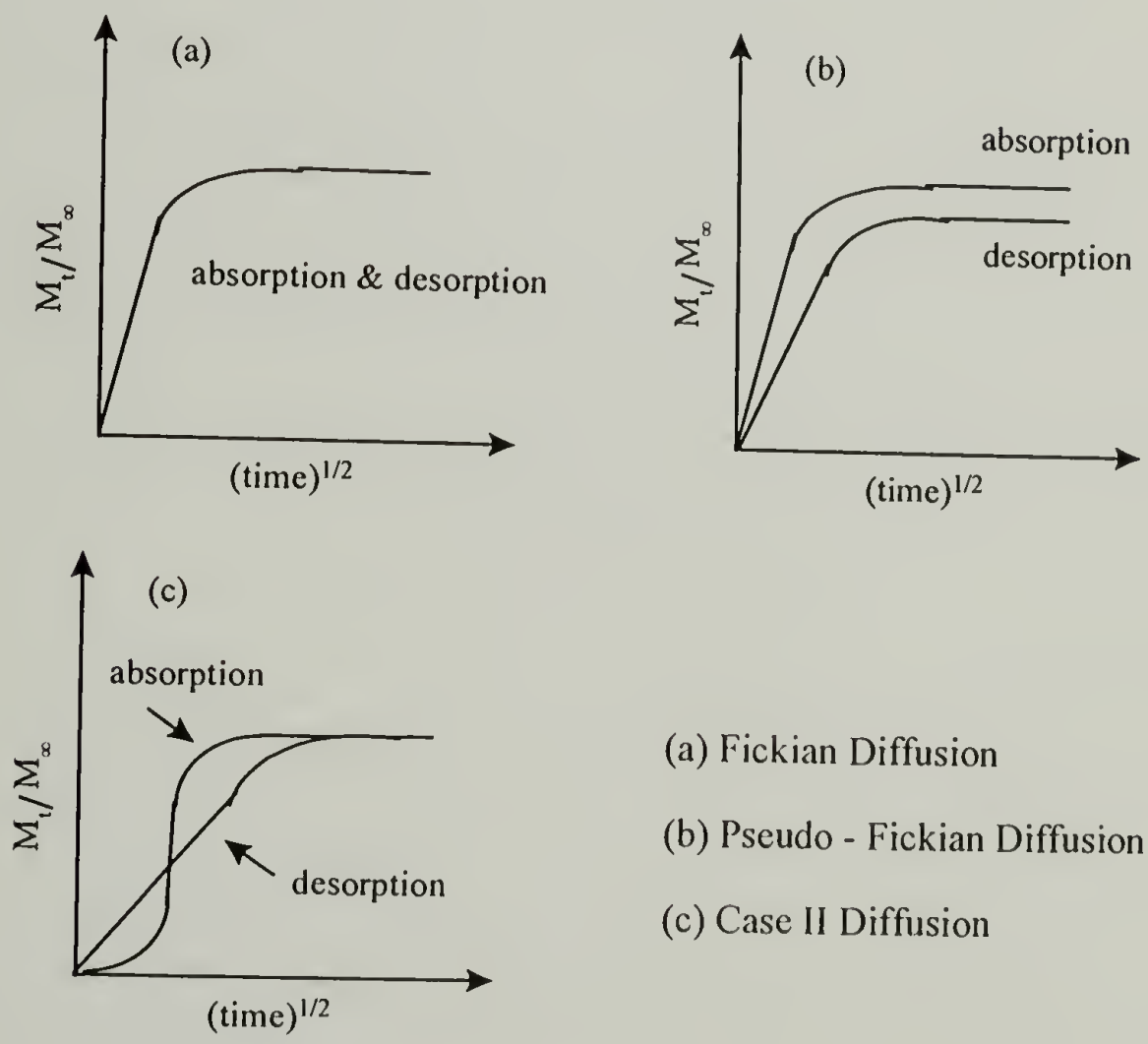

Figure 8.1 : Absorption and desorption curves for various types of diffusion behavior.

As mentioned above, from the plot between M_t / M_∞ vs. $\sqrt{t}$, the diffusion coefficient can be calculated by the initial slope method [12] and the half-time [2] method as follows:

(1) Initial Slope Method

$$D_{eff} = \pi\left[\frac{(slope)h}{4}\right]^2 \tag{8.4}$$

(2) Half-Time Method

$$D_{eff} = \frac{0.0492h^2}{t_{1/2}} \tag{8.5}$$

where $t_{1/2}$ is defined as the time where $M_t / M_\infty = 1/2$

In addition, the diffusion coefficient can also be calculated from the plot between $\log(1 - M_t / M_\infty)$ vs. time by the limiting slope method [13] and the moment method [13] as follows:

(3) Limiting Slope Method

$$D_{eff} = -(slope)\left[\frac{4h}{\pi}\right]^2 \tag{8.6}$$

(4) Moment Method

$$D_{eff} \frac{h^2}{12\left[\int_0^{\infty}\left(1-\frac{M_t}{M_\infty}\right)dt\right]} \tag{8.7}$$

Moreover, Long and Thompson [10] have shown that the diffusion coefficient can also be obtained from equation (8.8) in which the slope is derived from the plot between $\log(M_\infty - M)$ vs. time.

$$D_{eff} = -2.3\left(\frac{h}{\pi}\right)^2(\text{slope}) \tag{8.8}$$

Basically, the diffusion coefficient can be determined by monitoring the mass uptake as a function of time using a conventional gravimetric method e.g. a Cahn Electrobalance that is capable of measuring weights within 0.1 micrograms.[14] However, the instrument is very expensive and controlling the conditions are very critical. Moreover, it is a very time consuming and tedious method. Therefore, other techniques have been designed which are simpler and easier than the conventional gravimetric method.[1,15] By applying one dimensional hygrothermal elasticity theory [11], the changes in stress or strain with time at specific relative humidities can be correlated to the mass uptake as shown in equation (8.9). The details regarding the derivation of this equation were developed elsewhere [11] and was outlined by Jou [1] as presented in an Appendix B.

$$\frac{M_t}{M_\infty} = \frac{\Delta\bar{C}(t)}{\Delta\bar{C}(\infty)} = \frac{\Delta\bar{\sigma}_{xx}(t)}{\Delta\bar{\sigma}_{xx}(\infty)} = \frac{\Delta\bar{\varepsilon}_{xx}(t)}{\Delta\bar{\varepsilon}_{xx}(\infty)} \tag{8.9}$$

As a result, the experiments designed to measure stress or strain as a function of time can be employed to determine the diffusion coefficient as well. For example, Sackinger [15] developed the force-strain technique to measure swelling stress and swelling strain and then related all these properties to mass uptake. Vrtis [16] also applied a real time holographic interferometry to determine the diffusion coefficients by measuring the swelling stress of the materials. The results from these techniques are proven to be consistent with the conventional gravimetric method.

In this research, a commercially available thermomechanical analyzer (TMA) is applied to measure swelling strain of photographic gelatin films exposed to moisture. The diffusion coefficient can then be determined from the plot between normalized swelling strain ($\varepsilon_t/\varepsilon_\infty$) vs. $\sqrt{t}$.

Experimental

Swelling Strain Associated with Diffusion Behavior

Generally, the swelling strain apparatus designed by Sackinger [15] is similar to the thermomechanical analyzer (TMA). In this work, a relative humidity generator is connected to the TMA 2940 from TA Instruments and the length change of the film due to moisture exposure was monitored *in situ*. The changes in the film dimension are called

swelling strains. An experimental set-up equivalent to that described in chapter 6 , Figure 6.2, was used to determine the swelling strain as a function of time at various relative humidities. A thin gelatin film with the dimensions of 5 x 25 mm was held under a small force of 0.001N. The film was initially dried at 0% RH. After there was no further change of the axial dimension, 30% RH was introduced and the length increase as a function of time was monitored until equilibrium was reached. The film was once again exposed to 0% RH and the length decrease monitored. Three cycles of absorption and desorption, 30% RH, 60% RH, and 80% RH, were performed sequentially. The humidity swelling strains were recorded as a function of time. The transient swelling strains were then normalized with respect to the equilibrium swelling strain as described in equation(8.9). The normalized swelling strain vs. time ½ was plotted. The initial slope method was employed to calculate the diffusion coefficient of the film.

Results and Discussion

Swelling Strain Associated with Diffusion Behavior

Figure 8.2 shows the three sorption cycles of gelatin film exposed to moisture at three different relative humidities measured by TMA. Obviously, the swelling strain associated with the diffusion process is reversible with an axial strain that increases by absorption and decreases to the initial state after desorption. The sample presented in

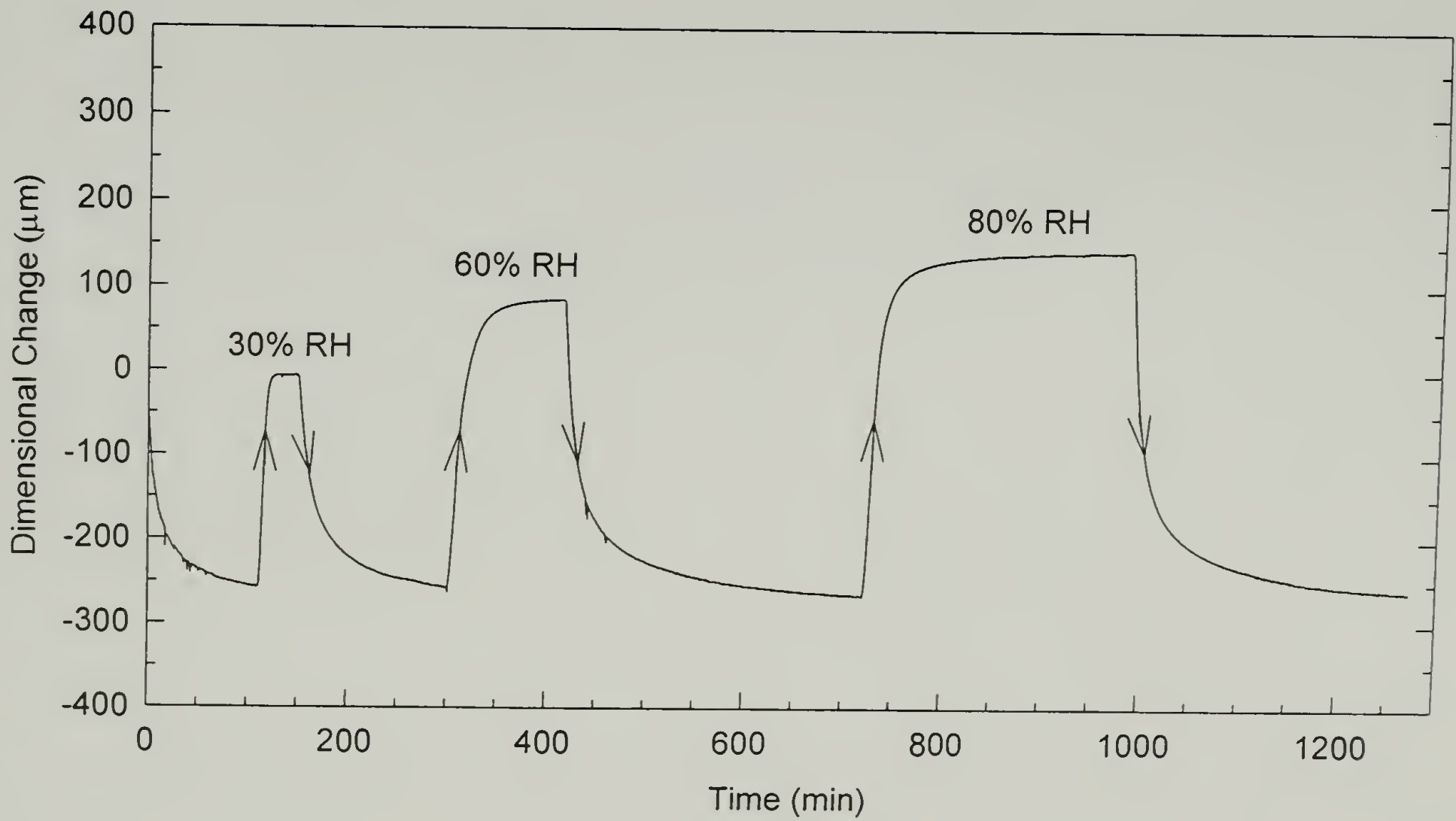

Figure 8.2 : Dimensional Change as a function of time during three sorption cycles for a gelatin-PEMA (BF 8483-412) film measured by the thermomechanical analyzer (TMA).

Figure 8.2 is gelatin-PEMA film (BF 8483-412). Similar behavior can also be obtained for pure gelatin and gelatin-PEA films.

According to the third criterion of Fickian diffusion, the curves should be superimposed when $\varepsilon_t/\varepsilon_\infty$ is plotted against $\sqrt{t}/h$ for various thicknesses of the samples. Such experiments at various dimensions, however, are impractical due to limited thickness variation in the available samples. In this experiment the thickness of the gelatin film is about 10 μm; thus, the diffusion behavior is considered as Fickian if criteria (1) and (2) are valid.

With the information shown in Figure 8.2, the transient swelling strains are then normalized with respect to the equilibrium swelling strain, and the results are presented in Figure 8.3(a) through (c). It can be seen that the absorption of moisture by gelatin is different than its desorption. As shown in Figure 8.3(a), the plot of normalized swelling strain vs. time$^{1/2}$ at 30% RH indicates that the diffusion is "Pseudo-Fickian". In a Pseudo-Fickian diffusion (Figure 8.1(b)), the absorption and desorption curves would not intersect except at the origin. Nevertheless, for the film exposed to moisture at 60% RH and 80% RH, the plot of ($\varepsilon_t/\varepsilon_\infty$) vs. $\sqrt{t}$ are a little different. Up to $\varepsilon_t/\varepsilon_\infty < 0.6$, the absorption and desorption curves are identical. Beyond $\varepsilon_t/\varepsilon_\infty = 0.6$, the diffusion appears to increase with concentration as indicated by the higher absorption curve. Nevertheless, it does necessary imply that the diffusion is "Pseudo-Fickian" as well. In addition, it should be mentioned here that the development of the absorption and desorption curves from 30% RH to 80% RH suggests that the diffusion behavior of gelatin has a tendency to move towards the Fickian diffusion as the relative humidity

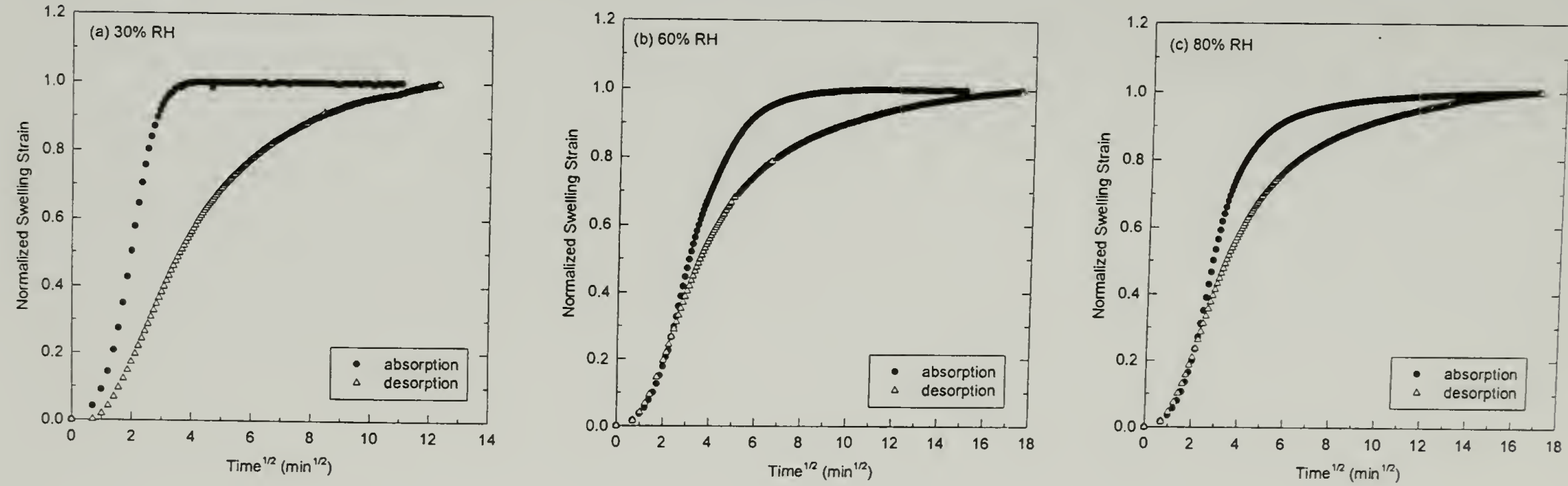

Figure 8.3 : Normalized swelling strain vs. time $^{1/2}$ for a gelatin-PEMA (BF 8483-412) film exposed to moisture at (a) 30% RH, (b) 60% RH, and (c) 80% RH with the data calculated from the swelling strain presented in Figure 8.2.

increases. The anomaly between the absorption and desorption curves is inherent of the moisture sorption hysteresis exhibited by this material.

This is not unexpected behavior since diffusion studies on polymer films have shown that most polymeric materials exhibit typical Fickian diffusion above their Tg, while the diffusion process is more complex below or in the proximity of Tg. This has been attributed to the difference in the mobility of the polymeric chain segments above and below Tg, i.e., above Tg the polymeric chains are capable of some motion which allows diffusion of smaller molecules in between the chains. Recall from chapter 4 that the glass transition temperature of gelatin is moisture dependent. Its Tg decreases with increasing moisture content. At 30% RH, its Tg is much greater than room temperature; hence, gelatin behaves as a glassy material. As a result, the motion of gelatin chains are not rapid enough to entirely homogenize the penetrant. The relaxation rate is much slower than the diffusion rate resulting in an anomalous diffusion namely as the Pseudo-Fickian diffusion. In the case of 60% RH and 80% RH, even though its Tg is lowered due to the presence of absorbed moisture, and the gelatin chains become softer compared to those at 30% RH; however, its glass transition temperatures are still in the vicinity of room temperature. This means that the relaxation rate of gelatin chains is still not fast enough to compete with the diffusion rate of moisture. In fact the diffusion and the relaxation rates are comparable. Therefore, the diffusion behavior at these two relative humidities are more likely to be the Pseudo-Fickian diffusion as well. Additionally, it should be pointed out that the mass transport through the polymer wall, in other words the diffusion coefficient, may increase drastically above the glass transition temperature

due to the transition of the polymer from the glass to the rubber-like state. In the latter the segmental motion promotes the transport of solute molecules.

The diffusion coefficients of the gelatin-PEMA film (BF 8483-412) presented in Figure8.3(a) through (c) were calculated based on the method of initial slope and summarized in Table 8.1. As can be seen, the diffusion coefficients for the absorption path are greater than those of the desorption path. In addition, they increase as a function of relative humidity, particularly at 80% RH where the gelatin-PEMA film shows the greatest diffusion coefficient. These results lead to the conclusion that the diffusion coefficients of the gelatin samples investigated are dependent upon concentration of penetrant. As explained earlier, at 30% RH gelatin behaves as a glassy material; thus, it responds slowly to the presence of moisture. Whereas at the 80% RH, gelatin becomes softer and more rubbery, the motion of gelatin chains reacts faster to the presence of the penetrant toward an equilibrium state; hence, the diffusion coefficients at this condition are greater than the other two relative humidities. In other words, the diffusion coefficient in the plasticized region (80% RH) is taken to be greater than the diffusion coefficient in the glassy region (30% RH and 60% RH).

It has been reported that for diffusion by a Fickian mechanism the rate of desorption is usually less than the rate of absorption if the diffusion coefficient is concentration dependent.[17] This should also apply to the values presented in this work, even though the diffusion behavior is shown to be the Pseudo-Fickian diffusion, because the diffusion coefficients values are proven to be dependent upon the concentration of moisture.

Table 8.1: Diffusion Coefficient of a Gelatin-PEMA Film (BF 8483-412)

Relative Humidity (%)	Diffusion Coefficient (cm^2/sec)		
	Absorption	Desorption	Average
30	3.37E-10	1.39E-10	2.38E-10
60	3.14E-10	1.39E-10	2.27E-10
80	3.97E-10	2.33E-10	3.15E-10

The initial slope and other methods given in equation (8.4) through (8.8) are valid for the situation when the diffusion coefficient is constant, i.e., it is not a function of concentration of penetrant or time. In this work, we shall assume that the diffusion coefficient is independent of time, but as shown in Figure 8.3(a) through (c) the diffusion appears to increase with concentration as indicated by the higher absorption curve. Also, the data shown in Table 8.1 indicate that the diffusion coefficients are dependent upon concentration. In such cases, Crank and Henry [18] developed a mathematical procedure to deduce quantitatively how the diffusion coefficient is related to concentration. From the initial gradient of each absorption or desorption curve, or the half-time, a mean diffusion coefficient, D_{avg}, is obtained of the variable diffusion coefficient averaged over the range of concentration appropriate to that experiment. Their calculations show that for any one experiment, the effective diffusion coefficient D_{avg} suitable for describing transport processes over a range of concentration from C1 to C2 can be defined as:

$$D_{avg} = \frac{\int_{c_1}^{c_2} D(c)dc}{\int_{c_1}^{c_2} dc} \tag{8.10}$$

These calculations are usually very lengthy, however. Crank [12] has extended this method to use both absorption and desorption data as shown in equation (8.11) which is a good approximation to equation (8.10).

$$D_{avg} = \frac{D_a + D_d}{2} \tag{8.11}$$

where D_a and D_d are the diffusion coefficients from the absorption and desorption paths, respectively. This method has been found very satisfactory and was used without further correction by Long and Prager [19] and Hayes and Park [20]. The mean diffusion coefficients, D_{avg}, calculated from the initial slope values of sorption and desorption for the gelatin-PEMA film (BF 8483-412) are also provided in Table 8.1.

In summary, as shown in Figure 8.3(a) through (c) although both absorption and desorption curves are concave to the abscissa axis, the criteria of an initial linear region extending up to 60% of the total swelling strain is not satisfied, and the curves are not identical when superimposed. As a result, we can conclude that the moisture transport for the gelatin film is Pseudo-Fickian diffusion and the diffusion coefficient is concentration dependent. This Pseudo-Fickian diffusion behavior of gelatin film has also been observed by others.[16] Although in their work, the reason for the larger in the diffusion coefficients in the absorption path was not discussed.

However, not every gelatin film examined behave similarly to the gelatin-PEMA film (BF 8483-412) presented in Figure 8.2. Surprisingly, some gelatin films show an exceptional behavior when exposed to moisture at 30% RH as displayed in Figure 8.4 for pure gelatin film (BF 8483-143). Initially, the sorption strain curves show an overshoot, i.e., an abrupt and fast initial straining followed by a decline to the true equilibrium value. This overshoot is not observed in the desorption path and the other two sorption cycles (60% RH and 80% RH). The desorption swelling strain is reversible with an axial strain that decreases to the initial state. The overshooting is not an experimental artifact and is associated with some type of polymer relaxation. In fact, this anomalous behavior can be observed in gelatin-latex films as well. Figure 8.5(a) through (c) provide the normalized swelling strain vs. time$^{1/2}$ at 30% RH for pure gelatin (BF 8483-143), gelatin-PEA (BF 8505-43), and gelatin-PEMA (BF 8483-123) films, respectively.

Published papers in the literature also support this phenomenon.[21-30] Different aspects of the overshoot phenomenon have been addressed. Nevertheless, no work has been carried out for gelatin. Kambour et al. [21], Titow et al. [22], and Overbergh et al. [23] have observed maxima in sorption curves for penetrant transport in various polymers. They attributed the overshoots to crystallization brought about by the presence of the penetrant. They stated that ordered regions formed during the transport process reject the penetrant which was sorbed before the ordered regions existed. Since gelatin does not crystallize to any substantial degree, this explanation is not feasible for the systems studied. Aminabhavi et al. [24,25] studied the diffusion of aromatic and aliphatic liquids into blends of ethylene-propylene random copolymer and isotactic polypropylene, also called Santoprene®, over the temperature interval of 25-70°C.

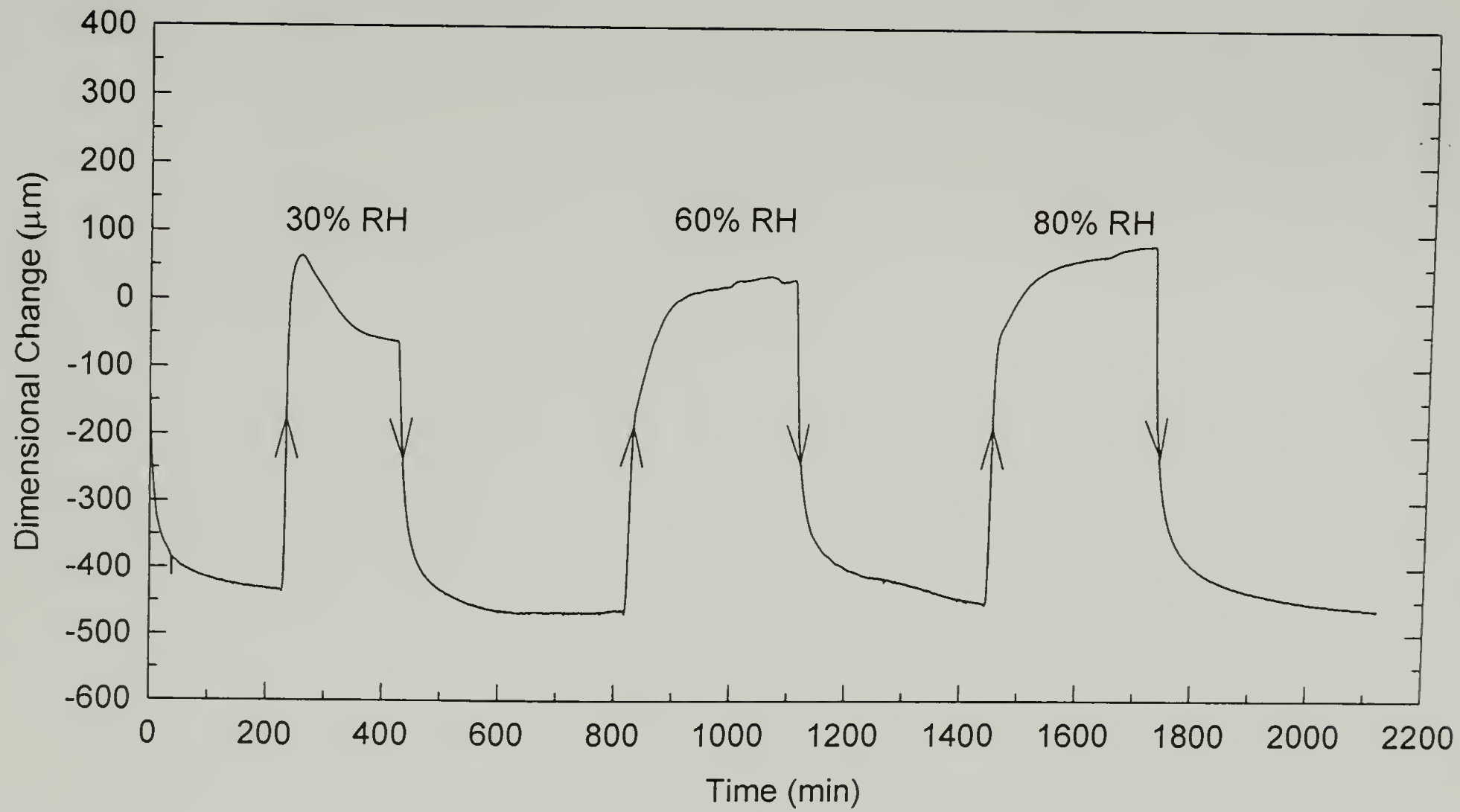

Figure 8.4 : Dimensional Change as a function of time during three sorption cycles for a pure gelatin (BF 8483-143) film measured by the thermomechanical analyzer (TMA).

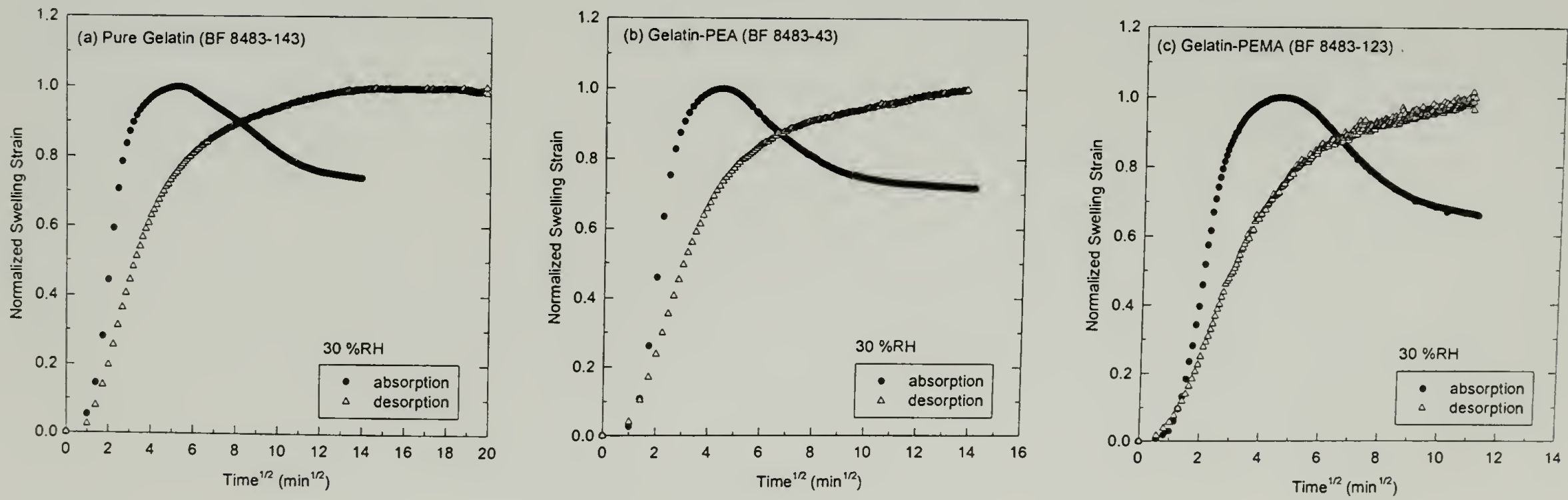

Figure 8.5 : Normalized swelling strain vs. time $^{1/2}$ for (a) pure gelatin (BF 8483-143), (b) gelatin-PEA (BF 8483-43), and (c) gelatin-PEMA (BF 8483-123) films exposed to moisture at 30% RH.

Sorption-desorption-resorption-redesorption (S-D-RS-RD) experiments were conducted to determine the sorption equilibrium and diffusion coefficients. For all liquids, results indicated an overshoot effect in the absorption curves, i.e., the uptake curves for Santoprene® immersed in solvents show a decrease after reaching a maximum. They claimed that the overshoot effect may have been associated with a polymer relaxation effect as well as the leaching out phenomenon (i.e., the loss of additives from the polymer during sorption). In other studies, such overshooting is the result of a loss of residuals/additives from the polymer.[26-30] However, overshoot was not observed with desorption, resorption, and redesorption runs. These results are comparable to our work that the overshoot was not observed with the desorption path of 30% RH, 60% RH cycle, and 80% RH cycle. Since the sorption cycles at 60% RH and 80% RH were performed consecutively after the film was exposed to 30% RH ;thus, these two relative humidities can be considered as resorption-redesorption cycles in Aminabhavi's work.

In our case, according to Alfrey's classical work [5], in the glassy polymer, the motions of polymer chains are not rapid enough to thoroughly homogenize the penetrant, and it causes some anomalous diffusion. Consequently, at 30% RH in which the gelatin film is in the glassy state, an overshoot is attributed to moisture diffusion into the gelatin network before its chains have sufficient time to relax (i.e., moisture diffusion is faster when compared to polymer relaxation). This results in the initial overshoot reaching a maximum. When gelatin chains finally relax, the equilibrium is attained.

After all, it should be note that this overshoot behavior occurred randomly in both pure gelatin and gelatin-latex films investigated, no systematic correlation can be found at

this stage. To elucidate the relationship among these films which exhibit this exceptional behavior, more investigation to resolve this anomaly is needed.

Latex Concentration vs. Diffusion Coefficient

Table 8.2 presents the effect of latex concentration on the diffusion coefficient for the gelatin-latex films. Clearly, the diffusion coefficients of the gelatin films increase with an increase in the latex concentration. The gelatin films containing 40 parts latex, either PEA or PEMA, have the greatest diffusion coefficients. No significant difference is observed between the two latex systems. In fact, the magnitude of the diffusion coefficients in both gelatin-latex systems are in the same range. Furthermore, similar to the results provided in Table 8.1, the diffusion coefficients of the gelatin films are dependent upon the concentration of the moisture, i.e., the diffusion coefficient values of the absorption curves are greater than those of the desorption curves; the diffusion coefficients increase with increasing relative humidity. All these observation can also be found from the data presented in Tables 8.3 through 8.5.

The increase in the diffusion rate with the latex content can be explained in terms of the relation between the physical structure, i.e., the effect of the degree of order, or crystallinity, of the investigated gelatin samples and their sorption of moisture. It is well established that sorption occurs mainly, if not exclusively, in the noncrystalline regions of a polymer. Also, diffusion is much faster in amorphous regions than in crystalline regions. Recall from chapter 4 (Table 4.2 and Figure 4.8(c)) that the degree of

Table 8.2 : Effect of Latex Concentration on the Diffusion Coefficient (D_{eff}) for Gelatin-Latex Films at Three Different Relative Humidities

Sample ID	Sample Description	Latex Conc (part)	Diffusion Coefficient (cm^2/sec)								
			Absorption			Desorption			Average		
			30% RH	60% RH	80% RH	30% RH	60% RH	80% RH	30% RH	60% RH	80% RH
BF 8483-133	Gelatin-PEA	0	2.65E-10	3.09E-10	3.28E-10	1.34E-10	1.34E-10	1.41E-10	2.00E-10	2.22E-10	2.35E-10
BF 8483-43		20	2.82E-10	2.78E-10	3.75E-10	1.45E-10	1.59E-10	1.75E-10	2.14E-10	2.19E-10	2.75E-10
BF 8505-372		40	3.41E-10	3.09E-10	4.91E-10	1.16E-10	1.63E-10	2.09E-10	2.29E-10	2.36E-10	3.50E-10
BF 8483-133	Gelatin-PEMA	0	2.65E-10	3.09E-10	3.28E-10	1.34E-10	1.34E-10	1.41E-10	2.00E-10	2.22E-10	2.35E-10
BF 8483-163		20	3.06E-10	2.90E-10	3.77E-10	1.49E-10	1.88E-10	2.27E-10	2.28E-10	2.39E-10	3.02E-10
BF 8505-412		40	3.37E-10	3.14E-10	3.97E-10	1.39E-10	1.39E-10	2.33E-10	2.38E-10	2.27E-10	3.15E-10

crystallinity of gelatin decreases with increasing latex concentration at all relative humidities investigated, and there is no difference between the two latex systems. Pure gelatin film has the greatest degree of crystallinity among all the films considered. Accordingly, the diffusion of moisture through the gelatin film is slowest for the pure gelatin film and fastest for the gelatin film with 40 parts latex.

Latex Particle Size vs. Diffusion Coefficient

The effect of latex particle size on the diffusion coefficient for gelatin-PEA and gelatin-PEMA films is provided in Table 8.3. In both latex systems, results indicate that the diffusion coefficients of the gelatin films with smaller latex particle size (0.051 μm or 0.067 μm) are less than those of the gelatin films with larger latex particle size (0.112 μm or 0.150 μm). In other words, the diffusion rate of moisture through the gelatin-latex film increases with an increase in the latex particle size. This is true for all the investigated relative humidities and sorption paths. Also, as already mentioned, the diffusion coefficients of all the gelatin-latex films are concentration dependent.

The effect of latex particle size on the diffusivity of gelatin-latex films can be explained by comparing the amount of surface area between the two phases, i.e., gelatin matrix and latex particles, of the two latex particle sizes. The surface area between the two phases plays an important role in the diffusion process. At the same weight fraction of latex particle, which was 20 parts in this case, the surface area is expected to increase as the size of latex particle becomes smaller. In other words, the gelatin film which

Table 8.3 : Effect of Latex Particle Size on the Diffusion Coefficient (D_{eff}) for Gelatin-Latex Films at Three Different Relative Humidities

Sample ID	Sample Description	Latex Size (μm)	Diffusion Coefficient (cm^2/sec)								
			Absorption			Desorption			Average		
			30% RH	60% RH	80% RH	30% RH	60% RH	80% RH	30% RH	60% RH	80% RH
BF 8483-173	Gelatin-PEA	0.051	2.60E-10	2.62E-10	3.34E-10	1.39E-10	1.45E-10	1.62E-10	2.00E-10	2.04E-10	2.48E-10
BF 8483-43		0.112	2.82E-10	2.78E-10	3.75E-10	1.45E-10	1.59E-10	1.75E-10	2.14E-10	2.19E-10	2.75E-10
BF 8483-123	Gelatin-PEMA	0.067	2.92E-10	2.72E-10	3.25E-10	1.43E-10	1.57E-10	1.99E-10	2.18E-10	2.15E-10	2.62E-10
BF 8483-163		0.15	3.06E-10	2.90E-10	3.77E-10	1.49E-10	1.88E-10	2.27E-10	2.28E-10	2.39E-10	3.02E-10

contains smaller latex particle size (0.051 μm or 0.067 μm) possesses a larger surface area compared to the gelatin film with the larger latex particle size (0.112 μm or 0.150 μm). This means that the diffusion path of the moisture through the gelatin samples is increased when smaller latex particles are present. Consequently, the diffusion rate of the moisture through the gelatin-latex films decreases with decreasing the latex particle size.

Gelatin Concentration at Set Point vs. Diffusion Coefficient

As shown in Table 8.4, gelatin concentration at set point also has an effect on the diffusion coefficient in both pure gelatin and gelatin-latex films. For the pure gelatin film, it was observed that increasing the gelatin concentration at set point on the emulsion layer showed a decrease in the diffusion coefficient. At every relative humidity for both absorption and desorption paths, the values of diffusion coefficient for the films containing 15% gelatin concentration are lower than those for the films with 10% gelatin concentration, and these values increase from 30% RH to 80% RH. The same trend as observed for the pure gelatin films was obtained for the gelatin-latex films as well.

These results again can be explained in term of the gel structure or the degree of crystallinity of the gelatin samples. Recall from Figure 4.11(c) in chapter 4 that the heat of fusion for both pure gelatin and gelatin-latex films containing 15% gelatin concentration are higher than that of the films with 10% gelatin concentration. This result suggests that the films with 15% gelatin concentration have more gel structure and a higher degree of crystallinity; as a result, the diffusion rate of moisture through these

Table 8.4 : Effect of Gelatin Concentration at Set Point on the Diffusion Coefficient (D_{eff}) for Pure Gelatin and Gelatin-Latex Films at Three Different Relative Humidities

Sample ID	Sample Description	Gelatin Conc (%)	Diffusion Coefficient (cm^2/sec)								
			Absorption			Desorption			Average		
			30% RH	60% RH	80% RH	30% RH	60% RH	80% RH	30% RH	60% RH	80% RH
BF 8483-133	Pure Gelatin	10	2.65E-10	3.09E-10	3.28E-10	1.34E-10	1.34E-10	1.41E-10	2.00E-10	2.22E-10	2.35E-10
BF 8483-83		15	2.16E-10	2.98E-10	3.23E-10	1.32E-10	1.31E-10	1.38E-10	1.74E-10	2.15E-10	2.31E-10
BF 8483-173	Gelatin-PEA	10	2.60E-10	2.62E-10	3.34E-10	1.39E-10	1.45E-10	1.62E-10	2.00E-10	2.04E-10	2.48E-10
BF 8505-482		15	2.22E-10	2.38E-10	3.06E-10	1.34E-10	1.34E-10	1.48E-10	1.78E-10	1.86E-10	2.27E-10
BF 8483-123	Gelatin-PEMA	10	2.92E-10	2.72E-10	3.25E-10	1.43E-10	1.57E-10	1.99E-10	2.18E-10	2.15E-10	2.62E-10
BF 8483-93		15	2.48E-10	2.52E-10	3.16E-10	1.32E-10	1.36E-10	1.69E-10	1.90E-10	1.94E-10	2.43E-10

samples is slower when compared to the films with 10% gelatin concentration at set point.

Drying Condition at Vitrification vs. Diffusion Coefficient

The experimental data regarding the dependence of the diffusion coefficient on the drying condition at vitrification for pure gelatin and gelatin-latex films at various relative humidities are presented in Table 8.5. Apparently, the diffusion coefficients of the films dried at the HMERH condition (80 F / 29% RH) are lower than those of the films dried at the LMERH condition (130F / 5.5% RH) for all the relative humidities studied. Once again the greater the diffusion rate of moisture through the gelatin films in the absorption path compared to that of the desorption path, including the increase in these values with increasing relative humidity, suggest that the diffusion coefficients of the gelatin films depend upon the concentration of moisture.

Similar to the effect of the latex concentration and the gelatin concentration at set point on to the diffusion coefficient of the gelatin film, the degree of crystallinity is likely responsible for the difference in diffusion rate of the gelatin films dried at two distinct conditions. As described earlier in chapter 4, both pure gelatin and gelatin-latex films dried at the HMERH condition have a greater amount of crystalline structure compared to the films dried at the LMERH condition. Thus, moisture can easily penetrate into the relatively large amount of amorphous structure of the films dried at the LMERH condition resulting in the faster diffusion rate of moisture through the films.

Table 8.5 : Effect of Drying Condition at Vitrification on the Diffusion Coefficient (D_{eff}) for Pure Gelatin and Gelatin-Latex Films at Three Different Relative Humidities

Sample ID	Sample Description	Drying Condition	Diffusion Coefficient (cm^2/sec)								
			Absorption			Desorption			Average		
			30% RH	60% RH	80% RH	30% RH	60% RH	80% RH	30% RH	60% RH	80% RH
BF 8483-133	Pure Gelatin	HMERH	2.65E-10	3.09E-10	3.28E-10	1.34E-10	1.34E-10	1.41E-10	2.00E-10	2.22E-10	2.35E-10
BF 8483-143		LMERH	2.81E-10	3.12E-10	3.33E-10	1.39E-10	1.46E-10	1.66E-10	2.10E-10	2.29E-10	2.50E-10
BF 8483-173	Gelatin-PEA	HMERH	2.60E-10	2.62E-10	3.34E-10	1.39E-10	1.45E-10	1.62E-10	2.00E-10	2.04E-10	2.48E-10
BF 8483-183		LMERH	3.01E-10	3.08E-10	3.43E-10	1.48E-10	1.47E-10	2.03E-10	2.25E-10	2.28E-10	2.73E-10
BF 8483-123	Gelatin-PEMA	HMERH	2.92E-10	2.72E-10	3.25E-10	1.43E-10	1.57E-10	1.99E-10	2.18E-10	2.15E-10	2.62E-10
BF 8483-113		LMERH	3.11E-10	2.79E-10	3.57E-10	1.50E-10	1.71E-10	2.02E-10	2.31E-10	2.25E-10	2.80E-10

Conclusions

The moisture diffusion behavior of pure gelatin and gelatin-latex films was investigated using a Thermomechanical Analyzer (TMA). Although both absorption and desorption curves are concave to the abscissa axis, the criteria of an initial linear region extending up to 60% of the total swelling strain was not satisfied, and the plots of normalized swelling strain vs. time$^{1/2}$ between the absorption and desorption curves of gelatin films were not identical when superimposed and only intersected at the origin. These results indicate that the transport of moisture through the gelatin and gelatin-latex films is "Pseudo-Fickian" diffusion.

An interesting result occurred at 30% RH where the absorption strain curve increased initially and after attaining a maximum, it decreased. The observed overshoot effect is characteristic of the relative importance of moisture diffusion and polymer relaxation phenomena. It is related to a relaxation process of the macromolecular chains occurring in the polymer after the material has become rubbery, but before the real equilibrium has been attained. However, more investigation is still needed to explain the cause of this phenomenon including the relationship among the gelatin samples studied.

The criteria of Fickian diffusion states the diffusion coefficient is independent of concentration of the penetrant. One can either carry out absorption-desorption experiments to determine the concentration dependence of the diffusion coefficient, or perform the sorption experiments at the same temperature for samples exposed to various concentration of the penetrant. In this experiment, we chose to do both categories by running the absorption and desorption tests at three different conditions (30% RH, 60%

RH, and 80% RH). From the absorption-desorption experiments, the diffusion appeared to increase with concentration as indicated by the higher absorption curve. And from the second method, data tabulated in Table 8.1 through 8.5 confirm that the diffusion coefficients of gelatin films increased with increasing relative humidity. Accordingly, we can conclude that the diffusion coefficient of gelatin film is dependent upon concentration of the penetrant, which is the moisture in this case.

The diffusion coefficients of moisture molecules through various gelatin films, as calculated from the sorption curves using the initial slope method, indicated a strong dependence between the diffusion coefficient and the relative humidity. The transport rate increased with an increase in the relative humidity. This is because the diffusion coefficients are dependent on the glass transition temperature (Tg) of the gelatin films.

The diffusion coefficients show a dependence on the latex concentration and latex particle size as well as drying condition at vitrification and gelatin concentration at set point. In both latex systems, the increase in the values of diffusion coefficients with increasing the latex concentration was apparent. The gelatin films with 40 parts latex, either PEA or PEMA, had the greatest diffusion coefficients. For the latex particle size, the gelatin-latex films with smaller latex particle size (0.051 μm or 0.067 μm) show a slower diffusion rate of moisture than the gelatin films with larger latex particle size (0.112 μm or 0.150 μm). Increasing the latex particle size resulted in increasing the moisture diffusion coefficients. Additionally, it was observed that there was no significant difference in the moisture diffusion coefficients between the two latex systems.

It was also found that the gelatin concentration at set point and the drying condition at vitrification affected the diffusion coefficients of the gelatin films. The diffusion rate of moisture through the pure gelatin and gelatin-latex films decreased as the gelatin concentration increased. Thus, the films with 15% gelatin concentration had lower diffusion coefficients. Also, the diffusion coefficients of moisture for the films dried at the HMERH condition (80 F / 29% RH) were slightly less than those of the films dried at the LMERH condition (130F / 5.5% RH).

References

1. Jou, C.S., "Stress Associated with Transport in Polymer Films", Ph.D. Dissertation, University of Massachusetts, Amherst, MA (1993).

2. Crank, J. and Park, G.S., "An Evaluation of the Diffusion Coefficient for Chloroform in Polystyrene from Simple Absorption Experiments", *Transactions of the Faraday Society*, **45**, 240 (1949).

3. Thomas, A.M. and Gent, W.L., "Permeation and Sorption of Water Vapour in Varnish Films", *Proceedings of the. Physical. Society, London.*, **57**, 324 (1945).

4. Crank, J. In *Diffusion in Polymers*; Crank, J. and Park, G.S., Eds.; Academic Press: New York, 1968.

5. Alfrey, T., Gurnee, E.F., and Lloyd, W.G., "Diffusion in Glassy Polymers", *Journal of Polymer Science, Part C.*, **12**, 249 (1966).

6. Hopfenberg, H.B. and Frisch, H.L., "Transport of Organic Micromolecules in Amorphous Polymers", *Journal of Polymer Science , Part B.*, 7, 405 (1969).

7. Vrentas, J.C. and Duda, J.L., "Molecular Diffusion in Polymer Solutions", *AICHE Journal*, **25**, 1 (1979).

8. Newns, A.C., "The Sorption and Desorption Kinetics of Water in a Regenerated Cellulose", *Transactions of the Faraday Society*, **52**, 1533 (1956).

9. King, G., "Sorption of Vapors by Keratin and Wool", *Transactions of the Faraday Society*, **41**, 325 (1945).

10. Long, F.A. and Thompson, L.J., "Diffusion of Water Vapor in Polymers", *Journal of Polymer Science*, **15**, 413 (1955).

11. Sih, G.C., Michopoulos, J.G., and Chou, S.C., Eds.; *Hygrothermoelasticity*; Martinus Nijhoff Publishers: Dordrecht, Netherlands, 1986.

12. Crank, J. *The Mathematics of Diffusion*; Oxford Clarendon Press: London, 1956.

13. Felder, R.M. and Huvard, G.S. *Methods of Experimental Physics*; Academic Press: New York, 1980.

14. Cahn Instruments, Inc., Cerritos, CA 90701.

15. Sackinger, S.T., "The Determination of Swelling Stress in Polyimide Films", Ph.D. Dissertation, University of Massachusetts, Amherst, MA (1989).

16. Vrtis, J.K., "Stress and Mass Transport in Polymer Coating and Films", Ph.D. Dissertation, University of Massachusetts, Amherst, MA (1995).

17. Watt, I.C., "Determination of Diffusion Rates in Swelling Systems", *Journal of Applied Polymer Science*, **8**, 2835 (1964).

18. Crank, J. and Henry, E., "Diffusion in Media with Variable Properties. Part I. The Effect of a Variable Diffusion Coefficient on the Rates of Absorption and Desorption", *Transactions of the Faraday Society*, **45**, 636 (1949).

19. Prager, S. and Long, F., "Diffusion of Hydrocarbons in Polyisobutylene", *Journal of the American Chemical Society*, **73**, 4072 (1951).

20. Hayes, M. and park, G., "The Diffusion of Benzene in Rubber", *Transactions of the Faraday Society*, **52**, 949 (1956).

21. Kambour, R.P., Karasz, F.E., and Daane, J.H., "Kinetic and Equilibrium Phenomena in the System: Acetone Vapor and Polycarbonate Film", *Journal of Polymer Science, Part A-2*, **4**(3), 327 (1966).

22. Titow, W.V., Braden, M, Currel, B.R., and Loneragan, R.J., "Diffusion and Some Structural Effects of Two Chlorinated Hydrocarbon Solvents in Bisphenol A Polycarbonate", *Journal of Applied Polymer Science*, **18**, 867 (1974).

23. Overbergh, N, Berghmans, H., and Smets, G., "Crystallization of Isotactic Polystyrene Indued by Organic Vapors", *Polymer*, **16**(10), 703 (1975).

24. Aminabhavi, T.M., Phayde, H.T.S., and Ortego, J.D., " Diffusion of Aromatic Liquids into Blends of Ethylene-Propylene Copolymers and Isotactic Polypropylene Membrane", *Polymer and Polymer Composites*, **4**(1), 13 (1996).

25. Aminabhavi, T.M., Phayde, H.T.S., and Ortego, J.D., "Sorption/Desorption and Diffusion Anomalies in Santoprene-Alkane Systems", *Polymer and Polymer Composites*, **4**(2), 103 (1996).

26. Peppas, N.A. and Urdahl, K.G., " Anomalous Penetrant Transport in Glassy Polymers VII. Overshoots in Cyclohexane Uptake in Crosslinked Polystyrene", *Polymer Bulletin*, **16**, 201 (1986).

27. Urdhal, K.G. and Peppas, N.A., " Anomalous Penetrant Transport in Glassy Polymers V. Cyclohexane Transport in Polystyrese", *Journal of Applied Polymer Science*, **33**, 2669 (1987).

28. Walker, C.M. and Peppas, N.A., " Solute and Penetrant Diffusion in Swellable Polymers: X. Swelling of Multiethylene Glycol Dimethacrylate Copolymers", *Journal of Applied Polymer Science*, **39**, 2043 (1990).

29. Kim, D., Caruthers, J.M., and Peppas, N.A., " Penetrant Transport in Cross-Linked Polystyrene", *Macromolecules*, **26**, 1841 (1993).

30. Johnson, H.E., Clarson, S.J., and Granick, S., " Overshoots as Polymer Adsorb", *Polymer*, **34**, 1960 (1993).

CHAPTER 9

CONCLUSIONS AND FUTURE WORK

Conclusions

Gelatin has been used for many years as a binder or protective colloid for light-sensitive silver halide photographic products because of its exceptional properties. It has the ability to keep the silver halide crystals finely dispersed and inherently has the ability of imparting non-optical sensitivity to the grains. However, the gelatin layer is very sensitive to changes in atmospheric conditions, especially humidity changes. Although this sensitivity to moisture is favorable when film is processed, it is also a drawback to the use of gelatin in an emulsion layer because it can cause dimensional instability in photographic film.

Attempts have been made to find a synthetic material which would be suitable as a dispersing agent and colloid carrier for silver halide crystals, and which would overcome the deficiencies of gelatin. Such an emulsion must possess the sensitometric characteristics and permeability to the usual photographic processing solutions comparable to an emulsion comprising gelatin as the sole binder.

At present, materials are still pursued which will render photographic layers mainly consisting of gelatin less brittle, and which instill greater dimensional stability to the photographic material and also decrease its tendency to curl. First, these substances should be compatible with gelatin and the photographic emulsions. Secondly, they

should not impair the optical properties of the photographic layers. Finally, they should be completely inert to light sensitive compounds, dyes, sensitizing agents, etc. These conditions are satisfied to a large extent by mixing the gelatin with certain polymer latices.

This work has focused on the hygroscopic effects on gelatin when it is used as a binder in the emulsion layer of photographic materials. Pure gelatin and gelatin with additives applied to a PET substrate were studied. Two types of polymer latices, PEA and PEMA, were used as modifiers and compared. The moisture sorption behavior, thermal and tensile properties, dimensional stability, swelling stress, and moisture diffusion behavior were investigated as a function of relative humidity, latex particle size, latex concentration, drying conditions at vitrification, and concentration of gelatin at set point.

A Cahn 2000 recording electrobalance was employed to determine the moisture uptake of pure gelatin, gelatin-latex, and PET films as a function of time at various relative humidities. In both gelatin and PET films, the amount of absorbed moisture increased as the relative humidity increased. However, due to the strong hydrophilic nature, gelatin can absorb much more moisture than the PET substrate. The very high moisture absorption of the gelatin film, when compared to the very low moisture absorption of the PET substrate, is one of the reasons for the curling effect which gelatin has on the dimensional stability of photographic film.

The incorporation of a polymer latex can reduce the moisture sensitivity of the emulsion layer. The amount of sorbed moisture in the emulsion layer decreased when polymer latices were added to the system, especially for the gelatin-PEA film. This is the

favorable effect because it can reduce the mismatch of the moisture swelling between the emulsion layer and the PET substrate. As a result, the dimensional stability of the photographic film is improved. Other factors, such as the gelatin concentration at set point or the drying conditions at vitrification, also affected the moisture absorption of the emulsion layer. The gelatin film with the lower gelatin concentration picked up more moisture. The moisture uptake of the gelatin film dried at the HMERH condition (130F / 5.5% RH) was slightly greater than the film dried at the LMERH condition (130F / 5.5% RH).

In addition, results have shown a moisture sorption hysteresis in the gelatin films, which is a general phenomenon observed in paper, polymer, and protein sorption systems. It is a phenomenon in which different paths exist for absorption and desorption isotherms of moisture at the same relative humidity. Typically, the desorption path is always greater than the absorption path. Several attempts have been made to explain this phenomenon and are highlighted in chapter 3.

Effect of moisture on thermal transition temperatures was characterized by a differential scanning calorimetry (DSC). The decrease in both the melting temperature and the glass transition temperature of pure gelatin and gelatin-latex films with an increase in moisture content were observed, and can be explained by the effect of crystallization temperature and the plasticization effect of water, respectively. The thermodynamic theory of the effect of composition on the glass transition temperature (Tg) in polymer / diluent (i.e. the Couchman-Karasz equation) was adopted to describe the plasticization effect of water on the films. The experimental results show fair agreement to the theoretical prediction.

In both latex systems, an absenec of any Tg shift with latex eoneentration demonstrates that the blend eomponents are immiseible. The heat of fusion of gelatin decreased as the latex coneentration incrcased. This is beeause thc latex particlcs eould interfere with the crystallization of thc gelatin by interaeting with thc gelatin in sueh a way as to prevent an interchain hydrogcn bonding, rcsulting in the suppression of the gelation, or more precisely, decreasing the degree of erystallinity.

Latcx particle size had no effect on the calorimetric propertics, whercas both thc gelatin concentration at set point and the drying condition at vitrification showcd significant effects on thc thermal properties of the gelatin films. Thc greater amorphous structure in the film containing 10% gelatin concentration enabled the film to absorb more moisture and hence, show a lower Tg and heat of fusion. Similarly, due to thc plasticization effect of moisture, thc Tg of the film dried at the HMERH condition (80F / 29% RH) was lowcr than that of the film dried at the LMERH eondition (130F / 5.5% RH). Also, the lower Tm and higher ΔH for the film dried at the HMERH eondition compared to the film dried at the LMERH condition can be described by the crystallization theory. The lower the gelation temperature, thc higher the crystallinity, but the smaller and less perfect are its crystallites.

Tensile propertics of the gelatin and gelatin-latex films werc determined as a function of relative humidity using a Sintcch tensile testcr (MTS Systcm Corporation). Results have shown that both tensile strength and Young's modulus decreascd with incrcasing moisturc content, whcrcas the clongation to break increased. In other words,

the tensile properties of both pure gelatin and gelatin-latex films range from hard glass-like at lower relative humidities, to soft rubber-like at higher relative humidities.

Both latices showed similar effects on the thermal properties; however, the effects of these two latices on the tensile properties of the gelatin film were significantly different. The inclusion of PEA latex in the gelatin matrix increased the elongation to break and toughness but reduced the Young's modulus and tensile strength of the gelatin film. However, this is not the case for gelatin-PEMA films. Although the PEMA latex also lowered the tensile strength and Young's modulus, it reduced the toughness and elongation to break of the gelatin films.

In both latex systems, the tensile modulus decreased with increasing latex concentration. The pure gelatin films had the highest Young's modulus, while the gelatin films with 40 parts PEA had the lowest Young's modulus. The experimental values of the Young's modulus of the gelatin-PEA films were in closed agreement with those predicted by the semi-empirical composite models. No effect of latex particle size was observed on the tensile properties of the gelatin-latex films in the investigated diameter range. Similarly, neither the drying condition at vitrification nor the gelatin concentration at set point affected the Young's modulus of both pure gelatin and gelatin-latex films.

An optical microscope and a SEM were used to investigate the deformation morphology of the fractured gelatin film surfaces. Observation revealed the presence of either micro-voids or bubbles of entrapped air, small cracks, crazes, and shear banding.

The effect of moisture and temperature on the dimensional stability of the gelatin film was investigated in chapter 6. For comparison, the hygrothermal effect on the dimensional stability of PET substrate was also studied. A thermomechanical analyzer

(TMA) was used to measure the dimensional change of a film as a function of time, temperature, and relative humidity. Results have shown a great influence of moisture on the dimensional stability of the gelatin film. Even though the effect of humidity on the dimensional stability of the gelatin film is much more pronounced than the effect of temperature, results suggest that both the mismatch in the humidity expansion coefficient (HEC) and the coefficient of thermal expansion (CTE) between the gelatin layer and PET substrate contribute to the dimensional instability in a photographic film.

From the humidity swelling strain experiment, it was determined that the PET substrate was an in-plane anisotropic material (i.e., biaxial oriented in the plane of the film) and displayed two humidity expansion coefficients, 10.5 and 5.97 μm/m %RH. In contrast, the gelatin film was an in-plane isotropic material having a single humidity expansion coefficient. The humidity expansion coefficient was determined from the slope of the plot between the humidity swelling strain vs. relative humidity.

An addition of latex particles, either PEA or PEMA, into the gelatin film helped improve the dimensional stability (i.e. lowered the HEC of the gelatin emulsion layer) of the films exposed to the moisture. While the humidity expansion coefficient (HEC) decreased and the coefficient of thermal expansion (CTE) increased with increasing in the latex concentration, the latex particle size had no effect on both HEC and CTE. It was also found that the gelatin concentration at set point and the drying condition at vitrification did not affect the CTE; however, these two parameters showed significant effects on the HEC of the gelatin films.

Composite theories for the thermal expansion coefficient of an isotropic composite filled with spherical particles were applied to determine the humidity expansion coefficient of the gelatin-latex films. The experimental data for the CTE and HEC of the two gelatin-latex systems were in excellent agreement with the model prediction based on the rule of mixtures and the modulus-modified rules of mixtures or Turner's equation, respectively.

In comparing the gelatin-PEA and gelatin-PEMA films, the HEC values have been found to depend upon the bulk stiffness of the film. Chapter 5 showed that the stiffness of the film, in turn, depends upon the relative humidity, and therefore the moisture content. Consequently, the HEC is a combination of moisture content and stiffness. Thus, in order to obtain a gelatin film with the greatest dimensional stability to moisture exposure (i.e. lowest HEC), the film should have low moisture absorption and high bulk stiffness so that it can resist humidity expansion.

This statement was true for the PET film. Due to the lower moisture absorption and greater stiffness of the PET substrate, its HEC was considerably less than that of the gelatin film. However, in the case of pure gelatin vs. gelatin-latex films, although the pure gelatin film possesses higher stiffness, its HEC was greater than that of the gelatin-latex film. This is because of the strong hydrophilic nature of the gelatin. In contrast to the case of gelatin-PEA vs. gelatin-PEMA films, the greater moisture absorption of the gelatin-PEMA film was dominated by its greater stiffness; as a result, the gelatin-PEMA film has a higher resistance to the humidity expansion (i.e. lower HEC) than the gelatin-PEA film. In summary, based on the scope of this investigation, the gelatin film dried at the LMERH condition (130F / 5.5% RH) with 40 parts PEMA and 15% gelatin

concentration at set point has proved to be the film with the greatest dimensional stability (i.e. lowest HEC) to the moisture exposure.

In addition, results have shown a dimensional hysteresis in the gelatin film. This dimensional hysteresis coincided with the moisture sorption hysteresis when the desorption path was greater than the absorption path. Besides a typical dimensional hysteresis, a "reversed dimensional hysteresis" of the gelatin film, caused by moisture-induced relaxation shrinkage at a high relative humidity, was also observed. Furthermore, thermal-induced relaxation shrinkage was observed in both the gelatin film and the PET substrate when they were heated to the temperature above their Tgs. In the case of gelatin, the thermal-induced relaxation shrinkage was analogous to the moisture-induced relaxation shrinkage. In both cases, the gelatin molecules were stretched and then "frozen" in a position either by drying or cooling. When they were "unfrozen" at a later time by heat or moisture, their molecules were free to contract to their preferred position.

A vibrational holographic interferometry technique was adopted to determine the biaxial stress in the gelatin films as a function of relative humidity. The effect of moisture on the biaxial swelling stress of the gelatin film was also investigated as a function of the latex concentration, latex particle size, gelatin concentration at set point, and drying condition at vitrification. Results have shown that due to the swelling effect of moisture an increase in relative humidity decreased the magnitude of swelling stress in the gelatin film. Gelatin exhibited a hysteresis in the equilibrium biaxial swelling stresses with greater stresses generated during absorption path. In fact, this stress hysteresis agrees with the reversed dimensional hysteresis of the gelatin film. At 75-80% RH, the

gelatin / PET bilayer system was flat. This is equivalent to a zero state of stress in the coating. As the relative humidity was lowered, the bilayer curled to a smaller and smaller radius, resulting in an increase in biaxial swelling stress in the coating. This is because at low relative humidity, the emulsion is in tension and the support is in compression; as a result, the emulsion pulls the support into a curl. On the other hand, as the relative humidity was increased, the bilayer increased its cylindrical radius. This was seen as a large decrease in biaxial swelling stress. This phenomenon can be explained that at the very high relative humidity, the emulsion is in compression, it expands more than support, causing the emulsion to push the support into a convex configuration.

An incorporation of the latex particles into the gelatin decreases the swelling stress in the gelatin coating, especially for the film containing PEA as an additive. For both latex systems, the biaxial swelling stress decreased as the latex concentration increased. Thus, the pure gelatin film shows the highest swelling stress, whereas the gelatin film with 40 parts PEA yielded the lowest swelling stress. No effect of latex particle size was observed on the swelling stress of the gelatin-latex films in the investigated diameter range. However, the swelling stress was significantly affected by the gelatin concentration at set point and the drying condition at vitrification. The gelatin film dried at the LMERH condition (130F / 5.5% RH), with 40 parts PEA and 15% gelatin concentration at set point, has proved to be the film with the minimum biaxial swelling stress.

Lastly, the moisture diffusion behavior of the pure gelatin and gelatin-latex films was investigated using a Thermomechanical Analyzer (TMA) equipped with a relative humidity generator. The swelling strains induced during the absorption and desorption of

moisture were monitored as a function of time at various relative humiditics. A one dimensional hygrothermal elasticity theory was applied to correlate these swelling strains to the moisture diffusion through the thickness of the films. Both pure gelatin and gelatin-latex films exhibited a Pseudo-Fickian diffusion. An interesting observation in moisture transport in gelatin films was the appearance of a moisture induced strain overshoot at 30% RH, that was an increase of the normalized quantity up to a "pseudo-equilibrium" value, followed by an apparent decline to the true equilibrium value. This behavior may be attributed to the relaxation process of the gelatin molecules before the true equilibrium has been achieved. Nevertheless, this strain overshoot did not occur in all of the gelatin samples; thus, more insight investigation is needed to explain the cause of this phenomenon including the relationship among the samples studied.

The moisture diffusion coefficients were calculated from the initial slope of the sorption curves. These values increased with increasing relative humidity. The rate of absorption was greater than the rate of desorption for all the examined relative humidities. The concentration dependence of diffusion coefficients was also evaluated and discussed in terms of the latex concentration, latex particle size, gelatin concentration at set point, and drying condition at vitrification.

In both latex systems, the diffusion rate of moisture through the gelatin film increased with an increase in the latex concentration as well as the latex particle size. By increasing the amount of latex concentration in the continuous phase of the emulsion layer, the degree of crystallinity of gelatin decreased; as a result, the diffusivity of moisture through the gelatin-latex film increased. However, the diffusion coefficient values of the gelatin-PEA and gelatin-PEMA films did not show a significant differencc.

Moisture can permeate either the gelatin-PEA or gelatin-PEMA films at approximately the same rate. It was also found that the gelatin concentration at set point and the drying condition at vitrification affected the diffusion rate of moisture through the gelatin films. The increase in the gelatin concentration at set point of pure gelatin and the gelatin-latex films decreased the diffusion coefficients. The diffusion coefficients of moisture for the films dried at the HMERH condition (80 F / 29% RH) were slightly less than those of the films dried at the LMERH condition (130F / 5.5% RH).

In summary, recall that the incremental linear elasticity theory for an isotropic, linear elastic, homogeneous material indicates that the change in stress with relative humidity is proportional to the product of the modulus (E) and humidity expansion coefficient (HEC); thus, based on this theory the best material is the one which has the lowest $E\beta$ value.

Table 9.1 summarizes the $E\beta$ values along with the modulus and the HEC values for the gelatin-PEA and gelatin-PEMA systems. The $E\beta$ values for pure gelatin range between 0.87 MPa/%RH and 1.55 MPa/%RH. These values are higher than the gelatin-latex films' $E\beta$ values. For both latex systems the $E\beta$ values decrease with an increase in the latex concentration. In comparison with the gelatin-PEA films, the gelatin-PEMA films yield higher $E\beta$ values for the entire relative humidity range, although their β values are lower. This is a direct result of their high moduli. Accordingly, the highest $E\beta$ values of 1.55 MPa/%RH was observed for the pure gelatin film at 15% RH, whereas the lowest $E\beta$ values of 0.35 MPa/%RH was observed for the gelatin-40 parts PEA film

at 80% RH. In other words, the best material for low stress is the high content PEA film (i.e., gelatin film containing 40 parts PEA).

Also shown in Table 9.1 is the $d\sigma/dRH$ values of the pure gelatin and gelatin-latex films. Qualitatively, the $d\sigma/dRH$ values agree very well with the $E\beta$ values that they both decrease as the latex concentration increases. However, a comparison of the $d\sigma/dRH$ values and the $E\beta/(1-\nu)$ values shows discrepancies. In each case, the $d\sigma/dRH$ values are less than the $E\beta/(1-\nu)$ values. The first possible reason for this discrepancy could be the result of changes in the modulus with relative humidity, which do not follow the assumption of the linear elasticity theory that the modulus, expansion coefficient, and the Poisson's ratio are not functions of relative humidity. Another possible reason may be the differences in the experimental procedures. The β values reported in Table 9.1 used the slope of the swelling strain vs. %RH from the first absorption cycle after the film was dried at 0% RH. Although the $d\sigma/dRH$ values were also taken from the absorption cycle, the film was brought to only 30% RH. In addition, the β values were obtained in a nitrogen atmosphere, whereas the $d\sigma/dRH$ values were obtained in a helium atmosphere. The difference in the tested environments might be another possible reason for the discrepancy.

Figure 9.1 presents the relationship between the change in stress with relative humidity ($d\sigma/dRH$) and the latex concentration. Clearly, the $d\sigma/dRH$ values decreased with an increase in the latex concentration. The gelatin film with 40 parts PEA lowered the $d\sigma/dRH$ value most. Figure 9.2 shows the $E\beta$ values at 50% RH as a function of latex concentration. Similar to the plot between the $d\sigma/dRH$ vs. latex concentration, the

Table 9.1 : Summary of the Modulus, Humidity Expansion Coefficient, $E\beta$, and $d\sigma/dRH$ Values for the Gelatin-PEA and Gelatin-PEMA Systems

Latex Conc. (parts)	E (GPa)					β (μm/m%RH)	Eβ (MPa/%RH)					-dσ/dRH (MPa/%RH)
	15 %RH	30 %RH	50 %RH	70 %RH	80 %RH		15 %RH	30 %RH	50 %RH	70 %RH	80 %RH	
PEMA												
0	4.51	4.28	3.92	3.75	2.55	343	1.55	1.47	1.34	1.29	0.87	0.437
20	4.23	3.69	3.67	3.40	2.07	305	1.29	1.12	1.12	1.04	0.63	0.373
40	3.70	3.46	3.11	3.08	1.87	274	1.01	0.95	0.85	0.84	0.51	0.272
PEA												
0	4.51	4.28	3.92	3.75	2.55	343	1.55	1.47	1.34	1.29	0.87	0.437
20	3.97	3.54	3.20	2.60	1.80	320	1.27	1.13	1.02	0.83	0.58	0.317
40	3.01	2.70	2.52	2.43	1.17	297	0.89	0.80	0.75	0.72	0.35	0.187

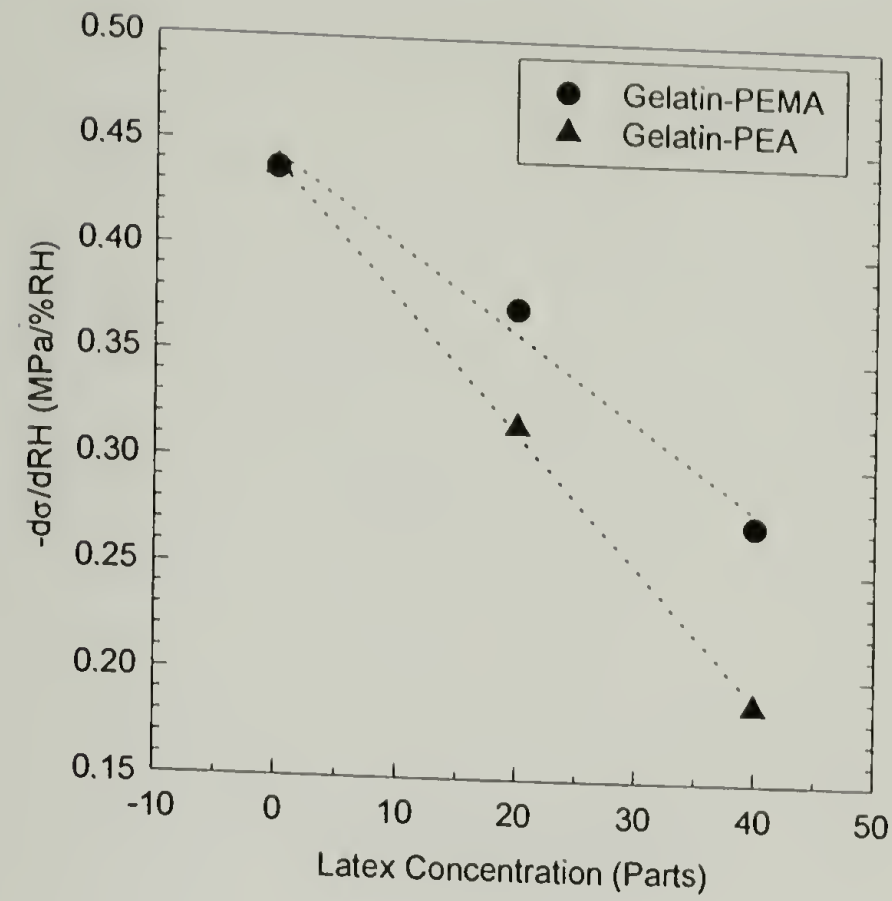

Figure 9.1 : Effect of latex concentration on the $d\sigma/dRH$ values for gelatin-PEMA and gelatin-PEA films.

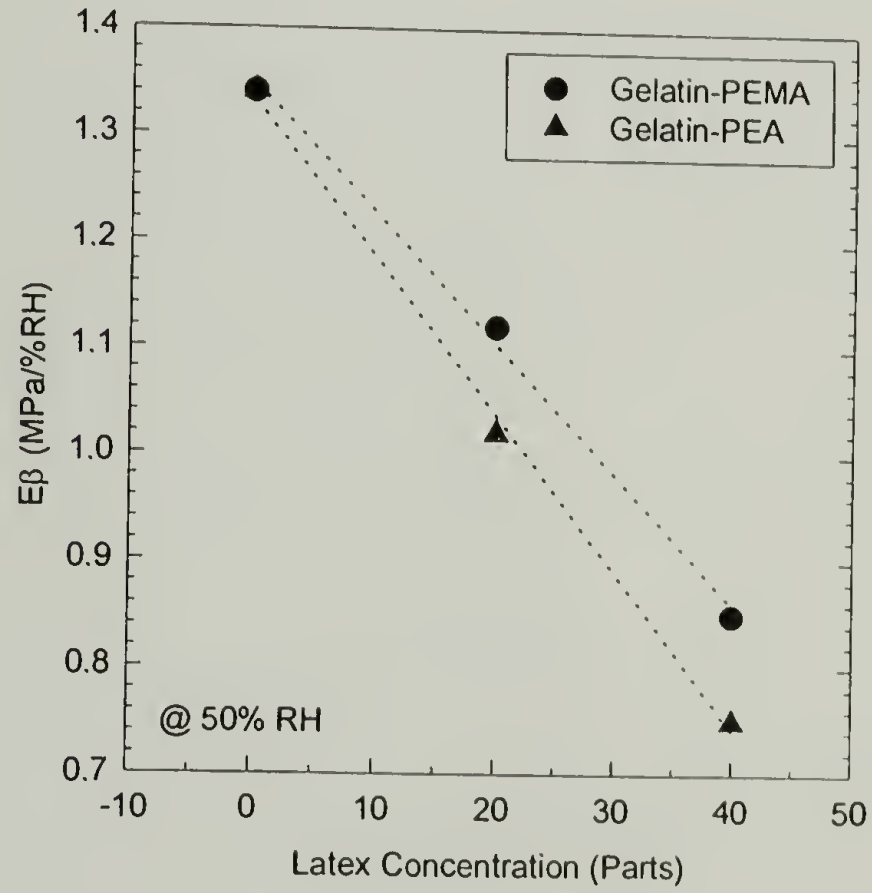

Figure 9.2 : Effect of latex concentration on the $E\beta$ values at 50% RH for gelatin-PEMA and gelatin-PEA films.

$E\beta$ values for both systems decreased as the latex concentration increased, the gelatin film with 40 parts PEA had the lowest $E\beta$ value.

Figure 9.3 presents the normalized $d\sigma/dRH$ values vs. latex concentration for both latex systems. Obviously, the addition of 40 parts PEMA and PEA into the gelatin film decreases the $d\sigma/dRH$ values approximately 40% and 60%, respectively. Similarly, the plot of normalized $E\beta$ values vs. latex concentration at 50% RH is provided in Figure 9.4. From these two plots, the addition of 40 parts PEMA decreases both the $d\sigma/dRH$ and the $E\beta$ values equally by 40%. However, for the case of the gelatin-PEA films, the inclusion of 40 parts PEA decreases the $d\sigma/dRH$ and the $E\beta$ values approximately 60% and 50%, respectively.

Figure 9.5 (a) and (b) present the plots between the $E\beta$ values as a function of the latex concentration at various relative humidities for the gelatin-PEMA and gelatin-PEA films, respectively. As can be seen, in both systems the $E\beta$ values decreased with an increase in relative humidity. The lowest $E\beta$ values for each system were obtained at 80% RH for the gelatin films with 40 parts latex.

Table 9.2 summarizes the effect of latex (type, size, and concentration), drying condition at vitrification, and the gelatin concentration at set point on the swelling stress, modulus, humidity expansion coefficient, and the moisture uptake of the gelatin film. Obviously, the modulus and the humidity expansion coefficient are important in determining the state of stress in the film. Qualitatively, the incremental linear elasticity theory has been shown to be appropriate for describing the biaxial swelling stress of the gelatin film exposed to moisture at room temperature. Therefore based on thc scope of

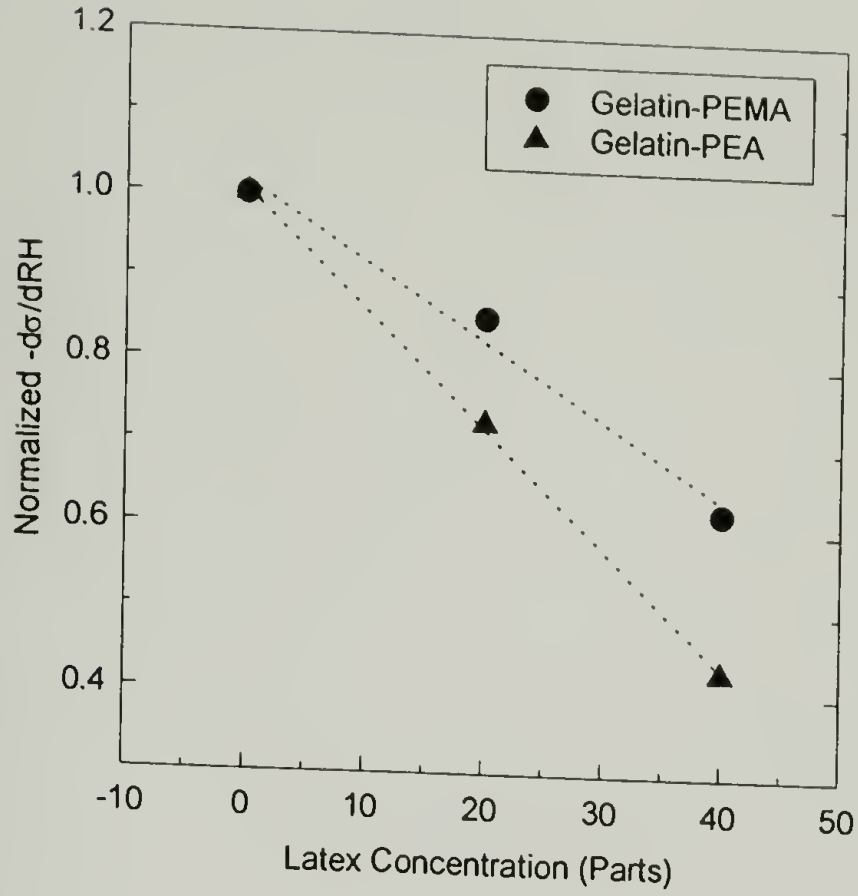

Figure 9.3 : Normalized $d\sigma/dRH$ vs. latex concentration for gelatin-PEMA and gelatin-PEA films.

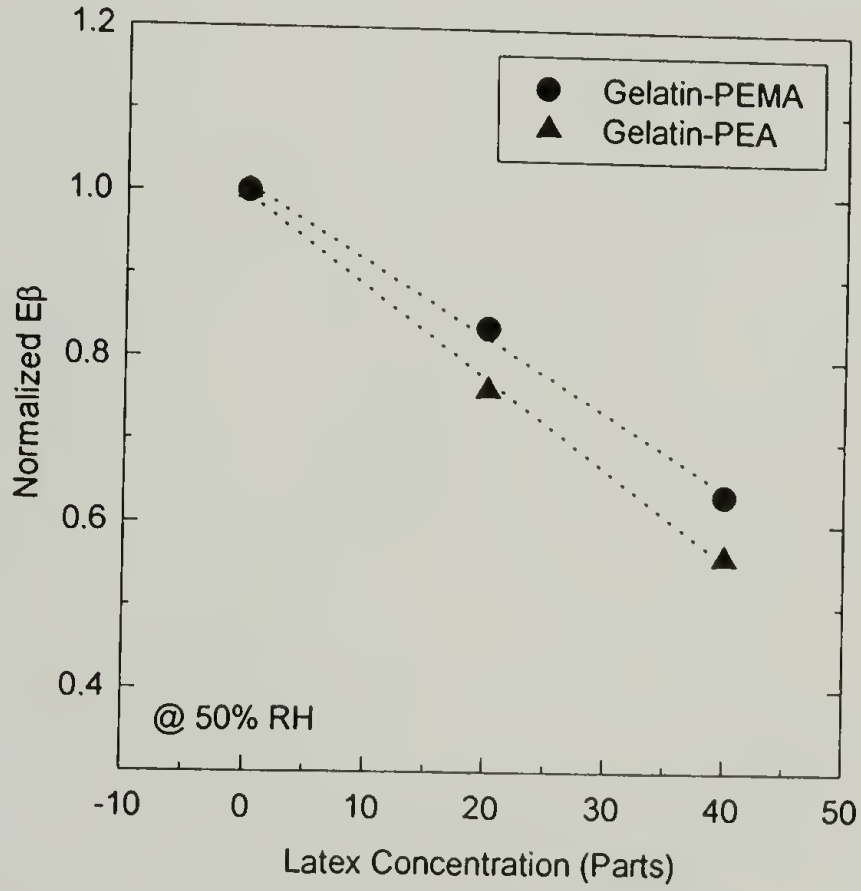

Figure 9.4 : Normalized $E\beta$ vs. latex concentration for gelatin-PEMA and gelatin-PEA films exposed to moisture at 50% RH.

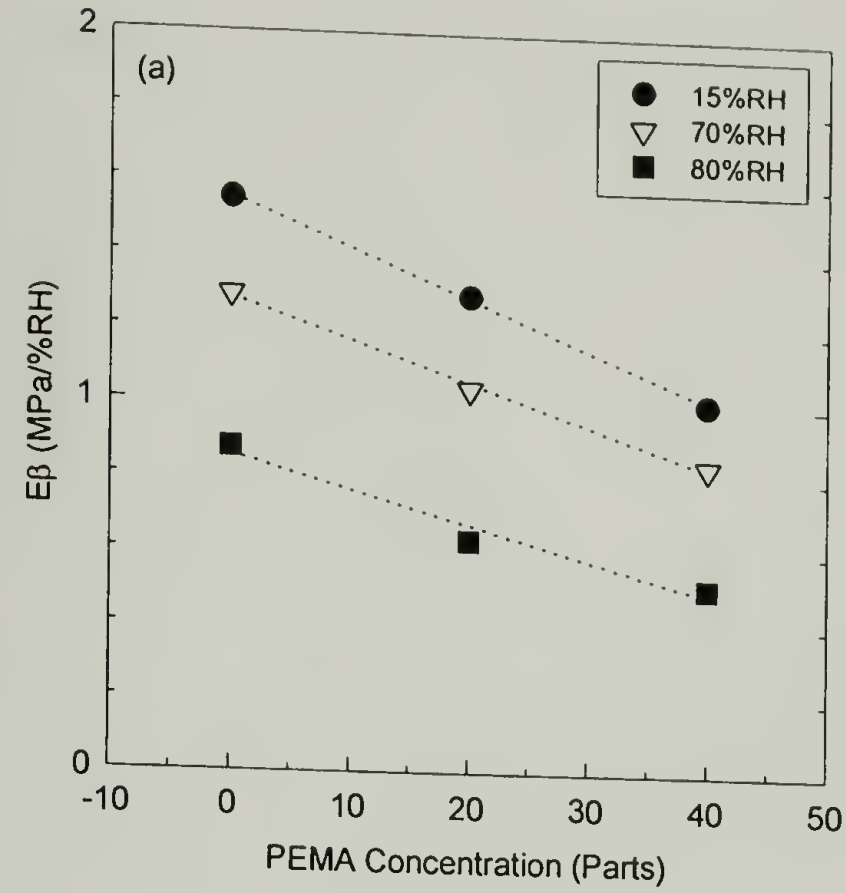

Figure 9.5 : Effect of latex concentration on the $E\beta$ values at various relative humidities for (a) gelatin-PEMA and (b) gelatin-PEA films, respectively.

Table 9.2 : Summary of the Effect of Latex (Type, Size, and Concentration), Drying Condition at Vitrification, and the Gelatin Concentration at Set Point on the Swelling Stress, Modulus, Humidity Expansion Coefficient, and the Moisture Uptake of the Gelatin Film

	Swelling Stress (MPa)	$d\sigma/dRH = -E\beta / (1-\upsilon)$		
		Moisture Uptake (%)	HEC (μm/m%RH)	Modulus (GPa)
Latex Type	Gel-PEMA > Gel-PEA	Gel-PEMA > Gel-PEA	Gel-PEMA < Gel-PEA	Gel-PEMA > Gel-PEA
Latex Concentration (parts)	0 > 20 > 40	0 > 20	0 > 20 > 40	0 > 20 > 40
Latex Particle Size (μm)	no effect	-	no effect	no effect
Drying Condition	HMERH > LMERH	HMERH > LMERH	HMERH > LMERH	no effect
Gelatin Concentration (%)	10 > 15	10 > 15	10 > 15	no effect

this investigation, the best material (i.e., minimum biaxial swelling stress, lowest $E\beta$ value) was found to be the gelatin film with 40 parts PEA and 15% gelatin concentration at set point, and was dried at the LMERH condition (130F / 5.5% RH).

Future Work

This research on this topic is far from complete. The addition of silver halides and/or other photographic components to the gelatin emulsion layer containing a polymer latex is one of the promising challenges. It will be interesting to investigate the interactionof the silver halides, polymer latex, and gelatin on the stress, mechanical properties, and dimensional stability of the gelatin film.

All of the properties reported in this thesis have been studied in the in-plane direction. The out-of-plane properties or the properties across the thickness of the films are also important for the materials that are used or stored in a roll form. Thus, the out-of-plane properties, such as the out-of-plane Young's modulus, the out-of-plane coefficient of thermal expansion (CTE), and the out-of-plane humidity expansion coefficient (HEC), for the gelatin film (with and without polymer latex) and for the bilayer should be further investigated. The out-of-plane Young's modulus and out-of-plane CTE can be determined using a Pressure-Volume-Temperature (PVT) Apparatus in combination with other techniques such as vibrational holographic interferometry, high pressure gas dilatometry, tensile testing, and thermomechanical analysis (TMA).[1,2]

The out-of-plane HEC can be measured using an optical technique known as Double Slit Laser Interferometry.[3]

In this research we were unable to produce a 100% latex film, especially for the PEMA film. Because of its high Tg, the PEMA film was very brittle and difficult to handle. Hence, a comparison between the experimental values of Young's modulus and the model predictions presented in chapter 5 have been only for the case of the gelatin-PEA film. A need exits to form PEMA films and to determine its mechanical properties (i.e. Young's modulus, shear modulus) and Poisson's ratio for use in the mechanical modeling of the gelatin-PEMA film.

As discussed in chapter 4 that the gelatin film has a different microstructure and properties depending upon the temperature of drying. Further investigation of the microstructure of the gelatin film as a function of the drying conditions at vitrification and the gelatin concentration at set point would make an interesting study. Wide-angel x-ray diffraction (WAXD) is a powerful technique for this purpose. Using this technique, the in-plane orientation and molecular order of the gelatin chains, the degree of crystallinity, and the size and the perfection of crystals in the gelatin film can be determined. The quantitative evaluation of the crystallite orientation is made by measuring the angular spread and the intensity of the ares from the plot between the diffracted intensity (I) versus the azimuthal angle (ϕ). The width of the ares is inversely proportional to the degree of orientation. The degree of crystallinity can be evaluated from the plot between intensity and two theta. Although it should be kept in mind that differing results are usually obtained from different techniques, the qualitative

comparison of the degree of crystallinity assessed from the WAXD and the DSC techniques could be made.

Adhesion between the gelatin layer and the PET substrate should be another area of interest. Adhesion of a coating to the substrate is crucial for reliability in any practical application. The coating could delaminate if the stored energy in the coating is sufficient to overcome the work of adhesion to the substrate. The stored energy is directly proportional to the thickness of the coating and the square of the stress in the coating. Therefore, the greater the stress, the higher the stored energy. A coating with good adhesion to the substrate would not yield to delamination failure. The adhesion energy between the gelatin coating and the PET substrate can be measured using the most common method, peel testing, or a residual stress based self-delamination method [4]. The peel testing is used for measuring the "practical" adhesion of the coating, whereas the self-delamination method is useful for evaluating the true adhesion of the coating to the substrate. The adhesion improvement by using a subbing layer as an adhesion promoter between the gelatin coating and the PET substrate should be evaluated as well. Peel testing on the gelatin coatings tested by a self-delamination method would help provide a good comparison between the two methods, with and without the subbing layer.

A few studies could be pursued in the area of moisture diffusion behavior. The diffusion coefficients of the gelatin films presented in chapter 8 were determined using the swelling strain technique. As stated earlier, the swelling strain or swelling stress can be related to the mass uptake through the application of linear elasticity theory. Thus, a comparison of the swelling strain method to the swelling stress and the gravimetric techniques should be carried out. The vibrational holographic interferometry and the

Cahn 2000 microbalance would work well for this objective.[3] The validity of these three techniques to determine the moisture diffusion coefficient should also be verified using a known diffusion coefficient material such as a PMDA-ODA polyimide film. Lastly, it was observed that the overshoot phenomenon occurred randomly among the gelatin samples tested at 30%RH. Although some explanation based on the published literature for other materials were discussed, a more complete understanding of this exceptional behavior is still needed. In fact, the results from the swelling stress method and gravimetric analysis might as well be helpful in validating this behavior.

References

1. Sheth, K.C., "Stress, Mechanical and Thermal Characterization of Anisotropic Polyimide Thin Films and Coatings", Ph.D. Dissertation, University of Massachusetts, Amherst, MA (1996).

2. Chen, M.J., "Pressure-Volume-Temperature and Wave Propagation Studies of Polyimide Films", Ph.D. Dissertation, University of Massachusetts, Amherst, MA (1998).

3. Vrtis, J.K., "Stress and Mass Transport in Polymer Coating and Films", Ph.D. Dissertation, University of Massachusetts, Amherst, MA (1995).

4. Farris, R.J. and Bauer, C.L., "A self-Delamination Method of Measuring the Surface Energy of Adhesion of Coatings", *Journal of Adhesion*, **26**, 293 (1988).

APPENDIX A

DESCRIPTION OF GELATIN AND GELATIN-LATEX SYSTEMS

Kodak Sample ID	Latex Type	Latex Size (μm)	Latex Concentration (parts)	Gelatin Concentration at Set Point (%)	Drying Condition at Vitrification
BF 8483-13	-	-	-	10	HMERH
BF 8483-133	-	-	-	10	HMERH
BF 8483-23	-	-	-	10	LMERH
BF 8483-143	-	-	-	10	LMERH
BF 8483-173	PEA	0.051	20	10	HMERH
BF 8483-183	PEA	0.051	20	10	LMERH
BF 8483-43	PEA	0.112	20	10	HMERH
BF 8483-33	PEA	0.112	20	10	LMERH
BF 8483-123	PEMA	0.067	20	10	HMERH
BF 8483-113	PEMA	0.067	20	10	LMERH
BF 8483-163	PEMA	0.150	20	10	HMERH
BF 8483-153	PEMA	0.150	20	10	LMERH
BF 8483-83	-	-	-	15	HMERH
BF 8483-203	-	-	-	15	HMERH
BF 8483-73	-	-	-	15	LMERH
BF 8483-193	-	-	-	15	LMERH
BF 8505-482	PEA	0.051	20	15	HMERH
BF 8505-472	PEA	0.051	20	15	LMERH
BF 8505-362	PEA	0.112	20	15	HMERH
BF 8505-352	PEA	0.112	20	15	LMERH
BF 8483-93	PEMA	0.067	20	15	HMERH
BF 8483-103	PEMA	0.067	20	15	LMERH
BF 8483-213	PEMA	0.150	20	15	HMERH
BF 8483-223	PEMA	0.150	20	15	LMERH

Continued, next page

continued

Kodak Sample ID	Latex Type	Latex Size (μm)	Latex Concentration (parts)	Gelatin Concentration at Set Point (%)	Drying Condition at Vitrification
BF 8505-252	-	-	-	10	HMERH
BF 8505-322	-	-	-	10	HMERH
BF 8505-262	-	-	-	10	LMERH
BF 8505-312	-	-	-	10	LMERH
BF 8505-372	PEA	0.112	40	10	HMERH
BF 8505-382	PEA	0.112	40	10	LMERH
BF 8505-402	PEMA	0.067	40	10	HMERH
BF 8505-392	PEMA	0.067	40	10	LMERH
BF 8505-412	PEMA	0.150	40	10	HMERH
BF 8505-422	PEMA	0.150	40	10	LMERH
BF 8505-332	-	-	-	15	HMERH
BF 8505-452	-	-	-	15	HMERH
BF 8505-342	-	-	-	15	LMERH
BF 8505-462	-	-	-	15	LMERH
BF 8505-292	PEA	0.051	40	15	HMERH
BF 8505-302	PEA	0.051	40	15	LMERH
BF 8483-63	PEA	0.051	40	15	LMERH
BF 8505-442	PEA	0.112	40	15	HMERH
BF 8505-432	PEA	0.112	40	15	LMERH
BF 8505-282	PEMA	0.067	40	15	HMERH
BF 8505-272	PEMA	0.067	40	15	LMERH
BF 8505-242	PEMA	0.150	40	15	HMERH
BF 8505-232	PEMA	0.150	40	15	LMERH

APPENDIX B

DERIVATION OF THE RELATIONSHIP BETWEEN NORMALIZED STRESS, STRAIN, AND MASS UPTAKE

From linear elastic theory, the stress-strain relationship of a homogeneous, elastic, isotropic material is:

$$E\left[\delta\varepsilon_{ij} - \delta_{ij}\left(\beta\delta C + \alpha\left(T - T_0\right)\right)\right] = (1+\upsilon)\delta\sigma_{ij} - \upsilon\delta_{ij}\delta\sigma_{kk} \qquad \text{(B.1)}$$

For a one dimensional stress and strain:

$$\sigma_{xx} = E\left[\varepsilon_{xx} - \alpha\Delta T(x,y,z,t) - \beta\Delta C(x,y,z,t)\right] \qquad \text{(B.2)}$$

At isothermal condition:

$$\sigma_{xx} = E\left(\varepsilon_{xx} - \beta\Delta C(x,y,z,t)\right) \qquad \text{(B.3)}$$

For the average property through the volume:

$$\overline{\Gamma} = \frac{1}{V}\int\Gamma(x,y,z,t)dV \qquad \text{(B.4)}$$

where $\Gamma = \varepsilon_{xx}, \sigma_{xx}$ or ΔC and V = volume of the sample

The average mass uptake per unit volume is:

$$\Delta\bar{C}(t) = \frac{1}{V}\int \Delta C(x, y, z, t)\, dV \tag{B.5}$$

The total amount of moisture absorbed by the film is:

$$M_t(t) = V\Delta\bar{C}(t) = \int \Delta C(x, y, z, t)\, dV \tag{B.6}$$

Integrate equation (B.3) through the volume:

$$\bar{\sigma}_{xx}(t) = E\left[\bar{\varepsilon}_{xx}(t) - \beta\Delta\bar{C}(t)\right] \tag{B.7}$$

Therefore, at constant stress, $\Delta\bar{\sigma}_{xx}(t) = 0$:

$$\Delta\bar{\varepsilon}_{xx}(t) = \beta\Delta\bar{C}(t) \tag{B.8}$$
where $\Delta\bar{\varepsilon}_{xx}(t) = \bar{\varepsilon}_{xx}(t) - \bar{\varepsilon}_{xx}(0)$

Analogously, at constant strain, $\Delta\bar{\varepsilon}_{xx}(t) = 0$:

$$\Delta\bar{\sigma}_{xx}(t) = -E\beta\Delta\bar{C}(t) \tag{B.9}$$
where $\Delta\bar{\sigma}_{xx}(t) = \bar{\sigma}_{xx}(t) - \bar{\sigma}_{xx}(0)$

By normalizing equation (B.6), (B.8), and (B.9):

$$\frac{M_t}{M_\infty} = \frac{\Delta\bar{C}(t)}{\Delta\bar{C}(\infty)} = \frac{\Delta\bar{\sigma}_{xx}(t)}{\Delta\bar{\sigma}_{xx}(\infty)} = \frac{\Delta\bar{\varepsilon}_{xx}(t)}{\Delta\bar{\varepsilon}_{xx}(\infty)} \tag{B.10}$$

BIBLIOGRAPHY

Adelstein, P.Z. and Calhoun, J.M., "Interpretation of Dimensional Changes in Cellulose Ester Base Motion-Picture Films", *Journal of the SMPTE*, **69**, 157 (1960).

Adelstein, P.Z. In *SPSE Handbook of Photographic Science and Engineering*; Thomas, W., Ed.; John Wiley & Sons: New York, 1973; Section 8, pp. 473-500.

Agarwal, N., Hoagland, D.A., and Farris, R.J., "Effect of Moisture Absorption on the Thermal Properties of Bombyx mori Silk Fibroin Films", *Journal of Applied Polymer Science*, **63**, 401 (1997).

Alfrey, T., Gurnee, E.F., and Lloyd, W.G., "Diffusion in Glassy Polymers", *Journal of Polymer Science, Part C.*, **12**, 249 (1966).

Allentoff, N. and Minsk, L.M., "Photographic Silver Halide Emulsions Having High Wet Density Retention", U.S. Patent No. 3,271,158 (September 6, 1966).

Aminabhavi, T.M., Phayde, H.T.S., and Ortego, J.D., " Diffusion of Aromatic Liquids into Blends of Ethylene-Propylene Copolymers and Isotactic Polypropylene Membrane", *Polymer and Polymer Composites*, **4**(1), 13 (1996).

Aminabhavi, T.M., Phayde, H.T.S., and Ortego, J.D., "Sorption/Desorption and Diffusion Anomalies in Santoprene-Alkane Systems", *Polymer and Polymer Composites*, **4**(2), 103 (1996).

Arfken, G. *Mathematical Methods for Physicists, 3rd Ed.*; Academic Press: New York, 1985; pp. 572.

Armour, E., Campbell, G.A., and Upson, D.A. In *Encyclopedia of Polymer Science and Engineering, 2nd ed.*; Mark, H.F., Bikales, N.M., Overberger, C.G., Menges, G., and Kroschwitz, J.I., Eds.; John Wiley & Sons: New York, 1985; Vol. 11, pp. 175-185.

Ashton, J.E., Halpin, J.C., and Petit, P.H. *Primer on Composite Analysis*; Technomic: Lancaster, Pennsylvania, 1969.

Bear, R.S., "The Structure of Collagen Fibrils", *Advance Protein Chemistry*, **7**, 69 (1952).

Berry, B.S. and Pritcher, W.C., "Bending-Cantilever Method for the Study of Moisture Swelling in Polymers", *IBM Journal of Research and Development*, **28**(6), 662 (1984).

Bonsignore, K., personal communication, 1996.

Bourdygina, G.I. and Kozlov, P.V., "Modification of the Physico-Mechanical Properties of Gelatin in the Coiled Conformation", *European Polymer Journal*, **28**(2), 135 (1992).

Brendley, W.H., "Acrylic Polymers", *Paint and Varnish Production*, 19 (1973).

Cahn Instruments, Inc., Cerritos, CA 90701.

Calhoun, J.M. and Leister, D.A., "Effect of Gelatin Layers on the Dimensional Stability of Photographic Film", *Photographic Science and Engineering*, **3**(1), 8 (1959).

Calhoun, J.M., "Properties and Dimensional Stability of Safety Aerographic Film", *Photogrammetric Engineering*, **13**, 163 (1974).

Centa, J.M., "Effect of Base and Emulsion Thickness on Dimensional Stability of Graphic Arts Films", *Proceeding of the Annual Technical Meeting: Technical Associates of Graphic Arts*, **8**, 75 (1956).

Chen, M.J., "Pressure-Volume-Temperature and Wave Propagation Studies of Polyimide Films", Ph.D. Dissertation, University of Massachusetts, Amherst, MA (1998).

Christensen, R.M. *Mechanic of Composite Material*; Wiley-Interscience: New York, 1979; Chapter 2, pp.31-72.

Christensen, R.M. *Mechanics of Composite Materials*; John-Wiley & Sons: New York, 1979; pp. 208, 337.

Cohan, L.H., "Hysteresis and the Capillary Theory of Adsorption of Vapors", *Journal of American Chemical Society*, **66**, 98 (1944).

Cohan, L.H., "Sorption Hysteresis and the Vapor Pressure of Concave Surfaces", *Journal of American Chemical Society*, **60**, 433 (1938).

Colton, E.K. and Wiegand, E.J., "Moisture in Photographic Film and Its Measurement", *Photographic Science and Engineering*, **2**(3), 170 (1958).

Coover, H.W.,Jr., "Modified Gelatins Obtained by Polymerizing and Alkenyl Carbonamide in an Aqueous Gelatin Solution", U.S. Patent No. 2,794,787 (June 4, 1957).

Couchman, P.R. and Karasz, F.E., "A Classical Thermodynamic Discussion of the Effect of Composition on Glass Transition Temperature", *Macromolecules*, **11**, 117 (1978).

Couchman, P.R., "Compositional Variation of Glass Transition Temperature. 2. Application of the Thermodynamic Theory to Compatible Polymer Blends", *Macromolecules*, **11**, 1156 (1978).

Crank, J. and Henry, E., "Diffusion in Media with Variable Properties. Part I. The Effect of a Variable Diffusion Coefficient on the Rates of Absorption and Desorption", *Transactions of the Faraday Society*, **45**, 636 (1949).

Crank, J. and Park, G.S., "An Evaluation of the Diffusion Coefficient for Chloroform in Polystyrene from Simple Absorption Experiments", *Transactions of the Faraday Society*, **45**, 240 (1949).

Crank, J. In *Diffusion in Polymers*; Crank, J. and Park, G.S., Eds.; Academic Press: New York, 1968.

Crank, J. *The Mathematics of Diffusion*; Oxford Clarendon Press: London, 1956.

Cribb, J.L., "Shrinkage and Thermal Expansion of a Two Phase Material", *Nature, London*, **220**, 576 (1968).

Crossman, F.W. and Wang, A.S.D., "Stress Field Induced by Transient Moisture Sorption in Finite-Width Composite Laminates", *Journal of Composite Materials*, **12**, 2 (1978).

Crossman, F.W., Warren, W.J., and Pinoli, P.C., "Time and Temperature Dependent Dimensional Stability of Graphite-Epoxy Composites", *Proceedings of the 21st National SAMPE Symposium*, **21**, 424 (1976).

Cuevas, J.E., "Effective Moduli Calculations of Isotropic Composites", *Journal of Composite Materials*, **2**(1), 113 (1968).

D'Arcy, R.L. and Watt, I.C., "Analysis of Sorption Isotherms of Non-Homogeneous Sorbents", *Trans. Faraday Soc.*, **66**, 1236 (1970).

D'Arcy, R.L. and Watt. In *Water Activity: Influences on Food Quality*; Rockland, L.B. and Stewart, G.F., Eds.; Academic Press: New York, 1981; pp. 111-142.

Dewey, J.M., "The Elastic Constants of Materials Loaded with Non-Rigid Fillers", *Journal of Applied Physics*, **18**, 578 (1947).

Donald, A.M. In *Rubber Toughened Engineering Plastics*; Collyer, A.A., Ed.; Chapman & Hall: New York, 1994; Chapter 1, pp.1-28.

Dubosc, J-P.C.G. and Thiebaut, R.P.J.G., "Photographic Emulsion Having a Low Modulus of Elasticity and Process for Its Manufacture", U.S. Patent No. 3,359,108 (December 19, 1967).

Eliassaf, J. and Eirich, F.R., "Creep Studies on Gelatin at 100% relative Humidity", *Journal of Applied Polymer Science*, **4**(11), 200 (1960).

Fakirov, S. et al., "Mechanical Properties and Transition Temperatures of Crosslinked Oriented Gelatin II Effect of Orientation and Water Content on Transition Temperatures", *Colloidal Polymer Science*, **275**, 307 (1997).

Farber, J.N. and Farris, R.J., "Model for Prediction of Elastic Response of Reinforced Materials over Wide Ranges of Concentration", *Journal of Applied Polymer Science*, **34**, 2093 (1987).

Farris, R.J. and Bauer, C.L., "A self-Delamination Method of Measuring the Surface Energy of Adhesion of Coatings", *Journal of Adhesion*, **26**, 293 (1988).

Felder, R.M. and Huvard, G.S. *Methods of Experimental Physics*; Academic Press: New York, 1980.

Fleischer, C.A., Bauer, C.L., Massa, D.J., and Taylor, J.F, "Film as a Composite material", *MRS Bulletin*, **21**(7), 14 (1996).

Fu, T.Z., Durning, C.J., and Tong, H.M., "Simple Model for Swelling-Induced Stresses in a Supported polymer Thin Film", *Journal of Applied Polymer Science*, **43**, 709 (1991).

Fuzek, J.F. In *Water in Polymers*; Rowland, S.P., Ed.; American Chemical Society: Washington, D.C., 1980; Chapter 31, pp. 515-530.

Gal, S. In *Water Activity: Influences on Food Quality*; Rockland, L.B. and Stewart, G.F., Eds.; Academic Press: New York, 1981; pp. 89-110.

Gal, S. In *Water Relations of Foods*; Duckworth, R.B., Ed.; Academic Press: London, 1975; pp. 139-153.

Godard, P., Biebuyck, J.J., Daumerie, M., Naveau, H., and Mercier, J.P., "Crystallization and Melting of Aqueous Gelatin", *Journal of Polymer Science: Polymer Physics Edition*, **16**, 1817 (1978).

Gordon, J.M., Rouse, G.B., and Risen, W.M., Jr., "The Compositional Dependence of Glass Transition Properties", *The Journal of Chemical Physics*, **66**(11), 4971 (1977).

Gordon, M. and Taylor, J.S., "Ideal Copolymers and the Second-Order Transitions of Synthetic Rubbers. I. Non Crystalline Copolymers", *Journal of Applied Chemistry*, **2**, 493 (1952).

Greenspan, L, "Humidity Fixed Points of Binary Saturated Aqueous Solutions", *Journal of Research of the National Bureau of Standards: A. Physics and Chemistry*, **81A**(1), 89 (1977).

Halpin, J.C., "Stiffness and Expansion Estimates for Oriented Short Fiber Composites", *Journal of Composite Material*, **3**, 732 (1969).

Harper, C.A., Ed.; *Handbook of Plastics, Elastomers, and Composites, 2nd ed.*; McGraw-Hill, Inc.: New York, 1992; Chapter 1, pp. 49-52.

Hashin, Z. and Shtrikman, S., "A Variational Approach to Theory of the Elastic Behavior of Multiphase Materials", *Journal of the Mechanics and Physics of Solids*, **11**, 127 (1963).

Hashin, Z. *Proceedings of the IUTAM Symposium on Nonhomogeneity in Elasticity and Plasticity, Warsaw Poland*; Pergamon Press: New York, 1959; p. 463.

Hayes, M. and park, G., "The Diffusion of Benzene in Rubber", *Transactions of the Faraday Society*, **52**, 949 (1956).

Hopfenberg, H.B. and Frisch, H.L., "Transport of Organic Micromolecules in Amorphous Polymers", *Journal of Polymer Science , Part B.*, 7, 405 (1969).

James, T.H., Ed.; *The Theory of the Photographic Process, 4th ed.*; Macmillan Publishing Co.: New York, 1977.

Jennings, R.M., Taylor, J.F., and Farris, R.J., "Determination of Residual Stress in Coatings by a Membrane Deflection Techniques", *Journal of Adhesion*, **49**, 57 (1995).

Johari, J.P., Hallbrucker, A., and Mayer, E., "The Glass-Liquid Transition of Hyper Quenched Water", *Nature*, **330**, 552 (1987).

Johnson, H.E., Clarson, S.J., and Granick, S., " Overshoots as Polymer Adsorb", *Polymer*, **34**, 1960 (1993).

Jolley, J.E., "The Microstructure of Photographic Gelatin Binders", *Photographic Science and Engineering*, **14**(3), 169 (1970).

Jones, F.R. In *Handbook of Polymer-Fibre Composites*; Jones, F.R., Ed.; Longman Scientific & Technical: Burnt Mill, Harlow, Essex, 1994; Chapter 6.3, pp. 371-375.

Jou, C.S., "Stress Associated with Transport in Polymer Films", Ph.D. Dissertation, University of Massachusetts, Amherst, MA (1993).

Jou, J., Huang, R., Huang, P., and Shen, W., "Structure Effect on Water Diffusion and Hygroscopic Stress in Polyimide Films", *Journal of Applied Polymer Science*, **43**, 857 (1991).

Kambour, R.P., Karasz, F.E., and Daane, J.H., "Kinetic and Equilibrium Phenomena in the System: Acetone Vapor and Polycarbonate Film", *Journal of Polymer Science, Part A-2*, **4**(3), 327 (1966).

Kapsalis, J.G. In *Water Activity: Influences on Food Quality*; Rockland, L.B. and Stewart, G.F., Eds.; Academic Press: New York, 1981; pp. 143-177.

Kapsalis, J.G. In *Water Activity: Theory and Application to Food*; Rockland, L.B. and Beuchat, L.R., Eds.; Marcel Dekker, Inc.: New York, 1987; pp. 173-214.

Kelley, F.N. and Bueche, F., "Viscosity and Glass Temperature Relations for Polymer-Diluent Systems", *Journal of Polymer Science*, **50**, 549 (1961).

Kerner, E.H., "The Elastic and Thermo-Elastic Properties of Composite Media", *Proceedings of the Physical Society, London*, **69B**, 808 (1956).

Kerner, E.H., "The Elastic and Thermo-Elastic Properties of Composite Media", *Proceedings of the Physical Society*, **69**B, 808 (1956).

Kim, D., Caruthers, J.M., and Peppas, N.A., " Penetrant Transport in Cross-Linked Polystyrene", *Macromolecules*, **26**, 1841 (1993).

Kine, B.B. and Novak, R.W. In *Encyclopedia of Polymer Science and Engineering , 2nd ed.*, Mark, H.F., Bikales, N.M., Overberger, C.G., Menges, G., and Kroschwitz, J.I., Eds.; John Wiley & Sons: New York, 1985; Vol. 1, pp. 234-299.

King, G. and Cassie, A.B.D., "Propagation of Temperature Changes Through Textiles in Humid Atmosphere : Part I. Rate of Absorption of Water Vapor by Wool Fibers", *Trans. Faraday Soc.*, 36, 445 (1940).

King, G., "Sorption of Vapors by Keratin and Wool", *Transactions of the Faraday Society*, **41**, 325 (1945).

Koleske, J.V. and Faucher, J.A., "Transitions in Gelatin and Vitrified Gelatin-Water Systems", *The Journal of Physical Chemistry*, **69**(11), 4040 (1965).

Kraemer, E.O. *A Treatise on Physical Chemistry*; Van Nostrand: New York, 1931.

Leaderman, H., "Elastic and Creep Properties of Filamentous Materials and Other High Polymers"; Textile Foundation, Inc.: Washington, D.C., 1943; pp. 98, 128.

Levenson, G.I.P., "Limiting Factors in Processing", *Journal of Photographic Science*, **17**, 2 (1969).

Levin, V.M., "On the Coefficients of Thermal Expansion of Heterogeneous Materials (in Russian)", *Mekhanika Tverdogo Tela*, **1**, 88 (1967).

Lewis, T.B. and Nielsen, L.E., " Dynamic Mechanical Properties of Particulate-Filled Composites", *Journal of Applied Polymer Science*, **14**, 1449 (1970).

Long, F.A. and Thompson, L.J., "Diffusion of Water Vapor in Polymers", *Journal of Polymer Science*, **15**, 413 (1955).

Macsuga, D.D., "Thermal Transitions in Gelatin: Optical Rotation and Enthalpy Changes", *Biopolymers*, **11**, 2521 (1972).

Maden, M.A. and Farris, R.J., "Stress Analysis of Thin Polyimide Films Using Holographic Interferometry", *Experimental Mechanics*, **31**(2), 178 (1991).

Maden, M.A., "The Determination of Stresses and Material Properties of Polyimide Coatings and Films Using Real Time Holographic Interferometry", Ph.D. Dissertation, University of Massachusetts, Amherst, MA (1992).

Maden, M.A., Tong, K., and Farris, R.J., "Measurement of Stresses in Thin Films Using Holographic Interferometry : Dependence on Atmospheric Conditions", *Material Research Society Symposium*, **188**, 29 (1990).

Marshall, A.S. and Petrie, S.E.B., "Thermal Transitions and Physical Aging in Gelatin", *Proceedings of the Eleventh North American Thermal Analysis Society Conference*, **2**, 183 (1981).

Marshall, A.S. and Petrie, S.E.B., "Thermal Transitions in Gelatin and Aqueous Gelatin Solutions", *Journal of Photographic Science*, **28**, 128 (1980).

McBain, J.W., "An Explanation of Hysteresis in the Hydration and Dehydration of Gels", *Journal of American Chemical Society*, **57**, 699 (1935).

Morinaka, A. and Asano, Y., "Residual Stress and Thermal Expansion Coefficients of Plasma Polymerized Films", *Journal of Applied Polymer Science*, **27**, 2139 (1982).

Moy, P. and Karasz, F.E. In *Water in Polymers*; Rowland, S.P., Ed.; American Chemical Society: Washington, D.C., 1980; Chapter 30, pp. 505-513.

Newns, A.C., "The Sorption and Desorption Kineties of Water in a Regenerated Cellulose", *Transactions of the Faraday Society*, **52**, 1533 (1956).

Ni, B.Y. and Faou, A.L., "Crystalline Structure and Moisture Effects on Deformation Mechanisms of Gelatin Films under Mode I Stress Field", *Mat. Res. Soc. Symp. Proc.*, **292**, 229 (1993).

Nielsen, L.E. and Landel, R.F. *Mechanical Properties of Polymers and Composites, 2nd ed.*; Marcel Dekker, Inc.: New York, 1994; Chapter 7, pp. 377-459.

Nielsen, L.E., "Mechanical Properties of Particulate-Filled Systems", *Journal of Composites Materials*, **1**, 100 (1967).

Oberth, A.E. and Shacklett, C.D., "Gelatin-Anion Soap Complex Dispersion in Polyvinyl Alcohol Photographic Emulsions", U.S. Patent No. 3,067,035 (December 4, 1962).

O'Brien, F.E.M. "Control of Humidity by saturated Salt Solutions", *Journal of Scientific Instrumentation*, **25**, 73 (1948).

Oosterbroek, M., Lammers, R.J., Van Der Van, L.G.J., and Perera, D.Y., "Crack Formation and Stress Development in an Organic coatings", *Journal of Coatings Technology*, **63**(797), 55 (1991).

Overbergh, N, Berghmans, H., and Smets, G., "Crystallization of Isotactic Polystyrene Induced by Organic Vapors", *Polymer*, **16**(10), 703 (1975).

Paesschen, A.J.V. and Vranken, M.N., "Photographic material", U.S. Patent No. 3,397,988 (August 20, 1968).

Peppas, N.A. and Urdahl, K.G., " Anomalous Penetrant Transport in Glassy Polymers VII. Overshoots in Cyclohexane Uptake in Crosslinked Polystyrene", *Polymer Bulletin*, **16**, 201 (1986).

Perera, D.Y. and Vanden Eynde, D., "Moisture and Temperature Induced Stresses (Hygrothermal Stresses) in Organic Coatings", *Journal of Coatings Technology*, **59**(748), 55 (1987).

Petrie, S.E.B. and Becker, R. In *Analytical Calorimetry*; Porter, R.S. and Johnson, J.F., Eds.; Plenum Press: New York, 1970; Vol. 2, pp.225-238.

Pinhas, M-F., Blanshard, J.M.V., Derbyshire, W., and Mitchell, J.R., "The Effect of Water on the Physicochemical and Mechanical Properties of Gelatin", *Journal of Thermal Analysis*, **47**, 1499 (1996).

Plepys, A., "A Study of the Evolution of residual Stresses in Three Dimensionally Constrained Epoxy Resins", Ph.D. Dissertation, University of Massachusetts, Amherst, MA (1992).

Prager, S. and Long, F., "Diffusion of Hydrocarbons in Polyisobutylene", *Journal of the American Chemical Society*, **73**, 4072 (1951).

Pritchard, J.G. *Poly(vinyl alcohol)-Basic Properties and Uses*; Gordon and Breach Science Publishers: New York, 1970; pp. 60.

Rao, K.S., "Hysteresis in Sorption. I-IV", *Journal of Physical Chemistry*, **45**, 500 (1941).

Rogers, H.G. and Lutes, H.W., "Photographic Process", U.S. Patent No. 3,239,336 (March 8, 1966).

Rose, P.I. In *Encyclopedia of Polymer Science and Engineering*; Mark, H.F., Bikales, N.M., Overberger, C.G., Menges, G., and Kroschwitz, J.I., Eds.; John Wiley & Sons: New York, 1978; Vol. 7, pp. 488-573.

Rosen, B.W., "Thermal Expansion Coefficients of Composite Material", Ph.D. Dissertation, University of Pennsylvania, PA (1968).

Ryan, W.H., "Process for Producing Silver Halide Emulsions Containing gelatin Derivatives", U.S. Patent No. 3,186,864 (June 1, 1965).

Sackinger, S.T., "The Determination of Swelling Stress in Polyimide Films", Ph.D. Dissertation, University of Massachusetts, Amherst, MA (1990).

Scandola, M. and Pezzin, G. In *Water in Polymers*; Rowland, S.P., Ed.; American Chemical Society: Washington, D.C., 1980; Chapter 13, pp. 225-234.

Schapery, R.A., "Thermal Expansion Coefficients of Composite Materials Based on Energy Principles", *Journal of Composite Materials*, **2**(3), 380 (1968).

Sheldon, R.P. *Composite Polymeric Materials*; Applied Science Publishers: London, 1982; Chapter 4, p. 98.

Sheth, K.C., "Stress, Mechanical and Thermal Characterization of Anisotropic Polyimide Thin Films and Coatings", Ph.D. Dissertation, University of Massachusetts, Amherst, MA (1996).

Shimbo, M., Ochi, M., and Arai, K., "Effect of Solvent and Solvent Concentration on the Internal Stress of Epoxide Resin Coatings", *Journal of Coatings Technology*, **57**(728), 93 (1985).

Sih, G.C., Michopoulos, J.G., and Chou, S.C., Eds.; *Hygrothermoelasticity*; Martinus Nijhoff Publishers: Dordrecht, Netherlands, 1986.

Spiess, W.E.L. and Wolf, W. In *Water Activity: Theory and Applications to Food*; Rockland, L.B. and Beuchat, L.R., Eds.; Marcel Dekker, Inc.: New York, 1987; pp. 215-233.

Starkweather, Jr., H.W. In *Water in Polymers*; Rowland, S.P., Ed.; American Chemical Society: Washington, D.C., 1980; Chapter 25, pp. 433-440.

Steel, T.R., "Determination of the Constitutive Coefficients for a Mixture of Two Solids", *International Journal of Solids and Structures*, **4**, 1149 (1968).

Stroebel, L., Compton, J., Current, I., and Zakia, R., Eds.; *Photographic Materials and process*; Focal Press: Boston, 1986.

Sugisaki, M., Suga, H., and Seki, S., "Calorimetric Study of the Glass State. IV. Heat Capacities of Glassy Water and Cubic Ice", *Bull. Chem. Soc. Jpn.*, **41**, 2591 (1968).

Thomas, A.M. and Gent, W.L., "Permeation and Sorption of Water Vapour in Varnish Films", *Proceedings of the Physical Society, London.*, **57**, 324 (1945).

Titow, W.V., Braden, M, Currel, B.R., and Loneragan, R.J., "Diffusion and Some Structural Effects of Two Chlorinated Hydrocarbon Solvents in Bisphenol A Polycarbonate", *Journal of Applied Polymer Science*, **18**, 867 (1974).

Tong, H.M. and Saenger, K.L., "Bending Beam Characterization of Thin Polymer Films" In *New Characterization Techniques for Thin Polymer Films*; Tong, H.M. and Nguyen, L.T., Eds.; John Wiley and Sons, Inc.: New York, 1990.

Treloar, L.R.G. *The Physics of Rubber Elasticity, 2nd ed.*; Clarendon Press: Oxford, 1958; p. 135.

Tsai, S.W., U.S. Government Report AD 834851, 1968.

Turner, P.S., "Thermal-Expansion Stresses in Reinforced Plastics", *Journal of Research of the National Bureau of Standards*, **37**(4), 239 (1946).

Umberger, J.Q., "The Fundamental Nature of Curl and Shrinkage in Photographic Films", *Photographic Science and Engineering*, **1**(2), 69 (1957).

Urdhal, K.G. and Peppas, N.A., " Anomalous Penetrant Transport in Glassy Polymers V. Cyclohexane Transport in Polystyrese", *Journal of Applied Polymer Science*, **33**, 2669 (1987).

Van Der Poel., C., "On the Rheology of Concentrated Dispersions", *Rheologica Acta*, **1**, 198 (1958).

Veis, A. *The Macromolecular Chemistry of Gelatin*; Academic Press: New York, 1964; pp. 367-387.

Vrentas, J.C. and Duda, J.L., "Molecular Diffusion in Polymer Solutions", *AICHE Journal*, **25**, 1 (1979).

Vrtis, J.K. and Farris, R.J., "Experimental Stress Analysis and Some Thin Film Applications", *Materials Research Society Symposium Proceedings*, **338**, 527 (1994).

Vrtis, J.K. and Farris, R.J., "Hysteresis of Biaxial Swelling Stresses in Humidity Sensitive Polymer Coatings", *Proceedings of the American Chemical Society: Division of Polymeric Materials: Science and Engineering*, **69**, 440 (1993).

Vrtis, J.K., "Stress and Mass Transport in Polymer Coating and Films", Ph.D. Dissertation, University of Massachusetts, Amherst, MA (1995).

Walker, C.M. and Peppas, N.A., " Solute and Penetrant Diffusion in Swellable Polymers: X. Swelling of Multiethylene Glycol Dimethacrylate Copolymers", *Journal of Applied Polymer Science*, **39**, 2043 (1990).

Walker, I. and Collyer, A.A. In *Rubber Toughened Engineering Plastics*; Collyer, A.A., Ed.; Chapman & Hall: New York, 1994; Chapter 2, pp.29-56.

Watt, I.C., "Determination of Diffusion Rates in Swelling Systems", *Journal of Applied Polymer Science*, **8**, 2835 (1964).

Weast, R.C., Ed.; *Handbook of Chemistry and Physics, 55th ed.*; CRC Press: Ohio, 1974.

Wetzel, R., Buder, E., Hermel, H., and Hüttner, "Conformations of Different Gelatins in Solutions and in Films: An Analysis of Circular Dicroism (CD) Measurements", *Colloid and Polymer Science*, **265**, 1036 (1987).

Wexler, A. and Brombacher, W.G., "Methods of Measuring Humidity and Testing Hygrometers. A Review and Bibliography", U.S. Government Printing Office (1951).

Williams, H.L., *Polymer Engineering*; Elsevier: New York, 1975; pp.110-113.

Windle, J.J., "Sorption of Water by Wool", *Journal of Polymer Science*, **21**, 103 (1956).

Wolff, E.G. In *Handbook of Polymer-Fibre Composites*; Jones, F.R., Ed.; Longman Scientific & Technical: Burnt Mill, Harlow, Essex, 1994; Chapter 6.1, pp. 362-366.

Wolff, E.G. In *International Encyclopedia of Composites, Vol.4*; Lee, S.M., Ed.; VCH Publishers: New York, 1991; pp. 279-323.

Yannas, I.V and Tobolsky, A.V., "High-Temperature Transformations of Gelatin", *European Polymer Journal*, **4**, 257 (1968).

Yannas, I.V and Tobolsky, A.V., "Transitions in Gelatin-Nonaqueous-Diluent Systems", *Journal of Macromolecular Chemistry*, **1**(4), 723 (1966).

York, P., "Analysis of Moisture Sorption Hysteresis in Hard Gelatin Capsules and Maize Starch: Drug Powder Mixtures", *Journal of Pharmaceutical and Pharmacology*, **33**, 269 (1981).

Young, R.J. and Lovell, P.A. *Introduction to Polymers, 2nd ed.*; Chapman & Hall: New York, 1991; Chapter 5, pp.310-428.

Zoller, P., "PVT Manual (Version 2.01)", Gnomix Inc., Boulder, CO, 1987.

Zoller, P., Bolli, P., Pahud, V., and Ackermann, H., "Apparatus for Measuring Pressure-Volume-Temperature Relationships of Polymers to 350°C and 2200 kg/cm^2", *Review of Scientific Instruments*, **47**(8), 948 (1976).

Zsigmondy, R., "Structure of Gelatious Silicic Acid. Theory of Dehydration", *Journal of Organic Chemistry*, **71**, 356 (1911).

Unknown Author

"Physical and Chemical Behavior of Kodak Aerial Films", *Properties of Kodak Materials for Aerial Photographic Systems*; Eastman Kodak Co.: Rochester, NY, 1972; Vol. III.

"Physical Properties of Kodak Aerial Films", *Properties of Kodak Materials for Aerial Photographic Systems*; Eastman Kodak Co.: Rochester, NY, 1972; Vol. II.

"The Measurements of Humidity in Closed Spaces", Food Investigation Special Report No. 8 (1993).